STUDIES ON HIGH TEMPERATURE

HEAT PUMP SYSTEMS

BY

SAM SUNDAY ADEFILA

Dissertation Submitted for the Degree of PhD

Department of Chemical Engineering

University of Salford

Salford

England

1983

DEDICATION

This thesis is dedicated to the Glory

of God.

A B S T R A C T

STUDIES ON HIGH TEMPERATURE HEAT PUMP SYSTEMS

There is no shortage of heat energy in the world. However, the thermodynamic degradation of energy when used and inefficient use of high grade energy may result in a shortage of high grade energy. The conservation of primary energy through recycling is imperative. The application of heat pump systems could be used to save significant amounts of energy.

Three experimental heat pump systems were built and evaluated using water (R718) which is a potentially useful high temperature working fluid.

Two of the heat pumps were open vapour compression systems using small compressors. Similar performance data were obtained from the two machines even though different compressors with different design compression ratios (CR) were used. The average values of the experimental gross temperature lift , compression ratio and Rankine heat pump effectiveness were $8^{o}C$, 1.3 and 0.2 respectively.

The third experimental heat pump was a conventional water-lithium bromide absorption system, constructed from stainless steel. The maximum delivery temperature obtained was $147.5^{o}C$. Actual coefficients of performance were in the range 1.20 and 1.30, decreasing as the generator temperature increased. The gross temperature lifts were in the range 25 to $46^{o}C$. The highest generator temperature was $197^{o}C$. Concentrations of solutions were varied between 50 and 54

weight per cent (LiBr). Studies showed that stainless steel AISI 316 corroded in the solutions (in the range of concentrations and temperatures investigated) only in the presence of contaminants.

Actual coefficients of performance up to 1.4 were obtained using an existing conventional glass absorption system operated at generator temperatures of about 110°C.

An experimental water-water closed vapour compression heat pump system was also used to obtain performance characteristics using trichlorofluoroethane (R113). The maximum condensing temperature obtained was 94.9°C. The gross temperature lifts were in the range 22.4 to 36.3°C and the corresponding Rankine heat pump effectiveness factors were in the range 0.31 to 0.43. The results obtained using R113 in this system were compared with the results obtained by previous workers using R12, R11 and R114.

These studies show that water and R113 produce high delivery temperatures in heat pump systems. Furthermore, they show that the conventional absorption heat pump system for certain applications is superior in performance and more likely to save money than the vapour compression heat pump system particularly for small capacities. However, both systems result in a significant reduction in primary energy requirements.

Enthalpy-concentration-temperature data in the temperature range 60-220°C were obtained from limited vapour pressure-concentration-temperature data for aqueous solutions of lithium bromide. The data were represented by polynomial equations and compared with the data obtained from the literature. The data were used to analyse a

conventional absorption system and the results were used as a basis for comparing experimental data.

Suggestions for further work are outlined.

ACKNOWLEDGEMENT

I wish to thank the authorities of Ahmadu Bello University, Samaru-Zaria, Nigeria, for allowing me to undertake this study. My thanks are also due to the Kwara State Government of Nigeria and the Netherlands Universities Foundation for international cooperation for their financial support at the initial and final stages of this work respectively.

I am most obliged to Professor F A Holland, Chairman and Head of Department of Chemical Engineering, University of Salford, and Mr F A Watson, formerly Senior Lecturer, Department of Chemical Engineering, University of Salford, for the guidance they offered me. I wish to note that the monthly departmental technical memoranda for the Heat Pump Research Group have been of immense use to me.

My gratitude is due to the entire members of the Heat Pump Research Group whose comments and help have been very useful.

I do express my gratitude to the technical staff for their assistance.

My thanks go to Mr T O Omideyi for his encouragement in his capacity as a colleague and a pastor.

I wish to thank my wife for her cooperation without which this work could not have been completed.

NOMENCLATURE

NOMENCLATURE

A	the slope of the Duhring line,	dimensionless
(COP)	coefficient of performance,	dimensionless
$(COP)_A$	actual coefficient of performance for vapour compression heat pump system,	dimensionless
$(COP)_{AHA}$	actual coefficient of performance for absorption heat pump system,	dimensionless
$(COP)_{AHC}$	Carnot coefficient of performance for absorption heat pump system,	dimensionless
$(COP)_{AHMO}$	maximum obtainable coefficient of performance for absorption heat pump system,	dimensionless
$(COP)_C$	Carnot coefficient of performance for vapour compression heat pump system,	dimensionless
$(COP)_P$	predicted coefficient of performance,	dimensionless
$(COP)_R$	Rankine coefficient of performance for vapour compression heat pump system,	dimensionless
C_p	heat capacity per unit mass	$kJ\ kg^{-1}K^{-1}$
(CR)	compression ratio = P_{CO}/P_{EV},	dimensionless
D	diffusion coefficient of gas through liquid,	$m^2\ s^{-1}$
d	column diameter,	m

dT	differential temperature,	K
E	primary energy consumed,	kW
F	packing factor,	dimensionless
(FRX)	reflux ratio,	dimensionless
$\bar{H}$	partial enthalpy of water in the solution,	kJ kg^{-1}
H_o	enthalpy of base concentration,	kJ kg^{-1}
$(\Delta H)_{LOSS}$	heat loss,	kJ kg^{-1}, kJ m^{-3}
HGE	high grade energy,	kW
$(HPE)_C$	Carnot heat pump effectiveness,	dimensionless
$(HPE)_R$	Rankine heat pump effectiveness,	dimensionless
(HPV)	enthalpy per unit volume,	kJ m^{-3}
H_X	enthalpy per unit mass at state condition X,	kJ kg^{-1}
K_L	the absorption coefficient of water vapour into the absorber solution,	m s^{-1}
m	circulation ratio = M_{AB}/M_W,	dimensionless
M_{AB}	mass flow rate of solution in the absorber,	kg s^{-1}
M_R	mass flow rate of water-rich solution recirculated through the absorber,	kg s^{-1}

M_X	mass flow rate at position X,	$kg\ s^{-1}$
M_W	mass flow rate of working fluid,	$kg\ s^{-1}$
P_{AB}	saturation pressure of solution in the absorber,	Nm^{-2} or bar
P_{CO}	condensing pressure of working fluid,	Nm^{-2} or bar
PER	primary energy ratio,	dimensionless
P_{EV}	evaporating pressure of working fluid,	Nm^{-2} or bar
P_{GE}	saturation pressure of solution in the generator,	Nm^{-2} or bar
P_S	saturated vapour pressure,	Nm^{-2} or bar
q	heat load per unit mass of working fluid,	$kJ\ kg^{-1}$
Q_{AB}	heat delivered by the absorber,	kW
Q_{CO}	heat delivered by the condenser,	kW
Q_D	heat delivered by the heat pump system,	kW
Q_{EV}	heat supplied to the evaporator,	kW
Q_{GE}	heat supplied to the generator,	kW
Q_{LOSS}	heat loss,	kW
Q_S	heat supplied to the heat pump system,	kW
R	universal gas law constant,	$J\ (kmole)^{-1}\ K^{-1}$

t'	the life time of a liquid surface element,	s
T	temperature of solution,	^{o}C
(TA)	temperature approach in the economiser heat exchanger,	^{o}C
T_{AB}	temperature of solution in the absorber,	^{o}C
T_{CO}	condensing temperature of working fluid,	^{o}C, K
T_{D}	delivery temperature of heat pump system,	^{o}C, K
T_{EV}	evaporator temperature,	^{o}C, K
T_{GE}	temperature of solution in the generator,	^{o}C
$(T_{AB}-T_{EV})$	gross absorber temperature lift,	^{o}C, K
$(T_{CO}-T_{EV})$	gross condenser temperature lift,	^{o}C, K
T_{S}	supply temperature of heat pump system,	K
T_{X}	temperature at position X,	^{o}C
T_{W}	temperature of working fluid,	^{o}C, K
V	volume of solution,	m^3

ΔV	volume difference,	m^3
V_C	volumetric flow rate of working at inlet of compressor,	$m^3\ s^{-1}$
(VPH)	volume per unit enthalpy,	$m^3\ kJ^{-1}$
(VR)	ratio of volume of working fluid in vapour state to its volume in liquid state,	dimensionless
W	work supplied to heat pump system,	kW
X	weight/weight per cent of salt in solution,	per cent
X^*	equilibrium concentration of working fluid at the interface,	mole m^{-3}
X_W	fractional weight of working fluid in solution,	dimensionless
Z	height of the absorber column,	m
γ	activity coefficient,	dimensionless
λ	latent heat of vaporisation per unit mass,	$kJ\ kg^{-1}$
μ	viscosity,	$kg\ m^{-1}\ s^{-1}$
ρ	density,	$kg\ m^{-3}$
ϕ	entropy per unit mass,	$kJ\ kg^{-1}\ K^{-1}$

ψ	ratio of density of water/ density of liquid,	dimensionless

SUBSCRIPTS

A	actual
AB	absorber
CO	condenser
CW	cooling water
D	delivered
EV	evaporator
GE	generator
L	liquid
O	reference state or pure state
R	reversible
S	solution, source
V	vapour
W	working fluid

LIST OF TABLES

		Page
1.1	Growth of commercial energy consumption (per cent) 1960-78	13
2.1	Working fluids and maximum temperatures obtained in heat pumps at the Department of Chemical Engineering, University of Salford, U.K.	20
4.1	Volumetric throughput required for compressor heat intake rate of 1 MW for some working fluids	91
4.2	Compressor cost correlations	92
5.1	Chemical names and formulae for some working fluids	127
5.2	Performance data for ICE1 with R112 as the working fluid	128
5.3	Heat losses and efficiencies of ICE1 compressor operating on R12 at a condensing temperature of 56°C	129
5.4	Performance factors at given mean condensing temperatures for R12, R11, R114 and R113	130
5.5	Performance data for heat pump 1 and heat pump 2 with R718 as working fluid	131
6.1	Chebyshev coefficients of the polynomial for the enthalpy-concentration-temperature data for solutions of lithium bromide	160
6.2	Chebyshev coefficients of the Chebyshev polynomial for the temperature of solutions-concentration-saturation temperature of water data for solutions of lithium bromide	160
6.3	Errors in enthalpy per unit mass due to specified errors in the Dubring line slope over a 10 per cent range of concentrations	161

		Page
6.4	Duhring constant, correlation coefficient of the Duhring curve, mean error of the Duhring constant and standard deviation of the mean error for temperature of solutions 60-220°C and a range of concentrations of aqueous solutions of lithium bromide	161
6.5	Errors in the enthalpy-concentration correlation for concentrations of lithium bromide 50 to 68 per cent in aqueous solutions of lithium bromide	162
6.6	Error in the concentration saturation temperature of water correlation for concentrations of lithium bromide 50 to 68 per cent in aqueous solutions of lithium bromide	162
6.7	Saturation temperature of water from data derived in this exercise and those reported by McNeely for a range of temperatures and concentrations for solutions of lithium bromide	163
6.8	Observed saturation temperature of water and those reported by McNeely for a range of temperatures and concentrations for solutions of lithium bromide	164
6.9	Enthalpy per unit mass from data derived in this exercise and those reported by McNeely for a range of temperatures and concentrations for solutions of lithium bromide	165
7.1	Mass and energy balances over a conventional absorption heat pump system	182
7.2	Heat pump effectiveness factors at a gross condenser temperature lfit of 40°C and generator temperatures of 190°C and 210°C	183
8.1	List of equipment parts	238
8.2	Raw experimental data and computed values for the water-lithium bromide system for a generator temperature of 171.8°C	239
8.3	Raw experimental data and computed values for the water-lithium bromide system for a generator temperature of 171.8°C	243

		Page
8.4	Raw experimental data and computed values for the water-lithium bromide system for a generator temperature of 197°C	247
8.5	Raw experimental data and computed values for the water-lithium bromide system for a generator temperature of 100.5°C	251
8.6	Raw experimental data and computed values for the water-lithium bromide system for a generator temperature of 110.7°C	255
A.I.1	Theoretical volume flowrate at T_{EV} for a heat intake rate of 1 MW for a range of lifts and condensing temperatures for R718	318
A.I.2	Theoretical volume flowrate at T_{EV} for a heat intake rate of 1 MW for a range of lifts and condensing temperatures for R114B2	323
A.I.3	Theoretical volume flowrate at T_{EV} for a heat intake rate of 1 MW for a range of lifts and condensing temperatures for R113	326
A.I.4	Theoretical volume flowrate at T_{EV} for a heat intake rate of 1 MW for a range of lifts and condensing temperatures for R11	329
A.I.5	Theoretical volume flowrate at T_{EV} for a heat intake rate of 1 MW for a range of lifts and condensing temperatures for R216	331
A.I.6	Theoretical volume flowrate at T_{EV} for a heat intake rate of 1 MW for a range of lifts and condensing temperatures for R21	333
A.I.7	Theoretical volume flowrate at T_{EV} for a heat intake rate of 1 MW for a range of lifts and condensing temperatures for R600	335
A.I.7	Theoretical volume flowrate at T_{EV} for a heat intake rate of 1 MW for a range of lifts and condensing temperatures for R12B1	337

		Page
A.I.9	Theoretical volume flowrate at T_{EV} for a heat intake rate of 1 MW for a range of lifts and condensing temperatures for R114	339
A.I.10	Theoretical volume flowrate at T_{EV} for a heat intake rate of 1 MW for a range of lifts and condensing temperatures for R506	341
A.I.11	Theoretical volume flowrate at T_{EV} for a heat intake rate of 1 MW for a range of lifts and condensing temperatures for R142B	343
A.I.12	Theoretical volume flowrate at T_{EV} for a heat intake rate of 1 MW for a range of lifts and condensing temperatures for R600A	345
A.I.13	Theoretical volume flowrate at T_{EV} for a heat intake rate of 1 MW for a range of lifts and condensing temperatures for R717	347
A.I.14	Theoretical volume flowrate at T_{EV} for a heat intake rate of 1 MW for a range of lifts and condensing temperatures for R505	349
A.I.15	Theoretical volume flowrate at T_{EV} for a heat intake rate of 1 MW for a range of lifts and condensing temperatures for RC318	350
A.I.16	Theoretical volume flowrate at T_{EV} for a heat intake rate of 1 MW for a range of lifts and condensing temperatures for R12	351
A.I.17	Theoretical volume flowrate at T_{EV} for a heat intake rate of 1 MW for a range of lifts and condensing temperatures for R500	352
A.I.18	Theoretical volume flowrate at T_{EV} for a heat intake rate of 1 MW for a range of lifts and condensing temperatures for R290	353
A.I.19	Theoretical volume flowrate at T_{EV} for a heat intake rate of 1 MW for a range of lifts and condensing temperatures for R22	354

		Page
A.I.20	Theoretical volume flowrate at T_{EV} for a heat intake rate of 1 MW for a range of lifts and condensing temperatures for R115	355
A.IV.1	Specifications of the anhydrous lithium bromide	375
A.IV.2	Properties of hydrated lithium bromide	376

LIST OF FIGURES

		Page
1.1	World energy consumption by region	14
1.2	World energy consumption by source	14
1.3	Double-effect heat pump system for cooling and heating	15
1.4	Dryer and heat pump system	16
1.5	Fractionation column with heat pump	17
3.1a	Mechanical vapour compression heat pump	74
3.1b	Conventional absorption heat pump	74
3.2a	Reversed absorption heat pump	75
3.2b	Resorption heat pump	75
3.2c	Absorption-resorption heat pump	75
3.3	A periodic absorption heat pump	76
3.4	Three stage heat pump	76
3.5	Heat engine and heat pump components of a continuous absorption heat pump system	77
3.6	Heat flow in a power station	77
3.7	IFP Thermosorb	78
3.8	Vapour pressure against temperature for a range of concentrations for ammonia-water and ammonia-water-lithium bromide mixtures	79

		Page
3.9	The CDE engine	80
3.10	Temperature against concentration for a favourable absorbent mixture	81
3.11	Pressure against temperature for an absorbent mixture	81
4.1	Enthalpy per unit volume against temperature for some common working fluids	93
4.2	Enthalpy per unit volume versus temperature for some working fluids	94
4.3	Enthalpy per unit volume against temperature for some working fluids	95
4.4	Enthalpy per unit volume against temperature for some high temperature working fluids	96
4.5	Volume per unit enthalpy against temperature for some working fluids	97
4.6	Volume per unit enthalpy against temperature for some working fluids	98
4.7	Volume per unit enthalpy against temperature for some working fluids	99
4.8	Volume per unit enthalpy against temperature for some working fluids	100
4.9	Pressure against enthalpy per unit mass for a working fluid	101
4.10	Ratio of volume of vapour to volume of liquid against temperature for some working fluids	102
4.11	Ratio of volume of vapour to volume of liquid against temperature for some working fluids	103

		Page
4.12	Ratio of volume of vapour to volume of liquid against temperature for some working fluids	104
4.13	Ratio of volume of vapour to volume of liquid against temperature for some working fluids	105
5.1	Non-ideal Rankine cycle	132
5.2	Pressure against enthalpy per unit mass for R12	133
5.3	Pressure against enthalpy per unit mass for R113	133
5.4	Experimental heat pump 1	134
5.5	Power intake against speed for the unloaded motor and gear for heat pump 1	135
5.6	Experimental heat pump 2	136
5.7	Power intake against speed for the unloaded motor and fear box for heat pump 2	137
5.8	Actual and predicted coefficients of performance against temperature lift at mean $T_{CO}=56^{o}C$ for R12 and at mean $T_{CO}=62^{o}C$ for R114	138
5.9	Actual and predicted coefficients of performance and Rankine heat pump effectiveness factor against temperature lift at mean $T_{CO}=84^{o}C$ for R113	138
5.10	Actual and predicted coefficients of performance against temperature lift at mean $T_{CO}=83^{o}C$ for R11	139
5.11	Heat loss against compression ratio for a reciprocating compressor and a rotary vane compressor for outlet temperature of $59^{o}C$ for R729	140
6.1	Enthalpy per unit mass of aqueous solutions of lithium bromide against concentration for various saturation temperatures	166

		Page
6.2	Saturation temperature of water vapour against saturation temperature of aqueous solution of lithium bromide	167
6.3	Saturation pressure against enthalpy per unit mass for water (R718)	168
7.1	Conventional absorption heat pump unit	184
7.2	Cycle of conventional absorption heat pump	185
7.3	Flow chart for the main computer programme for calculating $(COP)_{AHMO}$ for a conventional absorption heat pump	186
7.4	Carnot coefficient of performance against gross temperature lift for an evaporator temperature of $100^{o}C$ and a range of generator temperatures for a conventional absorption heat pump system	187
7.5	Maximum obtainable coefficient of performance against gross temperature lift for equal condenser and absorber temperatures for evaporator temperature of $100^{o}C$ and a range of generator temperatures for water-lithium bromide system	188
7.6	Maximum obtainable coefficient of performance against gross temperature lift showing the influence of generator temperature for an absorber temperature lift of $35.1^{o}C$, an evaporator temperature of $100^{o}C$ and a weight fraction of water in the absorber of 0.49 for the water-lithium bromide system	189
7.7	Maximum obtainable coefficient of performance against gross temperature lift showing the influence of water-rich solution flow rate to unit flow rate of vapour (FR) for a range of evaporator temperatures, a generator temperature of $190^{o}C$ and a weight fraction of water in the absorber of 0.49 for the water-lithium system	190
7.8	Maximum obtainable coefficient of performance against gross temperature lift of $47.8^{o}C$ and evaporator temperature of $110^{o}C$ and a weight fraction of water in the absorber of 0.44 for the water-lithium bromide system	191

		Page
7.9	Solubility of lithium bromide in water	192
7.10	Compression ratio and maximum obtainable coefficient of performance against gross temperature lift for a gross absorber temperature lift of 35°C and a weight fraction of water in the absorber of 0.49 for various generator temperatures for the water-lithium bromide system	193
7.11	Maximum obtainable coefficient of performance against gross temperature lift for various temperatures (TA) in the economiser for an evaporator temperature of 100°C, a generator temperature of 200°C and a weight fraction of water in the absorber of 0.49 for the water-lithium bromide system	194
8.1a	Simplified absorption heat pump	260
8.1b	Simplified vapour compression heat pump	260
8.2	Experimental conventional metal absorption heat pump	261
8.3	Generator/evaporator of the experimental conventional metal heat pump system	262
8.4	Coefficient of performance against gross condenser temperature lift for a gross absorber temperature lift of 32°C, an evaporator temperature of 100°C, a generator temperature of 172°C and a concentration of lithium-bromide of 50.5 weight per cent in the absorber for the water-lithium bromide system	263
8.5	Coefficient of performance against gross condenser temperature lift for a gross absorber temperature lift of 35°C, an evaporator temperature of 94°C, a generator temperature of 172°C and a concentration of lithium bromide of 52.5 weight per cent in the absorber for the water-lithium bromide system	264
8.6	Coefficient of performance against gross condenser temperature lift for a gross absorber temperature lift of 35°C, an evaporator temperature of 101°C, a generator temperature of 197°C and a concentration of lithium bromide of 51.5 weight per cent in the absorber for the water-lithium bromide system	265

		Page
8.7	Experimental conventional absorption heat pump	266
8.8	Generator of the glass heat pump	267
8.9	Coefficient of performance against gross condenser temperature lift for a gross absorber temperature lift of 24.4°C, an evaporator temperature of 46.7°C, a generator temperature of 100°C and a concentration of lithium bromide of 48.8 weight per cent in the absorber for water-lithium bromide system	268
8.10	Coefficient of performance against gross condenser temperature lift for a gross absorber temperature lift of 20.8°C, an evaporator temperature lift of 47.6°C, a generator temperature of 110°C and a concentration of lithium bromide of 48.5 weight per cent in the absorber for water-lithium bromide system	269
8.11	Comparison of actual coefficients of performance against temperature lift for the water-lithium bromide system	270
A.II.1	Schematic diagram of experimental water-to-water heat pump	360
A.II.2	Instrumentation of the experimental water-to-water heat pump	361
A.III.1	Conventional absorption heat pump unit	373
A.IV.1	Calibration of lithium bromide solutions at 30°C	377
A.IV.2	Calibration of the solution rotameter for the metal equipment	378
A.IV.3	Calibration of the solution rotameter for the glass equipment	379
A.V.1a	Simplified absorption heat pump	384
A.V.1b	Simplified vapour compression heat pump	384

CONTENTS

		Page
CHAPTER 1	INTRODUCTION	1
	1.1 Sources of primary energy	2
	1.2 World energy reserves and distribution	2
	1.3 World energy consumption	8
	1.4 The need to conserve energy	9
	1.5 The means to conserve energy	11
CHAPTER 2	RESEARCH OBJECTIVE	18
CHAPTER 3	HEAT PUMP SYSTEMS	22
	3.1 Types of heat pumps	23
	3.1.1 Vapour compression heat pumps	23
	3.1.2 Vapour sorption heat pumps	23
	3.1.2.1 Absorption heat pumps	24
	3.1.2.2 Derivatives of the vapour compression and absorption heat pumps	25
	3.2 Literature survey on absorption heat pump systems	27
	3.2.1 Theoretical reports	28
	3.2.2 Experimental research	36
	3.2.3 Installed heat pumps	45
	3.3 Absorption power cycle	47
	3.4 Working fluid-absorbent mixtures for absorbent heat pumps	48
	3.4.1 Characteristics of working fluids and absorbent mixtures	51
	3.4.1.1 Thermodynamic characteristics	52
	3.4.1.2 Kinetic characteristics	59
	3.4.1.3 Thermophysical properties	59
	3.4.1.4 Safety considerations	60
	3.4.1.5 Corrosivity	61

		Page
3.4.2	Physical and thermodynamic data reference for working fluid-absorbent mixtures	61
3.4.2.1	General	61
3.4.2.2	Water as working fluid	63
3.4.2.3	Alcohols as working fluids	66
3.4.2.4	Ammonia based compounds as working fluids	67
3.4.2.5	Halogenated hydrocarbons as working fluids	69
3.4.2.6	Miscellaneous compounds as working fluids	72
CHAPTER 4	THERMODYNAMIC CONSIDERATIONS	83
4.1	Introduction	84
4.2	Compressor size and cost	86
4.3	Compressors for non-isentropic compression	87
4.4	Discussion	89
CHAPTER 5	PERFORMANCE CHARACTERISTICS OF WORKING FLUIDS IN VAPOUR COMPRESSION HEAT PUMP SYSTEMS	106
5.1	Introduction	107
5.1.1	Inefficiencies in a vapour compression heat pump system	109
5.1.2	Selection of working fluids	111
5.1.3	Prediction of performance	113
5.2	Experimental operation of ICE1 using R113	114
5.3	Heat pump 1	115
5.3.1	Description of heat pump 1	115
5.3.1.1	Instrumentation	117
5.3.2	Experimental technique	118
5.4	Heat pump 2	119
5.4.1	Description of heat pump 2	119
5.4.2	Instrumentation	120
5.4.3	Experimental technique	120

			Page
	5.5	Results and discussion	120
	5.6	Conclusions	126
	5.7	Recommendations	126
CHAPTER 6	ENTHALPY-CONCENTRATION-TEMPERATURE RELATION FOR WATER-LITHIUM BROMIDE SOLUTIONS		141
	6.1	Introduction	142
	6.2	The Duhring equation	147
	6.3	Vapour pressure data	149
	6.4	Determination of the enthalpy-concentration-temperature data	151
		6.4.1 The Haltenberger's relation	152
		6.4.2 Reference state	152
		6.4.3 Determination of the enthalpy of the base concentration solution	152
		6.4.4 Heat capacity data	153
		6.4.5 The partial enthalpy of water in the solutions	153
	6.5	Computer programme	154
	6.6	Accuracy	155
	6.7	Results and discussion	156
CHAPTER 7	THERMODYNAMIC ANALYSIS OF A CONVENTIONAL WATER-LITHIUM BROMIDE ABSORPTION HEAT PUMP SYSTEM		169
	7.1	Introduction	170
	7.2	Theory of absorption heat pumps	170
	7.3	Conventional absorption heat pump cycle	171
	7.4	Expressions for coefficient of performance	172
		7.4.1 $(COP)_{AHC}$	172
		7.4.2 $(COP)_{AHMO}$	174
	7.5	Computer programme	176
	7.6	Discussion of derived data	178

		Page
CHAPTER 8	PERFORMANCE STUDIES USING WATER-LITHIUM BROMIDE SOLUTIONS IN CONVENTIONAL ABSORPTION HEAT PUMP SYSTEMS	195
	8.1 Introduction	
	8.2 Performance studies using water-lithium bromide solutions in a metal absorption heat pump system	199
	8.2.1 Equipment	199
	8.2.2 Instrumentation	207
	8.2.3 Commissioning the equipment	209
	8.2.4 Experimental procedure	212
	8.2.4.1 Preparation and standardisation of aqueous lithium bromide solution	212
	8.2.4.2 Experimental technique	214
	8.2.5 Results and discussion	219
	8.3 Performance studies using water-lithium bromide solutions in a glass absorption heat pump system	228
	8.3.1 Introduction	228
	8.3.2 Equipment	229
	8.3.3 Accuracy of instrument	231
	8.3.4 Experimental technique	233
	8.3.5 Results and discussion	233
	8.4 Summary of experimental results and conclusion	236
CHAPTER 9	CONCLUSIONS AND RECOMMENDATIONS FOR FUTURE WORK	271
	9.1 Conclusions	272
	9.1.1 Mechanical vapour compression systems	273
	9.1.1.1 Water-to-water system operating on R113	273
	9.1.1.2 Comparison of performance data for R12, R11, R114 and R113	273
	9.1.1.3 Small heat pumps operating on air and water vapour	274
	9.1.1.4 General conclusions concerning mechanical vapour compression heat pump systems	274

		Page
9.1.2	Conventional absorption heat pump systems	275
9.1.2.1	Metal absorption heat pump systems	275
9.1.2.2	Glass absorption heat pump systems	275
9.1.2.3	General conclusions concerning the effect of varying operating parameters	276
9.1.3	General conclusions concerning the mechanical vapour compression and conventional absorption heat pump systems	277
9.2	Recommendations for future work	277
REFERENCES		280
APPENDIX I	COMPUTER PROGRAMMES AND RESULT	301
APPENDIX II	DESCRIPTION OF ICE1	356
APPENDIX III	DESIGN OF THE ABSORBER COLUMN	362
APPENDIX IV	PROPERTIES OF LITHIUM BROMIDE	374
APPENDIX V	THERMAL EFFICIENCY OF HEAT PUMPS	380

CHAPTER 1

INTRODUCTION

CHAPTER 1

INTRODUCTION

1.1 SOURCES OF PRIMARY ENERGY

The various sources of primary energy available to mankind include solar energy, wind energy, wave energy, hydro energy, geothermal energy, animal dung, agricultural wastes, wood, natural gas, oil, oil shale, tar sand, peat,coal and nuclear energy. Most primary energies exist as a result of solar energy.

1.2 WORLD ENERGY RESERVES AND DISTRIBUTION

The total amount of solar energy intercepted by the earth is about 5,500,000 EJ per annum (1 EJ = 10^{18}J). The solar energy reaching the earth is very diffuse; it comes for the most part in the daytime and even then, changes constantly during the day and the season of the year; it is considerably reduced for various periods of time on cloudy and rainy days, depending on the geographical location and the season. Conversion of solar energy into organic material by photosynthesis is a most important natural way of storing solar energy.

The average surface temperature of the earth due to solar interception is 7^{o}C and the additional energy contained in the land mass of a large tropical country such as Nigeria is enormous. In Nigeria the mean ambient temperature is 26^{o}C and the mean soil temperature at 5 cm below the surface is about 30^{o}C.

The differential heating and cooling of the various parts of the earth's surface by the sun induces wind with varying speeds from and to different parts of the world. The wind speed at a given location is furthermore a function of the topology of the area.

The power of a windmill is proportional to the cube of the wind velocity approaching the rotor at right angles. Typical windmill efficiencies are 50 per cent and outputs of 1.25 MW have been achieved with blade disc diameters of 60 m ["Compact shrouds for wind turbines, Ingra, O., Energy Conservation, 16, 149-157 (1977)].

As with wind power, wave power is variable from one part of the ocean body to another. The amount of wave power which could be harnessed for use depends on the coastline of a particular country. For example the U.K. has a coastline of approximately 1,500 km. This could be used for the location of a practical wave power system. The potential for the generation of electrical energy is of the order of 30,000 MW or about 50 per cent of the current installed capacity of the C.E.G.B. ["Industrial energy conservation", Reay, D.A., Pergamon Press Ltd., Oxford, 296 (1977)]. The work at the University of Edinburgh and other centres has demonstrated experimentally that more than 80 per cent of the total wave power from water waves could be extracted using a specially contoured rocking device ["Wave power", Salter, S.H., Nature, 249, 720-724 (1974)], ["Characteristics of a rocking wave power device, Salter, S.H., Nature, 254, 504-506 (1975)].

There is plenty of energy to be obtained from the world's rivers and waterfalls. Hydro power installations are now invariably used to produce electricity. The total hydroelectric potential of the world is about 2,261,100 MW. The potential of some individual rivers are particularly notable. The potential of the Yenisey-Angara in the USSR is estimated at 64,000 MW, about the same as the whole electricity generating capacity of all kinds in the U.K. The potential of the Inga River in Zaire is estimated to be

25,000 MW, and that of the Bramaputra in India to be 20,000 MW.

Geopressurised zones are known to occur in several parts of the world. The form and quality of available geothermal energy also vary widely. Natural streams, mixtures of steam and hot water at 160°C (in France), hot water at 81°C to 90°C (in Hungary), water from 40°C to 90°C (in Egypt), and very hot brine at 340°C (in California) are known. Some of these contain important elements such as uranium, copper and silver.

Animal dung is distributed widely in the world but it is not universally used as a primary energy source.

Using various tree-planting patterns, 2 to 5 per cent of farm land can be used to grow tress for fuel and other purposes without any loss in agricultural production ["Fuelwood production in traditional farming systems", Salem, B. and Van Nas, T., Food and Agricultural Organisation of United Nations, Rome, 33, (131) (1981)]. Currently, 3.04 x 10^9ha, have a 20 per cent tree cover - roughly one third of the world's land surface and about the same average percentage as that for the U.S.A. as a whole. Latin American and the tropical regions of Africa and Southeast Asia have most of the hardwood forests, while the softwood areas are concentrated in North America and the Soviet Union. Fuelwood is now a major forest product in the U.S.A. There is an adequate supply of unused wood annually which could provide 10 to 15 per cent of the energy needs in the U.S.A. ["Wood fuel resources in the United States, Hornick, J.R., ASHRAE Annual Meeting, (June 27-30 1982)].

It is difficult to predict exact quantities of recoverable reserves of fossil fuel in the world. Established reserves of natural gas are about 2,500 EJ, whilst remaining undiscovered resources were estimated to be about 8,100 EJ ["The future of world natural gas supply", McCormick, W.T., Kalishi, R.B. and Wonder, T.J., World Energy Resources, 1985-2020, World Energy Conference 1978, IPC Science and Technology Press, 50-51 (1978)]. Though natural gas reserves seem plentiful, over 50 per cent of them are in the developing countries ["Natural gas - prospects in developing countries and the role of LNG transportation", Ovcharenko, V.A., Natural Resources Forum, 4, (3), 277-290 (1980)]. The developed (industrialised) countries include Australia, Canada, various countries in Eastern Europe, the Soviet Union, Japan, New Zealand, the United States of America and the various countries in Western Europe. The rest of the world is commonly referred to as the developing countries.

The world total of recoverable reserves of petroleum were estimated to be about 9752 EJ in 1978 ["World petroleum supply limits", Pierre Des Praires, World Energy Resources, 1985-2020, World Energy Conference 1978, IPC Science and Technology Press, 2-14 (1978)]. In 1979, the recoverable oil reserve in Mexico was put at about 1250 EJ. This value is three times higher than the pre-1979 estimates ["Oil and world power", Odell, P.R., Pelican Books, 6th Edition, 272 (1981)]. The 1979 estimates put Mexico almost into the Saudi Arabian class. China was estimated, conservatively, to have 438 EJ of oil resources ["Oil and world power", Odell, P.R., Pelican Books, 6th Edition, 272 (1981)]. Moreover, the non-communist world's potentially valuable offshore recoverable oil reserves are greater than the on-shore reserves from which, to date,

almost all of the world's oil production has come ["Oil and world power, Odell, P.R., Pelican Books, 6th Edition, 266 (1981)]. In fact, Odell expects that by 2035 an oil industry about two and a half times its present size may have developed.

The richest single proven deposit of oil shale in the world is in the U.S.A. where the estimated quantity is 5737 EJ. The total world reserve of oil shale is estimated at about 5,441,800,000 EJ ["McGraw-Hill encyclopaedia of energy", Parker, S.P., McGraw-Hill Book Company, New York, 8 and 494 (1981)].

The largest single proven reserve of tar sand in the world is in the Canadian province of Alberta.

Although peat occurs throughout the world in wet environments, the full extent of the reserves has not yet been established ["Peat resources - classification, properties and geographical distribution", Farnham, R.S., Symposium on Management and Assessment of Peats as an Energy Resources, Arlington, Va. (22-24 July, 1979), (7-18 June 1980)].

Over 50 per cent of the world's proven reserves of coal are in the Soviet Union. The U.K. and Western Germany may have to import coal by 1995 ["British say coal reserves overstated", The Royal Society, Coal Age, 85, (5), 52 (May, 1980)], ["West German plans project large coal imports before 1995", Coal Age, 85, (5), 45 (May 1980)]. These imports may be met from Australia, Canada, Indonesia, South Africa and the U.S.A. where the resources could be developed at lower costs.

In general, the developing countries have a greater potential

for the development of both renewable and non-renewable forms of energy compared with the developed countries ["A new energy emphasis for the United States: transfering energy-intensive industry from the United States to developing countries", Stingel, D.E., Natural Resources Forum, The Division of Natural Resources and Energy of the United Nations, United Nations, New York, 4, (3), 260 (July, 1980)]. However, the development of energy potentials in developing countries has been hampered due to their lack of indigenous capital, meagre technological skills, and poor management. For example, the cost of the proposed 305 TJ (1 TJ = 10^{12}J) LNG plant in Nigeria, which could be commissioned by 1985, is estimated at about US $14 billion ["Vast gas program looms in Nigeria", Roger Vielvoye, Oil and Gas Journal, 61 (Jan. 1981)]. This amount can be afforded only by the central government in that region. Nigeria's proven unassociated gas reserves are estimated, extremely conservatively, as about 6.5 EJ. The Iran-Iraqi war which disrupted oil supplies to the West brought about intensified oil and gas exploration in West Africa. This exploration opened up large reserves of easily accessible oil and gas in West Africa ["West African crude suddenly is crucial", Roger Vielvoye, Oil and Gas Journal, 47 (Jan. 1981)]. Less than 1 per cent of the fossil energy resources in Africa have been developed ["Oil and world power", Odell, P.R., Pelican Books, 6th Edition, 268 (1981)]. On the other hand, up to 60 per cent of the recoverable oil in the U.S.A. has been produced ["Estimating undiscovered oil resources: an engineering approach, Uri, N.D., Energy Sources, 5, (3), 197 (1980)]. The solar, hydro and geothermal energy resources in the developing countries are yet to be developed.

1.3 WORLD ENERGY CONSUMPTION

The total primary energy consumption of the world in 1978 was about 265 EJ, of which about 75 per cent was consumed by the industrial countries ["Energy strategies for developing nations", Dunkerly, J., Ramsay, L.G. and Cecelski, E., John Hopkins University Press, London, 1st Edition, (1981)]. Energy from commercial sources (hydroelectricity, gas, oil, coal and nuclear energy) constituted 92 per cent of total consumption in the same period while the rest was from traditional sources (mainly firewood and charcoal, animal dung and agricultural wastes). Nigeria consumed 0.024 EJ in 1976. ["Energy production and consumption", U.N. Statistical Year Book 1978, U.N. Publication, New York, 389-392 (1979)]. Figure (1.1) shows the predicted annual rate of world energy consumption (by region) between 1960 and 1990. Table (1.1) shows that it is extremely difficult to predict future energy consumption. The developing countries with three-quarters of the world's population accounted for a share of about 47 per cent out of the world's consumption of traditional energy in 1978. India and Nigeria consumed 1.3 EJ and 0.7 EJ respectively of fuelwood in 1977 ["Energy strategies for developing nations", John Hopkins University Press, London, 1st Edition, 175 (1981)]. Currently, the U.S.A. derives 2 to 2.5 per cent of its energy requirements from wood.

Table (1.1) gives the annual percentage growth of commercial energy consumption for the industrialised and developing nations between 1960 and 1978. In 1955 and 1978 the developing countries consumed 9.5 per cent and 20.3 per cent respectively of the world's total commercial energy and their share is estimated to be about 30 per cent by the year 2000.

The developing nations have continued to derive most of their domestic and commercial energy requirements from wood. In fact, even in oil-rich Nigeria, 90 per cent or more of the people cook with wood [["Societies can no longer afford to harvest forests just for lumber or fuel", Smith, N., Worldwatch papeer-wood: an ancient fuel with a new future, Worldwatch Institute, Washington, 9 (Jan, 1981)]].

The end uses of all the primary energy available to man are for heating, cooking, lighting, transport and manufacturing. The fuel industries in the process of converting the primary energy into forms usable, for the above purposes consume about 30 per cent of the total available. That is, the effeciency of the energy industry is about 70 per cent.

1.4 THE NEED TO CONSERVE ENERGY

In the context of the current and expected development of energy demand, there are no medium-term energy-supply problems. Oil production of OPEC member countries increased in 1979 by 5 per cent over 1978, while consumption increased by only 2 per cent in the corresponding period [["OPEC oil for Western Europe", Awnis, A., The Challenge of energy-policies in the making, Edited by Khouja, M.W., Longman Group Ltd., Essex, 81 (1981)]]. However, there is a need to conserve energy.

Oil constituted 52 per cent of the world's total energy consumption in 1979. Figure (1.2) indicates that throughout the foreseeable future, fossil fuels will continue to be the world's

main energy source. Unfortunately, less fossil energy reserves are available in the industrialised parts of the world than in the developing parts. Therefore, politics are likely to continue to cause disruptions in the energy supply/demand balance. Furthermore, because fossil fuels are not renewable forms of energy the cost of winning them will increase progressively.

The world's primary energy consumption of about 265 EJ per annum arises for the most part from the utilisation of various forms of energy with differing degress of efficiency so that the energy usefully used is only a small fraction of the total consumed. For example, the efficiency of the fuel industries in the U.K. is about 70 per cent ["How we use fuels", Chapman, P., Fuel's paradise, energy options for Britain, Penguin Books, 40-57 (1979)]. The efficiency of most power stations in the United Kingdom is only 15 to 35 per cent of the thermal content of fuel used and in some installations it is even less.

The efficiency of energy usage by end users is even less than by the fuel industries. In addition, variations occur in different parts of the world. Currently, the coefficient of energy use in the developing countries is about 2; this means that for each percentage rise in economic activity there is a 2 per cent rise in energy use ["Oil and world power, Odell, P.R., Pelican Books, 6th Edition, 169 (1981)]. The value of this coefficient is high compared with that of 0.4 for the inudstrialised countries. The traditional use of wood for cooking has an efficiency of about 17 per cent ["Heat pumps: Part 1, The potential for heat pumps in India" F.A. Holland, Indian Chemical Engineer, XXI, 2, (3) (1979)].

The opportunity cost of using some forms of primary energy is another important aspect. In India the use of cow dung cakes for cooking reduces the quantity of animal waste available for use as fertilizer by about 35 per cent per annum [["An imporved solar cooker", Malhotra, K.S., Nahar, N.M. and Ramana, B.V., International Journal of Energy Research, 6, (3), 227 (July-September, 1982)]]. Worldwide, the use of livestock droppings as fuel is thought to lower grain production by some 20 million tons, enough food to nourish 100 million people. In Brazil, the programme of sugar-ethanol conversion has resulted in a shortage of fertile land needed for the production of food in the rural areas.

All the foregoing considerations indicate that the adoption of energy conservation policies has to be implemented globally. This is essential if the quality oflife which depends so much on energy is to be retained and improved.

1.5 THE MEANS TO CONSERVE ENERGY

The objects of energy conservation are to use the available resources more efficiently and to recover fundamentally unavoidable waste energy.

The key to a successful energy conservation programme is good management. This has been proved in the developed nations where the energy GDP coefficient (this measures the relationship between the rate of increase in energy use and the rate of increase in the level of economic activities) has been reduced from 0.8 before 1973 to about 0.4 in 1980 [["Oil and world power", Odell, P.R., Pelican Books,

6th Edition, 259 (1981)] through good management of their energy conservation programmes.

Fossil energy can be conserved if supplemented with other sources of energy like geothermal and solar energy. Fuelwood, being a major renewable energy source should constitute an important component of primary energy consumption in the developing countries. Wood burning is, in many cases, the most cost effective form of solar energy utilization. Compared with liquid fuel like oil, handling of wood is more expensive and boiler design more complicated. However, a good annual efficiency and economics can be obtained with careful design. The utility of wood and other cellulosic materials can be widened by converting the solids to bioliquids or biogas by fermentation. The solids can also be converted to gas by gasification.

Generally, the main cause of inefficiency in the use of high grade energy like fossil fuels is the loss of heat. This, together with the solar energy reaching the earth, means that a great deal of thermal energy is available at a comparatively low temperature with progressively less thermal energy being available at higher and more useful temperatures. Therefore, a considerable quantity of energy can be conserved by recovering the maximum possible from waste heat while the temperatures are still relatively high. For example, an annual saving of about 7,168 TJ (1 TJ = 10^{12} J) could acrue by increasing the thermal efficiency of all power stations in the U.K. by 0.1 per cent [["Energy conservation for new measures and long term strategy", Energy Paper No. 33, Department of Energy, H.M.S.O., London, 34-35 (February, 1979)]. Enormous amounts of energy can be recovered from low temperature waste heat. This can be achieved with a heat pump.

A heat pump is the only existing practical system which can raise the temperature of low grade heat energy to a more useful level using a relatively small amount of high grade energy [1]. Heat pumps are currently used in domestic and commercial applications to provide space heating and hot water. However, they have vast potential in industrial applications. Figure (1.3) shows a proposal for the integrated application of heat pumps in water conservation and the drying of agricultural products. Figure (1.4) shows a simplified heat pump for drying. Figure (1.5) shows the application of a heat pump in fractional distillation.

In Nigeria the potential for the application of heat pumps in domestic, commercial and industrial sectors is enormous. The proposal in Figure (1.3) would be useful on some of the river basins being developed in Nigeria. The Nigerian government should particularly welcome this idea to boost the production and preservation of food as a matter of immediate introduction.

	1960-65	1965-73	1960-73	1973-78
World	4.2	5.1	4.7	2.5
All industrial nations	5.0	4.7	4.9	1.5
All developing nations	-0.1	6.9	4.2	7.3

TABLE 1.1 GROWTH OF COMMERCIAL ENERGY CONSUMPTION (per cent) 1960-78.

Source: "World Energy Supplies", United Nations Publication, New York, Series Journal 19, 1950-74, and 22, 1973-78 (1975) and (1979)

[1] "The potential for heat pumps in India, Holland, F.A., Indian Chemical Engineer, 21, (2), 1-8 (April-June, 1979)".

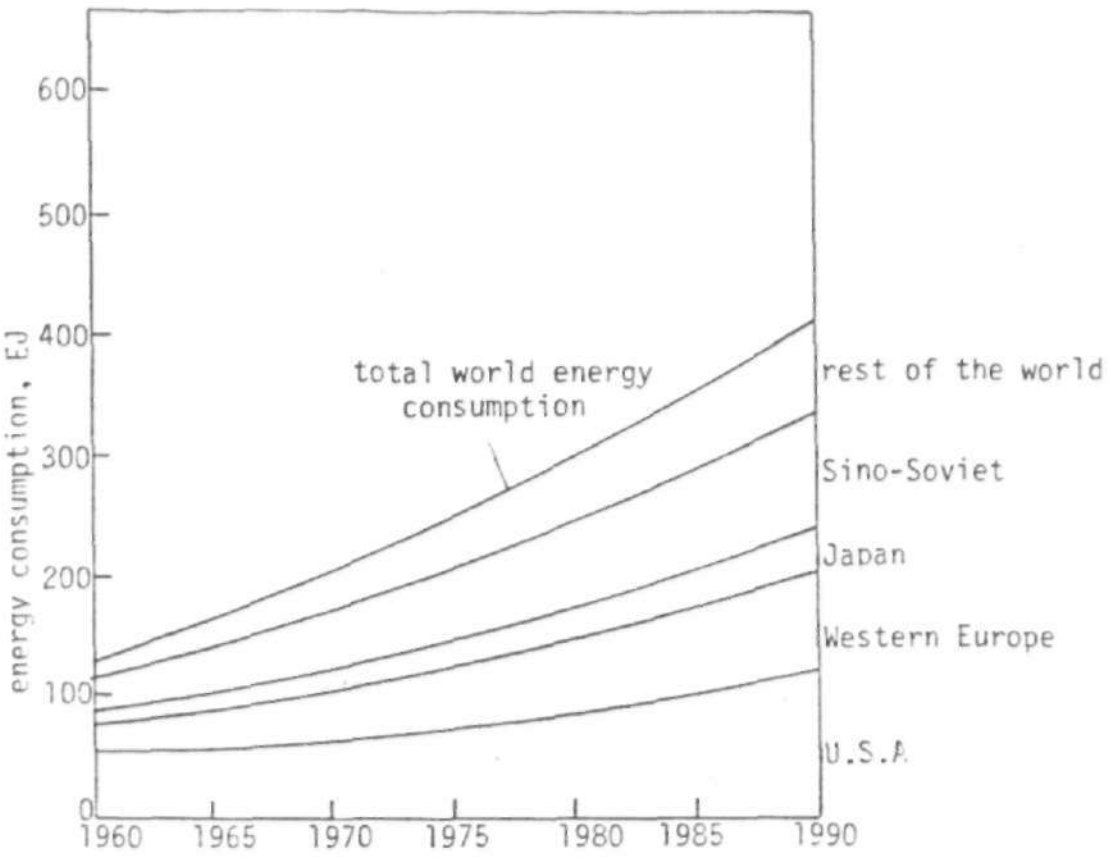


FIGURE (1.1) WORLD ENERGY CONSUMPTION BY REGION
Source: "Energy Handbook", Loftness, R.L., 183, Litton Educational Publishing, Inc., New York (1978).

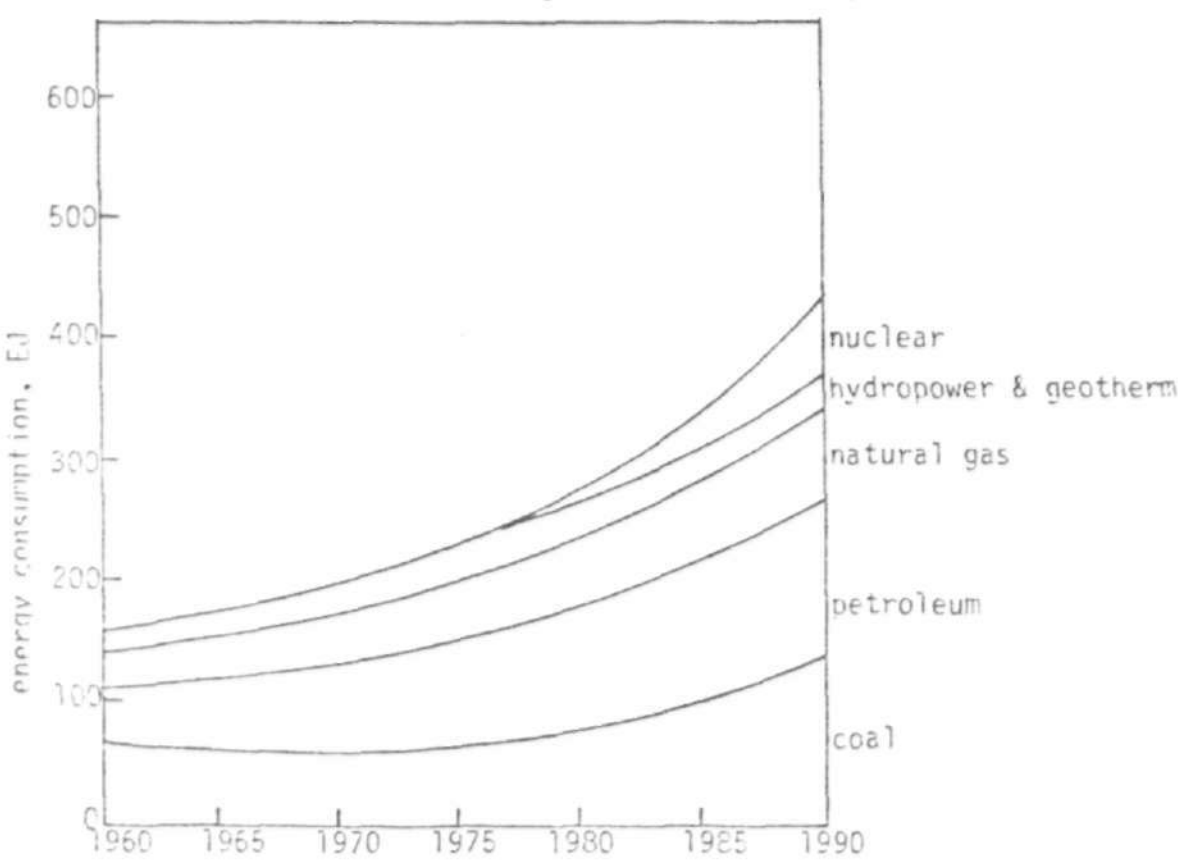


FIGURE (1.2) WORLD ENERGY CONSUMPTION BY SOURCE

Source: "Energy perspectives: a presentation of major energy and energy-related data", Hermann, E., Walter, D. and Stanley, M., U.S. Department of the Interior, Washington (Feb. 1975).

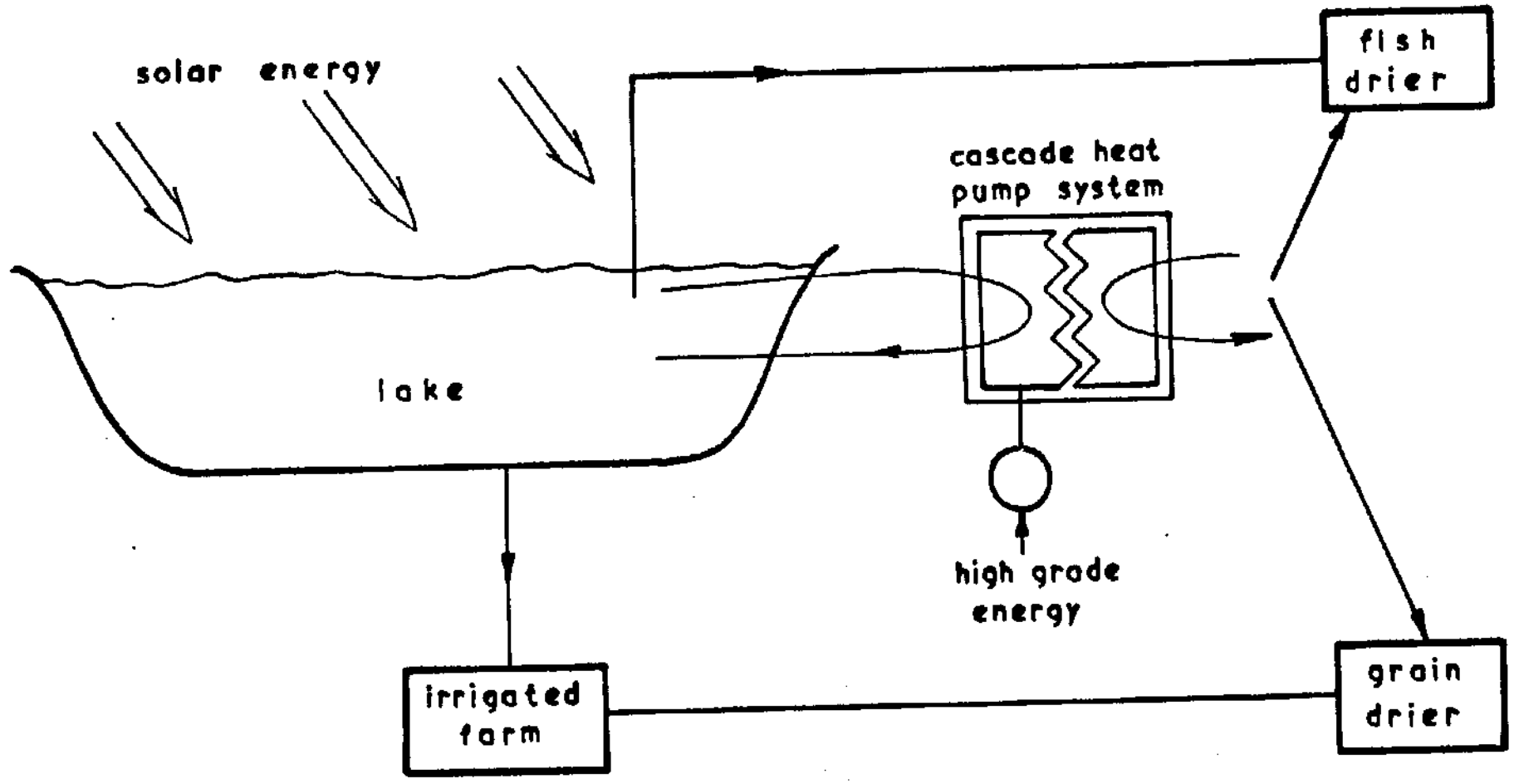


FIGURE 1.3 DOUBLE-EFFECT HEAT PUMP SYSTEM FOR COOLING AND HEATING

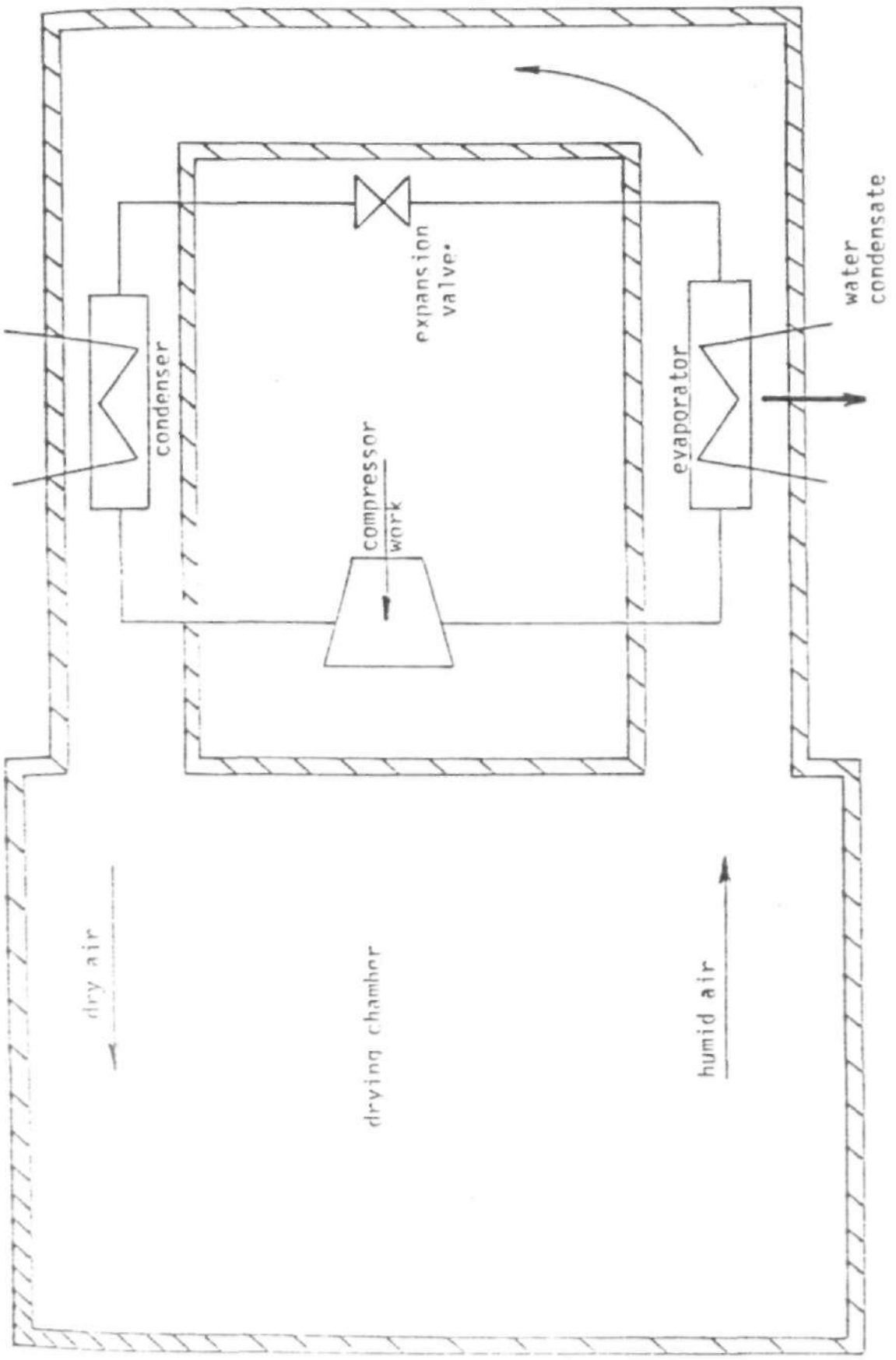


FIGURE (1.4) DRYER AND HEAT PUMP SYSTEM

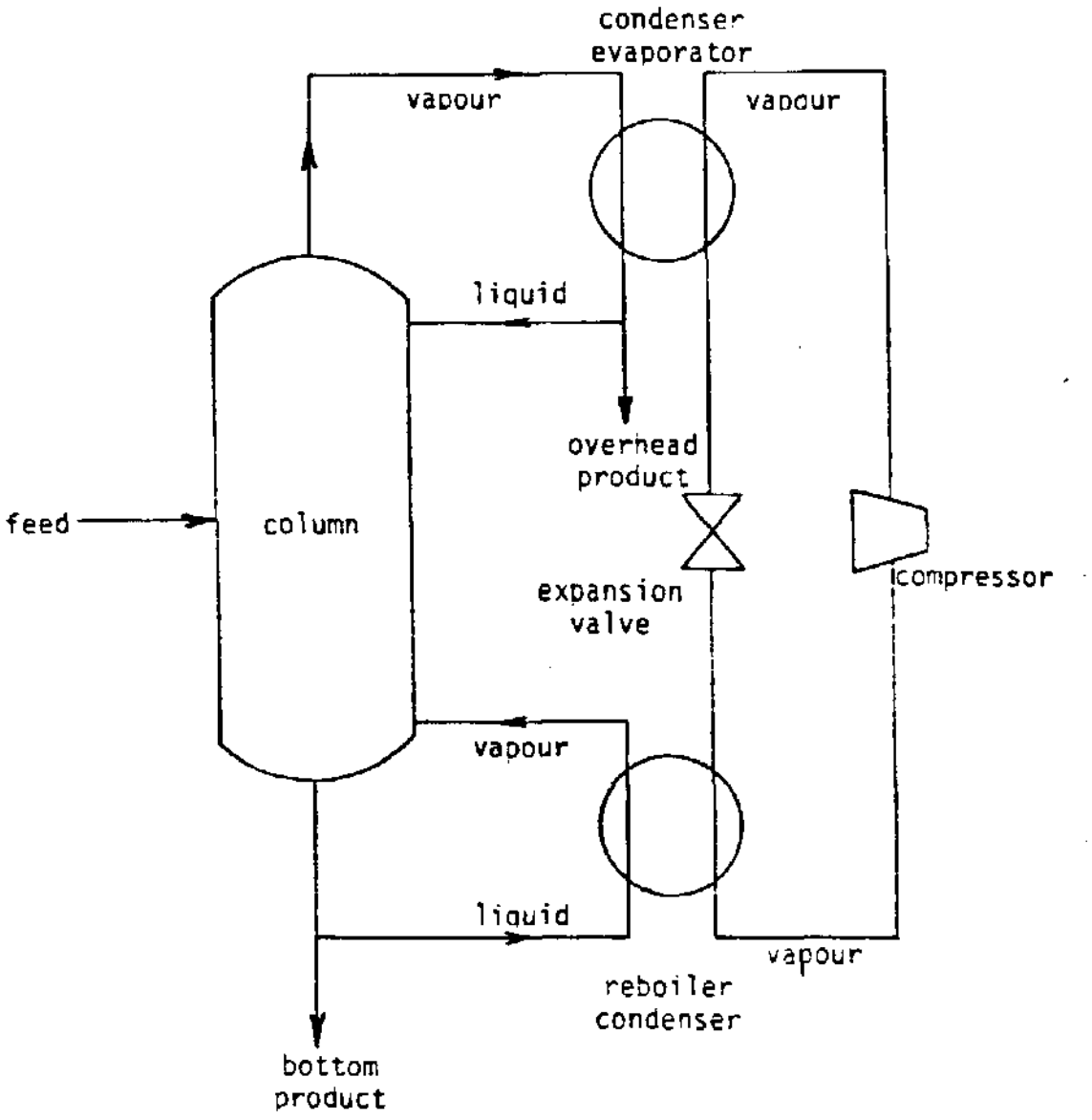


FIGURE (1.5) FRACTIONATION COLUMN WITH HEAT PUMP

CHAPTER 2

RESEARCH OBJECTIVE

CHAPTER 2

RESEARCH OBJECTIVE

The objective of this study was to obtain performance data on high temperature heat pump systems.

An evaluation of a number of potentially suitable compounds showed that water possesses the most attractive thermodynamic properties in the range 100-300^{o}C. Moreover it is chemically stable and it is cheap.

Based on the thermodynamic properties of water, it can be used as a working fluid in heat pumps to deliver temperatures up to 300^{o}C. The requirement in industry for temperatures in this range is enormous. About 20 per cent of industrial process heat in the developed nations is used at temperatures between 100 and 300^{o}C.

In order that the results from this study should be universally useful for the design of high temperature heat pump systems, it was decided to use another high temperature working fluid in addition to water. Trichlorotrifluoroethane (R113) was selected for this purpose because it is a thermodynamically attractive working fluid for delivering heat at temperatures in the range 70-150^{o}C in heat pump systems. In the Department of Chemical Engineering, University of Salford, heat pump systems have been developed to deliver low and medium temperatures. The ranges of temperatures produced and the working fluids used are presented in Table (2.1). Vapour compression heat pump systems were used. On the basis of the results from Salford and the consciousness of the need in industry for heat in the

temperature range 100-300°C, Holland ["Heat pumps, energy savers for the process industries", Holland, F.A., Symposium Papers (3), Institution of Chemical Engineers, North Western Branch, (3), 1.1-1.15 (7/8 April, 1981)] proposed a three stage heat pump system. He suggested an absorption heat pump as the third stage of the cascade

Working fluid	Maximum delivery temperature	Source-sink
R12	70°C	water-water
R22	70°C	water-water
R12B1	100°C	water-water sand-water
R114	125°C	water-water
R11	125°C	water-water

TABLE 2.1 WORKING FLUIDS AND MAXIMUM TEMPERATURES OBTAINED IN HEAT PUMPS AT THE DEPARTMENT OF CHEMICAL ENGINEERING, UNIVERSITY OF SALFORD, SALFORD, UK.

Adapted from ["Heat pumps, energy savers for the process industries", Holland, F.A., Symposium papers (3), Institution of Chemical Engineers, North Western Branch, (3), 1.1-1.15 (7/8 April, 1981)].

A heat pump operating with R113 as working fluid is capable of delivering heat at temperatures higher than the maximum temperatures listed in Table (2.1) but below the temperature range deliverable using R718.

An analysis of the results in the above investigations showed that the compressor is the most important apparatus in the system and that it was the major cause of inefficiency. Furthermore, inefficiencies became more significant when fluids capable of delivering heat at higher temperatures were used as working fluids in a given compressor.

It was therefore decided to investigate the performance of R718 in vapour compression and also absorption heat pump systems. A particularly important point was to do this using small units with heat delivery rates below 3kW.

The results would be a basis for the comparison of the performances of vapour compression and absorption heat pump systems for the purpose of selecting the better. Consequently, the more efficient and economic heat pump capable of delivering heat in the temperature range 100 -300^{o}C would be used in the third stage of the three stage heat pump system.

CHAPTER 3

HEAT PUMP SYSTEMS

CHAPTER 3

HEAT PUMP SYSTEMS

3.1 TYPES OF HEAT PUMPS

A heat pump is a device for raising the temperature of heat from a low grade to a more useful temperature using a relatively small quantity of high grade energy. Heat pumps may be classified into three broad groups. They are the vapour compression heat pump, the vapour sorption heat pump and the electrodynamic heat pump. Hybrids of these basic groups exist.

3.1.1 Vapour compression heat pumps

The vapour compression heat pump consists of an evaporator heat exchanger, a condenser heat exchanger, a compressor, an expansion valve and a working fluid. Figure (3.1) shows a simplified diagram of a vapour compression heat pump.

In the evaporator heat exchanger, the working fluid evaporates at a temperature T_{EV} by extracting heat from the heat source. The vapour is then compressed and gives up its latent heat at a higher temperature T_{CO} in the condenser heat exchanger. The condensed liquid is expanded through the expansion valve and is returned to the evaporator to complete the cycle.

3.1.2 Vapour sorption heat pumps

The absorption heat pump and the adsorption heat pump are the two main types of sorption heat pumps. In the absorption heat pump a working fluid combines with an absorbent in the liquid phase. In the adsorption heat pump the working fluid combines with the adsorbent which is in the solid state. If a large heat of combination is developed, in either of the two types, the system is known as a chemical heat pump. The absorption heat pump is currently more commonly exploited than the adsorption heat pump.

3.1.2.1 Absorption heat pumps

A simplified diagram of a conventional absorption heat pump is presented in Figure (3.1). In a conventional absorption heat pump, heat is released in the condenser by the working fluid, while condensing at a temperature T_{CO}. The condensed liquid passes through a pressure reducing valve into the evaporator where the working fluid evaporates at a temperature T_{EV}, as in the vapour compression heat pump. However, the compression takes place in a thermodynamic process involving the working fluid and an absorbent in the generator heat exchanger, where heat is absorbed at a temperature T_{GE}. In the absorber heat exchanger heat is released at a temperature T_{AB}. In the system $T_{GE} > T_{CO} = T_{AB} > T_{EV}$.

3.1.2.2 Derivatives of the vapour compression and the absorption heat pumps

Four derivatives of the vapour compression and the absorption heat pumps are the reversed absorption heat pump, the resorption heat pump, the absorption-resorption heat pump and the chemical heat pump. Simplified diagrams of the reversed absorption heat pump, the resorption heat pump and the absorption-resorption heat pump are presented in Figures (3.2a), (3.2b) and (3.2c) respectively.

In the reversed absorption heat pump system, the direction of flow of liquids through the system and the relative pressure levels in the heat exchangers are reversed compared with the conventional absorption heat pump system. Thus, in the reversed absorption heat pump $T_{AB} > T_{GE} = T_{EV} > T_{CO}$.

The resorption heat pump system consists of a solution circuit which is equivalent to the solution circuit of the reversed absorption heat pump system in the concentrations and pressure and temperature levels. The pure working fluid circuit is completed through a compressor as in the vapour compression heat pump. The compressed vapour is then absorbed by working fluid-poor solution in the resorber. Heat is removed from the

resorber at a temperature T_{RE}. The working fluid-rich solution from the resorber passes through an expansion valve into the desorber. It takes in heat to generate working fluid vapour at a temperature T_{DE}. Working fluid-poor solution is pumped into the resorber and the working fluid vapour passes to the compressor to complete the cycle.

The absorption-resorption heat pump consists of the equivalent of the generator-absorber solution circuit of the conventional absorption heat pump system in conjunction with the equivalent of the resorber-desorber solution circuit of the resorption heat pump system. The absorption-resorption cycle makes it possible to operate at temperatures up to the critical temperature of the working fluid.

A chemical heat pump is essentially a sorption heat pump in which the heat of sorption is significantly higher than in the heat pump systems described above. The chemical heat pumps are usually used for storing heat and are also commonly known as storage heat pumps. Since the process of heat storage is usually intermitent, chemical heat pumps are operated discontinuously unlike the heat pumps described previously. Solid as well as liquid absorbents are used in chemical heat pumps.

Currently, over 90 per cent of the heat pumps being

exploited are of the vapour compression type which includes absorption heat pump systems. There are comprehensive reports on the history and the latest developments of vapour compression heat pumps ["An investigation into the operating characteristics of water and sand source heat pump systems, El-Meniawy, S.A.K., Ph.D Thesis, University of Salford, Salford, U.K. (1981)] and ["Heat pumps for industry and commerce", one day course material, Department of Chemical Engineering, University of Salford, Salford, U.K., (14th April, 1983)] . Such compilations on absorption heat pump systems are not available. In this section, a review of the research and development work which has been reported in the literature is presented.

3.2 LITERATURE SURVEY ON ABSORPTION HEAT PUMP SYSTEMS

In 1810 Leslie ["Professor Leslie's process for making ice", Leslie, J., Mechanics Magazine, (1) 311-314 and 322-323 (1824)] produced ice by the absorption of water vapour on to the open surface of sulphuric acid. In his apparatus, shown in Figure (3.3), sulphuric acid was placed in one container and water in the other. The containers were connected by a tube and a hand pump created vacuum in order to increase the rate of diffusion of the water vapour. If Leslie had reconcentrated the diluted acid and condensed the water vapour, he would

have produced the first continuous absorption heat pump.

By 1859, Carre ["Appreils et procedes propres a produire du froid et fabriquer de la glance", French Patent 41958 (1859)] published a report on the operation of a truly continuous absorption heat pump using ammonia as the working fluid and ammonia-water mixture as the absorbent. Carre used his system to cool water. The cycle described by Carre is still used today. However, different working fluid-absorbent combinations and modified equipment designs are employed.

A review of the literature shows that the absorption heat pump has been used predominantly for the purpose of cooling. The working fluid-absorbent combinations most commonly used were ammonia-ammonia/water and water-water/lithium bromide. The operation of an absorption heat pump for cooling using the water-water/lithium bromide system was reported in 1950 by Berestneff ["Absorption refrigeration", Berestneff, A.A., Mechanical Engineering, 72, 216-220 (March 1950)]. Currently, working fluids like fluorocarbons and alcohols are used. Other absorbents ranging from liquids such as the dimethylether of tetraethylene glycol(DMETEG) to solids such as $LiNO_3$ are being used.

Notable researchers in the field of absorption heat pumps for cooling between 1940 and 1960 were Hainsworth,

Buffington and Ellington. Recently, significant research contributions have been made by Uemura (Japan), Albright (U.S.A.) and Grossman (U.S.S.R.).

Currently, absorption heat pump systems for cooling are available for domestic, commercial and industrial applications. They are available both as single stage and multi stage units. A typical coefficient of performance for an absorption cooling system is 0.7. They are available for cooling at temperatures as low as -60°C.

3.2.1 Theoretical reports

An absorption heat pump system for heating using a 'reversed' absorption cycle was described in 1913 and 1914 by Altenkirch ["Reversible absorption machines", Altenkirch, E., Zeitschrift Gezamte Kalteindustrie, 20, 114, 150 (1913)], ["Reversible absorption machines", Altenkirch, E., Zeitschrift Gezamte Kalteindustrie, 21, 7, 21 (1914)]. The cycle described by Altenkirch is the reversed form of the conventional cycle employed by Carre. The thermodynamics of the system presented by Altenkirch was further illuminated by Nesselmann ["The theory of heat transformers", Nesselmann, K., Wissenseh. Verroffente. Siemens-Konzern, 12, 89-109 1933)]. Their calculations were based on the ammonia-ammonia/water system for delivering heat at temperatures below 100°C.

The development of the double acting compressor by Linde in 1877 and the low cost of energy led to the decline in the number of absorption heat pump systems used, even for cooling in industry. By the 1930s, the absorption refrigerator was gradually being replaced in households by compressor-driven refrigerators using freons. The current high cost of energy coupled with the necessity and will to conserve energy has led to active interest in the development of the absorption heat pump system for heating.

In 1974, Williams and Tiedemann ["A heat pump powered by natural thermal gradients", Williams, D.A., and Tiedemann, J.T., Proceedings of the Inter-society Energy Conversion Engineering Conference 9th, California, U.S.A., 538-540 (August 1974)] showed numerically, that a three-staged reversed absorption heat pump could be used to extract heat at about 1°C from the bottom of a frozen pool of water and discharged at about 43°C for domestic heating in the Arctic region. They estimated the over-all coefficient of performance to be about 1.9 for the system using ammonia as working fluid and ammonia-water as the absorbent. The system would be totally self-powered based on the Platen-Munters cycle.

Lower ["Sorption heat pumps as heating machines", Lower, H., Klima and Kalte Inginieur, 5(12) (1977)] emphasised that the maximum obtainable (COP) in an

absorption heat pump operated in the conventional mode is 2. However, he estimated the (COP) to be between 1.3 and 1.6 for an actual machine. With this assumption, he showed numerically that for identical conditions, the absorption heat pump was better, from an energy conservation point of view, than the vapour compression heat pump. In 1981, Lower ["Technical potentiality and development of the absorption heat pump", Lower, H., Die Klima Kaelte Heizungstechnik, 9(5), 255-262 (May 1982)] reiterated the principle of the absorption heat pump with particular reference to its application for domestic heating. He stated that heat pumps have been known for a long time and have been proven practically not only as refrigerating machines, but also in earlier years, as heating units.

Jenssen and Johnston ["Some thoughts on the domestic, gas-fired heat pump", Jenssen, P.F. and Johnston, I.W., Gas Engineering and Management, 553-557 (November 1979)] showed theoretically that a gas-fired absorption heat pump with a (COP) of 1.2 would surpass its electric counterpart having a (COP) of 3.0 from an energy utilisation stand-point. These calculations were based on a delivery temperature of 60^{o}C and a gross temperature lift of 60^{o}C. Moreover, the absorption heat pump system is relatively more reliable and less noisy than the electrically driven vapour compression heat pump.

From a search of world-wide literature, Hunderman ["Heat pumps, Volume 2, 1978 - February 1980", Hunderman, A.S., NTIS/PB80 - 805815/EES, (1980)] presented abstracts of one hundred and sixty (160) references on heat pumps covering the design, performance and application of heat pumps including absorption heat pumps.

From a theoretical basis, Schmidt ["Gas heat pumps using the absorption principle", Schmidt, K., VDI-Berichte, 353, 79-86 (1980)] showed that the cost of the heat delivered by a gas-fired absorption heat pump would be half that of the same quantity of heat delivered using an electrically powered vapour compression heat pump. He gave the cost of one kilowatt of heat delivered using a three kilowatt gas-fired absorption heat pump, with a (COP) of 1.3, as US ¢0.01. The price of gas with a calorific value of 10.09kW m^{-3} was US ¢0.013 kW^{-1}. Based on the price of electricity at US ¢0.06kW^{-1}, Schmidt gave the cost of one kilowatt of heat delivered, using a three kilowatt electrically driven vapour compression heat pump with a (COP) of 3.0, as US ¢0.02.

Smith and El-Shamarka ["Absorption heat pumps for space heating", Smith, I.E. and El-Shamarka, S.E., 3rd International Conference on Future Energy Concepts, Electrical Engineers' Conference, London (192) 232-237 (1981)] reiterated the principle of the absorption heat

pump and showed that a (COP) of 2 is the maximum theoretically obtainable in a conventional absorption heat pump. However, they explained that practical aspects, coupled with thermodynamic limitations, will reduce the (COP) to values below 2. For a system using methanol as the working fluid and a mixture of lithium bromide, zinc bromide and methanol as absorbent, it was shown numerically that a practical (COP) of 1.5 may be achieved at temperature levels that are of interest for space heating purposes.

In 1982, Smith and Carey ["Thermal transformers for up-grading industrial waste heat", Smith, I.E. and Carey, C.O.B., International Symposium on the Industrial Application of Heat Pumps, Coventry, England, 251-253 (1982)] discussed the principle of the reversed absorption heat pump system and stated that it should be developed to meet the wide range of potential applications in a large market.

The interest of Nakanishi, Furukawa, Sato, Shibamoto and Baba ["Industrial high temperature heat pump", Nakanishi, T., Furukawa, T., Sato, N. and Baba, H., Hitachi Zosen Technical Review, 42(1), 7-13 (March 1981)] was directed at the development of large scale absorption heat pumps which function at temperatures ranging from 5°C to 150°C utilising waste heat from industry. They noted that since industrial waste heat is expected to be cooler in the future, the performance of heat

exchangers must be improved. They suggested that one way of achieving the improvement is to use vertical shell and tube type heat exchangers and counter current flow in both absorption and regeneration processes. The other method is to use special tubes, which will yield higher heat transfer coefficients in the absorber.

As part of a programme to produce heat at high temperatures, Holland ["What is a heat pump", Holland, F.A., Symposium Papers of the Institution of Chemical Engineers, North Western Branch, U.K., (3), 1.1-1.15 (April 1981)] discussed an absorption heat pump using water as the working fluid as the highest temperature stage of a three stage heat pump. The system is capable of raising heat from ambient temperature to about 200°C. The three stage heat pump is schematically illustrated in Figure (3.4).

Stephan and Seher ["Heating with two-stage absorption heat pumps", Stephan, K. and Seher, D., Ki Klima Kaelte Heizungstechnik, 9(9), 431-438 (September 1981)] suggested the use of a two-stage absorption heat pump where water-sodium hydroxide would be used in the high temperature stage and ammonia-water would be used in the low temperature stage. They emphasised that this would improve the heating efficiency of a single stage process by 25 per cent. Their claim is based on the higher temperature at which heat flows into the process. Their choice of working fluid-absorbent mixtures was based on the availability of sufficient information on thermal properties

and corrosion effects on the material of construction. They noted that physical and thermodynamic data were not available in the required temperature ranges for most other suitable working fluids.

In 1981, Bjurstrom and Raldow ["The absorption process for heating, cooling and energy storage - an historical survey", Bjurstrom, H. and Raldow, W., Energy Research, 5, 43-59 (1981)] presented an historical survey of the absorption process for heating, covering the period from 1810 to 1979.

Recently, Alefeld ["New approaches to energy conversion by alternative working fluids", Alefeld, G., Advances in solid state physics, Edited by Dortmund, J.T., Freudenstadt, West Germany, XVIII, 53-76 (1978)], ["Sorption processes for heat storage and heat transformation", Alefeld, G., Proceedings from the International Seminar on thermo-chemical energy storage, Stockholm. Sweden, 47-64, (1980)] and ["Energy flux and energy storage in heat transformation devices", Alefeld, G., Institution of Chemical Engineering Symposium Series, (78), P6/1-P6/13 (1982)] high-lighted the principle of absorption heat pump systems and showed their relationships to vapour compression heat pump systems. In particular, he showed that the absorption heat pump system consists of two Clausius-Rankine processes, one work producing and the other work

absorbing. The concept is shown schematically in Figure (3.5) where the components to the left hand side of the dashed lines represent the heat engine in which a Clausius-Rankine cycle takes place, and the components on the right hand side represent the heat pump in which a reverse Clausius-Rankine cycle takes place. In 1978, he showed that by incorporating a conventional absorption heat pump as the topping cycle, the efficiency of a power station can be increased from 36 per cent to 54 per cent. Figure (3.6) shows his concept schematically. In 1980, he showed that the absorption heat pump can also be used as a heat storage system when it is operated discontinuously. In 1982, he showed the scope for a wide range of combinations of vapour compression heat pump systems, absorption heat pump systems and power cycle systems to obtain desired requirements of 'heat pumping'.

3.2.2 Experimental research

In 1958, Rozenfeld and Karnaukh ["Dynamic heating by means of a reversed absorption lithium bromide machine", Rozenfeld, L.M. and Karnaukh, M.S., Journal of Technical Physics (U.S.S.R), 28(7), 1460-1465 (1958)] gave experimental results from a reversed absorption heat pump system, using water as the working fluid and water-lithium bromide as absorbent. Heat was delivered

in the temperature range 60°C to 90°C while putting in waste heat into the evaporator and generator in the temperature range 35°C to 60°C. A typical set of his results is as follows:

temperature of weak solution at absorber outlet, °C	64.5
temperature of water-poor solution at generator outlet, °C	45.0
temperature of solution at absorber inlet, °C	64.5
temperature of water at evaporator outlet, °C	45.5
temperature of water at evaporator inlet, °C	49.4
temperature of water at condenser inlet, °C	9.4
temperature of water at condenser outlet, °C	11.5
temperature of water at generator outlet, °C	48.1
temperature of water at generator inlet, °C	49.9
temperature of water at absorber inlet, °C	57.4
temperature of water at absorber outlet, °C	59.6
steam pressure in condenser, mm Hg	19
steam pressure in evaporator, mm Hg	75
concentration of water-poor solution, per cent	50.0
concentration of water-rich solution, per cent	46.2

heat loading to generator, kW	3.349
heat loading to condenser, kW	3.105
heat loading to evaporator, kW	2.593
heat loading to absorber, kW	2.628
coefficient of performance, dimensionless	0.44

The inner tubes of the generator and absorber were made of copper-nickel alloy and the cylinders of two-layer metal using stainless steel.

Boldrin, Bolzan and Lazzarin ["Lithium bromide absorption cooling devices", Boldrin, B., Bolzan. M. and Lazzarin, R., Tagunsbericht Internationales Sonneforum 2nd, Hamburg, West Germany, 127-136 (1978)] carried out tests using an absorption chiller (Yazaki WFC 400 S) with a cooling capacity of 4.5kW in the conventional heating mode. They could not exceed a temperature of 95°C for the heating fluid in the machine. It was originally designed for use with solar energy. The absorber and condenser were cooled in parallel streams. There was no solution pump in the machine and circulation was by natural convection.

A typical set of their results is as follows :

temperature of solution in the generator, ^{o}C	90
temperature of evaporating fluid, ^{o}C	13
temperature of solution in the absorber, ^{o}C	47
temperature of condensing fluid, ^{o}C	47
coefficient of performance, dimensionless	1.31

In 1979, Janben and Olert ["Development of a primary driven absorption heat pump for domestic heating", Janben, H.A. and Olert, G., New ways to save energy - Commission of the European Communities, D. Reidel Publishing Company, 198-220, (1979)] initiated studies on the mixture, R22 and the dimethyether of tetraethylene glycol (DMTEG). The intention was to develop an absorption heat pump working with the pair R22-DMTEG for the heating of individual houses. It was based on the following specifications:

i) the heat source was the ambient or ground water,

ii) gas or fuel oil burned was to supply heat,

iii) heating was done with hot water,

iv) the heating power was 12kW for an external temperature of -2°C to increase the water temperature to 55°C,

v) the pump was also equipped with a special line so that a generator can be used as a conventional boiler when the external temperature was below the one in the design.

They obtained a coefficient of performance of 1.26 based on the ambient air temperature characteristics of an average heating period in the area of Hamburg, West Germany. Commercially availabe and low-price components were used for the construction of the prototype except for the pressurised generator boiler which was specially fabricated.

A large reversed absorption heat pump was studied by Cohen, Salvat and Rojey ["A new absorption-cycle process for up-grading waste heat", Cohen, G., Salvat, J. and Rojey, A., Proceedings of the 14th Inter-society Energy Conversion Engineering Conference, Boston, U.S.A., 2, 1720-1724 (1979)], ["Absorption heat pump developments", Cohen, G., Salvat, J. and Rojey, A., International Advanced Course On Heat Pump Fundamentals, Espinho, Portugal, (NATO Advanced Study Institutes Programme) (September 1980)] using mixtures of ammonia and water to produce heat at temperature up to 180°C. A typical set

of results obtained with the system is as follows :

heat recovered, MW	17.5
heat upgraded, MW	7.1
temperature of recovered heat, ^{o}C	105 - 140
temperature of upgraded heat, ^{o}C	152
coefficient of performance, dimensionless	0.402

The machine was code named 'IFP Thermosorb".
Figure (3.7) is a block diagram of the IFP Thermosorb process. Referring to Figure (3.7), the units A and S were incorporated into the system to enable irreversibility to be reduced as much as possible. The internal recycling heat exchanges occuring in unit EEX were reported to be optimised. Furthermore, an auxiliary desorption fluid was reported to have been used to enable the cycle to operate satisfactorily even with very low grade heat.

It was claimed that the system could produce heat at temperatures up to 220^{o}C. The target capacity was 10MW.

The results on the application of the IFP Thermosorb for heat recovery from a styrene production unit and from a cyclohexane production unit showed that the pay-back periods for the total installations would

be 2.1 and 4.5 years respectively in 1979.

Recently, Siddig Mohammed, Watson and Holland ["A study of the operating characteristics of a reversed absorption heat pump (heat transformer)", Siddig-Mohammed, B.E., Watson, F.A. and Holland, F.A., Transactions of the Institution of Chemical Engineers, Paper accepted for publication] carried out investigations on a reversed absorption heat pump using water as the working fluid and three types of absorbent mixtures. The absorbents were water-lithium bromide (H_2O-LiBr), water-calcium chloride (H_2O-$CaCl_2$) and water-lithium chloride/calcium chloride (H_2O-LiCl/$CaCl_2$) (30:100 wt/wt ratio of lithium chloride to calcium chloride). Their results showed that the performances of the water-lithium bromide mixture and the water-lithium chloride/Calcium chloride were comparable. The performance of the water-calcium chloride mixture was limited by relatively low solubility. Typical results are given below:

absorbent	absorber temperature (°C)	gross temperature lift (°C)	(COP)
H_2O-LiBr	119	37.9	0.257
H_2O-LiCl/$CaCl_2$	131.5	40.4	0.239
H_2O-$CaCl_2$	104.8	22.3	0.223

They noted that lithium chloride and calcium chloride are

cheaper than lithium bromide. Based on this observation and their results they recommended the use of water-lithium chloride/calcium chloride absorbent for use in reversed absorption heat pump systems.

The studies by Radermacher and Alefeld ["Working fluid combinations for absorption heat pumps", Radermacher, R. and Alefeld, G., Proceedings from the International Seminar on Thermo-chemical Energy Storage", Stockholm, 314-347 (1980)] on the formulation of new mixtures included a consideration of multi-component systems. They suggested the use of a minimum of two absorbents, where at least one is a liquid, in combination with a working fluid. This has two advantages over the binary system. Firstly, in the multi-component system, the temperature at which crystallisation occurs due to complete degassing of the solution is pushed upwards. Secondly, even if complete degassing occurs, the liquid absorbent would keep the other absorbent(s) in the solution. Their experimental results for the vapour pressure of ammonia-water and ammonia-water-lithium bromide solutions are reproduced in Figure (3.8). Referring to Figure (3.8), they showed that at a pressure of 20 bar and a temperature of 160^{o}C, the water content in the ammonia-water vapour is reduced from 0.18 to 0.07 by using the lithium bromide solution as absorbent

rather than water alone. This reduced water content in the vapour would have an additional advantage of reducing the size of the rectifier. They presented similar diagrams for methylamine-water and methylamine-water-lithium bromide solutions.

In addition to the above, Radermacher and Alefeld have mentioned mixtures of two working fluids, whose vapour line do not differ strongly. They pointed out that such mixtures would bring about reduced irreversibilities in the condenser and evaporator by yielding varying temperatures at constant pressure. This would yield higher (COP) values. The idea of using such working fluids is well established in vapour compression heat pumps ["Significance of the non-azeotropic binary refrigerants when used in heat pumps for refrigeration plants", Kruse, H., and Jacob, R., Klima Kälte Inginieur, 7(8), 253 (1977)].

Smith and El-Shamarka ["Absorption heat pumps for space heating", Smith, I.E. and El-Shamarka, S.E., 3rd International Conference on Future Energy Concepts, Electrical Engineers' Conference, (192), 232-237 (1981)] published the physical and thermal properties of methanol-lithium bromide/zinc bromide solutions (lithium bromide and zinc bromide were in the molar ratio 2:1).

The measurements were carried out over the temperature range 17°C to 120°C. The data are useful for the design of absorption heat pumps using methanol-lithium bromide/zinc bromide solutions in this temperature range.

3.2.3 Installed heat pumps

Niebergall ["Die absorptions-kalteanlagen in der braueritechnik", Niebergall, W., Die Kälte, 4, 237 (1951)] reported that the heat pumped from the storage premises in a brewery was used to provide hot water. Similarly, some attempts have been made to adapt absorption heat pumps to residential heating. ["Absorptionsheizanlagen", Niebergall, W., Kaltechnik, 9, 239 (1957)].

In 1977, Sarkes, Nicholis and Menzer ["Gas-fired heat pumps: emerging technology, Sarkes, L.A., Nicholis, J.A. and Menzer, M.S., ASHRAE Journal, 19(3), S.36-41 (1977)] reported that prototypes of an absorption heat pump with an organic working fluid-absorbent combination were already in use in the U.S.A.

A report in the literature ["An absorption heat pump heats the federal criminal court building, Anonymous, Sanitaere und Heizung Technologie, 46(3), 308-310 (March 1981)] shows that the largest absorption

heat pump installation in West Germany began operation in 1980. It was located in the re-built Federal Criminal Court in Meckenheim. It was driven by a gas motor and used the ground around the building as the heat source. The heat was collected with a 12km plastic piping through which brine was circulated. A $40m^3$ buffer heat store was incorporated for the low load periods. An electric boiler was used to cover peak loads when out-door temperatures dropped below $0^{o}C$.

The coefficient of performance was 1.3. It was claimed that the system had approximately 100 per cent higher output than a conventional boiler installation which operated with an annual efficiency of between 0.6 and 0.7.

Cohen, Salvat and Rojey ["Personal communication from Allied Chemical, Cohen, G., Salvat, J. and Rojey, A., International Advanced Course On Heat Pump Fundamentals", Espinho, Portugal (NATO Advanced Study Institutes Programme, (September 1980)] stated that Allied Chemical, U.S.A., was developing an absorption heat pump system for both the heating and cooling of houses. It was reported that production was planned to begin in 1983. Some expected performances given

are as follows :

	heating		refrigeration
ambient temperature, ^{o}C	8.3	-8.3	35
(COP), dimensionless	1.25	1.11	0.5
capacity, kW	26.3	23.4	10.5
water temperature, ^{o}C	56	53	10
electricity consumption, kW	1.0	1.1	1.0

3.3 ABSORPTION POWER CYCLE

An absorption heat pump may be coupled to another heat pump in any of the ways discussed by Alefeld ["Energy flux and energy storage in heat transformation devices", Alefeld, G., Institution of Chemical Engineers Symposium Series, (78), P6/1-P6/13 (1982)].

The absorption power cycle was discussed by Koenemann ["A new process for energy production using binary mixtures", Koenemann, E., 2nd World Power Conference, 5(10), (1930), VDI-Verlag, (15), (1930)] using the ammonia-zinc chloride mixture.

Recently, Isshiki ["Storage and generation of power and heat by aqueous solution of salts", Isshiki, N., Proceedings from the International Seminar on Thermo-chemical Energy Storage, Stockholm, 301-339 (1980)]

operated a car with an absorption power machine. He used water-calcium chloride/lithium chloride (2:3 weight ratio) mixture at 150°C. The machine, which Isshiki named "Concentration Difference Energy (CDE)", is schematically shown in Figure (3.9).

3.4 WORKING FLUID-ABSORBENT MIXTURES FOR ABSORPTION HEAT PUMPS

The thermodynamic, kinetic and thermophysical properties of absorbent mixtures and working fluids are critical in the design and evaluation of absorption heat pumps.

Fundamental and empirical information on solutions can be found in the literature. A detailed review of the subject is not given in this thesis. However, the basics of the nature of the forces between the component compounds in solutions are presented. They help to explain the non-ideal behaviour of mixtures.

The forces involved are:

i) primary forces and
ii) secondary forces.

Primary forces are those which hold atoms together in molecules (covalency) and the oppositely charged ions

in crystalline salts (electrovalency). A convenient measure of these forces is the total energy required to dissociate all the molecules in one mole of the substance into neutral atoms.

Secondary forces are those which operate between molecules which are 'saturated' so far as primary forces are concerned. A measure of these forces is the latent heat of vaporisation of the liquids.

There are four types of secondary attractive forces. They are :

i) dipole-dipole forces,
ii) dipole-induced dipole forces,
iii) dispersion forces, and
iv) hydrogen bonds.

Dipole-dipole forces arise between molecules if the distribution of charge over the molecules lacks symmetry in such a way that they become polar.

A dipole-induced dipole force operates between a polar molecule and any other molecule whether polar or not.

A dispersion force is due to the transient dipole moment created in a molecule. The dipole moment results from the relative motion of the electrons to the atomic

nuclei in a molecule.

A hydrogen bond is the interaction between molecule A-H (where H is hydrogen) and a second atom or molecule.

Repulsive forces must oppose attractive forces between atoms and molecules. Otherwise, matter would collapse. Repulsion arises when the electron-cloud round any atom is pushed up against the clouds round other atoms or molecules. The actual equilibrium positions of the atoms in stable molecular situations depend on a balance of attractive and repulsive forces.

Solution theories which describe non-ideality in terms of the forces described have been developed by Hildebrand, Prausnitz and Scott ["Regular and related solutions", Hildebrand, J.H., Prausnitz, J.M., and Scott, P.L., Van Nostrand Reinhold Company, New York, (1970)], and Coetzee and Ritchie ["Solute-solvent interactions", Coetzee,J.F., and Ritchie,E.,Marcel Dekker, Inc., New York,(1976)]

Solution theories provide a frame-work for correlating data in a useful way. The theories have proved successful for predicting the behaviour of two or more component systems for gas and liquid mixtures. The works conducted by Zellhoefer, Copley and Marvel

["Hydrogen bonds involving the C-H link", Zellhoefer, G.F., Copley, M.J. and Marvel, C.S., Journal of American Chemical Society, 60, 1337-1343 (1938)] and ["Hydrogen bonds involving the C-H link. IV. The effect of solvent association on solubility", Copley, M.J., Zellhoefer, G.F. and Marvel, C.S., Journal of American Chemical Society, 60, 2666-2673 (1938)] showed the effect of hydrogen bonds in suitable pairs of fluorocarbon polar solvents.

In the light of the foregoing, the required thermodynamic characteristics of working fluid-absorbent mixtures are discussed. Kinetic, thermophysical and other parameters are also considered.

A list of references from the literature containing thermodynamics, thermophysical and other parameters are presented. Many of the data were conceived for absorption cooling systems. However, they can be extrapolated to design or evaluate absorption heat pumps.

3.4.1 Characteristics of working fluids and absorbent mixtures

The working fluid, absorbent and the mixture of the two in an absorption heat pump, should possess certain thermodynamic, thermophysical and chemical characteristics which make them economical and safe to use within the required temperature.

The working fluid in an absorption heat pump undergoes a cyclic process of evaporation and condensation. This is similar to that in the mechanical vapour compression heat pump system. The requisite characteristics for the selection of working fluids in both types of heat pumps should be similar. A comprehensive presentation of these characteristics for mechanical vapour compression heat pumps was recently made available in a one-day course, held at the University of Salford, U.K. ["Heat pumps for industry and commerce", one day course material, Department of Chemical Engineering, University of Salford, Salford, U.K., (14th April 1983)].

3.4.1.1 Thermodynamic characteristics

The solubility of the absorbent in the working fluid, over the required temperature range, should be very high since the absorption heat pump cycles work on the phenomenon of dissolution. The implications of this are extensive.

When dissolution takes place, molecules or ions of the solute (absorbent in this case) are broken apart and solvated. Solubility increases as the heat of solvation exceeds the heat of dissociation of the solute. Since solids have high inter-molecular molecules, they could be expected to absorb large quantities of working

fluid at conditions under which they are deliquiscent to form solutions.

When using solid absorbents, the crystallisation limit of the working fluid-absorbent mixture should lie at the highest possible temperature. Invariably, this occurs when the heat of mixing is high. A high heat of mixing increases the quantity of heat delivered per unit volume of vapour. Furthermore, good separation of the mixture is achieved when the fraction of volatiles in the solution is high.

The solubility of solids in liquids, however, can not be readily predicted, but some approximations may be made on the basis of thermodynamics. If only pure solid solute separates out at saturation, the solubility of a solid solute should obey the following relationship. ["Regular and related solutions", Hildebrand, J.H., Prausnitz, J.M. and Scott, P.L., Van Nostrand Reinhold Company, New York, 22 (1970)]

$$\ln a_S = -\frac{(\Delta H_m)_f}{R}\left(\frac{T_m - T}{T_m T}\right) + \frac{\Delta C_p}{R}\left(\frac{T_m - T}{T}\right) - \frac{\Delta C_p}{R}\ln(T_m/T) \quad (3.1)$$

where

$$\Delta C_p = (C_p)_\ell - (C_p)_S$$

(ΔH_m) is the heat of fusion at the melting point (T_m)

and

a_S is the activity of the solute.

Solute with low melting points exhibit high solubilities and thus produce maximum heats of mixing and lowering of the vapour pressure. It is always preferable to obtain data experimentally from laboratory and pilot plants.

On a temperature-concentration diagram, it is desirable to have a working fluid saturation temperature curve which is flat up to a concentration near to $(X_W)_{GE}$ $\left[(X_W)_{GE}\right.$ is the fraction of working fluid-poor solution in the generator$\left.\right]$ and then steep as in Figure (3.10). The solution saturation temperature curve should be as straight as possible because the concentration width $\left[(X_W)_{AB} - (X_W)_{GE}\right]$ is higher simultaneously with a good solubility of the absorbent in the working fluid.

A high concentration width implies a low circulation ratio (FR). The circulation ratio (FR) is the ratio of the mass flow rate of working fluid-rich solution to the mass flow rate of working fluid in the system. The coefficient of performance (COP) of the system increases as the value of (FR) decreases.

The vapour pressures for the mixtures should be lower than those predicted by Raoult's law. The

physical absorption and desorption of a gas or vapour is governed by the characteristic phase equilibrium of the solution at the operating temperatures. In the case of ideal binary mixtures, the vapour pressure of each component in the solution at a given temperature is given by Raoult's law and is represented by Equations (3.2) and (3.3)

$$P_W = (P_O)_W X_W \qquad (3.2)$$

$$P_O = (P_O)_S X_S \qquad (3.3)$$

where P_W and P_S are the partial pressures of the working fluid and the solute in the vapour phase and X_W and X_S are the mole fractions of the working fluid and the solute in the liquid phase, and $(P_O)_W$ and $(P_O)_S$ are the vapour pressures of the pure components at the temperature of the system.

In practice, real systems deviate from ideality and Raoult's law can be modified and written as in Equations (3.4) and (3.5)

$$P_W = \gamma_W (P_O)_W X_W \qquad (3.4)$$

$$P_S = \gamma_S (P_O)_S X_S \qquad (3.5)$$

where γ_W and γ_S are the activity coefficients of the

components in solutions at the temperature and composition of the solution.

A single stage process works at two pressures. The higher pressure is determined by the delivery temperature and the lower pressure by the heat source temperature.

A large pressure difference ΔP is disadvantageous because an expensive pump will be required. Therefore, the vapour pressure curve of the working fluid-absorbent mixture ($\ell n P$ versus $1/T$) should be as flat as possible. This is shown in Figure (3.11) by the dashed lines. For a relatively flat pressure-temperature curve, a higher delivery temperature can be achieved. However, the mixtures with relatively flat vapour pressure curves possess lower heats of vaporisation per unit mass and in most cases, lower enthalpies of mixing. This is evident from the Clausius-Clapeyron equation:

$$\lambda = (T\Delta V)\, dP/dT \approx (RT^2/MP)\, dP/dT \qquad (3.6)$$

where

M is the molecular weight of the substance.

A small value of dP/dT yields a small value of the heat of vaporisation.

The latent heat of vaporisation per unit mass of the working fluid must be as high as possible to minimise the rate of circulation of the working fluid in the system and increase the coefficient of performance. Equation (3.6) shows that a low molecular weight compound will have a high latent heat of vaporisation. However, it would also possess a low saturation temperature at a given temperature. This is demonstrated in the homologous series of organic compounds presented below:

compound	molecular weight	saturation temperature at 1 bar	latent heat of vaporisation at 1 bar
	kg kmol^{-1}	(K)	(kJ kg^{-1})
methane	16	112	510.2
ethane	30	185	489.7
propane	44	231	426.1

Some low molecular weight compounds, which are polar, may possess high saturation temperatures as well as high latent heats of vaporisation. This is shown in the following table:

compound	molecular weight kg kmol^{-1}	saturation temperature at 1 bar (K)	latent heat of vaporisation at 1 bar kJ kg^{-1}
methane	16	112	510.2
ammonia	17	240	1369
water	18	373	2256

Unfortunately, these compounds do not retain their strong interactive forces in the vapour state. They possess relatively low vapour densities. Thus, the vapour would occupy a large space per unit enthalpy. This will affect the sizes of the evaporator, generator, absorber and pipes carrying the vapour.

The absorbent must possess a low saturation pressure within the range of operating temperatures. A low vapour pressure would prevent absorbent carry-over by the regenerated working fluid vapour. Therefore, a high molecular weight is desirable for the absorbent. An absorbent which possesses extra interactive forces, due to secondary forces, tends to have a relatively high saturation temperature.

The saturation temperature difference between the absorbent and the working fluid should be greater than 200K so that no rectification is required. This value is based on experience ["Solubility of working fluid

pairs for absorption heat pump processes", Renz, M., Vulkanverlag, (1978)].

It is desirable that the pressure in the evaporator and absorber is super-atmospheric. Under sub-atmospheric conditions, contaminants such as air, water vapour etc., may leak into the system if it is not properly sealed. Such contaminants may cause corrosion of the materials of construction or degradation of the working fluid-absorbent mixture.

3.4.1.2 Kinetic characteristics

A high reaction rate is desirable so that complete absorption of vapour would take place in a short time. A short absorption time would decrease the size of the absorber. The limiting effect of the absorption of vapour in absorption systems has been emphasised by Smith and El-Shamarka ["Absorption heat pumps for space heating", Smith, I.E. and El-Shamarka, S.E., 3rd International Conference on Future Energy Concepts, Electrical Engineers' Conferences, London, (192), 232-237 (1981)].

3.4.1.3 Thermophysical properties

The working fluid and absorbent mixture should have a low viscosity and a low surface tension in order

to reduce pressure drops within the system. However, they should not be too low, for the working fluid, to inhibit drop-wise condensation which improves heat transfer.

The thermal conductivity of the working fluid and the absorbent mixture should be high to provide good heat transfer in the heat exchangers.

The velocity of sound in the vapour phase of the working fluid should be reasonably high. It sets the maximum limit for the allowable velocity of gas in the pipings or narrow parts.

3.4.1.4 Safety considerations

Ideal working fluid and absorbent mixtures should be non-flammable, non-explosive, non-corrosive, non-expensive and the detection of any leak should be easy.

The toxicity of the fluids should be so low that they would not cause adverse effects in low concentrations and during the relatively short time of exposure. The degree of toxicity is expressed by the factor, Threshold Limit Value (TLV) ["Threshold limit values for chemical substances and physical agents in work-room environment", American Conference of Government Industrial Hygienists, 1-12 (1977)]. The

range of Threshold limit values extends from 0.001ppm (most toxic) to 1000ppm (least toxic).

Comprehensive information on the safety aspects of a wide range of chemical compounds is available ["Dangerous properties of industrial material", Sax, N.I., Van Nostrand Reinhold, 5th (1979)].

3.4.1.5 Corrosivity

Fluids which are corrosive to the materials of construction should be avoided. Detailed corrosion data on materials of construction for a wide range of chemicals are also available in the literature ["Chemical Engineers' Handbook", Perry, R.H. and Chilton, C.H., McGraw-Hill Book Company, New York, 5th, 23(3), 23-27 (1973)]. In certain cases, corrosive chemicals may be used with inhibitors.

3.4.2 Physical and thermodynamic data references for working fluid-absorbent mixtures

3.4.2.1 General

For general design purposes, the properties of water-lithium bromide and ammonia-water mixtures, were

given in ASHRAE Handbook [ASHRAE Handbook and Product Directory, ASHRAE Inc., New York (1977)], Uemura ["Physical properties of refrigerant-absorbent systems for absorption refrigeration", Uemura, T., Reito, 53(600), 929-940 (1970)] has presented a review of the physical and thermodynamic properties of working fluid-absorbent mixtures that are based on water, alcohols, ammonia and freons, listing eighty references.

Data on binary and ternary mixtures have been reported by Linke and Seidell ["Solubilities of inorganic and metal organic compounds", Linke, W.F. and Seidell, A., American Chemical Society 2(4), Washington D.C. (1965)], Stephen and Stephen ["Solubilities of Inorganic and Organic Compounds", Stephen, H. and Stephen, T. 1 and 2, Pergamon Press, Oxford (1963)], Hildebrand, Praustnitz and Scott ["Regular and Related Solutions", Hildebrand, J.H., Praustnitz, J.M. and Scott, P.L., Van Nostrand Reinhold Company, New York, (1970)] and Scrosati and Vincent ["Solubility Data Series, II: Solubility of Solids in liquids", Scrosati, B. and Vincent, C.A., Pergamon Press, Oxford (1980)]. The last reference presented an abstract of experimental values, methods and apparatus, procedures and references for solubility of various salts (for example, lithium bromide, lithium chloride, lithium thiocynate, etc.) in formamide,

N-Methylformamide, N,N-Dimethylformamide, acetamide, N-Methyllacetamide and N,N-Dimethylacetamide.

3.4.2.2 Water as working fluid

Water possesses physical and thermodynamic properties which make it quite suitable as a working fluid in heat pump systems. There are many references in the literature in which the physical and thermodynamic properties of water and its mixtures with many compounds have been presented. Water-lithium bromide mixture has been studied extensively. A good summary was presented by Foote Mineral Company ["Lithium bromide", Foote Mineral Company, Technical Data Bulletin, 145, Exton, Pa. (1934)]. McNeely ["Thermodynamic properties of aqueous solutions of lithium bromide", McNeely, L.A., ASHRAE Transactions, 85(1), 413-434 (1979)] presented a review of experimental data (physical and thermal) for this system and in most cases, the data were reduced to equations for use in computer programme. Other sources of data are those of Pennington ["How to find accurate vapour pressure of LiBr-water solutions", Pennington, W., Refrigerating Engineering, 57-61 (May 1955)], Kessis ["Le systeme eau-bromide de lithium", Kessis, J.J., Bulletin Societe Chemique, 7, 48-52 (1965)], Boryta ["Solubility of lithium bromide in water between -50°C and 100°C (45 to 50 per cent lithium bromide), Boryta, D.A., Journal of Chemical Engineering Data, 15(1), 142-144 (1970)],

Boryta, Maas and Grant ["Vapour pressure-temperature-concentration relationship for system lithium bromide and water (40 to 70 per cent, lithium bromide", Journal of Chemical Engineering Data, 20(3), 316-319 (1975)], Usyukin ["Thermodynamic diagrams of solution lithium bromide-water", Usyukin, I.P., Kholodilnaya Technika, 46(1), 25-29 (1969)], Schwartz and Lange ["Losung-und Verdunnungswarmer von Salzen von der Aussersten Verdunnung bis zur Sattigung", Schwartz, F. and Lange, E., Zeitschrift fur Physikalische Chemie, 133, 129-149 (1928)], Lower ["Thermodynamische Eigenschaften und Warmediagramme des binaren systems lithium bromide-Wasser", Lower, H., Kaltetechnik, 13(5) 178-184 (1961)] and Uemura and Hasaba ["Studies on the lithium bromide-water absorption refrigerating machine", Uemura, T. and Hasaba, S., Technological Reports of Kansai University, 6(6), 31-55 (1964)].

The solubility of lithium chloride in water has been investigated by Schimmel ["Solubilities of lithium chloride and lithium thiocynate at low temperature", Schimmel, F.A., Journal of Chemical Engineering Data, 5(4), 519-520 (1960)], Gibbard and Scatchard ["Liquid vapour equilibrium of aqueous lithium chloride from 25°C to 100°C and from 1.0 to 18.5 molal, and related properties", Gibbard, H.F. and Scatchard, G., Journal of Chemical Engineering Data, 18(3), 293-297 (1973)]. Bogatykh and Evnovich

["Investigations of densities of aqueous lithium bromide, lithium chloride and calcium chloride solutions in relation to conditions of gas drying", Bogatykh, S.A. and Evnovich, I.D., Journal of the Applied Chemistry of the U.S.S.R., 38(4), 932-933 (1965)], ["A study of the viscosities of aqueous solutions of lithium chloride, lithium bromide and calcium chloride applied to the normal drying of gases", Bogatykh, S.A. and Evnovich, I.D., Journal of the Applied Chemistry of the U.S.S.R., 36(8), 1808-1809 (1963)] published experimental data of the viscosity and density of aqueous solutions of lithium bromide and lithium chloride. The solubility of lithium iodide in water was reported by Bach and Boardman ["Vapour pressure of aqueous lithium iodide solutions", Bach, R.O. and Boardman, W.W., ASHRAE Journal, 9(11), 33-36 (1967)]. Phase diagrams for aqueous solutions of lithium chloride and calcium chloride have been investigated by Khandurdyer and Daikhanov ["Phase diagram for lithium chloride and calcium chloride aqueous solutions", Khandurdyer, A. and Daikhanov, S., Izvestia Akademie Nauk Turkmenskot U.S.S.R. Seriya, Fiziko - Tekhnicheskik Khimicheskikh Geologicheskikh Nauk, 5, 41-44 (1977)]. The vapour pressure of mixtures of three compounds, water-lithium bromide-lithium thiocynate and water-lithium bromide-Cesium bromide were reported by Macriss and Rush

["Lithium bromide-lithium thiocynate-water composition for an absorbent-refrigeration system", Macriss, R.A. and Rush, W.F., U.S. 3,541,013, (November 17, 1970)]. The vapour pressure of the mixtures of water-lithium bromide-lithium iodide were obtained by Hensel and Harlowe ["Lithium bromide-lithium iodide composition for absorption refrigeration system", Hensel, W.E. and Harlowe, W.W., U.S. 3,524,815, (August 18, 1970)].

3.4.2.3. Alcohols as working fluids

Methanol and ethanol, like water and ammonia, possess relatively attractive thermodynamic properties for use as working fluids in absorption heat pump systems. Reliable research works in the use of alcohols have been done by Uemura (Japan), Albright (U.S.A) and Grosman (U.S.S.R.).

Densities and viscosities of methanol-lithium bromide solutions were reported by Grosman ["Properties of solution of methanol and lithium bromide studied as working susbtances of absorption refrigeration machines", Grosman, E.R., Kholodilnaya Tecknika Tekhnologika, 11, 84-86 (1971)]. Thermodynamic properties were also reported by Grosman ["Temperature-pressure diagramm for methanol-lithium bromide solutions", Grosman, E.R., Zhuravlenko, V. Ya., Kholodilnaya Tekhnika, 46(11), 40-42 (1969)]. The

vapour pressure of mixtures of methanol and ethanol on lithium bromide and zinc bromide salts have been presented by Aker, Squires and Albright ["An evaluation of alcohol-salt mixtures as absorption refrigeration solution", Aker, J.E., Squires, R.G. and Albright, L.F., AHSRAE Journal, 7, 90-92 (1965)]. Physical and thermal properties of methanol-zinc bromide as well as methanol lithium bromide-zinc bromide and methanol-lithium bromide systems, were determined by Uemura ["Studies on the methanol-zinc bromide refrigerating machine", Uemura, T., Reito, 51, 1027-1036, (1976)] and ["Methanol-lithium iodide-zinc bromide absorption refrigerating machine", Uemura, T., Reito, 50(568) 95-101 (1975)].

3.4.2.4 Ammonia based compounds as working fluids

Physical and thermodynamic properties for the solutions of ammonia-water were presented by Perry et al ["Chemical Engineers' Handbook', 4th Edition, Perry, R.H., Chilton, C.H. and Kirkpatrick, S.D., McGraw-Hill, New York, (1969)]. Robertson, Lee, Squires and Albright ["Vapour pressure of ammonia and methylamines in solutions for absorption refrigeration systems", Robertson, J.P., Lee Ch. Y., Squires, R.G. and Albright, L.F., ASHRAE Transactions, 72(1), 198-208 (1966)] have measured the vapour pressures of

ammonia-organic solvents, ammonia-salts and methylamine-organic solvents. Their results clearly indicate that these combinations are of interest for absorption refrigeration systems. Furthermore, Blytas and Daniels ["Concentrated solutions of sodium thiocynate in ammonia: solubility, density, vapour pressure, viscosity, thermal conductance, heat of solution and heat capacity", Blytas, G.C., and Daniels, F., Journal of American Chemical Society, 84(7), 1075-1083 (1962)] reported experimental values for ammonia-sodium thiocynate mixture. This mixture was strongly recommended for use in absorption refrigeration by George and Birkett ["A study of liquid ammonia-salt system and their potential application in the absorption cooling process", George, J.H.B. and Birkett, J.D., Projects ZF-72 and 72(a), Library of Congress, No. 65-19567 (1965)].

Data on viscosities for aqueous ammonia and liquid ammonia and on description of experimental apparatus, were reported by Pinevitsch ["Viscosities of ammonia-water mixtures and liquid ammonia", Pinevitsch, G., Kholodilnaya Tekhnika, 20(3), 30-37 (1948)]. Density data for ammonia were determined by Rashkovskaya and Chernenkaya ["Densities of solutions of ammonium bicarbonate, sodium bicarbonate, ammonium chloride and ammonia in the 20°C to 100°C range", Rashkovskaya, E.A. and Chernenkaya, E.I., Zh. Prik. Khim., 40(2), 301-308 (1967)] in the

temperature range of 20°C to 100°C.

3.4.2.5 Halogenated hydrocarbons as working fluids

The results of the pioneering work of Zellhoefer, Copley and Marvel ["Hydrogen bonds involving the C-H link. The solubility of halogens in donor solvents", Zellhoefer, G.F., Copley, M.J. and Marvel, C.S., Journal of American Chemical Society, 60, 1337-1343 (1938)], ["Hydrogen bonds involving the C-H link, IV. The effect of solvent association on solubility", Copley, M.J., Zellhoefer, G.F. and Marvel, C.S., Journal of American Chemical Society, 60, 2666-2673 (1938)] formed an important basis for the rationalisation of working fluids and absorbent mixtures for use in absorption processes. They showed that the molecules of the large molecular compounds they used as absorbents contained high proportions of active atoms, each of which exerts a strong attractive force for selective atoms of the molecules of the working fluids.

Results of solubility studies of binary mixtures were presented by Kribel and Loffler ["Thermodynamische eigenschaften des binären systems difluoromonochloromethan (R22)-tetraathylenglycoldimethylather (E181)", Kribel, M. and Loffler, H.J., Kaltetechnik, 17(9), 266-271 (1965)], Albright, Shannon, Terrier and

Chueh ["Solubility of chlorofluoromethanes in non-volatile polar organic solvents", Albright, L.F., Shannon, P.T., Terrier, F. and Chueh, P.L., Journal of the American Institution of Chemical Engineering, 668-672 (November 1962)] and Mastranglo ["Solubility of some chlorofluorohydrocarbons in E181", Mastranglo, S.V.R., ASHRAE Journal, 64-67 (October 1959)]. Solubility data for the system R22-Isobutyl acetate were reported by Sellerio ["Absorption kaltmachine mit isobutylazetat-R22", Sellerio, V., Kaltetechnik, 18(1), 2-3 (1966)]. Diagrams of enthalpy against concentration for the mixtures of R22-dibutylphthalate and R22-E181 have been presented by Latyschev ["Enthalpy-concentration diagrams for Freon 22-dimethyl ether of tetraethylene glycol", Latyschev, V.P., Kholodilnaya Tekhnika, 46(7), 61-62 (1969)], ["Temperature-concentration diagram for a solution of Freon 22 in dibutyl phthalate and dimethylformamide", Latyschev, V.P., Kholodilnaya Tekhnika, 47(11), 61 (November 1970)] and Seliverstov ["Enthalpy-concentration diagrams for solution Freon 22-dibutyl phthalate", Seliverstov, V.M., Kholodilnaya Tekhnika, 43(4), 36-38 (1966)], ["Solubility of Freon 22 in a mixture of dibutyl phthalate and dimethyl formamide", Seliverstov, V.M., Kholodilnaya Tekhnika, 47(11), 34-36 (November 1970)]. Thermodynamic properties for the mixture R22-dimethyl ether of tetraethylene glycol (DMETEG (E181)) were measured by Kribel and Loffler

["Thermodynamische eigenschaften des binaren systems difuoromonochloromethan R22-tetraathylen glycol-dimethylather (E181)", Kribel, M. and Loffler, H.J., Kältetechnik, 17(9), 266-271 (1965)] in order to evaluate the suitability of this mixture for absorption cooling. Furthermore, the authors presented data for enthalpy-concentration diagrams, density and vapour pressure for this mixture. Jelink, Borde and Yaron ["Enthalpy-concentration diagram of the system R22-dimethyl formamide and performance characteristics of refrigeration cycle operating with this system", Jelink, M., Borde, J. and Yaron, I., ASHRAE Transactions, 84(2), 60-67 (1978)] presented an enthalpy-concentration diagram for the system R22-dimethyl formamide (DMF). Latyschev gave a description of an experimental apparatus to measure thermal capacity and heat of mixing for R22 in dimethyl phthalate and E181 ["Experimental investigation of thermal capacity of dimethyl phthalate of tetraethylene glycol dimethyl ether and heat of their mixing", Latyschev, V.P., Kholodilnaya Tekhnika, 46(8), 31-34 (1969)].

Equations for calculating thermodynamic and thermophysical properties of halogenated hydrocarbons were described by Perelshtein and Parushin ["Method to determine the thermodynamic properties of principal coolants from experimental data", Perelshtein, I.I. and Parushin, E.B., Kholodilnaya Tekhnika (1), 27-30

(1976)] and Downing ["Refrigerant equations", Downing, R.C., ASHRAE Transactions, 80(2), 158-169 (1974)]. Ackroyd ["Refrigerants: properties, selection and hazards", Ackroyd, K., The Chemical Engineer (May 1978)] conducted a survey on the properties and selection of fluorocarbons.

3.4.2.6 Miscellaneous compounds as working fluids

Other compounds which are potentially useful as working fluids, apart from those mentioned above, have been investigated on a relatively small scale. Albright, Shannon, Yu and Chueh ["Solubility of sulphur dioxide in polar organic solvents", Albright, L.F. Shannon, P.T., Yu, S.N. and Chueh, P.L., Chemical Engineering Progress Symposium Series, 59(44), 66-74 (1963)] published results of solubility of sulphur dioxide in DMETEG, DMF and DMA. They presented diagrams for N,N-dimethyl acetamide.

Pechatnikov and D'yachenko ["Selection of thermodynamic optimum pair for hydrocarbon absorption refrigerating machines", Pechatnikov, M.Z. and D'yachenko, Yu. I., Tr. Vsesoyuznov Konf. Thermodin. Sbornik Dokladov, Sektsii Novye Tepl., 379-386 (1968)] obtained experimental results for the mixtures of

ethane-pentane and ethane-heptane . They provided enthalpy-concentration diagrams as well as state equations for calculating the thermal properties of the mixtures.

Correlations of thermophysical properties for hydrocarbons, mainly using the Soave equations ["Equilibrium constants from a modified Redlich-Kwong equation of state", Soave, G., Chemical Engineering Science, 27, 1197-1203 (1972)] have been reported by Bier and Gorenflo ["Universal representation of the thermophysical properties of boiling liquids", Bier, K. and Gorenflo, D., Bull. Inst. Int. Froid, Annexe (4), 135-141 (1973)] and Dolotov ["Method of determination of thermodynamic properties of hydrocarbons for design calculation of process in a cycle of absorption refrigeration machine", Dolotov, A.G., Kholodilnye I. Ustreistva, 116-121 (1976)].

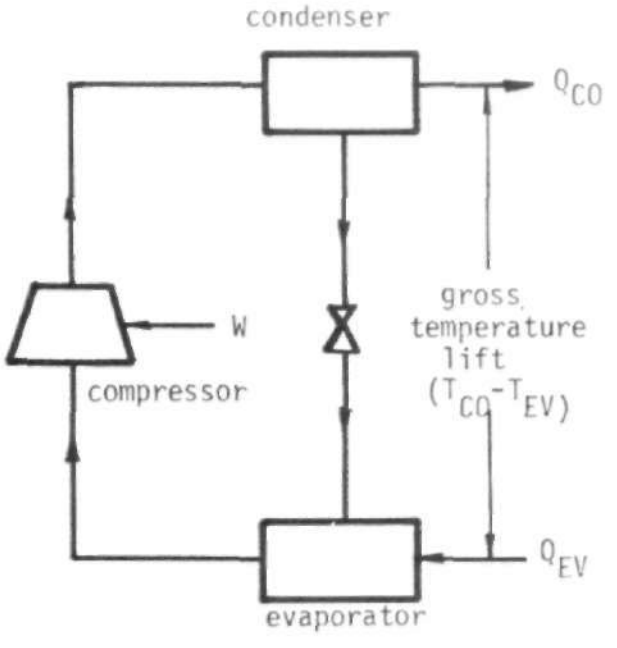


FIGURE (3.1a) MECHANICAL VAPOUR COMPRESSION HEAT PUMP

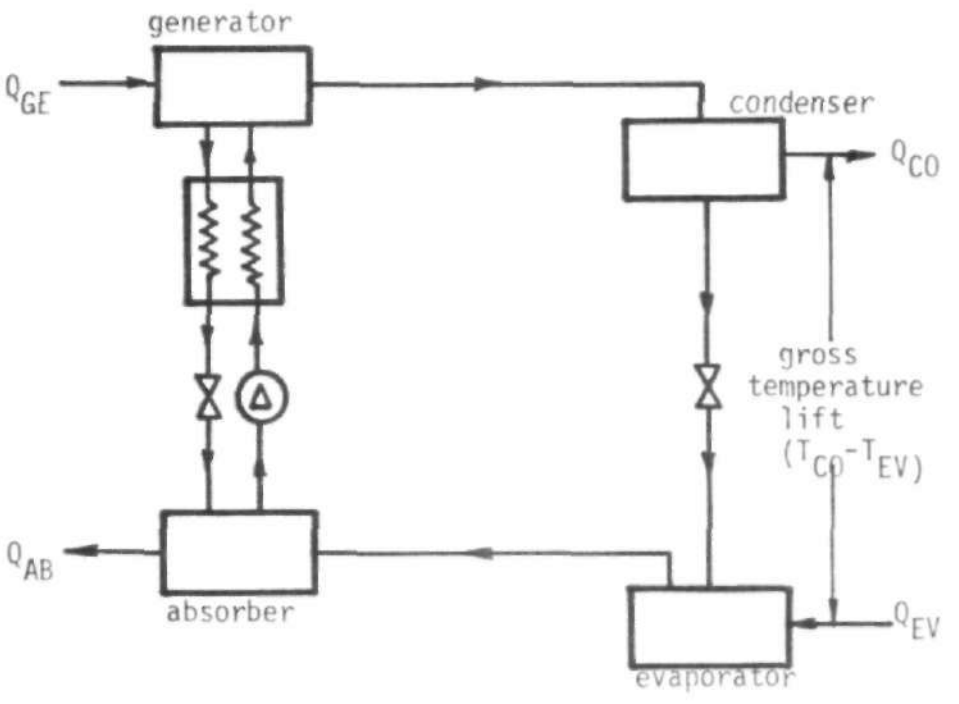


FIGURE (3.1b) CONVENTIONAL ABSORPTION HEAT PUMP

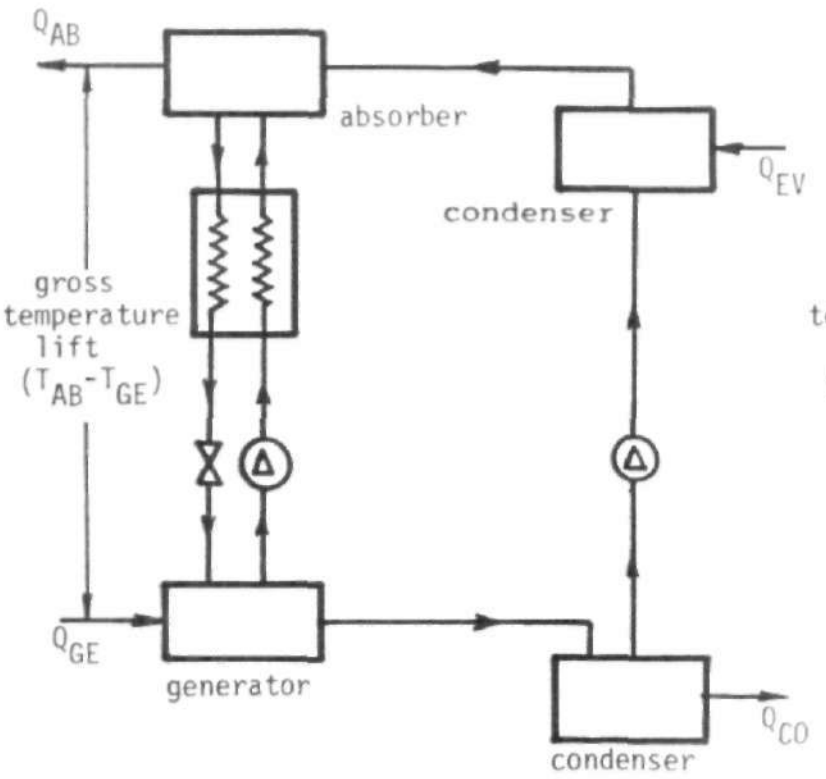


FIGURE (3.2a) REVERSED ABSORPTION HEAT PUMP

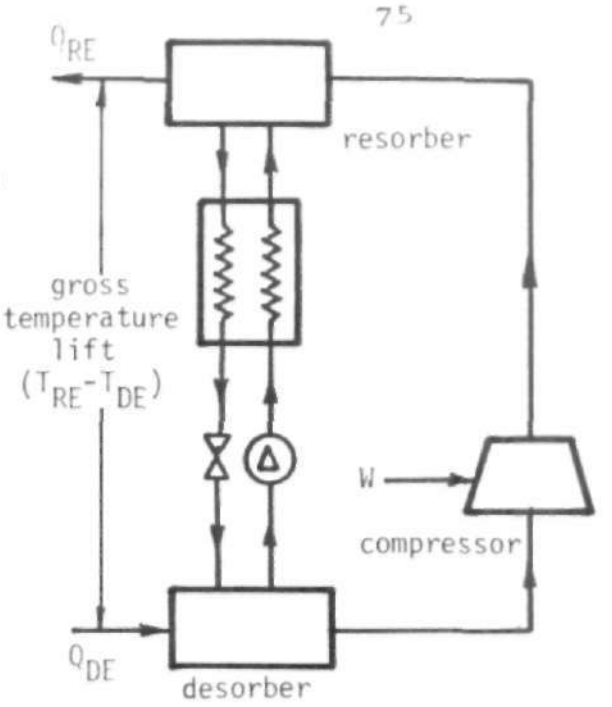


FIGURE (3.2b) RESORPTION HEAT PUMP

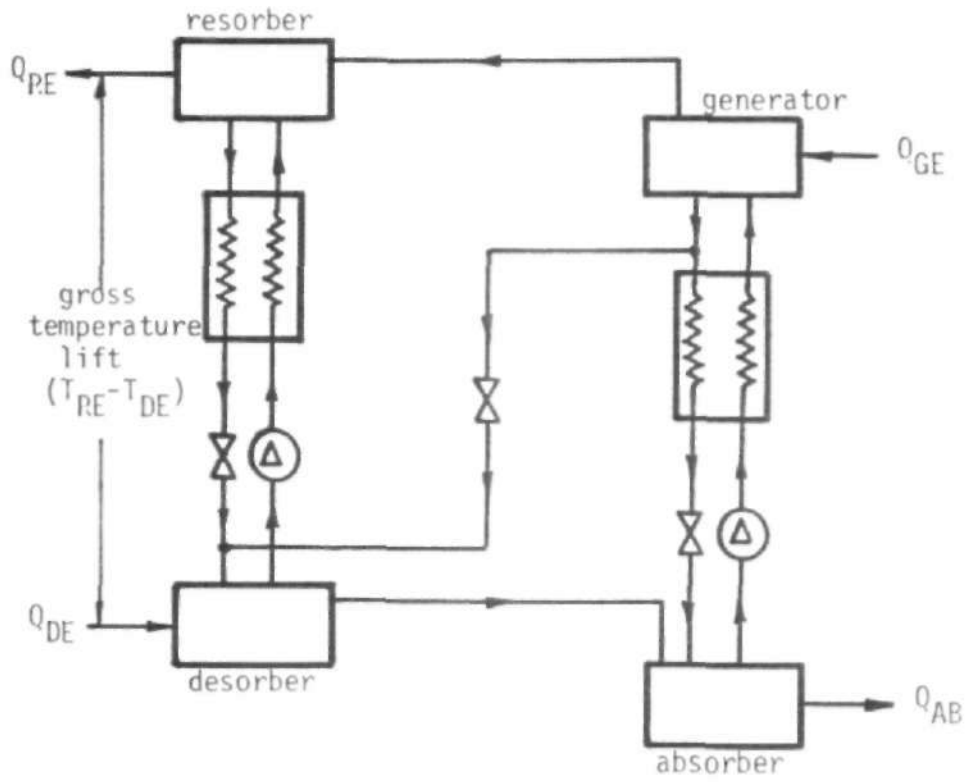


FIGURE (3.2c) ABSORPTION-RESORPTION HEAT PUMP

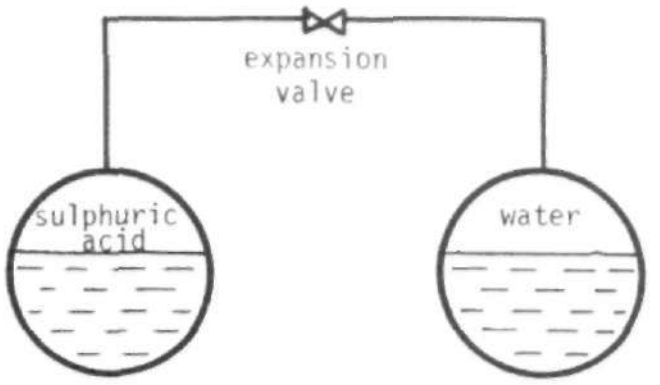


FIGURE (3.3) A PERIODIC ABSORPTION HEAT PUMP

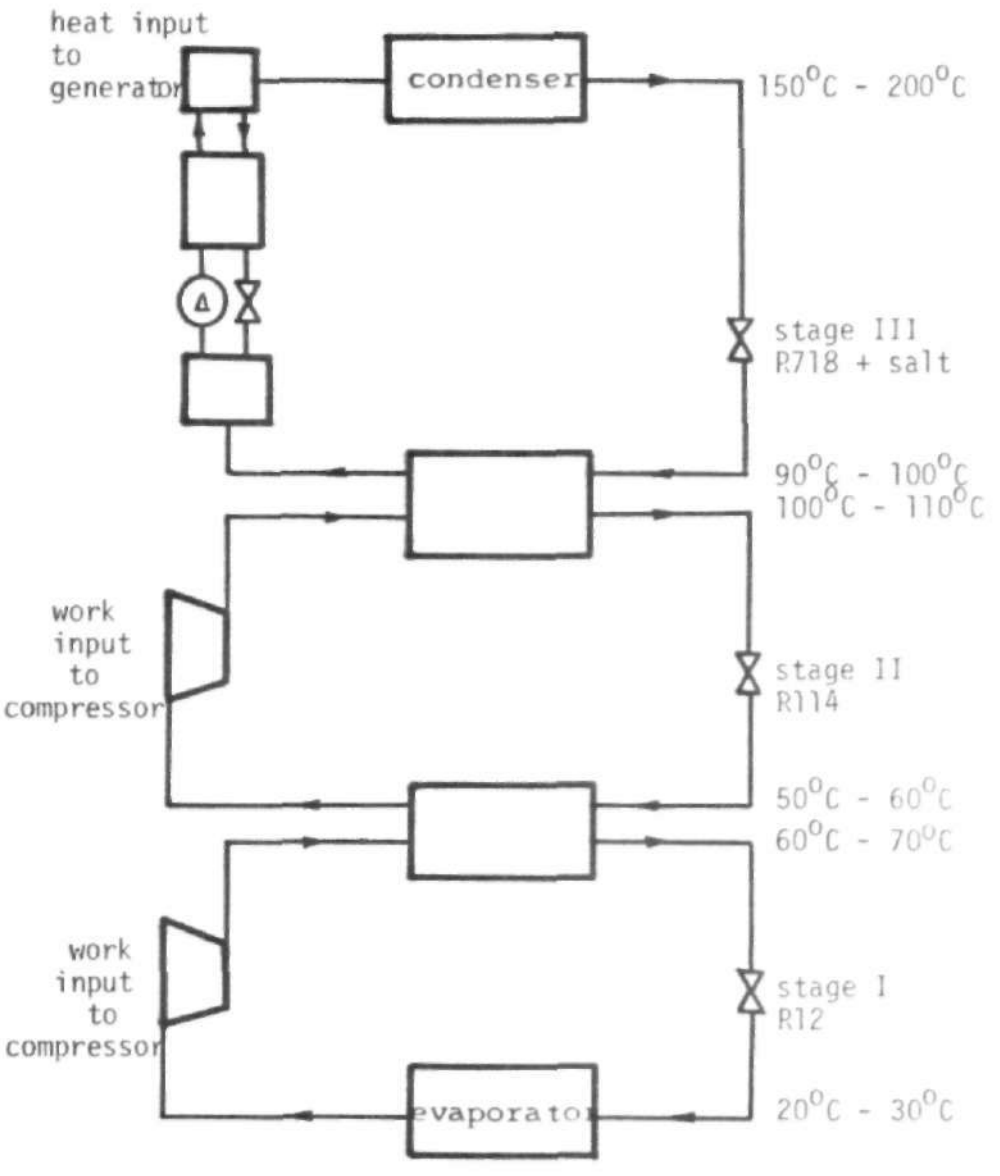


FIGURE (3.4) THREE STAGE HEAT PUMP

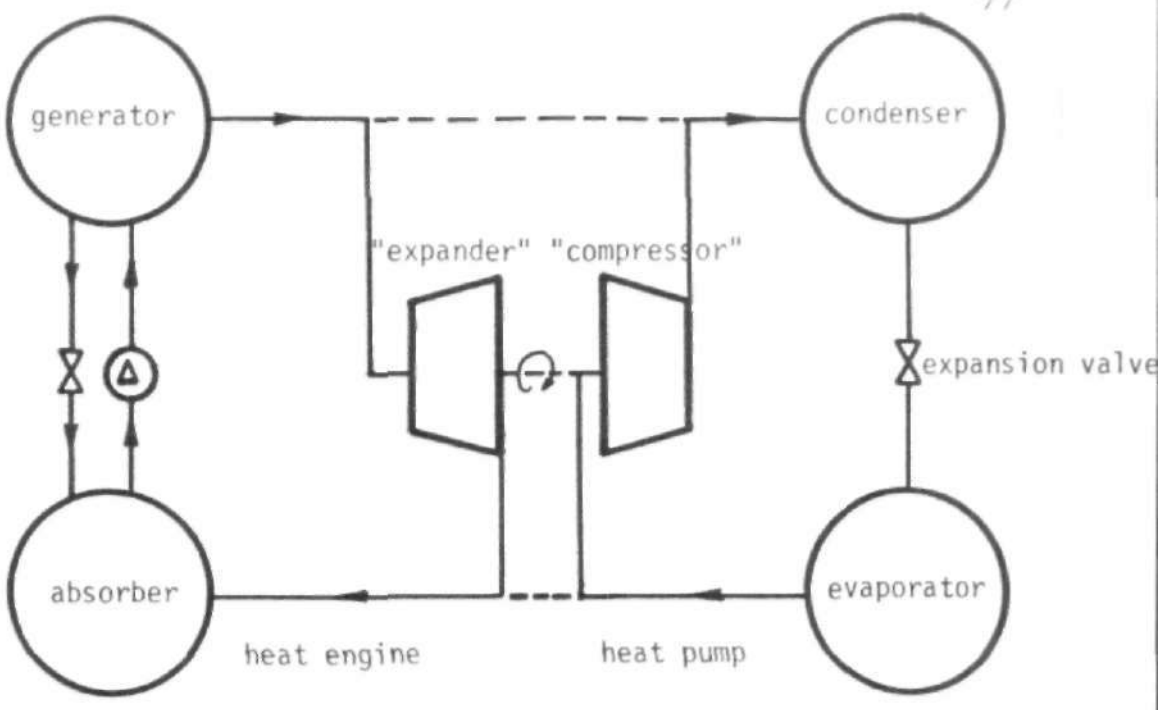


FIGURE (3.5) HEAT ENGINE AND HEAT PUMP COMPONENTS OF A CONTINUOUS ABSORPTION HEAT PUMP SYSTEM

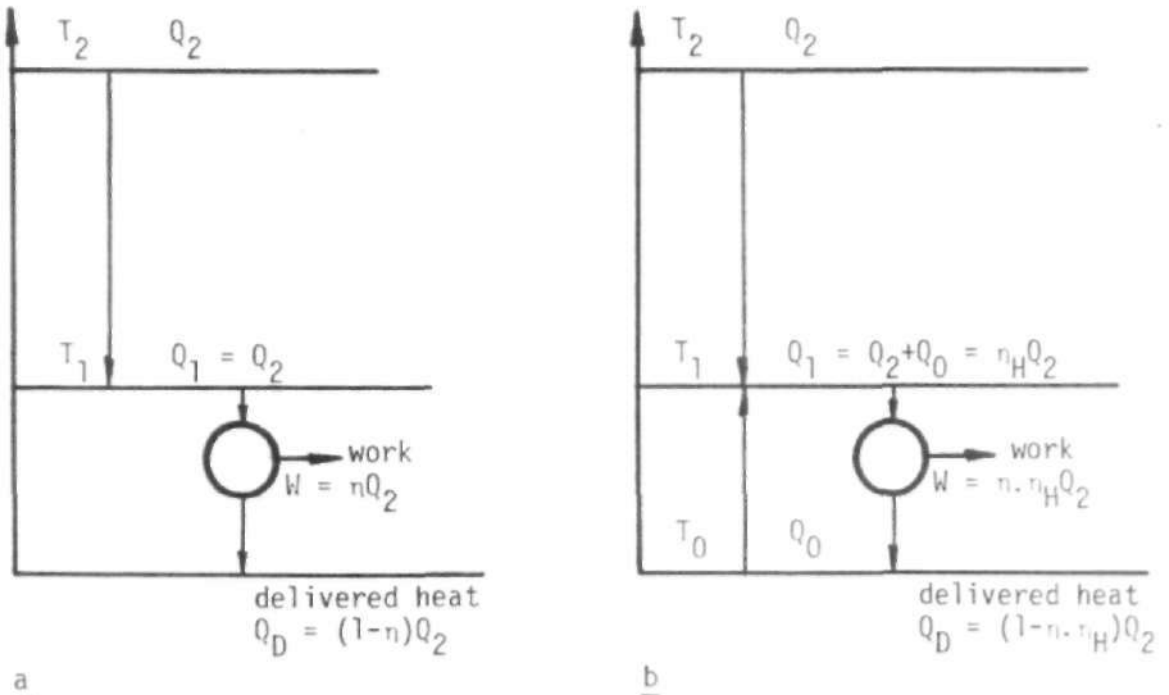


FIGURE (3.6) HEAT FLOW IN A POWER STATION (a) WITHOUT AND (b) WITH AN ABSORPTION HEAT PUMP (n = efficiency of power station without heat pump, n • 36 per cent; $n_H = Q_1/Q_2$ 1.5; $n.n_H$ = efficiency of power station with heat pump, n_{eff} = 54 per cent)

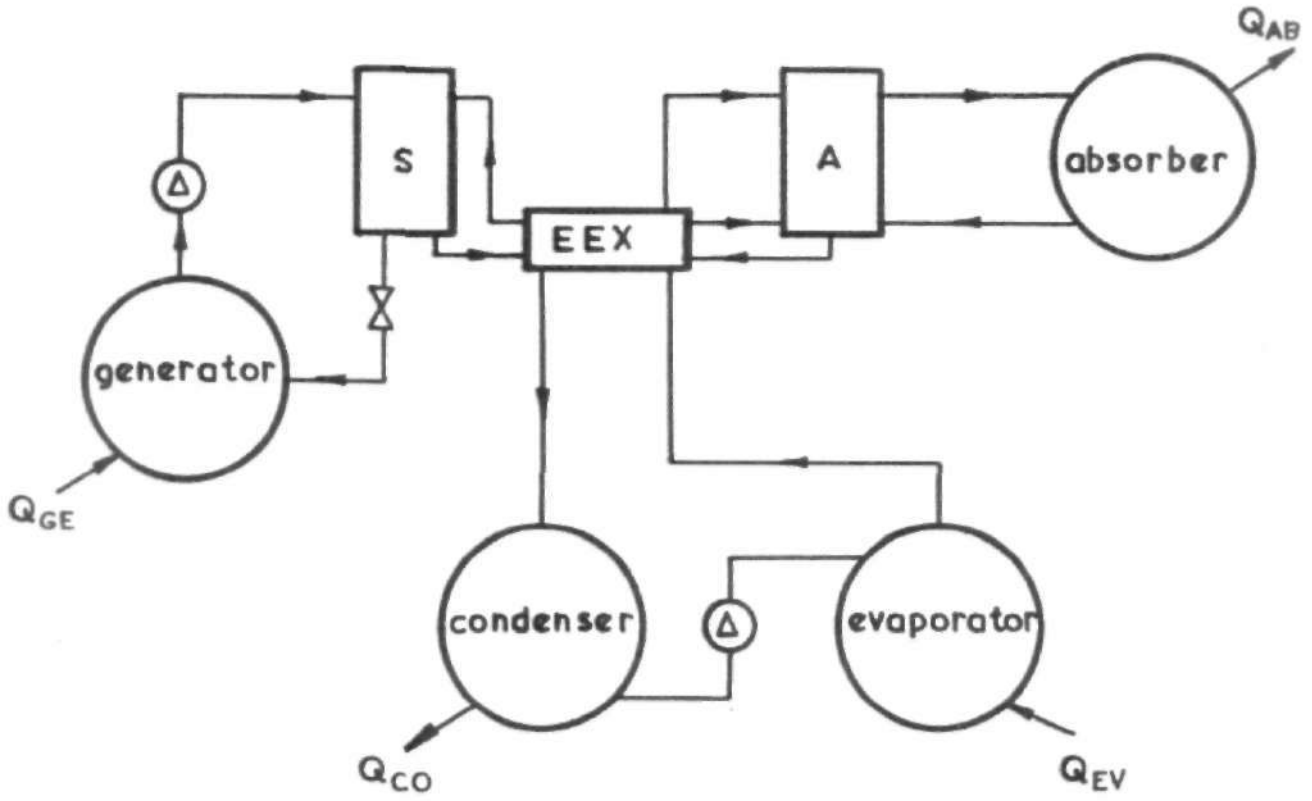
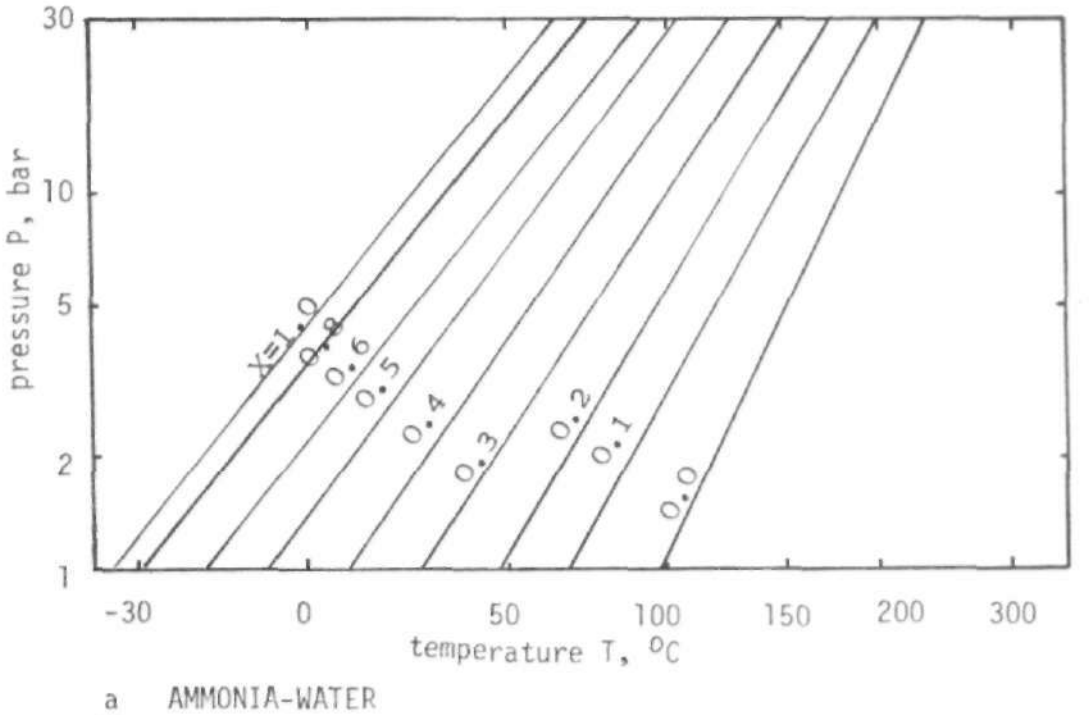
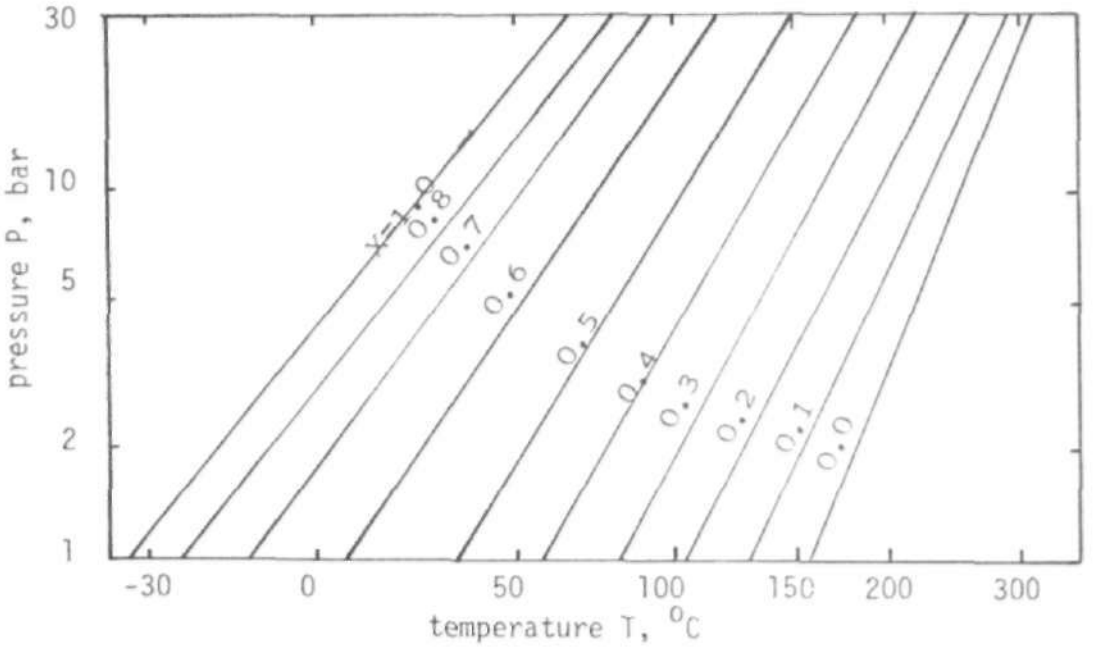


FIGURE 3.7 IFP THERMOSORB.



a AMMONIA-WATER



b AMMONIA-WATER-LITHIUM BROMIDE (Concentration of LiBr, X = 60 wt per cent)

FIGURE (3.8) VAPOUR PRESSURE AGAINST TEMPERATURE FOR A RANGE OF CONCENTRATIONS FOR AMMONIA-WATER AND AMMONIA-WATER-LITHIUM BROMIDE MIXTURES |Adapted from Radermacher, R. and Alefeld, G., (1980)|

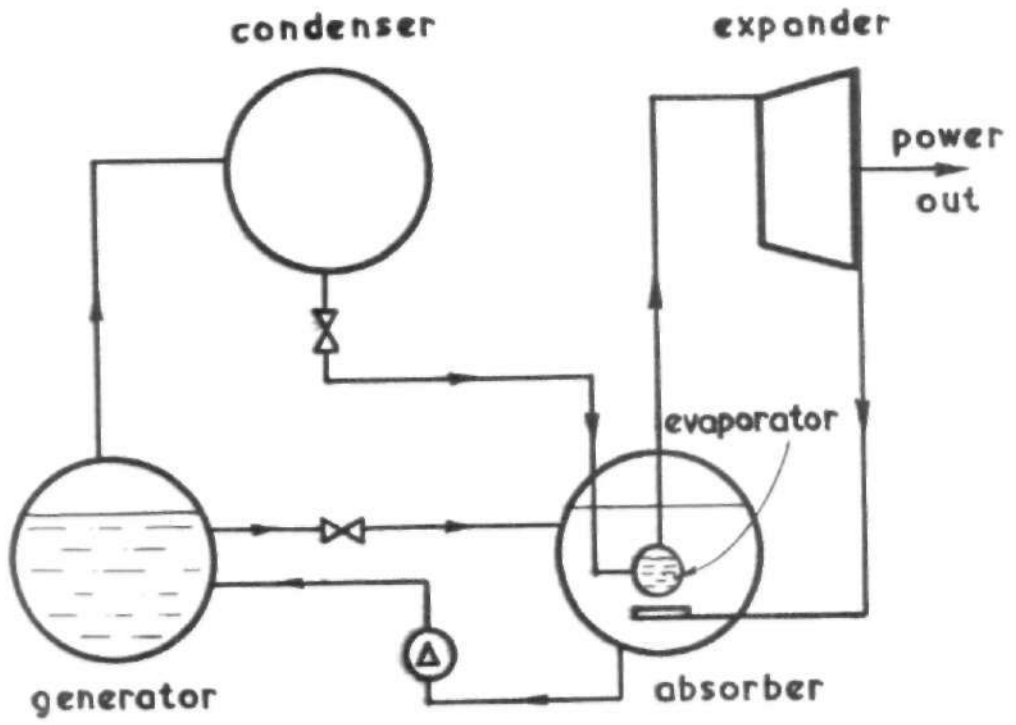


FIGURE 3.9 THE CDE ENGINE.

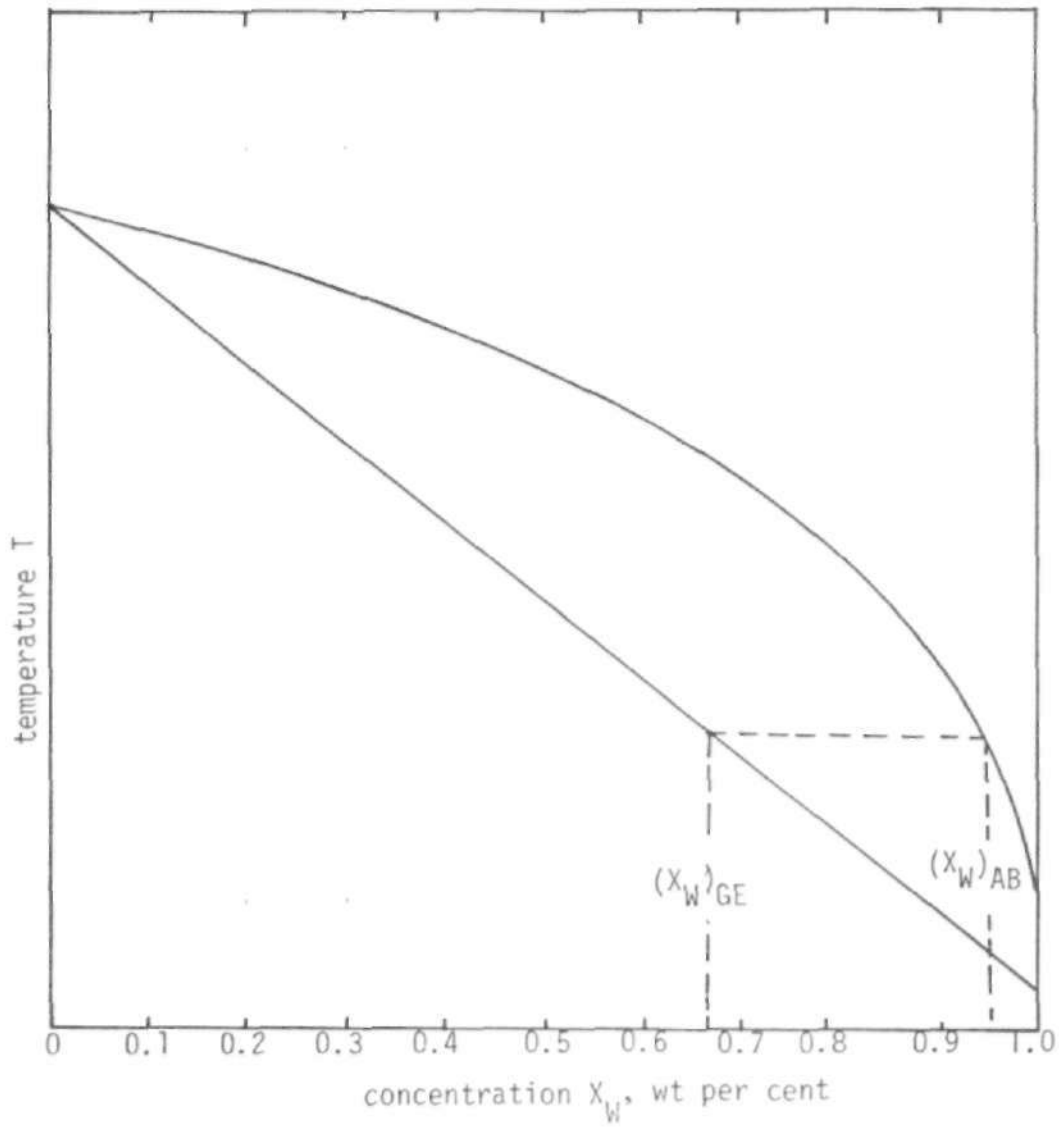


FIGURE (3.10) TEMPERATURE AGAINST CONCENTRATION FOR A FAVOURABLE ABSORBENT MIXTURE

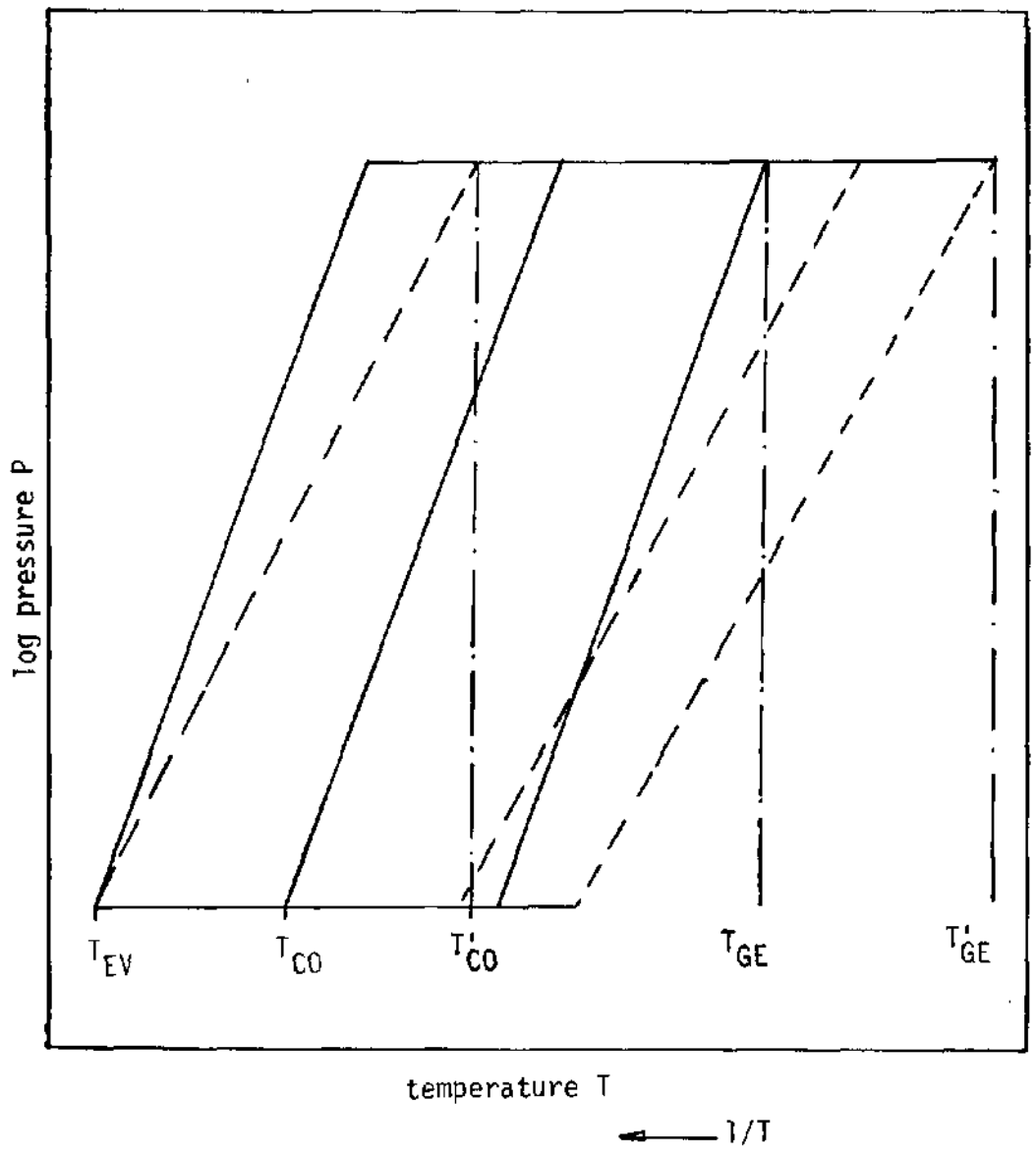


FIGURE (3.11) PRESSURE AGAINST TEMPERATURE FOR AN ABSORBENT MIXTURE

CHAPTER 4

THERMODYNAMIC CONSIDERATIONS

CHAPTER 4

THERMODYNAMIC CONSIDERATIONS

4.1 INTRODUCTION

The volumetric thermodynamic properties of a working fluid have more important implications than the mass-based properties in the design and performance of heat pump systems. Such thermodynamic properties are the volume per unit enthalpy (VPH) and the ratio of volume in vapour state to the volume in liquid state (VR) of the working fluid at a given temperature.

The volume per unit enthalpy of the working fluid determines the sizes of the component units in a heat pump system once the heat delivery rate is specified. In addition, when heat losses occur, the (VPH) and (VR) of the working fluid influence the efficiency of the pressure lifting device of the heat pump. These effects are more significant in the vapour compression heat pump system where the pressure lifting device is a compressor, than in the absorption heat pump system where the pressure lifting device is the combination of the generator, absorber and solution pump and expansion valve. This is because a compressor transports a volume of vapour which has a lower (VPH) than the liquid which the generator-absorber-pump unit transfers. The compressor is more prone to heat losses than the generator-absorber-pump unit.

The cost of a heat pump system depends inter alia on the sizes of the various component units and the overall performance.

Any one of a group of working fluids can be used to achieve a required temperature lift and hence a desired compression ratio, from a given evaporating temperature T_{EV} (evaporating pressure P_{EV}) in a heat pump. If the heat input Q_S is fixed, the volume of the compressor required to obtain the established duty will vary. This is because the different working fluids possess different enthalpies per unit volume at the same temperature. Furthermore, the design of other aspects of the compressor, like the sizes of the inlet and outlet parts, heat dissipation characteristics, have to be taken into consideration.

This work presents a comparative study of the enthalpy per unit volume and the ratio of volume of vapour to volume of liquid of twenty compounds for a range of temperatures. Furthermore, the volumetric flow rate of the compounds into a compressor for a heat intake rate of 1 MW, for a range of condensing temperatures and gross temperature lifts are given. The twenty compounds have been presented by Holland et al ["Thermodynamic design data for heat pump systems", Holland, F.A., Watson, F.A. and Devotta, S., Pergamon Press, Oxford (1982)] as potentially useful working fluids in heat pump systems. Table (4.1) gives a list of the twenty working fluids in order of decreasing critical temperature T_C.

The results of this exercise can be used to select the most cost effective working fluid for a heat pump system for a desired heat delivery rate and temperature lift. In addition, they can be used to determine the size and cost of the units of the equipment. They can also be used to explain the performance of heat pump systems based on any of the twenty fluids or by extrapolation for other working fluids.

4.2 COMPRESSOR SIZE AND COST

Figures (4.1), (4.2), (4.3) and (4.4) relate enthalpy per unit volume (HPV) and temperature T for different groups of working fluids for temperature ranges 0-120°C, 20-140°C, 20-140°C and 100-200°C respectively. Figures (4.5), (4.6), (4.7) and (4.8) show the relations between (VPH) and T for the same sets of working fluids as above for corresponding ranges of temperature. The size of a compressor is based on the volumetric flow rate of the required working fluid at the inlet temperature T_{EV}. The compression ratio (CR) is an additional parameter which further describes the compressor. Together, they determine the power of the motor to drive it.

It is most useful to correlate the compressor cost with its size rather than its power consumption W. This is because the same compressor can be operated at different power levels by using different working fluids and temperature lifts.

The volumetric flow rate of a fluid into a compressor can be determined from Equation (4.1)

$$V_C = Q_S/(HPV) \qquad (4.1)$$

Equation (4.1) can be used to calculate the required compressor throughput V_C for any desired condensing temperature T_{CO}, gross temperature lift $(T_{CO} - T_{EV})$ and heat energy input Q_S using the enthalpy per unit volume (HPV) of different working fluids taken at a given value of T_{EV}.

The values of V_C for the working fluids listed in Tables (1.1) to (1.20) have been calculated for a heat intake rate of 1 MW for gross temperature lifts between 10 and 75°C at intervals of 5°C and condensing temperatures at intervals of 5°C.

All the values of enthalpy per unit volume for the working fluids used were taken from published tables ["Thermodynamic design data for heat pump systems, Holland, F.A., Watson, F.A. and Devotta, S., Pergamon Press, Oxford (1982)].

Van Looveren, Verelst, Berghmans and Gelders ["Determining the capital cost of industrial heat pumps by correlation, Van Looveren, Verelst, J., Berghmans, J. and Gelders, L., International Symposium on the Industrial Application of Heat Pumps, BHRA Fluid Engineering, Cranfield, England (March 1982)] presented a set of correlations for costs of compressors, in Belgian francs, against volumetric displacement for a range of sizes. Table (4.2) gives an adapted form of the correlations in pounds sterling.

4.3 COMPRESSORS FOR NON-ISENTROPIC COMPRESSION

For reversible adiabatic, that is isentropic, compression, the power required by a compressor can be determined from Equation (4.3.1)

$$W_R = Q_S/[(COP)_R - 1] \qquad (4.3.1)$$

Referring to Figure (4.9) which is a plot of pressure against enthalpy per unit volume for a typical working fluid, the theoretical

Rankine coefficient of performance $(COP)_R$ of a heat pump can be defined as

$$(COP)_R = \frac{H_{D1} - H_{D3}}{H_{D1} - H_{S2}} \qquad (4.3.2)$$

The compression from S2 to D1 is isentropic.

Values of $(COP)_R$ for the fluids in Table (4.1) have been presented by Holland et al ["Thermodynamic design data for heat pump systems", Holland, F.A., Watson, F.A. and Devotta, S., Pergamon Press, Oxford (1982)]. The corresponding heat output rate Q_D can be obtained from Equation (4.3.3).

$$Q_D = Q_S + W \qquad (4.3.3)$$

which represents a heat balance over a heat pump system.

In practice, compressors for isentropic compression are not obtainable. The power required by an actual compressor can be obtained from Equation (4.3.4)

$$W_A = Q_S/\left[(COP)_A - 1\right] \qquad (4.3.4)$$

With reference to Equation (4.3.2) the actual coefficient of performance $(COP)_A$ is defined as

$$(COP)_A = \frac{H_{D1} - H_{D3}}{(H_{D1} - H_{D2})/\eta_C} \qquad (4.3.5)$$

This is obtained by dividing the denominator in Equation (4.3.2) by the efficiency η_c of a non-ideal compressor. The denominator in Equation (4.3.2) is the work required by a compressor for isentropic compression. The main causes of non-isentropic compression in a compressor have been discussed by Dossat ["Principles of refrigeration", Dossat, R.J., John Wiley and Sons, New York (1961)]. One of the causes is the loss of heat through the wall of the compressor. This may be particularly serious when a small heat flow rate is involved. If condensation of fluid takes place in the compressor due to heat loss, this will aggravate the volumetric inefficiency of the compressor. Normally, volumetric inefficiency arises due to the dead spaces in the compressor.

In addition, condensate may cause mechanical inefficiency during compression. This phenomena may be described as the (VR)-heat loss factor. This is because heat losses may cause a phase change from vapour to liquid. The extent of this factor may be evaluated from a (VR)-temperature relationship.

Figures (4.10) and (4.13) present (VR)-temperature relationships for the twenty working fluids given in Table (4.1).

4.4 DISCUSSION

Figures (4.1) to (4.4) show that the enthalpy per unit volume of a working fluid increases as the temperature increases. Alternatively, Figures (4.5) to (4.8) show that the volume per unit enthalpy of a working fluid decreases as the temperature increases. These plots imply that progressively smaller compressors are

required, for a given inlet heat rate and gross temperature lift, as the delivery temperature increases. The required compressor size for a particular working fluid increases from bottom to top on each of Figures (4.5) to (4.8), for a given heat delivery temperature and gross temperature lift. Figures (4.10) to (4.13) show the order of the inefficiency which may result in a compressor in which a working fluid is compressed. The inefficiency which may result from the compression increases as the (VR) increases for a given temperature in the compressor.

index	working fluid code number	chemical formula	critical temperature, ^{o}C	compressor throughput for (T_{CO}-T_{EV}) = 50^{o}C and T_{CO} = 120^{o}C $m^3 s^{-1}$	vapour pressure at T_{CO}=120^{o}C bar	safety class	safety group
1	R718	H_2O	374.15	2.1626	1.985	-	-
2	R114B2	$CBrF_2CBrF_2$	214.5	0.5133	6.824	-	-
3	R113	CCl_2FCClF_2	214.1	0.5094	6.870	1	4-5
4	R11	CCl_3F	198.0	0.2870	12.248	1	5
5	R216	$CF_3CCl_2CF_3$	180.0	0.3755	9.378	-	-
6	R21	$CHCl_2F$	178.5	0.1800	19.518	1	4-5
7	R12B1	$CClBrF_2$	154.4	0.1620	22.195	1	6
8	R600	$CH_3CH_2CH_2CH_3$	152.0	0.1474	24.176	3	5
9	R114	$CClF_2CClF_2$	145.7	0.1765	20.575	1	6
10	R506	R31(55.1 wt%)+R114	142.0	0.1036	35.275	-	5
11	R142b	CH_3CClF_2	137.0	0.1182	30.766	-	-
12	R600a	$CH(CH_3)_3$	135.0	0.1350	28.418	3	56
13	R717	NH_3	132.2	0.0400	91.025	2	2
14	R505	R12(78.0 wt%)+R31	117.8	NA	NA	-	5
15	RC318	C_4F_8	115.3	NA	NA	-	-
16	R12	CCl_2F_2	112.0	NA	NA	1	6
17	R500	R12(73.8 wt%)+R152a	105.4	NA	NA	1	5a
18	R290	$CH_3CH_2CH_3$	97.0	NA	NA	3	5b
19	R22	$CHClF_2$	96.0	NA	NA	1	5a
20	R115	$CClF_2CF_3$	79.8	NA	NA	-	-

NA = not applicable

TABLE 4.1 VOLUMETRIC THROUGHPUT REQUIRED FOR COMPRESSOR FOR A HEAT INTAKE RATE OF 1 MW FOR SOME WORKING FLUIDS

Type	Size range (V_C), $m^3\ s^{-1}$	Correlation
Semi-hermetic	0.075 - 2.9141	$C_C = 1.817\ (V_C)\ 0.70$
Open	0.056 - 0.2921	$C_C = 0.602\ (V_C)\ 0.48$
Open	0.539 - 1.4581	$C_C = 1.280\ (V_C)\ 0.75$
Open	1.661 - 26.61	$C_C = 6.884\ (V_C)\ 0.47$

TABLE 4.2 COMPRESSOR COST CORRELATIONS

[Adapted from Van Looveren, A., Verelst, J., Bergmans, J. and Golders, L., "Determining the cost of industrial heat pumps by correlation, *International Symposium on the Industrial* Application of Heat Pumps, BHRA Fluid Engineering, Cranfield, England (March 1982)].

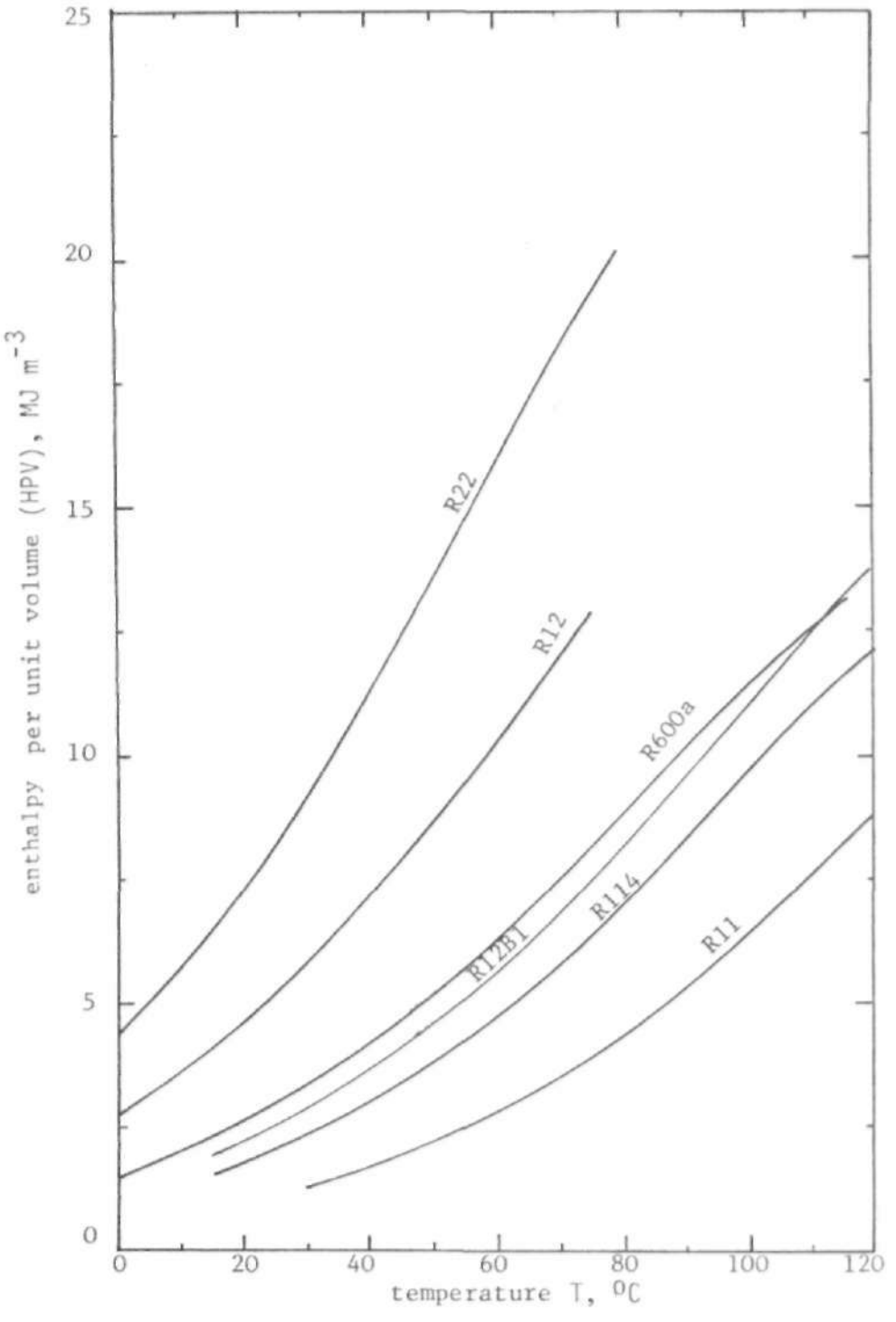


FIGURE 4.1 ENTHALPY PER UNIT VOLUME AGAINST TEMPERATURE FOR SOME COMMON WORKING FLUIDS

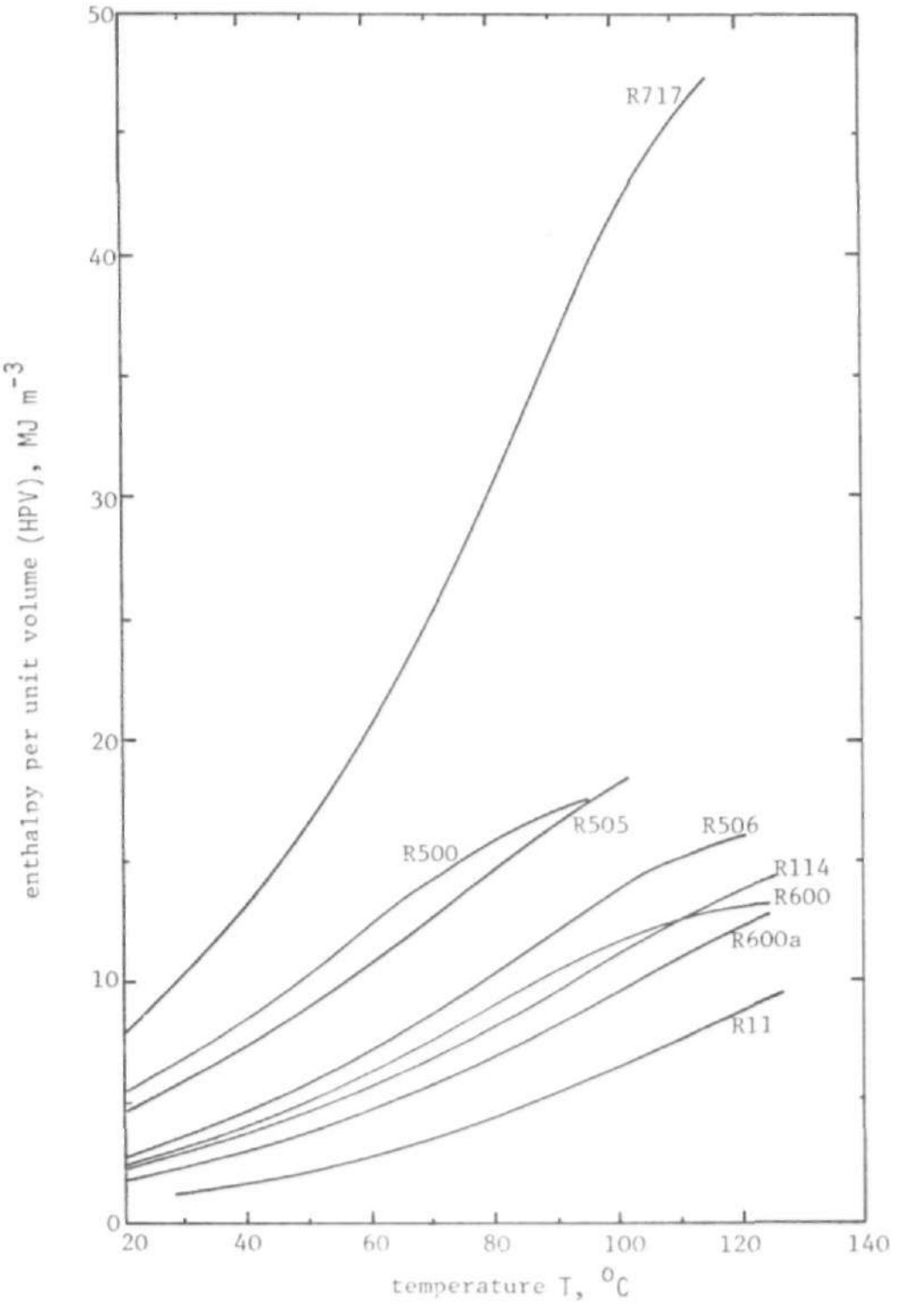


FIGURE 4.2 ENTHALPY PER UNIT VOLUME AGAINST TEMPERATURE FOR SOME WORKING FLUIDS.

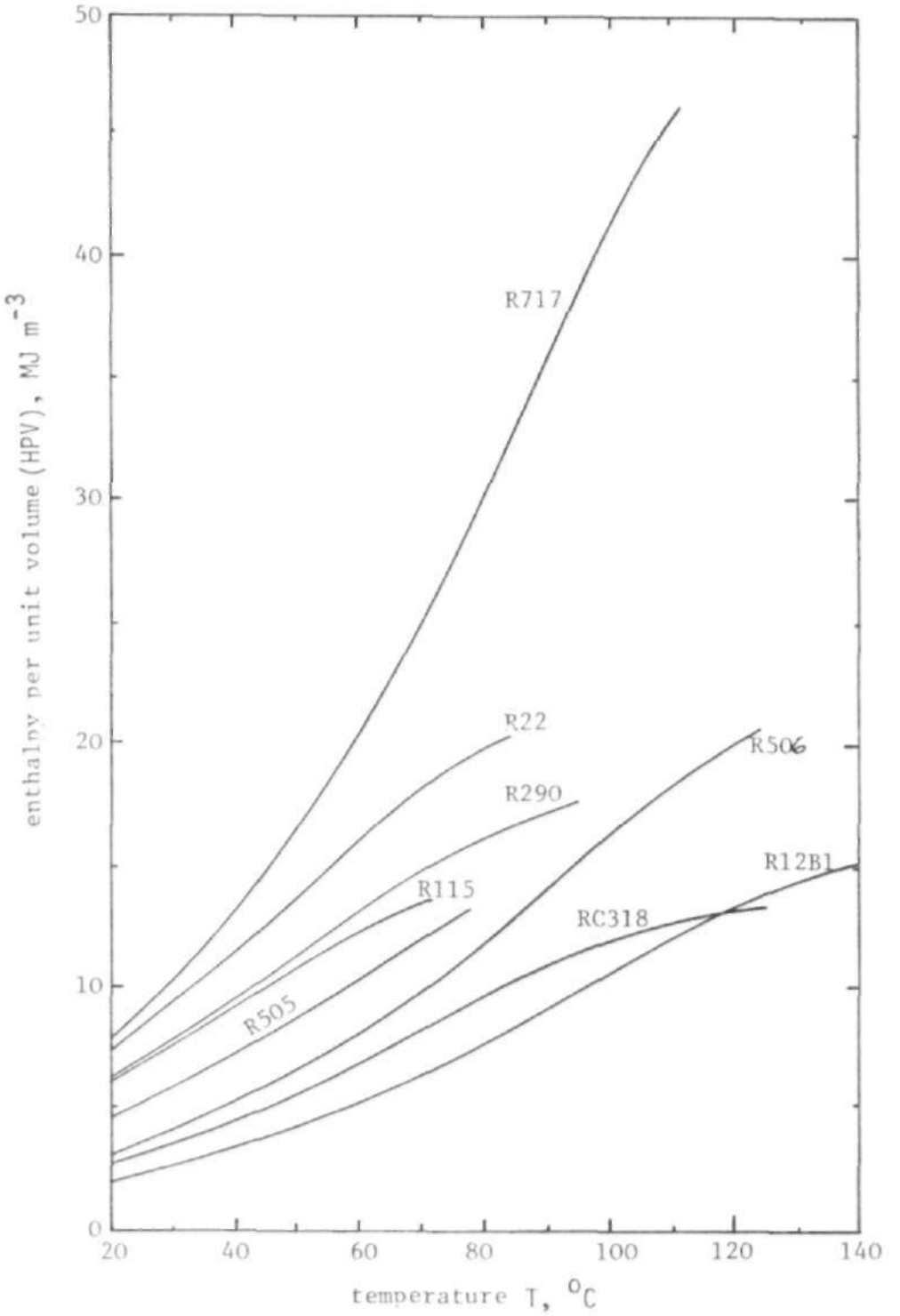


FIGURE 4.3 ENTHALPY PER UNIT VOLUME AGAINST TEMPERATURE FOR SOME WORKING FLUIDS

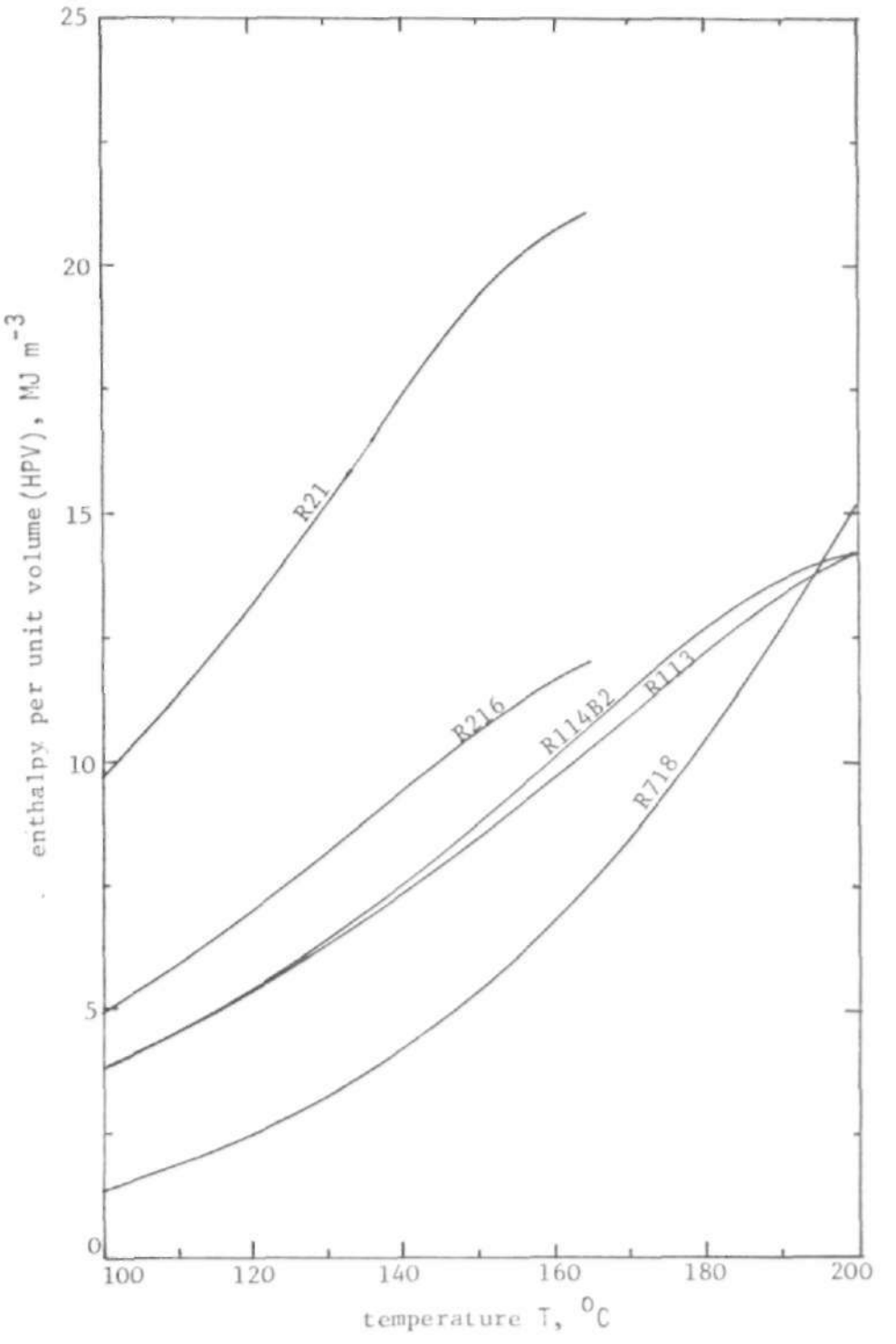


FIGURE 4.4 ENTHALPY PER UNIT VOLUME AGAINST TEMPERATURE FOR SOME HIGH TEMPERATURE WORKING FLUIDS

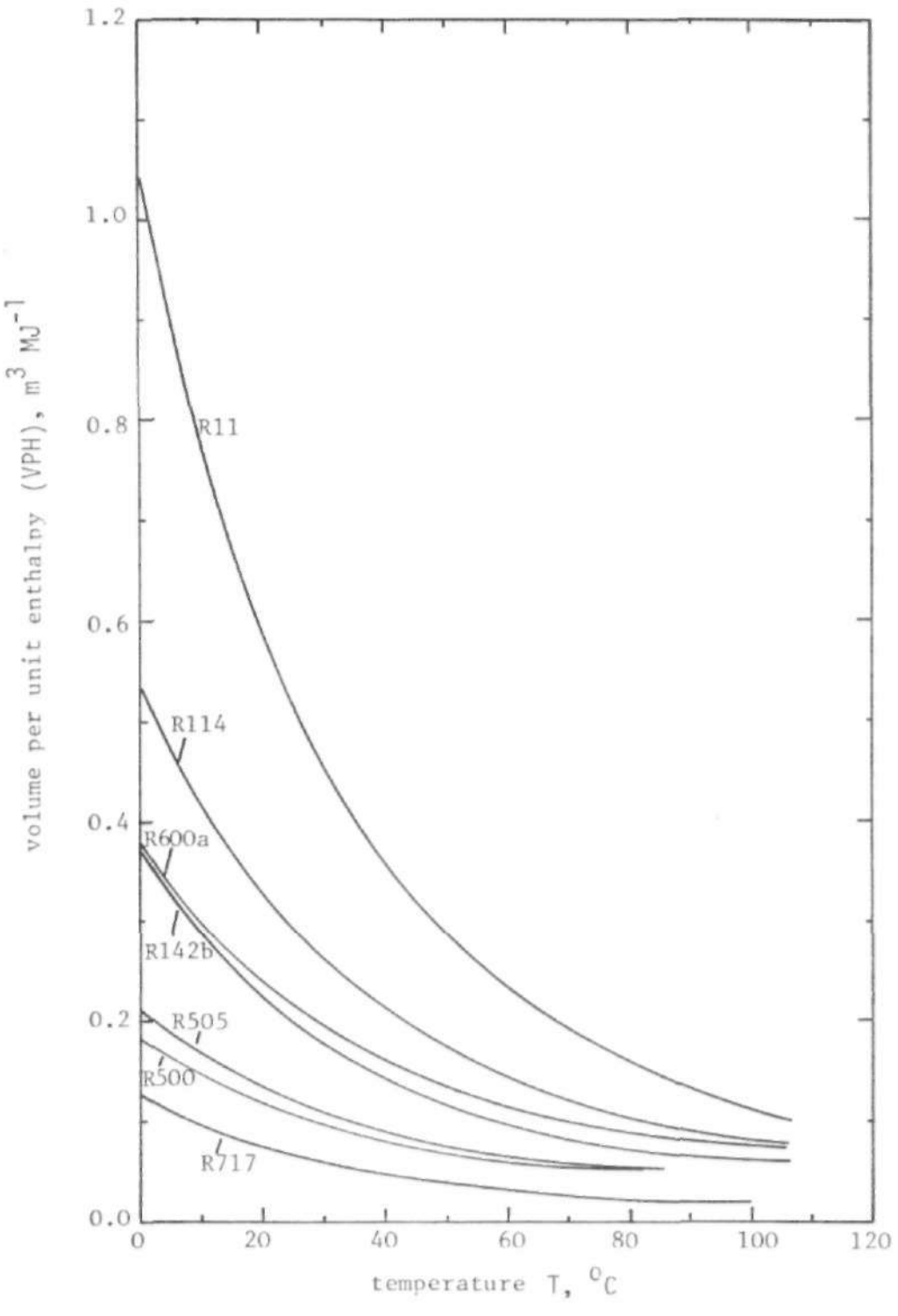


FIGURE 4.5 VOLUME PER UNIT ENTHALPY AGAINST TEMPERATURE FOR SOME WORKING FLUIDS

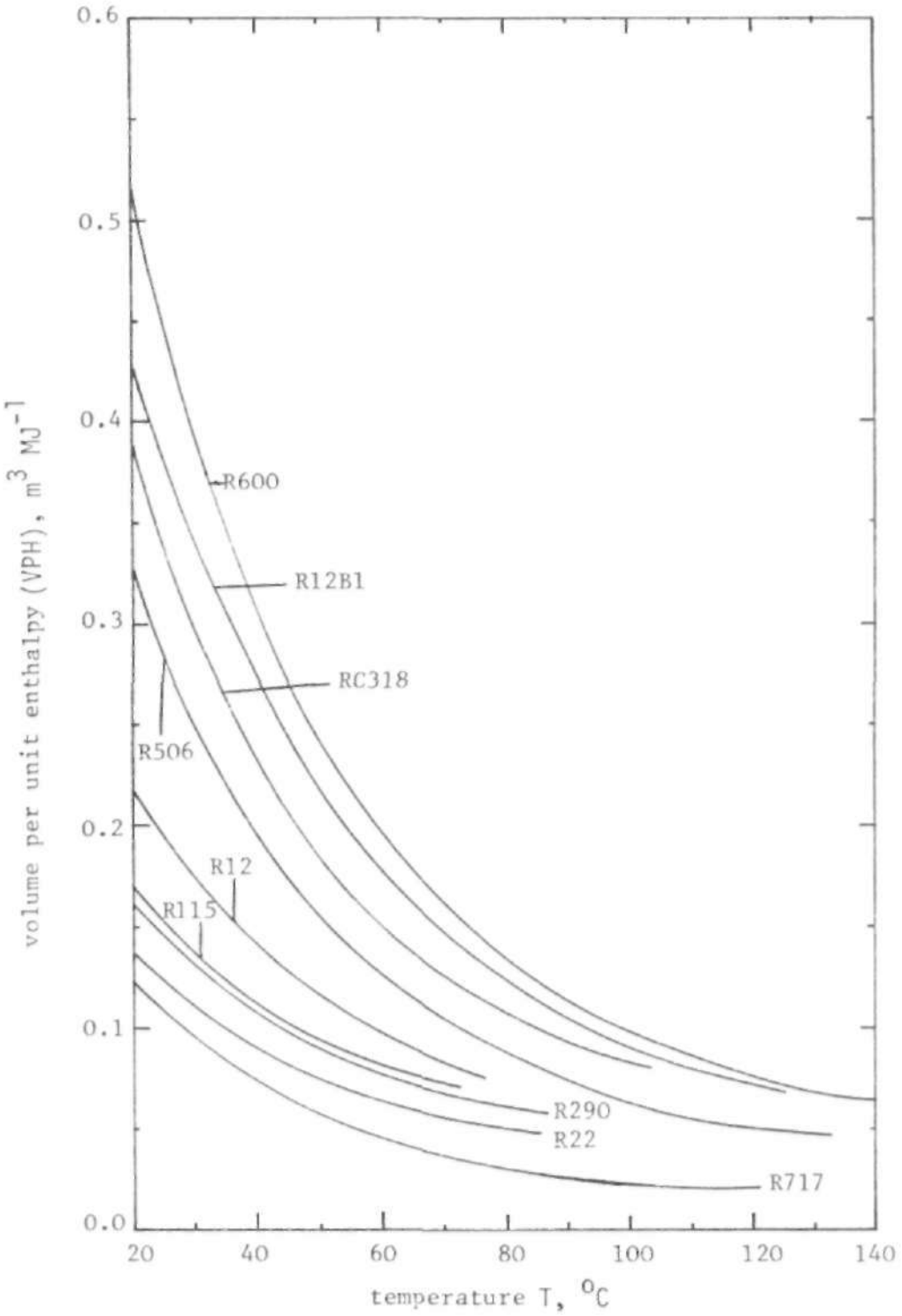


FIGURE 4.6 VOLUME PER UNIT ENTHALPY AGAINST TEMPERATURE FOR SOME WORKING FLUIDS

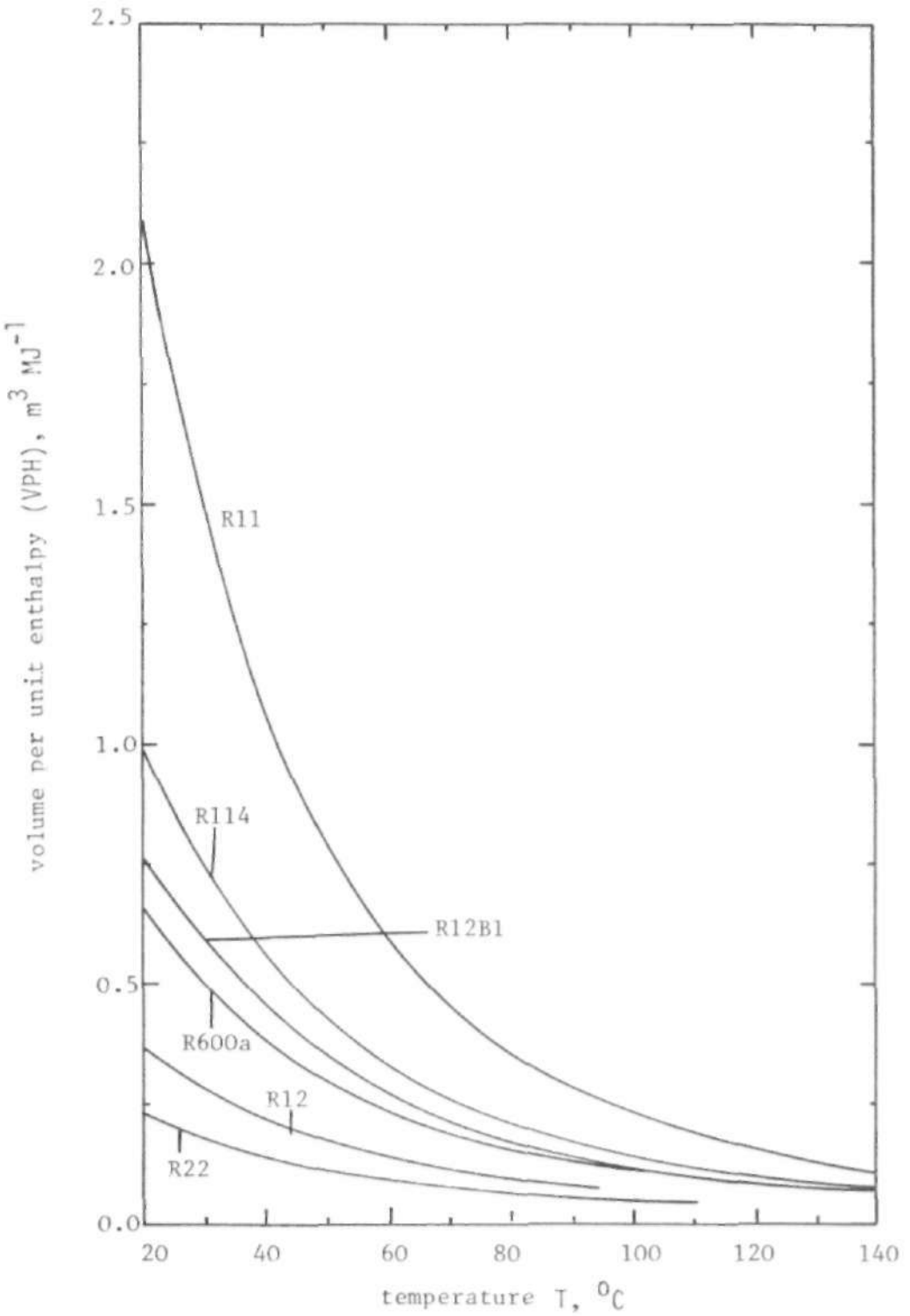


FIGURE 4.7 VOLUME PER UNIT ENTHALPY AGAINST TEMPERATURE FOR SOME WORKING FLUIDS

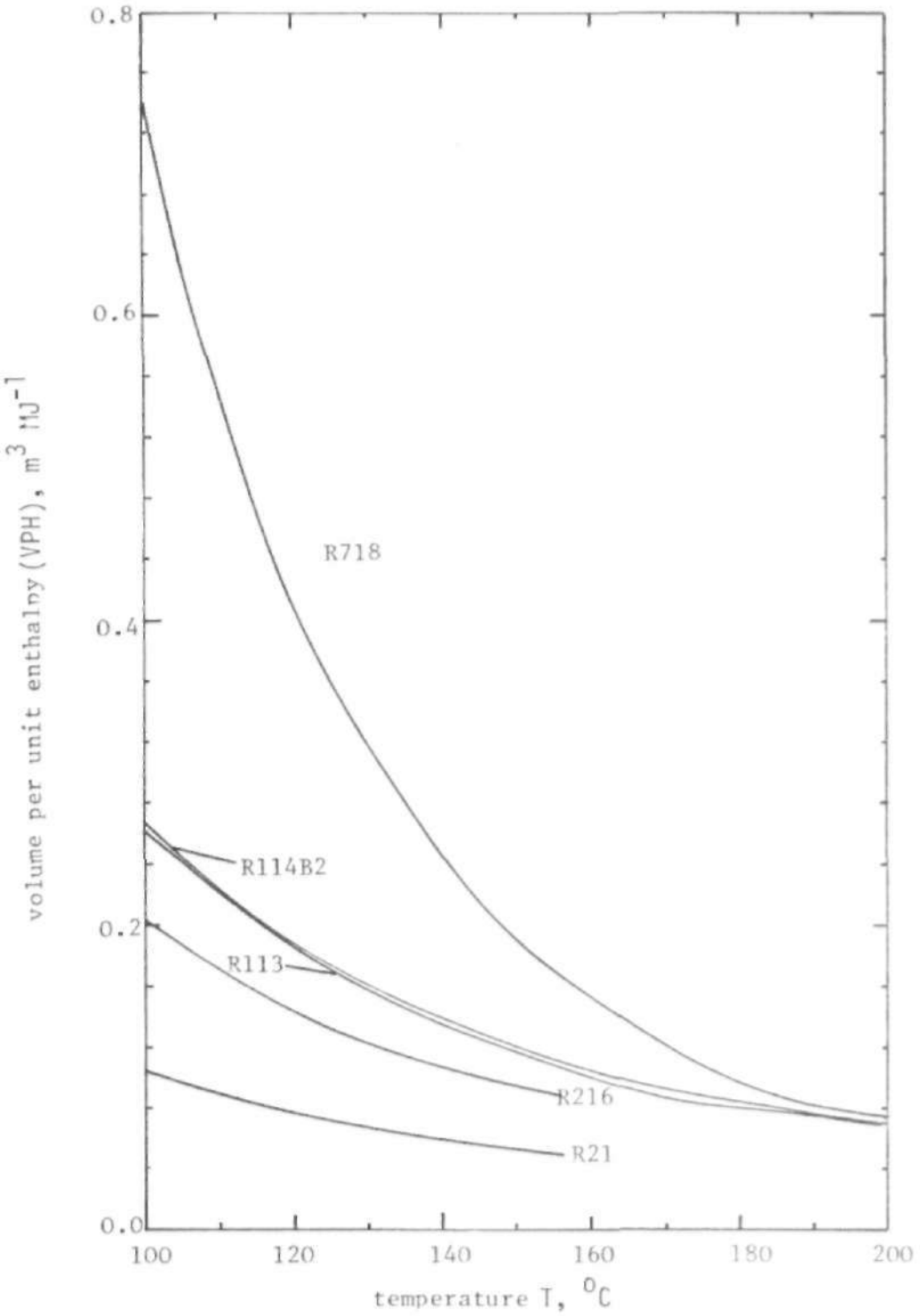
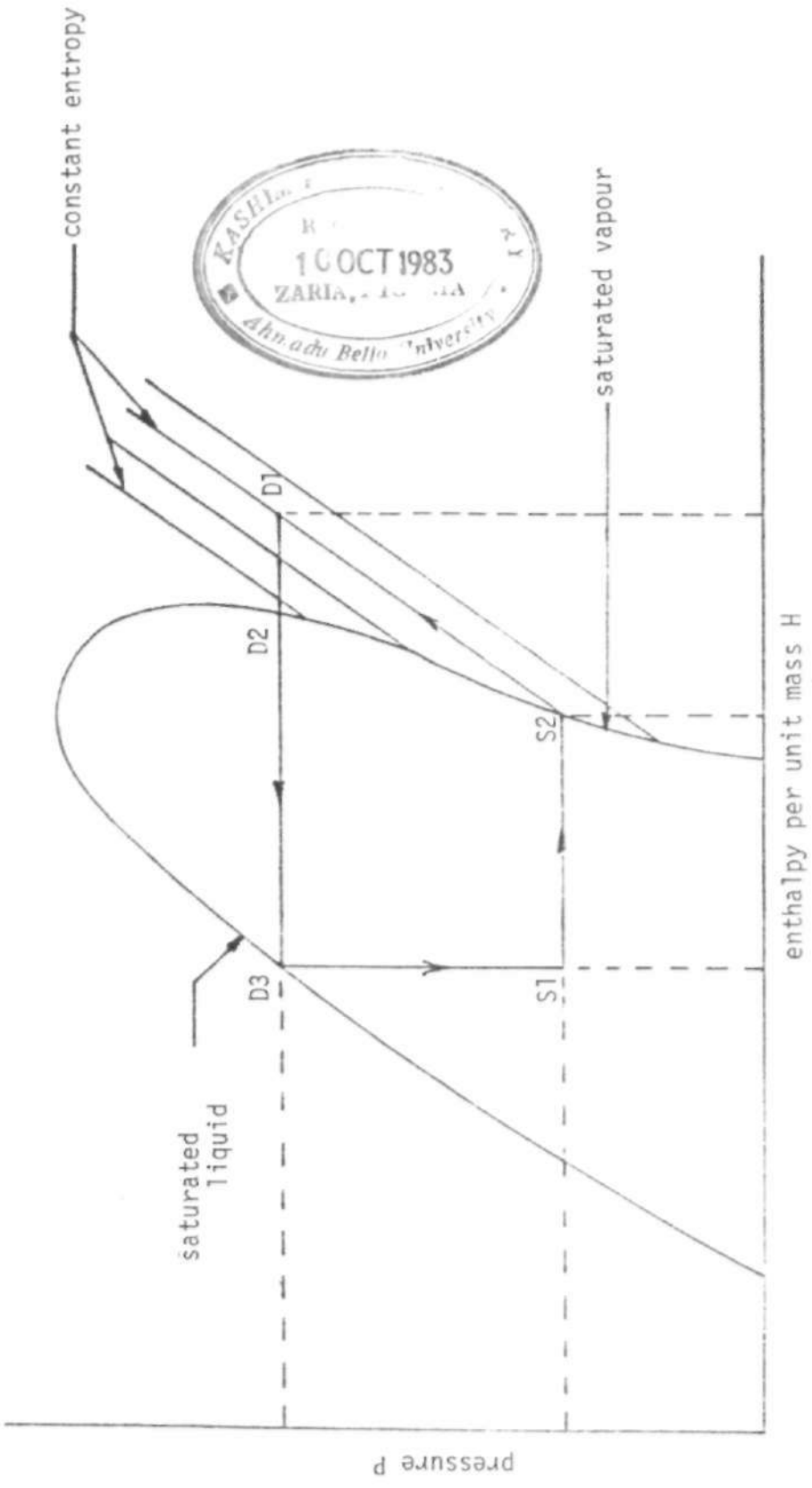


FIGURE 4.8 VOLUME PER UNIT ENTHALPY AGAINST TEMPERATURE FOR SOME WORKING FLUIDS



KASHIM
10 OCT 1983
ZARIA
Ahmadu Bello University

FIGURE (4.9) PRESSURE AGAINST ENTHALPY PER UNIT MASS FOR A WORKING FLUID

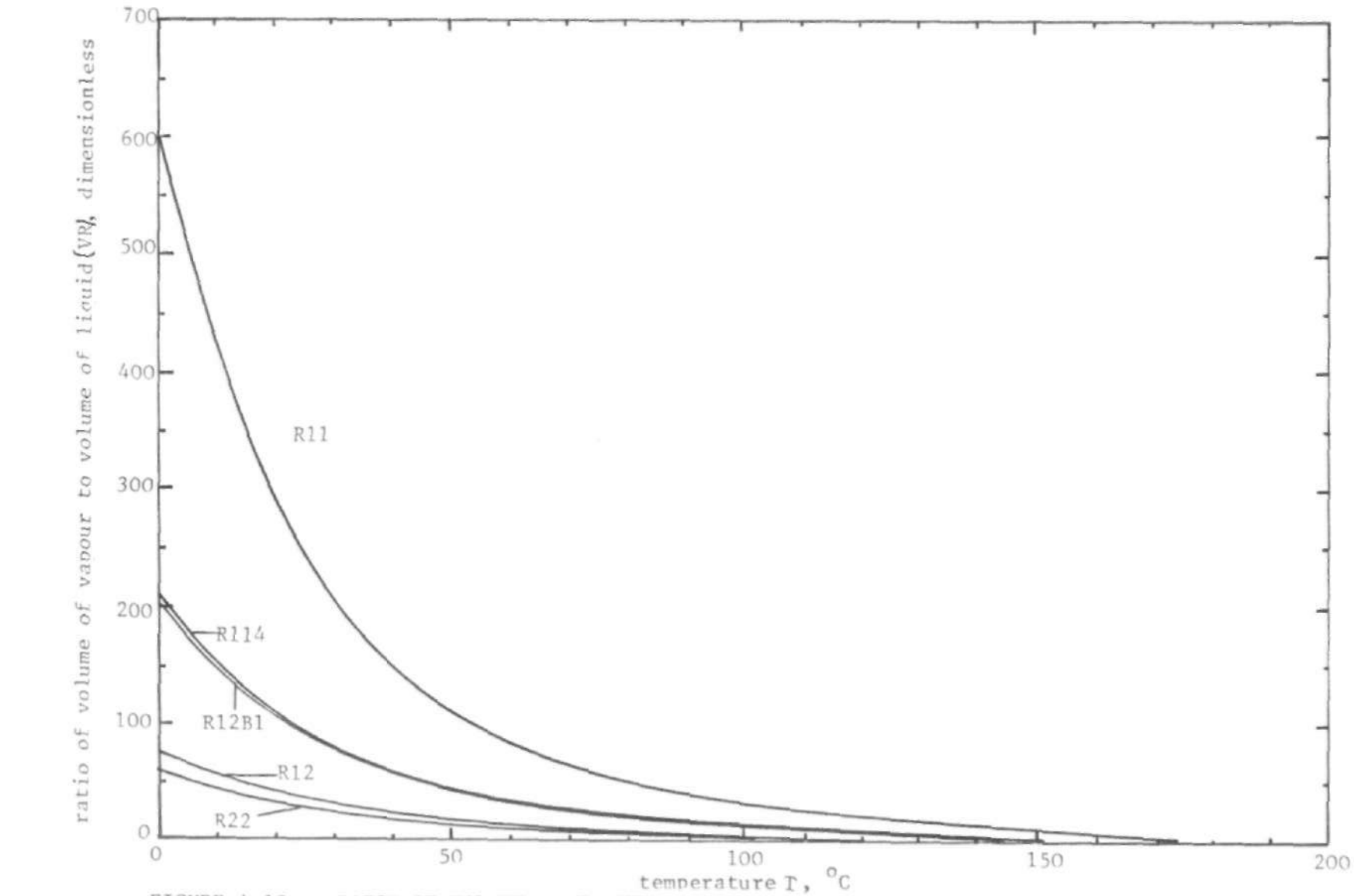


FIGURE 4.10 RATIO OF VOLUME OF VAPOUR TO VOLUME OF LIQUID AGAINST TEMPERATURE FOR SOME WORKING FLUIDS

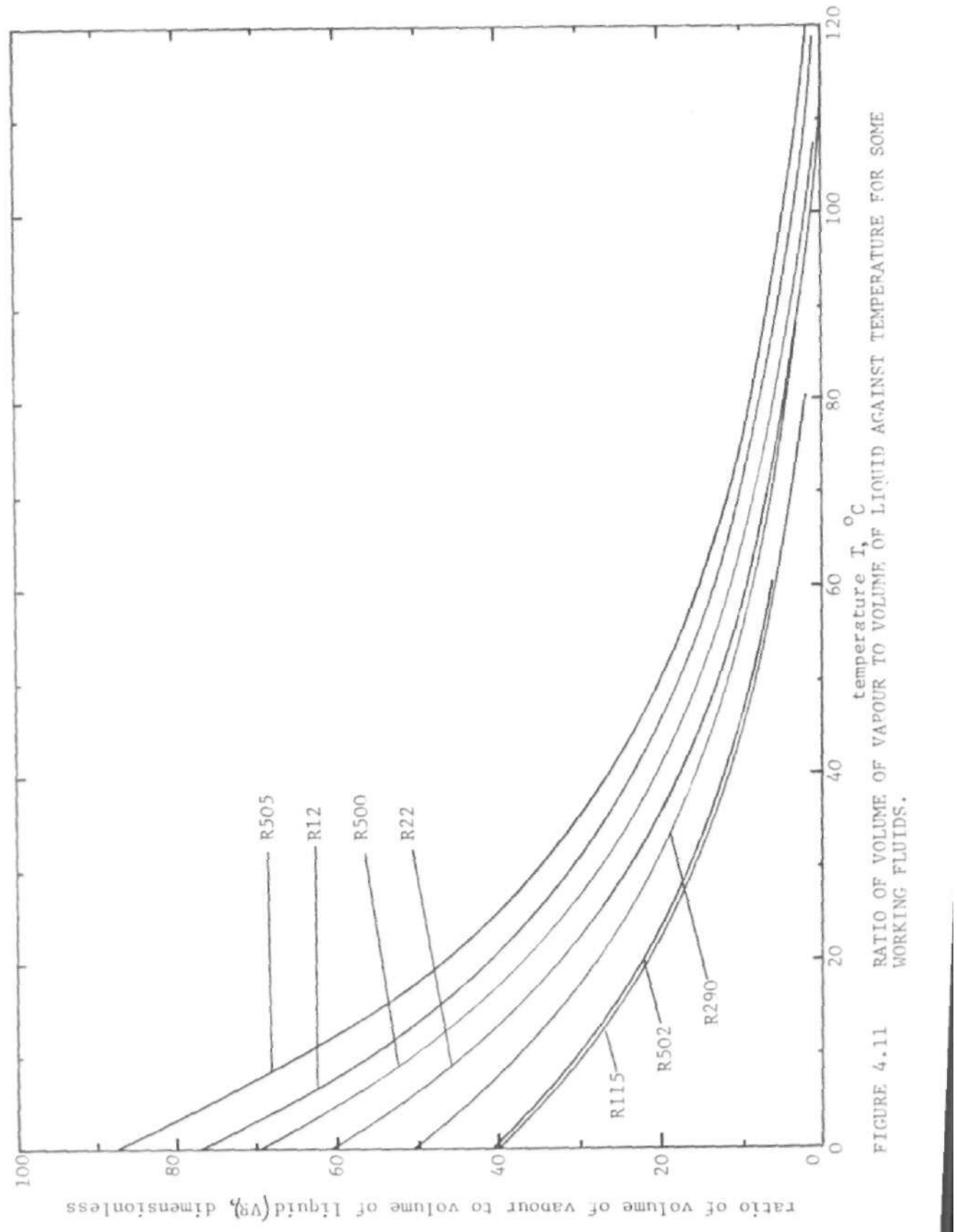


FIGURE 4.11 RATIO OF VOLUME OF VAPOUR TO VOLUME OF LIQUID AGAINST TEMPERATURE FOR SOME WORKING FLUIDS.

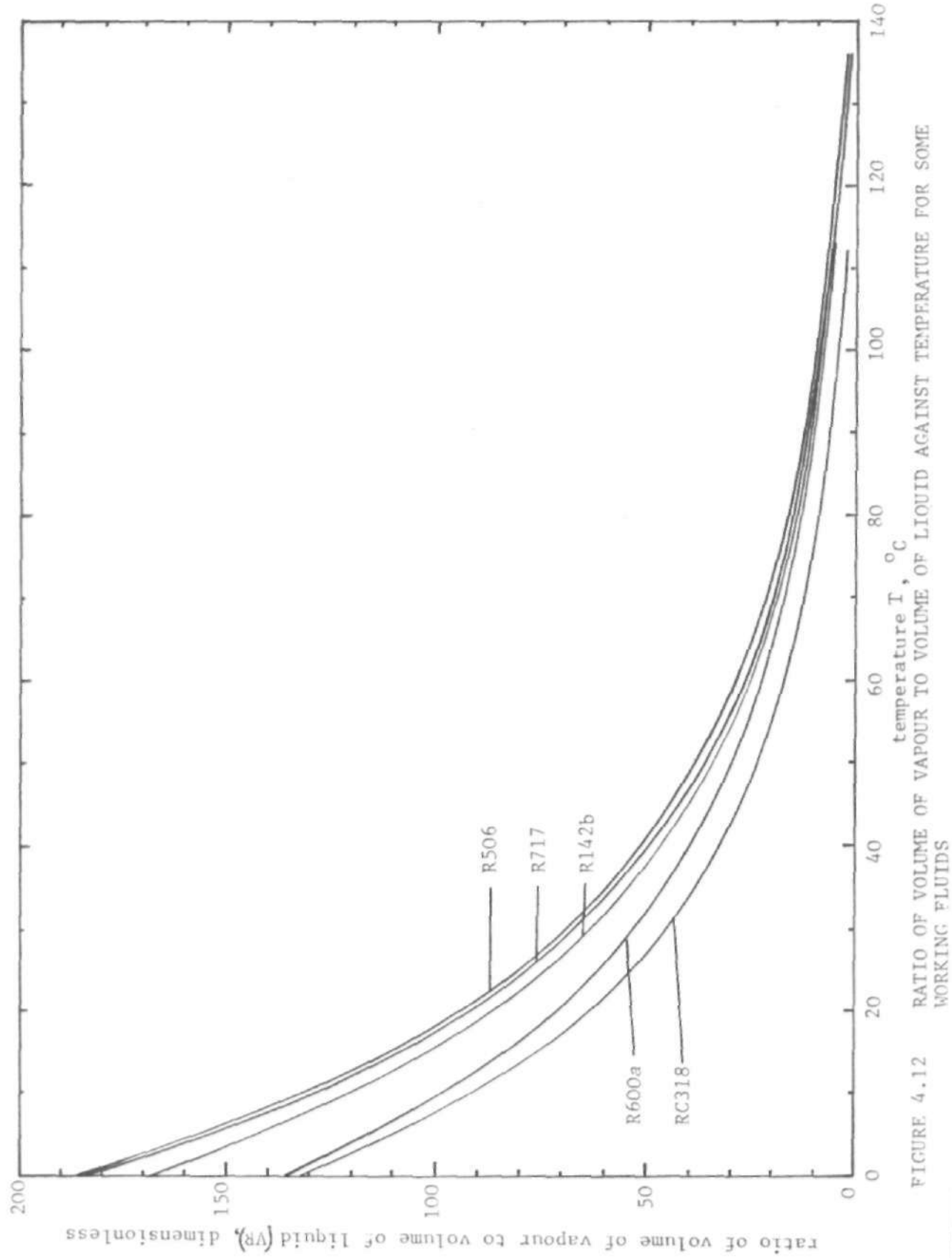


FIGURE 4.12 RATIO OF VOLUME OF VAPOUR TO VOLUME OF LIQUID AGAINST TEMPERATURE FOR SOME WORKING FLUIDS

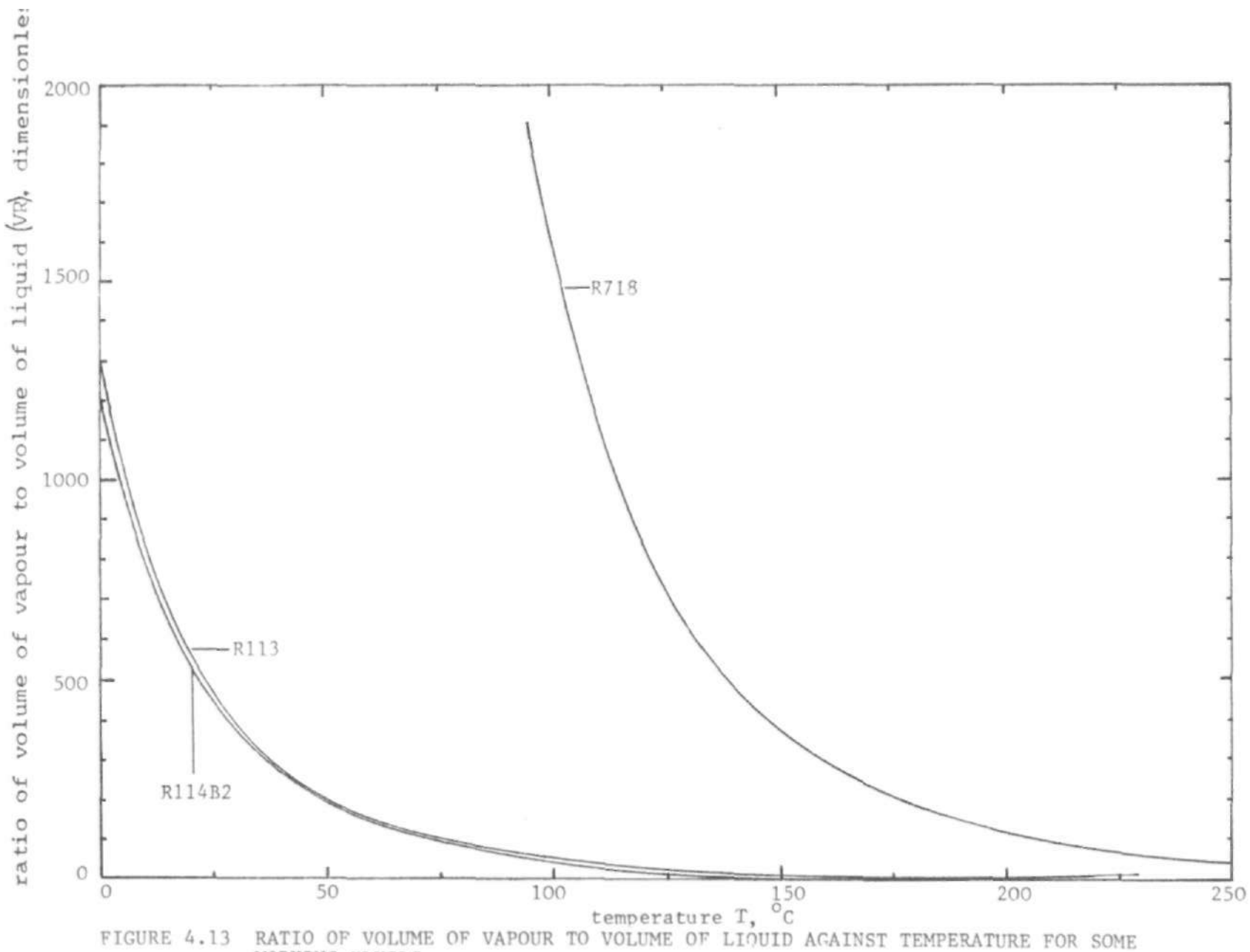


FIGURE 4.13 RATIO OF VOLUME OF VAPOUR TO VOLUME OF LIQUID AGAINST TEMPERATURE FOR SOME WORKING FLUIDS

CHAPTER 5

PERFORMANCE CHARACTERISTICS OF WORKING FLUIDS IN VAPOUR COMPRESSION HEAT PUMP SYSTEMS

CHAPTER 5

PERFORMANCE CHARACTERISTICS OF WORKING FLUIDS IN VAPOUR COMPRESSION HEAT PUMP SYSTEMS

5.1 INTRODUCTION

Performance and thermodynamic data of working fluids are required for the design of heat pump systems. Holland, Watson and Devotta ["Thermodynamic design data for heat pump systems", Holland, F.A., Watson, F.A. and Devotta, S., Pergamon Press, Oxford, U.K. (1982)] have presented the thermodynamic data for twenty-one working fluids which are potentially useful for producing heat in the temperature range 60°C to 300°C. Furthermore, they established a method for deriving such data for other working fluids. The performances of R11, R12, R12B1 and R114 [the chemical names and formulae for the working fluids used in this Chapter are listed in Table (5.1)] obtained from a water-to-water heat pump system were reported by Ogbeide ["Performance and heat transfer studies on a heat pump system", Ogbeide, S.E., PhD Thesis, University of Salford, Salford, U.K. (1981)], Guterriez, El-Meniawy, Watson and Holland ["Heat pumps: Part 5 - Operating characteristics of a water-water heat pump system using R12", Guterriez, A.G., El-Meniawy, S.A.K., Watson, F.A. and Holland, F.A., Indian Chemical Engineer, XXI(4), 19-26 (October-December 1979)] and El-Meniawy, Watson and Holland ["Heat pumps: Part 8 - Operating characteristics of a water-water heat pump system using R12B1 and R114", El-Meniawy, S.A.K., Watson, F.A. and Holland, F.A., Indian Chemical Engineer, XXLL(3), 3-12 (July-September 1980)] respectively. It would be very expensive to

obtain such performance data for all potentially useful working fluids in a given heat pump system. However, it should be possible to develop an empirical method for determining such data from limited experimental results.

The heat pump effectiveness factor $(HPE)_R$ of a vapour compression heat pump system is a useful parameter. The $(HPE)_R$ is the ratio of the coefficient of performance $(COP)_A$, actually obtained with a given working fluid in a given heat pump system, to the theoretical Rankine coefficient of performance $(COP)_R$ of that fluid when operating over the same temperature lift on an ideal Rankine cycle. The $(HPE)_R$ is, therefore, a measure of the overall efficiency of a heat pump system operating on a specific working fluid. If the individual inefficiencies of the system are isolated, it may be possible to assign individual efficiency factors to them. Some of these factors will be independent of the working fluid but others may be dependent on particular thermodynamic properties of the fluid. Using the dependent factors, it may be possible to predict the performance of a heat pump operating with other working fluids based on the experimental results obtained with a given working fluid. This could greatly simplify the design of such systems and reduce the costs of experimentation.

Heat may be lost from the compressor, expansion valve, heat exchangers or the piping of a given heat pump system. However, it will be shown that the compressor is likely to be the main source of energy loss in the system. The energy must then be dispersed as heat from the compressor or elsewhere. It will be assumed that other inefficiencies are negligible. With this assumption, a relationship between the actual coefficient of performance $(COP)_A$ of a heat pump system and the efficiency

of the compressor η_c should provide a basis for predicting the performance of the system. The relationship will probably involve volume related thermodynamic properties of the working fluid since a compressor transports a fixed volume of fluid per cycle.

5.1.1 Inefficiencies in a vapour compression heat pump system

The inefficiencies in a vapour compression heat pump system could be highlighted by comparing the ideal Rankine cycle and an actual cycle on a pressure-enthalpy diagram. This is presented schematically in Figure (5.1).

In Figure (5.1) the ideal Rankine cycle is shown by the dotted outline. The downward curving lines to the right represent isotherms in the superheated vapour region. The effect of various nonidealities has been exaggerated for clarity.

Assuming that the actual system is well insulated, inefficiencies due to heat losses to the environment are negligible. If the pipings are short, the parts where appreciable heat losses could occur are the evaporator and condenser heat exchangers, the expansion valve and the compressor.

The desuperheating, condensation and subcooling which take place from D1' to D2' and D2' to D3' respectively in the condenser heat exchanger is accompanied by a pressure drop and hence a corresponding temperature drop. In a well designed condenser the pressure and temperature drops would be small.

Nevertheless, the latent heat is delivered at a lower temperature and pressure, thus decreasing the (COP) obtainable. In theory, a

relatively large proportion of the condenser surface could be involved in desuperheating. However, in practice desuperheating and condensation take place throughout the heat exchanger. Provided that the temperature and pressure drops are not too large between D1' and D2', the specific volume of the vapour at the means of the temperatures and pressures between these two points may be used to estimate the pressure drop in the desuperheating section.

The evaporation and superheating which take place from S1' to S2 and from S2 to S2' respectively in the evaporator heat exchanger is also accompanied by a pressure drop and corresponding temperature drop. Though these changes are small, they result in the latent heat of vaporisation being absorbed at a slightly lower temperature and pressure. This results in a decrease of (COP) obtainable because the heat which would have been 'lifted' in the compressor and consequently delivered in the condenser is decreased. The required superheat is usually very small (about $3^{o}C$). Furthermore, the temperatures and pressures are lower in the evaporator than the corresponding temperatures and pressures in the condenser. Thus the relative inefficiencies in the evaporator are proportionately smaller than in the condenser.

If the flow of liquid to the expansion valve is smooth, the expansion which takes place in it from D3' to S1' will be almost insenthalpic.

In the compressor, vapour is compressed from S2' to D1'. The energy required in a real compressor will be greater than in an isentropic compressor for two reasons. Firstly, compression takes place in a finite time, and therefore irreversibly. The excess energy appears as heat when the turbulence dies away. Secondly, the volumetric

efficiency is less than unity. Effectively, this means that part of the vapour is repeatedly compressed and hence absorbs energy on each cycle, only some of which is recovered on the expansion stroke. The exact amount of the excess entropy, and hence enthalpy, due to these causes depends on the compressor design and on the thermodynamic properties of the working fluid. The location of point D1' can be established by measurement of the temperature and pressure at the outlet of the compressor.

From the foregoing it could be inferred that the major contribution to the inefficiency of a vapour compression heat pump system is from the compressor.

The performance of a vapour compression heat pump system can be related to an inefficiency factor for the compressor. This factor would vary if the heat pump is operated away from its design specification or is used with a different working fluid. The magnitude of the inefficiencies would depend on the enthalpy per unit volume, the condensing temperature and the temperature lift. The value of the inefficiency is likely to increase as the isothermal enthalpy per unit volume (HPV) decreases; the compressor would transport less quantity of heat per stroke and losses would constitute a greater proportion.

5.1.2 Selection of working fluids

Some representative working fluids are chosen for the empirical evaluation of their performance characteristics in vapour compression heat pump systems. The following thermophysical properties of the fluids are considered:

temperature

condensibility

slope of saturated vapour line

heat of vaporisation per unit volume (HPV)

isothermal ratio of volume of vapour to the volume of liquid (VR)

Working fluids can be classified on the basis of the range of temperature over which they can deliver heat.

low temperature	($50^{o}C$ - $70^{o}C$)
medium temperature	($70^{o}C$ - $140^{o}C$)
high temperature	($140^{o}C$ - $180^{o}C$)
extra-high temperature	($180^{o}C$ - $300^{o}C$)

On compression working fluids may be superheated, wet or saturated depending on whether the slope of the saturated vapour line on the T-S diagram is negative, positive or perpendicular to the entropy axis. These phenomena can be illustrated for Rankine heat pump cycles on a P-H diagram. Figures (5.2) and (5.3) show the Rankine heat pump cycles for R12 and R113 respectively. The working fluids selected for consideration are R11, R12, R113, R114, R718 and R729. Some of their special features are shown below.

working fluid / thermophysical properties	R11	R12	R113	R114	R718	R729
low temperature		X				X
medium temperature	X			X		
high temperature			X			
extra-high temperature					X	
condensible	X	X	X	X	X	
non-condensible						X
negative saturated vapour (T-S) curve		X		X	X	
positive saturated vapour (T-S) curve			X			
perpendicular saturated vapour (T-S) curve	X					

The order of magnitude of the values of (HPV) are R12 > R11 > R114 > R113 > R718. The order of magnitude of the values of (VR) are R12 < R114 < R11 < R113 < R718.

5.1.3 Prediction of performance

The performances of R11, R12, R113, R114, R718 and R729 in vapour compression heat pumps are considered using three heat pump systems. The first one is a closed cycle water-to-water system with a reciprocating compressor. The machine which is code named ICE1 is described in Appendix (A.II). The second system, code named Heat Pump 1, is an open cycle system with a small rotary vane compressor. The third one, code named Heat Pump 2, is an open cycle system with a small reciprocating compressor.

The results of the performance of R12 in ICE1 are used to predict the performances of R11, R114 and R113. The predicted results are then compared with experimental results for R12, R114 and R11 reported by Gutierrez, El-Meniawy, Watson and Holland ["Heat pumps: Part 5 - Operating characteristics of a water-to-water heat pump system using R12", Gutierrez, A.G., El-Meniawy, S.A.K., Watson, F.A. and Holland F.A., Indian Chemical Engineer, XXI(4), 19-26 (October-December 1979)], El-Meniawy, Watson and Holland ["Heat pumps: Part 8 - Operating characteristics of a water-to-water heat pump system using R12B1 and R114", El-Meniawy, S.A.K., Watson, F.A. and Holland, F.A., Indian Chemical Engineer XXLL(3), 3-12 (July-September 1980)] and Ogbeide ["Performance and heat transfer studies on a heat pump system", Ogbeide, S.E., PhD Thesis, University of Salford, Salford, U.K. (1981)] respectively. Experimental results were obtained using R113 in ICE1 as

part of this work.

The results of the performance of R729 in Heat Pump 1 and Heat Pump 2 are used to predict the performance of R718 in the same heat pump systems.

5.2 EXPERIMENTAL OPERATION OF ICE1 USING R113

The preparation of the heat pump system for charging with the required working fluid and the method of calculations have been described by Ogbeide ["Performance and heat transfer studies on a heat pump system", Ogbeide, S.E., PhD Thesis, University of Salford, Salford, U.K., (1981)].

The operation of the heat pump system using R113 as the working fluid posed some problems. As R113 is supplied by the manufacturer in plastic cans, a special vessel had to be fabricated in order to charge the heat pump with R113. The vessel with a capacity of three litres was filled with R113 until it overflowed in order to ensure that no air was present inside the vessel. This was then used to charge the condenser of the heat pump after the whole system had been evacuated. The total charge was about 9 kg.

Once the charging had been completed, water at a temperature of about 60^{0}C was passed through both the condenser and the evaporator to ensure that R113 was vaporised. The compressor was then started and the expansion valve slightly opened. For a particular temperature value at the outlet of the compressor T1, the pressure valve read from the pressure gauge P1 was higher than that obtained from the thermodynamic property tables ["Thermodynamic properties of Arcton 113 SI units", Imperial Chemical Industries Ltd., Imperial Chemical House,

Millbank, London]. Some non-condensibles were suspected and hence the unit was shut down. When the system had cooled down to room temperature, the pressure in the condenser was found to be higher than atmospheric pressure whereas the vapour pressure of R113 at room temperature (about $20^{o}C$) should be lower than atmospheric pressure. This confirmed the presence of non-condensibles. The non-condensibles were bled out and the unit restarted but the same phenomenon was observed again. This led to the suspicion that during start up the low pressure side of the unit was under vacuum due to the insufficient supply of the working fluid. This resulted in air leaking into the system. In order to overcome this problem water was circulated through both the condenser and the evaporator at $60^{o}C$ for a minimum period of three hours to warm up the system and the compressor was started only after the low pressure side reached a definite positive pressure. During the warm up period, the expansion valve was kept in a completely open position. This mode of operation eliminated the problem of air leaking into the system and further experiments were carried out using this method.

5.3 HEAT PUMP 1

5.3.1 Description of Heat Pump 1

Heat Pump 1 is shown schematically in Figure (5.4).

The compressor, Gast model 0740-P106A was an open rotary vane type. It was supplied by Gast Manufacturing Corporation, Michigan, U.S.A. The design compression ratio for air was 2 and its capacity was $3.2 \times 10^{-3}\ m^3 s^{-1}$. The graphite vanes weakened gradually and they got

crushed when the compressor was operated on superheated water vapour at about 110^{o}C. These were later replaced by aluminium vanes.

The compressor was modified for the compression of superheated water vapour by effecting the following:

(1) The washers, bearings and caps on the drive and dead ends were replaced by bearing houses made of brass. An O-ring rubber seal was installed on each bearing housing to prevent the leakage of steam. An oil inlet was provided on each of the bearing housings for the lubrication of the rotor shaft. The lubricant was prevented from flowing into the cylinder by lip seals. A tiny hole at the centre of each of the bearing housings was drilled to drain out the used lubricant.

(2) The air inlet filter was replaced by a T-joint and valves. This made it possible to open or isolate the system from the atmosphere.

The compressor drive was an Alpak 3-phase induction motor with a rated output of 1.5 kW at 50 Hz and 1420 rpm. The motor was supplied by G.E.C. Machines, Rugby, U.K. The speed of the motor was regulated by a hydraulic gear box with a rated output of 0.47 kW at 1420 rpm. The gear box was supplied by Carter Gears Ltd, Bradford, U.K. The shafts of the compressor and the gear box were coupled through a flexible joint.

The superheater consisted of a stainless steel shell containing an aluminium cylinder. Nichrome wire in insulated sleeve was wrapped on the cylinder.

The condenser was made of a cylindrical glass vessel containing a copper coil. The cylinder was 0.68 m tall and 0.26 m in diameter. The coil had a heat transfer area of 0.279 m^2. Cooling water passed through the coil while condensation occured on the outer tube.

A steam trap, model TD3-2 supplied by British Steam Specialists, Salford, U.K. was connected in series with a steel vessel steam trap. The vessel was 0.45 m tall and 0.16 m wide. Either the standard steam trap or the vessel could be bypassed.

5.3.1.1 Instrumentation

Figure (5.4) shows the locations of the instruments on the system.

Temperatures were measured to the nearest 0.1^{o}C using chromel-alumel thermocouples manufactured by BICC Pyrotenax Ltd., U.K. The thermocouples were connected to a digital temperature indicator model 206 type K supplied by Control and Readout Ltd., Worthing, U.K. The thermocouples on the inlet and outlet of the compressor were connected to a chart recorder model 3020 supplied by Chessel Ltd., Sussex, U.K.

Bourden gauges made by Budenberg Ltd., Manchester, U.K. were used to measure pressures. The gauge on the compressor inlet had a range 30 in Hg vacuum to 15 psi (0 to 1.035 bar) readable to $\pm$0.2 psi. The gauges on the compressor outlet and the steam supply line had a range 0 to 60 psi (0 to 4.14 bar) readable to $\pm$0.2 psi. The temperature of the steam was regulated by a pneumatic controller.

The power input to the motor was measured by a wattmeter. The wattmeter had a range 0 to 1.5 kW readable to $\pm$0.005 kW. The speed of the motor was measured using a tacheometer with a range 0 to 200 rpm

readable to ±5 rpm. The power input to the compressor was obtained through a calibration curve. Figure (5.5) shows the calibration curve.

The flow rate of the compressor water vapour was determined by collecting the condensate over a known period of time and weighing it. Similarly, the flow rate of cooling water was obtained by direct weighing. The flow rate of air was measured using a rotameter.

5.3.2 Experimental technique

Preliminary experiments showed that it was necessary to maintain the cylinder of the compressor dry. This ensured that the vanes slided out when the compressor was switched on. Referring to Figure (5.4) the following routine was followed before start up and after shut down:

(1) The liquid in the compressor was drained through valve (V4).

(2) The shaft of the compressor was lubricated through valve (V10).

(3) The cylinder of the compressor was lubricated through valve (V11).

(4) The compressor was operated with air for a minimum of ten minutes to ensure that the cylinder was dry. Then the compressor was stopped.

The system was prepared for the compression of steam by closing valves (V1), (V4), (V10), (V11), either (V5) or (V6) and either (V7) or (V8). All the other valves were left open. Steam was taken into the system from a central supply in the laboratory.

Stable conditions were obtained by controlling the speed of the compressor and by means of the valves (V2) and (V8). The maximum compression ratios were obtained when valve (V8) was almost closed. Compression could not be achieved when the water vapour from the compressor was cooled in the main condenser.

5.4 HEAT PUMP 2

5.4.1 Description of Heat Pump 2

The Heat Pump 2 is shown schematically in Figure (5.5).

The compressor, model PAB10, was an open reciprocating type. It was manufactured by Gast Manufacturing Corporation, Michigan, U.S.A. The design compression ratio for air was 7 and its capacity was $6.1 \times 10^{-4}\ m^3 s^{-1}$. The maximum working pressure was 7 bar.

The compressor was driven by a 3-phase induction motor with a rated output of 0.56 kW at 50 Hz and 1420 rpm. The motor was supplied by Brook Motors Ltd., Huddersfield, U.K. The speed of the motor was controlled by an hydraulic gear box with a rated output of 0.47 kW at 1420 rpm. The gear box was supplied by Carter Gears Ltd., Bradford, U.K. The shafts of the compressor and gear box were coupled through a flexible joint.

The condenser was a cylindrical steel vessel. It was 0.28 m tall and 0.08 m in diameter. A coil of copper tube outside the vessel carried the cooling water.

A cylindrical vessel 0.10 m tall and 0.04 m wide was used to disentrain droplets of water in the steam supply. The steam was then superheated by a 50 W electric heater before it entered the compressor.

5.4.2 Instrumentation

Figure (5.6) shows the locations of the instruments on the system. The instrumentation on this equipment is identical to that already described for Heat Pump 1.

Figure (5.7) shows the calibration curve for the power of the unloaded motor against speed.

5.4.3 Experimental technique

Identical experimental technique described for Heat Pump 1 was used.

5.5 RESULTS AND DISCUSSION

The results from experiments carried out using R113 are presented in Table (5.2). The condensing temperatures were limited by the boiling point of the cooling water which was used as the heat sink. Higher condensing temperatures could be obtained with a coolant having a normal boiling temperature significantly higher than $100^{o}C$.

The values of the total heat losses Q_{LOSS} presented in Table (5.2) were calculated using Equation (5.1).

$$Q_{LOSS} = \frac{(Q_S + W - Q_D)}{Q_S + W} \qquad (5.1)$$

A comparison of the corresponding values of Q_{LOSS} and $(HPE)_R$ shows that the inefficiency of the heat pump system may largely be due to heat losses. It has been shown in section (5.1.1) that the

heat losses may be mainly through the compressor. A comparison of the values of the mean $(HPE)_R$ for R12, R11, R114 and R113 and Figures (4.1), (4.2), (4.10) and (4.13) suggests the following relationships:

$$(\Delta H)_{LOSS} \propto T_{CO}/(HPV) \tag{5.2}$$

$$(\Delta H)_{LOSS} \propto (VR)T_{CO} \tag{5.3}$$

Referring to Figure (5.1), $(\Delta H)_{LOSS}$ is, in theory, obtainable from Equation (5.4).

$$(\Delta H)_{LOSS} = H_{D11'} - H_{D1} \tag{5.4}$$

Actual values of $(\Delta H)_{LOSS}$ can be computed from the relation

$$(COP)_A \approx \frac{H_{D1} - H_{D3}}{H_{D1} - H_{S2} + (\Delta H)_{LOSS}} \tag{5.5}$$

Similarly, the efficiency of the compressor η_c could be estimated using the relation

$$(COP)_A \approx \frac{H_{D1} - H_{D3}}{(H_{D1} - H_{S2})/\eta_c} \tag{5.6}$$

In order to predict the performance of different working fluids in the ICEI heat pump, the performance data for R12 were used as the basis since the machine was designed for R12. The values of $(\Delta H)_{LOSS}$ and η_c, calculated using Equations (5.5) and (5.6) for a range of gross temperature lifts $(T_{CO}-T_{EV})$ are presented in Table (5.3). The experimental results presented by Gutierrez, El-Meniawy, Watson and

Holland ["Heat pumps: Part 5 - Operating characteristics of a water-to-water heat pump system using R12", Gutierrez, A.G., El-Meniawy, S.A.K., Watson, F.A. and Holland, F.A., Indian Chemical Engineer, XXI(4), 19-26 (October-December 1979)] were used in the computations. The values of H_{D1} were obtained using Equation (5.7).

$$H_{D1} = H_{D2} + (\phi_{S2} - \phi_{D2})T_{CO} \qquad (5.7)$$

The values of H_{D3}, H_{S2}, ϕ_{S2} and ϕ_{D2} in Equations (5.5) to (5.7) were obtained from published tables ["Thermodynamic properties of Arcton 12 SI units", Imperial Chemical Industrial Ltd., Imperial Chemical House, Millbank, London].

For a mean gross temperature lift of 35°C and a condensing temperature of 56°C, it is seen from Table (5.3) that the value of $(\Delta H)_{LOSS}$ for R12 is 5.516 kJ kg^{-1} (292.31 kJ m^{-3}). The volumetric throughput of the compressor in the ICE1 heat pump is constant for any working fluid. Therefore for given values of T_{CO} and $(T_{CO}-T_{EV})$, the volumetric heat loss from the system should be the same irrespective of the working fluid. It was assumed that the volumetric heat loss is 292.31 kJ m^{-3} when the ICE1 heat pump is operated with any working fluid at T_{CO} = 56°C and $(T_{CO}-T_{EV})$ = 35°C. Based on this assumption the average values of η_c for R11, R114 and R113 were computed using Equation (5.8)

$$\eta_c = \frac{H_{D1} - H_{S2}}{H_{D1} - H_{S2} + (\Delta H)_{LOSS}} \qquad (5.8)$$

and presented in Table (5.4). The condensing temperatures for R11 and R114 are those reported by Ogbeide ["Performance and heat transfer

studies on a heat pump system", Ogbeide, S.E., PhD Thesis, University of Salford, Salford, U.K. (1981)] and El-Meniawy, Watson and Holland ["Heat pumps: Part 8 - Operating characteristics of a water-to-water heat pump system using R12B1 and R114", El-Meniawy, S.A.K., Watson, F.A. and Holland, F.A., Indian Chemical Engineer, XXLL(3), 3-12 (July-September 1980)] respectively. The value of T_{CO} for R113 is that obtained experimentally for this work. The value of H_{D1} for R113 was computed from Equations (5.9) and (5.10)

$$\emptyset_{D1} = \emptyset_{D3}X + \emptyset_{D2}(1-X) \qquad (5.9)$$

$$H_{D1} = H_{D3}X + H_{D2}(1-X) \qquad (5.10)$$

where X is the liquid fraction of wet vapour of D1.

The subscripts in Equations (5.9) and (5.10) refer to those in Figure (5.3).

Predicted coefficients of performance $(COP)_P$ were obtained from Equation (5.11)

$$(COP)_P = \frac{H_{D1} - H_{D3}}{(H_{D1} - H_{S2})/\eta_c} \qquad (5.11)$$

Figures (5.8) and (5.10) are plots of (COP) against $(T_{CO}-T_{EV})$ for R12 and R114, R113 and R11 respectively. The 'best fit' $(COP)_A$ curves are represented by the following equations:

R12

$$(COP)_A = \left[0.0348 + 3.912 \times 10^{-3} (T_{CO}-T_{EV})\right]^{-1} \quad (5.12)$$

mean error = 0.71 per cent

standard deviation of error = 6.11 per cent

R11

$$(COP)_A = \left[0.06144 + 3.7334 \times 10^{-3} (T_{CO}-T_{EV})\right]^{-1} \quad (5.13)$$

mean error = 0.11 per cent

standard deviation of error = 6.32 per cent

R114

$$(COP)_A = \left[0.0855 + 3.787 \times 10^{-3} (T_{CO}-T_{EV})\right]^{-1} \quad (5.14)$$

mean error = 0.56 per cent

standard deviation of error = 7.54 per cent

Table (5.4) shows the experimental values of $(HPE)_R$ and η_c. Within the limits of experimental error these values are in good agreement for each of the working fluids considered. It has been shown by Gutierrez, El-Meniawy, Watson and Holland [1979] that the experimental values of $(HPE)_R$ may be used in conjunction with the thermophysical properties of a working fluid to design a heat pump. It should also be possible to use the values of η_c for design.

The errors between $(COP)_P$ and $(COP)_A$ and the standard deviations of the errors are shown in Table (5.4). These errors are within the

same range as those presented for $(COP)_A$. Figures (5.8) to (5.10) show the plots of $(COP)_A$ and $(COP)_P$ against gross temperature lift. It can be seen that the values of $(COP)_P$ and $(COP)_A$ are in good agreement between $(T_{CO}-T_{EV})$ = 25°C and $(T_{CO}-T_{EV})$ = 45°C.

The results from the experimental investigations carried out with R729 in Heat Pumps 1 and 2 are presented in Figure (5.11). The results from the experiments carried out with R718 in the systems and the predicted results are presented in Table (5.5). The predictions for R718 were based on the experimental results for R729. Table (5.5) shows that the gross temperature lifts obtained for the compression of steam are about 8°C. The values of the compression ratio (CR) and heat pump effectiveness $(HPE)_R$ were about 1.3 and 0.2 respectively. It is significant to note that similar performance data were obtained in the two heat pump systems even though different compressors with different design (CR) values were used. However, both compressors were very small. The poor performances of the two machines with water could be due to heat losses. It has been shown previously that water vapour has relatively low values of isothermal (HPV) compared with other working fluids. In a heat pump with a small capacity, any heat loss would constitute a relatively high proportion of the total heat transported. In the extreme, this phenomenon might lead to condensation in the compressor, resulting in serious mechanical inefficiency. Operations at higher temperatures where the values of (HPV) are higher could be useful. However, the capacity of the heat pump may be more important.

It can be seen from Table (5.5) that the corresponding values of $(HPE)_R$ and η_c are in good agreement. The values of η_c may be used in

the design of heat pumps.

5.6 CONCLUSIONS

The inefficiency in a vapour compression heat pump appears to be due mainly to heat losses through the compressor. The values of η_c for the compressor of the ICEI heat pump, determined on this basis are similar to the corresponding values of $(HPE)_R$ for R12, R11, R114 and R113.

The values of $(COP)_P$ are in good agreement with the values of $(COP)_A$. The values of η_c may be used instead of $(HPE)_R$ to design a heat pump. Based on experimental results for one fluid, values of η_c may be obtained for others.

For a given heat pump the values of η_c decrease as the values of the isothermal (HPV) for the working fluid decreases. High temperature working fluids with low values of (HPV) are likely to have poor performances in small compressors.

Further work is required to establish the design requirements of compressors for water vapour and other high temperature working fluids.

5.7 RECOMMENDATIONS

It is recommended that an absorption heat pump and a mechanical vapour compression system of the same capacity and same delivery temperature be built and operated using water. It is expected that the performance of the absorption heat pump would be better than that of the mechanical vapour compression system.

ASHRAE code	chemical name	chemical formula
R11	trichloromonofluomethane	CCl_3F
R12	dichlorodifluoroethane	CCl_2F_2
R12B1	monochloromonobromodifluoroethane	$CClBrF_2$
R113	trichlorotrifluoroethane	CCl_2FCClF_2
R114	dichlorotrifluoroethane	$CClF_2CClF_2$
R718	water	H_2O
R729	air	-

TABLE (5.1) CHEMICAL NAMES AND FORMULAE FOR SOME WORKING FLUIDS

run number	T_{CO} ^{o}C	$(T_{CO}-T_{EV})$ ^{o}C	Q_D kW	Q_S kW	W kW	Q_{LOSS} dimensionless	$(COP)_A$	$(HPE)_R$	$(HPE)_C$
1	72.9	22.4	2.31	3.05	0.52	0.35	4.44	0.312	0.287
2	73.6	22.8	2.47	3.05	0.57	0.32	4.35	0.311	0.286
3	78.9	24.9	2.53	3.48	0.61	0.38	4.13	0.322	0.292
4	79.2	25.1	2.68	3.48	0.62	0.35	4.32	0.339	0.308
5	82.4	33.0	2.18	3.05	0.61	0.41	3.56	0.375	0.220
6	87.9	34.9	2.36	3.26	0.64	0.40	3.67	0.408	0.355
7	92.0	36.5	2.54	3.85	0.69	0.44	3.66	0.425	0.366
8	92.5	36.8	2.52	3.46	0.68	0.39	3.71	0.434	0.373
9	94.9	36.3	2.79	3.67	0.74	0.37	3.75	0.430	0.376

TABLE 5.2 PERFORMANCE DATA FOR ICE1 WITH R113 AS THE WORKING FLUID

T_{EV} ^{o}C	$(T_{CO}-T_{EV})$ ^{o}C	$(\Delta H)_{LOSS}$ kJ kg^{-1}	$(\Delta H)_{LOSS}$ kJ m^{-3}	$(COP)_A$	η_c
31.0	25	5.328	320.216	7.50	0.66
21.0	35	5.516	292.315	5.75	0.73
11.0	45	5.512	256.917	4.65	0.79
1.0	55	4.879	200.023	3.95	0.84
-9.0	65	4.121	147.440	3.42	0.89

TABLE 5.3 HEAT LOSSES AND EFFICIENCIES OF ICE1 COMPRESSOR OPERATING ON R12 AT A CONDENSING TEMPERATURE OF $56^{o}C$

working fluid	R12	R11	R114	R113
mean T_{CO}, ^{o}C	56.0	83.0	62.0	84.0
mean $(HPE)_R$	0.77	0.53	0.59	0.37
η_c	0.73	0.52	0.54	0.35
$(HPE-\eta)_R$	0.03	0.01	0.05	0.02
mean error of $(COP)_p$, per cent	0.26	-5.49	-5.33	-5.34
standard deviation of error, per cent	8.70	12.39	14.24	9.09

TABLE 5.4 PERFORMANCE FACTORS AT GIVEN MEAN CONDENSING TEMPERATURES FOR R12, R11, R114 and R113

type of heat pump	T_{CO} °C	$(T_{CO}-T_{EV})$ °C	P_{CO} bar	(CR)	Q_D kW	W kW	$(\Delta H)_{Loss}$ kJ kg^{-1}	$(COP)_A$	$(COP)_P$	$(HPE)_R$	η_c
heat pump 1	116.5	8.0	1.772	1.305	1.175	0.148	145.3	7.9	11.7	0.163	0.242
	111.1	8.0	1.482	1.311	1.128	0.113	174.4	10.0	10.2	0.209	0.213
heat pump 2	113.5	8.7	1.599	1.341	0.516	0.015	165.3	10.4	10.4	0.236	0.237
	109.0	6.9	1.386	1.256	0.207	0.020	181.5	10.4	10.2	0.189	0.185

TABLE 5.5 PERFORMANCE DATA FOR HEAT PUMP 1 AND HEAT PUMP 2 WITH R718 AS WORKING FLUID

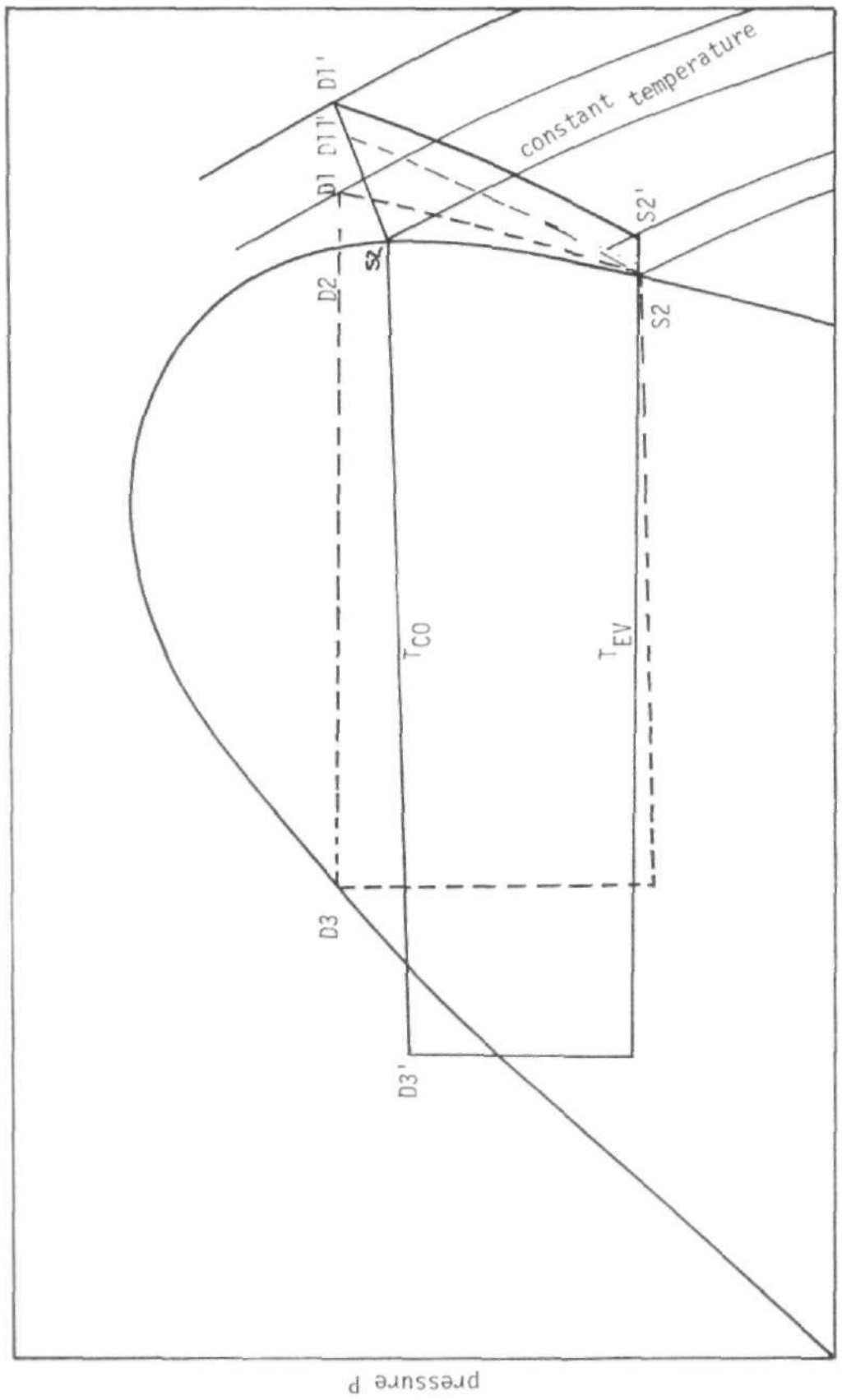


FIGURE (5.1) NON-IDEAL RANKINE CYCLE

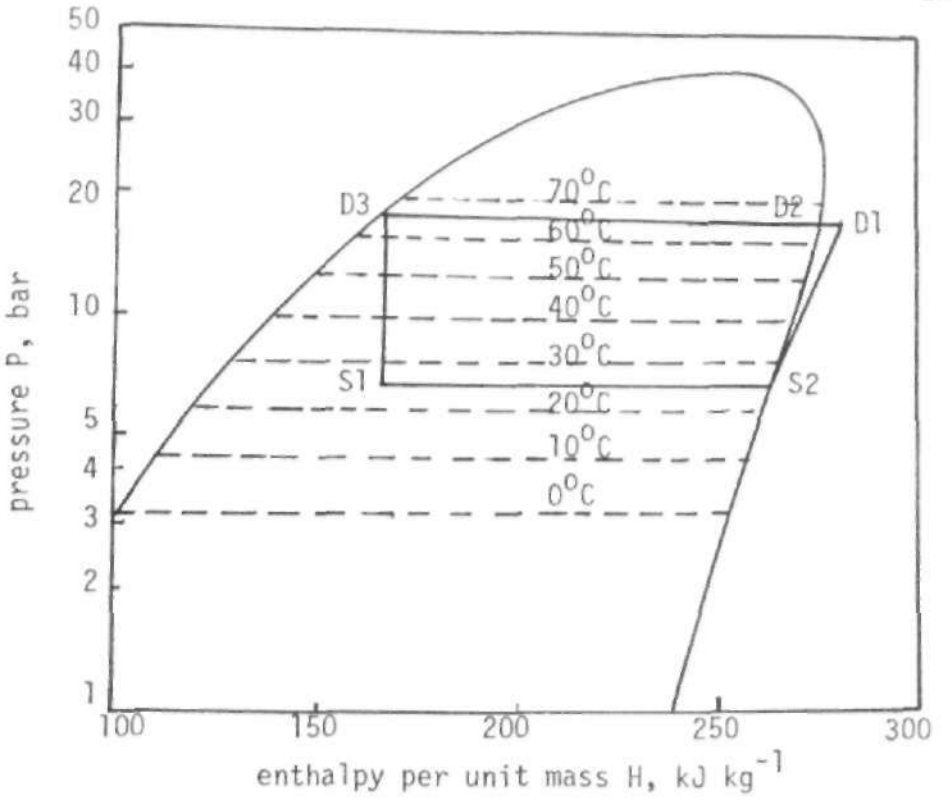


FIGURE (5.2) PRESSURE AGAINST ENTHALPY PER UNIT MASS FOR R12

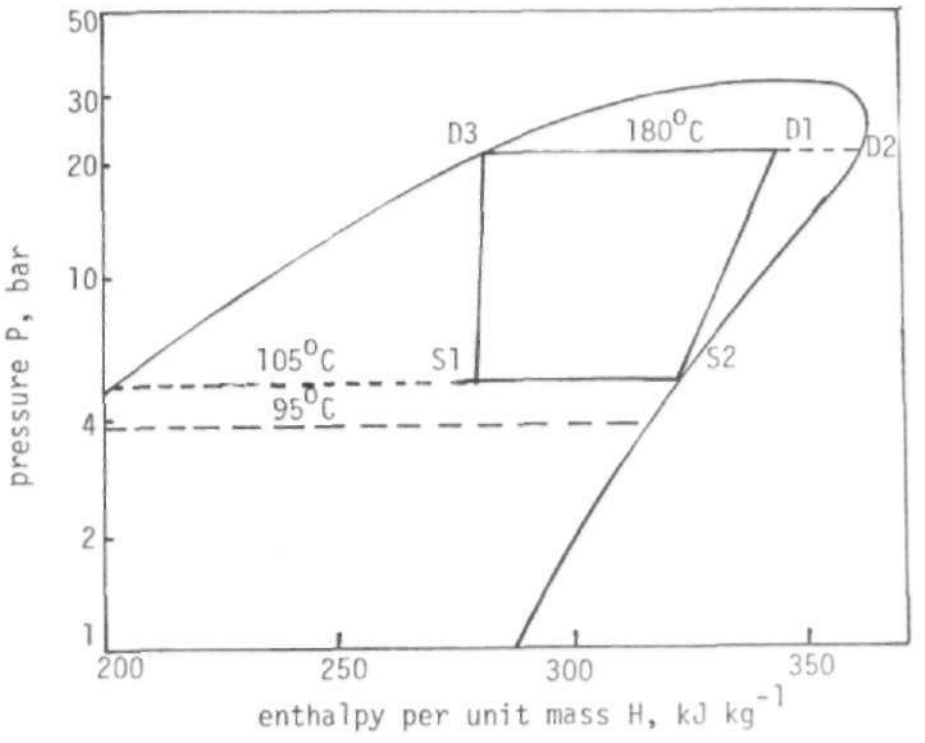


FIGURE (5.3) PRESSURE AGAINST ENTHALPY PER UNIT MASS FOR R113

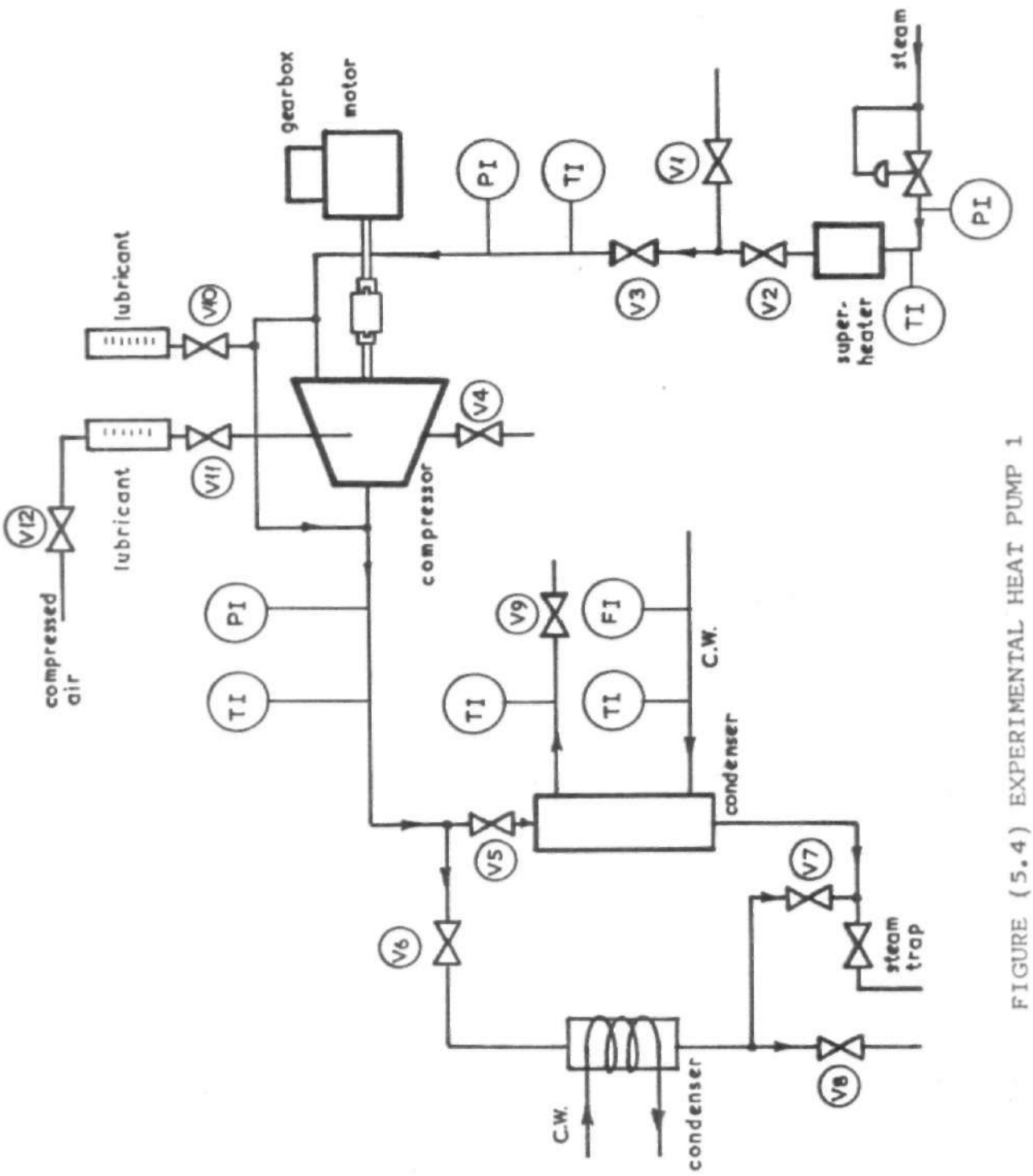
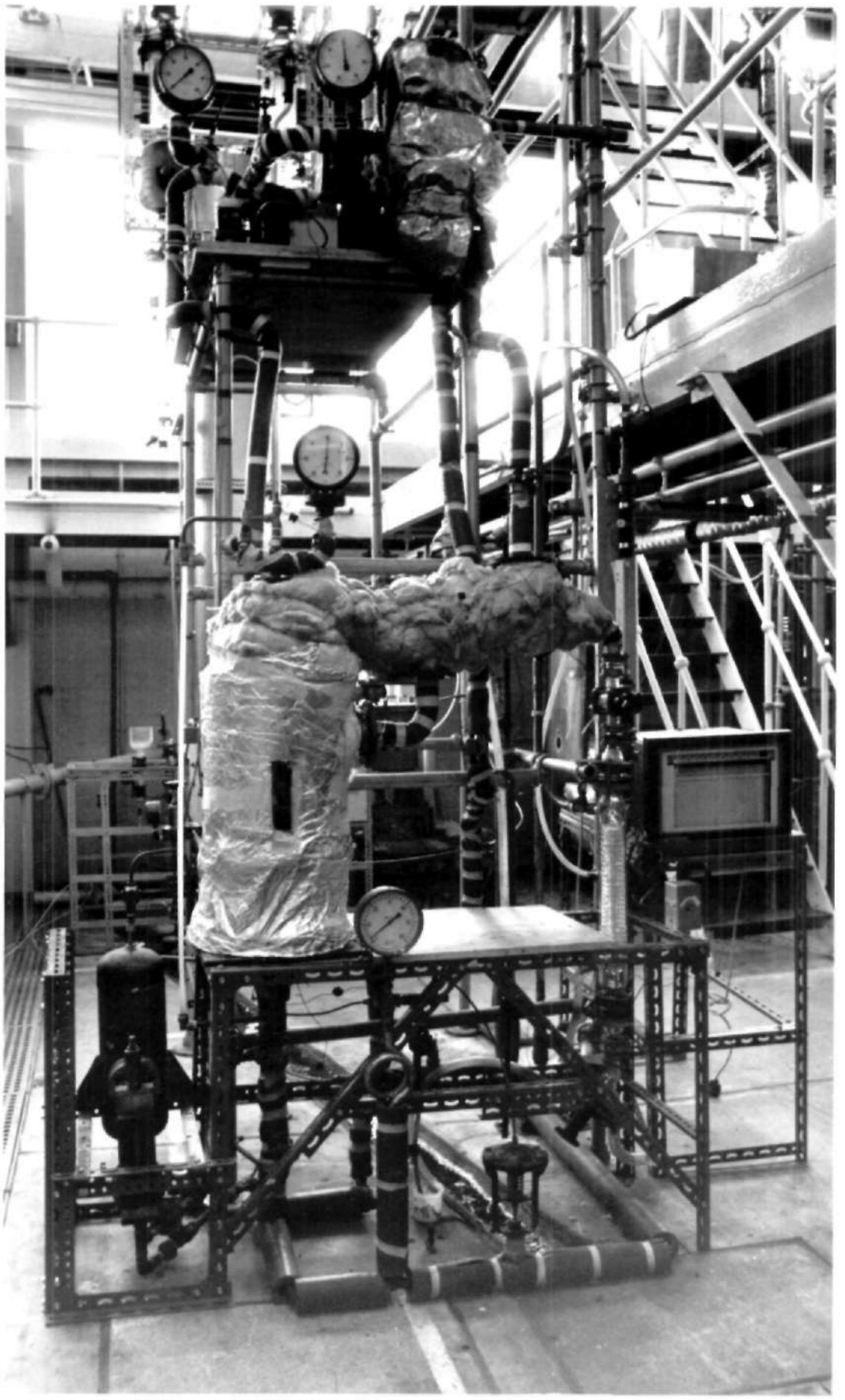


FIGURE (5.4) EXPERIMENTAL HEAT PUMP 1



EXPERIMENTAL HEAT PUMP 1

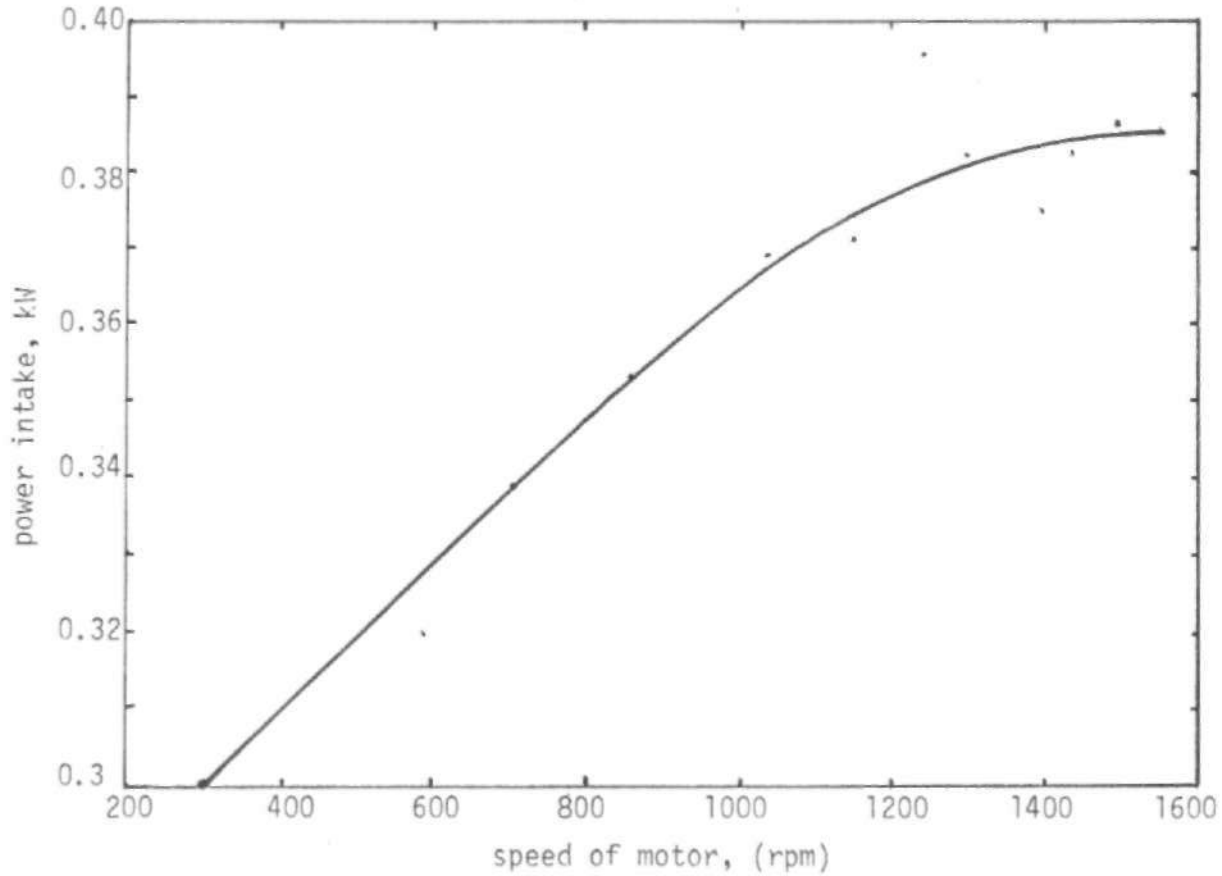


FIGURE (5.5) POWER INTAKE AGAINST SPEED FOR THE UNLOADED MOTOR AND GEAR BOX FOR HEAT PUMP 1

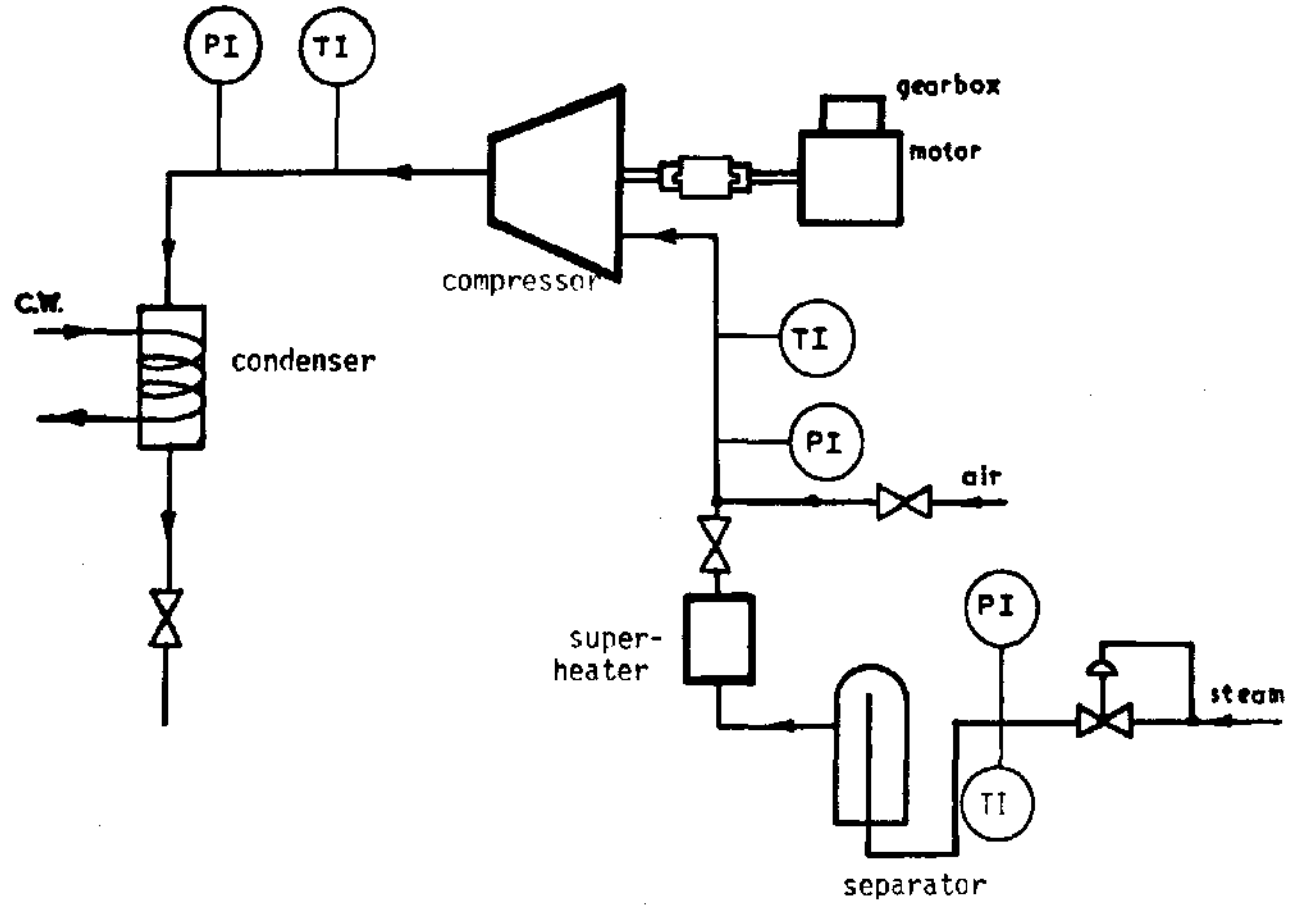
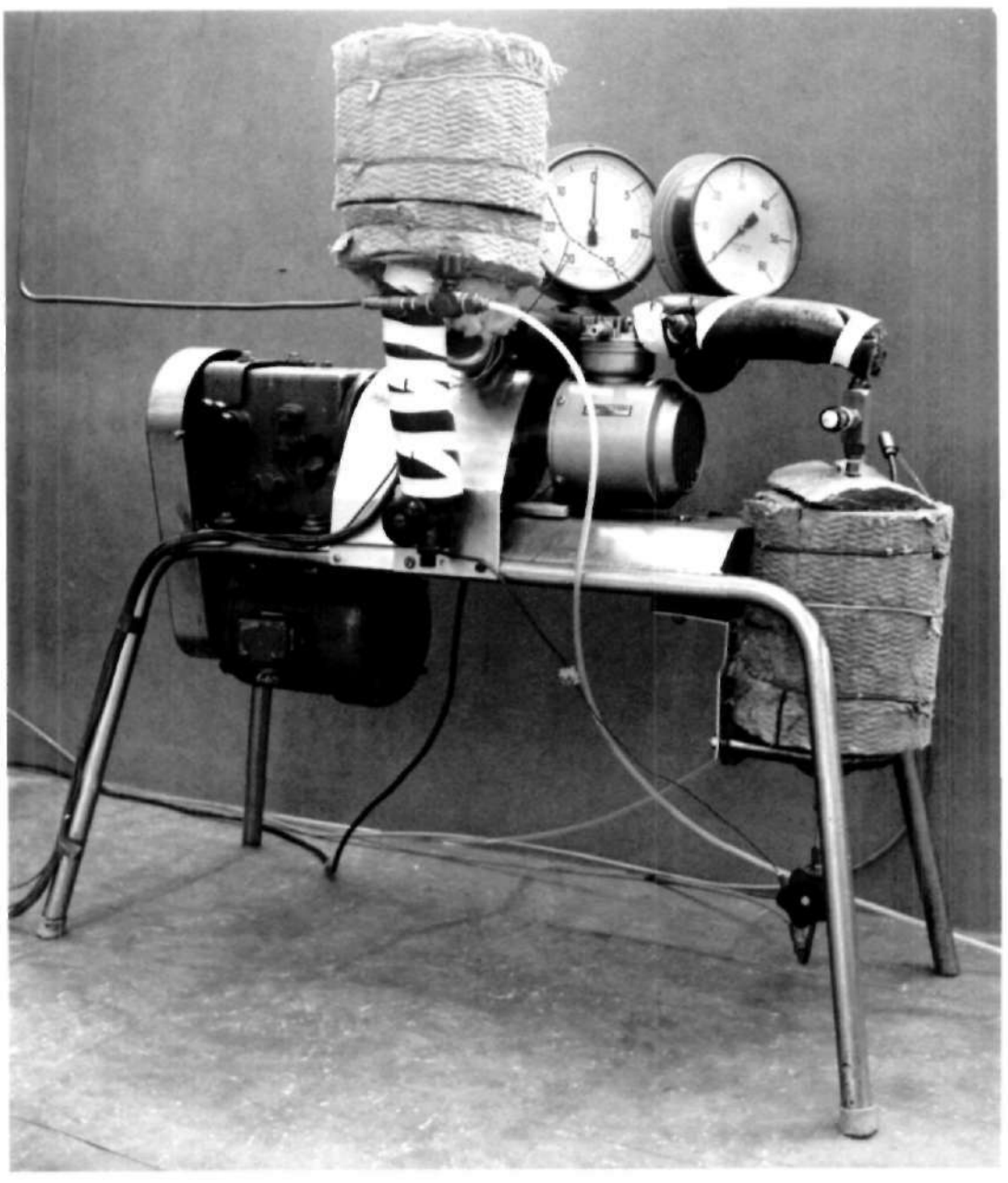


FIGURE (5.6) — EXPERIMENTAL HEAT PUMP 2



EXPERIMENTAL HEAT PUMP 2

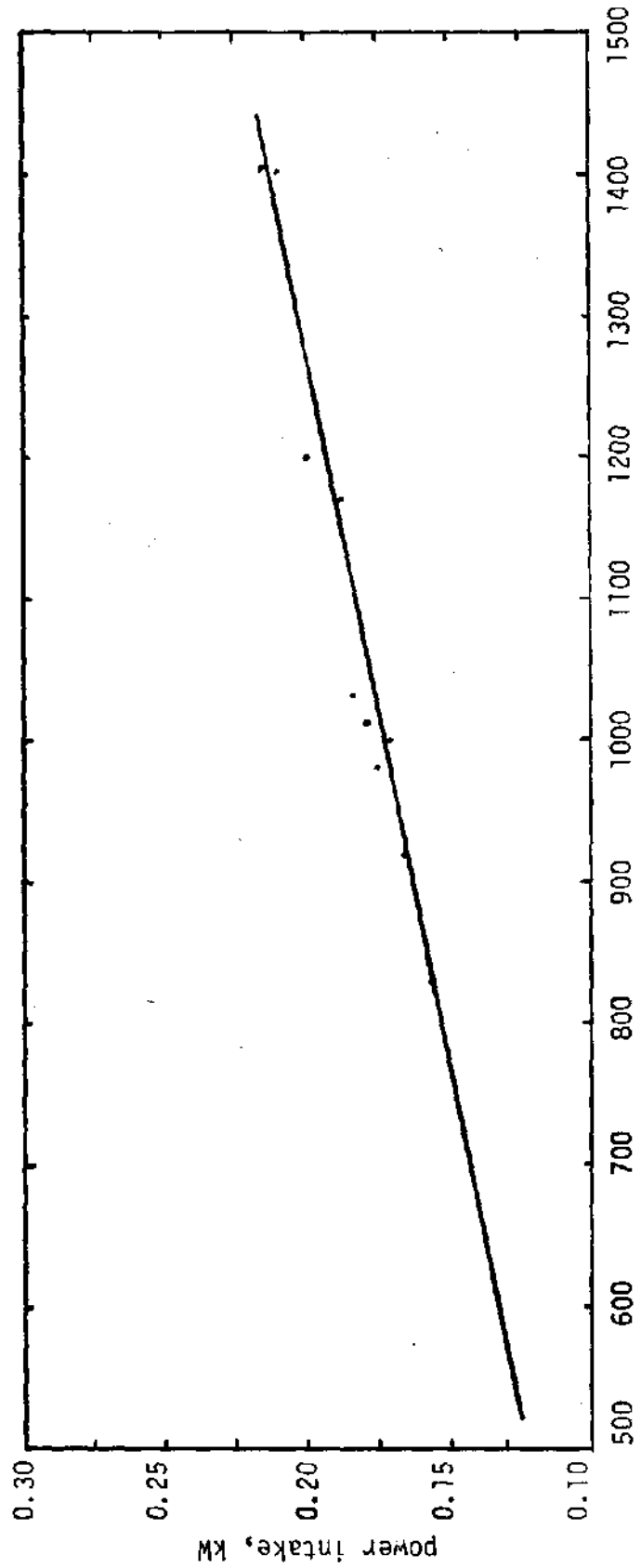


FIGURE (5.7) POWER INTAKE AGAINST SPEED FOR THE UNLOADED MOTOR AND GEAR BOX FOR HEAT PUMP 2

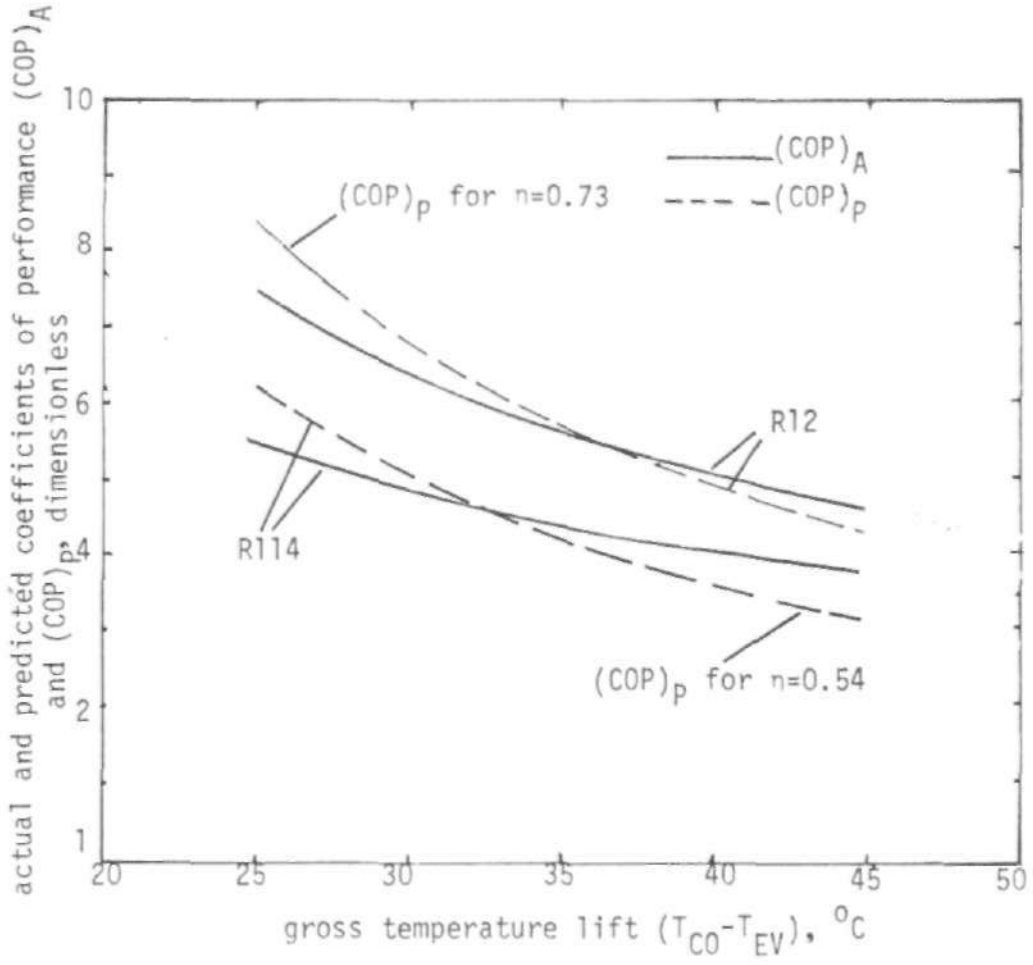


FIGURE (5.8) ACTUAL AND PREDICTED COEFFICIENTS OF PERFORMANCE AGAINST TEMPERATURE LIFT AT MEAN T_{CO} = 56^oC FOR R12 AND AT MEAN T_{CO} = 62^oC FOR R114.

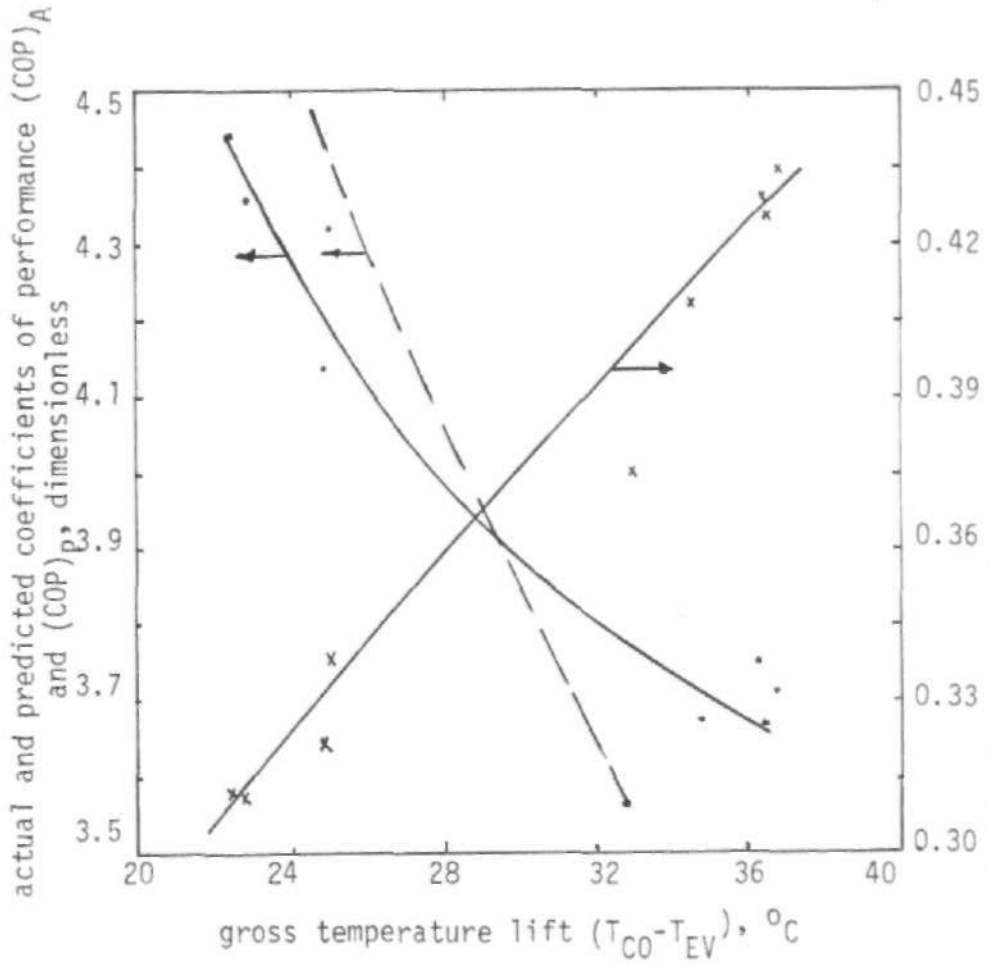


FIGURE (5.9) ACTUAL AND PREDICTED COEFFICIENTS OF PERFORMANCE . AND RANKINE HEAT PUMP EFFECTIVENESS FACTOR AGAINST TEMPERATURE LIFT AT MEAN T_{CO} = 84^oC FOR R113

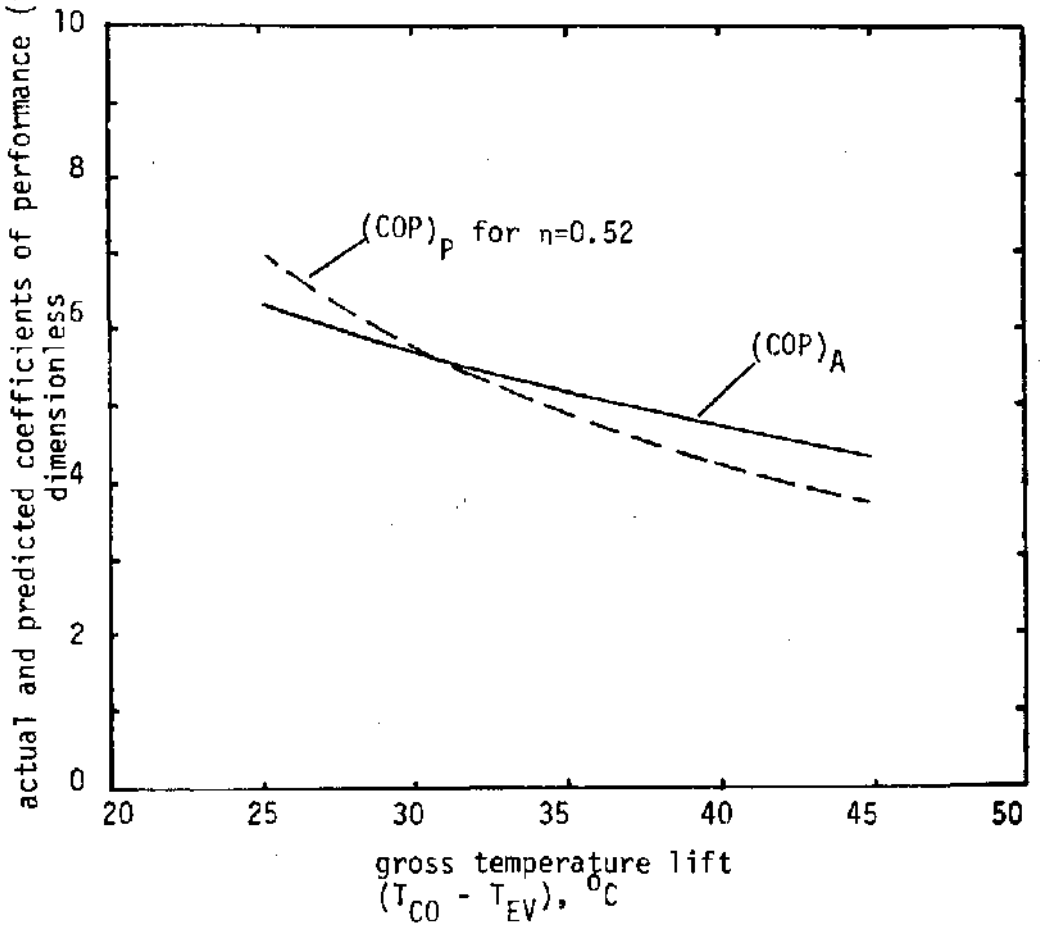


FIGURE (5.10) ACTUAL AND PREDICTED COEFFICIENTS OF PERFORMANCE AGAINST TEMPERATURE LIFT AT MEAN T_{CO} = 83^{o}C for R11

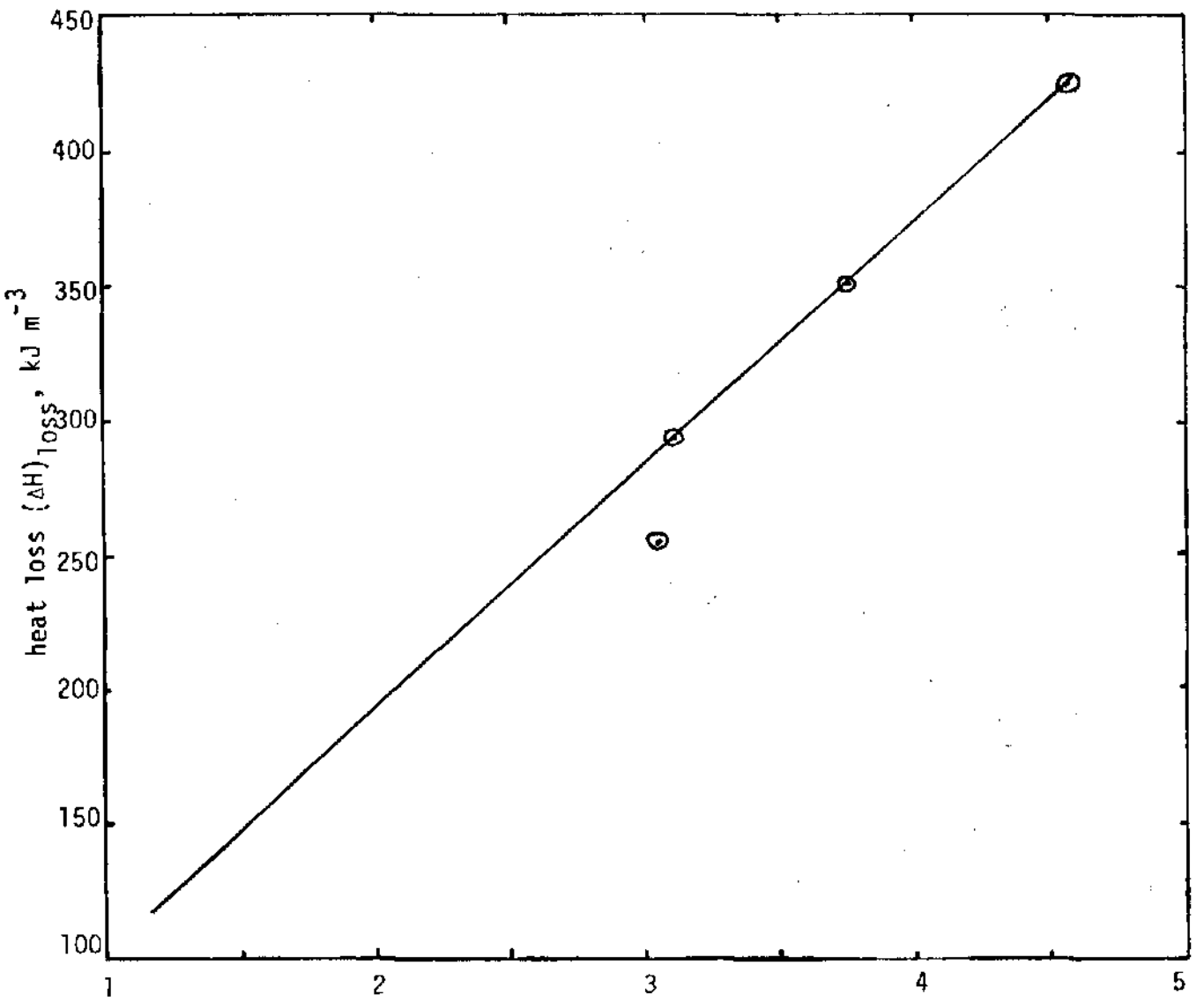


FIGURE (5.11) HEAT LOSS AGAINST COMPRESSION RATIO FOR A RECIPROCATING COMPRESSOR AND A ROTARY VANE COMPRESSOR FOR OUTLET TEMPERATURE OF 59^{o}C FOR R729

CHAPTER 6

ENTHALPY-CONCENTRATION-TEMPERATURE RELATION FOR WATER-LITHIUM BROMIDE SOLUTIONS

CHAPTER 6

ENTHALPY-CONCENTRATION-TEMPERATURE RELATION FOR WATER-LITHIUM BROMIDE SOLUTIONS

6.1 INTRODUCTION

Accurate enthalpy-concentration-temperature data of aqueous solutions of lithium bromide are required in order to develop and evaluate absorption heat pumps for the production of heat at temperatures above 180°C. The enthalpy data of aqueous solutions of lithium bromide currently available, were conceived in order to evaluate the suitability of water as a working fluid and the suitability of aqueous solutions of lithium bromide for use in absorption cooling machines. ["Absorption cooling process", Ellington, R.T., Kunst, G., Peck, R.E., Institute of Gas Technology, Chicago, Illinois, Research Bulletin 14 (1957)], ["Enthalpy-concentration diagram for lithium bromide-water solutions for calculating absorption cooling machines", Rozenfeld, L.M. and Karnaukh, M.C., Kholodilnaya Teknika (1), 37-42 (1958)], ["Thermodynamic and physical properties of aqueous lithium bromide solutions", Lower, H., Kaltetechnik, 13(5), 178-183 (1961)], ["Studies on the lithium bromide-water absorption refrigerating machine", Uemura, T. and Hasaba, S., Technical Report of Kansai University 6, 31-35 (1964)], ["Thermodynamic diagrams of lithium bromide-water solution", Usyukin, I.P., Kholodilnaya Teknika 46(1), 25-29 (1969)], [ASHRAE Handbook 1977 Fundamentals and Product Directory, American Society of Heating, Refrigerating and Air Conditioning Engineers, New York, 18.81-16.82 (1977)], ["Thermodynamic diagrams of solutions of lithium bromide",

McNeely, L.A., ASHRAE Transactions, 85(1), 413-434 (1979)].

The most comprehensive enthalpy-concentration-temperature data for aqueous solutions of lithium bromide available in the literature are those of McNeely ["Thermodynamic properties of aqueous solutions of lithium bromide", McNeely, L.A., ASHRAE Transactions, 85(1), 413-434 (1979)]. The data were presented in graphical and tabular forms covering the concentration range 0-70 per cent by weight of lithium bromide and the temperature range 0-180°C. McNeely presented the data for the solutions in the concentration and temperature ranges 45-70 per cent and 5-180°C respectively as Equations (6.1) to (6.4).

$$H = 2.326 \left[A + B\,(1.8T + 32) + C\,(1.8T + 32)^2\right] \qquad (6.1)$$

for $45 < x < 70$ per cent, $5 < T < 180^{o}C$

$$A = -1.0150E3 + (7.95387E1)X - 2.358016X^2 + (3.031583E-2)X^3 - (1.400261E-4)X^4 \qquad (6.2)$$

$$B = 4.68108 - (3.037766E-1)X + (8.44845E-3)X^2 - (1.047721E-4)X^3 - (4.80097E-7)X^4 \qquad (6.3)$$

$$C = -4.9107E-3 + (3.83184-4)X - (1.078963E-5)X^2 + (1.3152E-7)X^3 - (5.897E-10)X^4 \qquad (6.4)$$

The basis of McNeely's calculations is that Duhring's rule is valid within the concentration and temperature ranges considered. Duhring's rule states that the plot of the boiling temperatures of solutions against the corresponding saturation temperatures of the solvent at the same corresponding pressures is a straight line. In

the derivation of the equation of the Duhring line from the Clapeyron Equation, McNeely assumed that the volume of water in the liquid state was negligible compared with its volume in the vapour state at the same temperature. McNeely used the vapour pressure data in the International Critical Tables ["The International Critical Tables", III, 369, McGraw-Hill Book Company, New York, (1968)] and the data of the Dow Chemical Company [ACG Data Book, A-10-5, Dow Chemical Company, USA] to obtain the coefficients of the Duhring Equation for solutions below 45 per cent lithium bromide. Above 45 per cent lithium bromide, we used the vapour pressure data of Pennington ["How to find accurate vapour pressures of lithium bromide-water solutions", Pennington, W., Refrigerating Engineering, 63, 57-61 (1955)] and Lower ["Thermodynamic and physical properties of aqueous lithium bromide solutions", Lower, H., Kaltetechnik, 13(5), 1978-183 (1961)].

McNeely ["Thermodynamic properties of aqueous solutions of lithium bromide", McNeely, L.A., ASHRAE Transactions, 85(1), 413-434 (1979)] employed the method developed by Haltenberger ["Enthalpy-concentration charts for vapour pressure data", Haltenberger, W. (Jr), Industrial and Engineering Chemistry, 31(6), 783-786 (1939)], using the coefficients of the Duhring Equation plus the heat capacity for a single concentration over the range of temperatures desired in order to obtain enthalpy-concentration-temperature data. The heat capacity used in the calculations was that of a 50 per cent aqueous solution of lithium bromide. It was assumed to be constant at 0.531 kJ kg^{-1} $^{o}C^{-1}$ over the temperature range considered in the calculations.

In this thesis, enthalpy-concentration temperature data have been obtained for solutions of lithium bromide in the concentration

and temperature ranges 50-68 per cent lithium bromide and 60-220°C respectively. The general method adopted by McNeely was employed in the calculations. However, the vapour pressure data of Boryta, Maas and Grant ["Vapour pressure-temperature-concentration relationships for system lithium bromide and water (40-70 per cent lithium bromide)", Boryta, D.A., Maas, A.J. and Grant, C.B., Journal of Chemical and Engineering Data, 20(3) (1975)] were used to determine the dew point temperatures in the Duhring Equation. This is because these data are superior to all others since they were experimentally obtained compared with the mainly extrapolated data in the literature. Moreover, the data are available in the required concentration and temperature ranges. Furthermore, the volume of liquid water was calculated and included in the Clapeyron Equation for the determination of the Duhring coefficient. The heat capacity of 50 per cent lithium bromide solution was considered to vary with temperature. The heat capacity-concentration-temperature equations presented by Uemura and Hasaba ["Studies on the lithium bromide-water absorption refrigerating machine", Uemura, T. and Hasaba, S., Technical Report of Kansai University 6, 31-35 (1964)] were used. Uemura and Hasaba's equations are

$$C_p = A + BT + CT^2 \qquad (6.5)$$

for $10 < X < 66.2$ per cent, $25^{\circ}C < T < 130^{\circ}C$.

Where

$$A = 1.098 - 1.529E\text{-}2 + 6.220E\text{-}5X^2 \qquad (6.6)$$

$$B = - 3.651E\text{-}3 + 4.204E\text{-}5X \qquad (6.7)$$

$$C = 3.576E\text{-}5 - 4.238E\text{-}7X \qquad (6.8)$$

where the units of C_p are cal. $g^{-1}\ {}^{o}C^{-1}$. They stated that observed data show about 2 per cent mean deviation from Equations (6.5) to (6.8).

The results of the calculations based on the assumptions in this study were correlated with bivariate polynomials. The enthalpy-concentration-temperature equation for solutions was to the second degree in temperature and to the fourth degree in concentration of the solutions. The temperature of solutions-concentration-dew point temperature relation was to the first degree in dew point temperature and to the third degree in concentration of the solutions. The polynomials were represented in double Chebyshev series form, with arguments XCAP and tCAP which can be written as

$$H = \sum_{i=0}^{4} \sum_{j=0}^{2} A_{i,j}\, T_i\,(XCAP)\, T_j\,(tCAP) \qquad (6.9)$$

$$T = \sum_{i=0}^{3} \sum_{j=0}^{1} A_{i,j}\, T_i\,(XCAP)\, T_j\,(tCAP) \qquad (6.10)$$

where T_i (XCAP) is the Chebyshev polynomial of the first kind of degree in i with argument XCAP, and T_j is similarly defined.

For the enthalpy-concentration-temperature relations for the solutions, XCAP and tCAP are transformed concentrations and temperatures of the solutions, and the Chebyshev coefficients of the fit are presented in Table (6.1). Similarly, for the temperature of solutions-concentration-dew point temperature equation, XCAP and tCAP are transformed concentrations of solutions and dew point

temperature, and the Chebyshev coefficients of the fit are presented in Table (6.2).

6.2 THE DUHRING EQUATION

The Duhring relation can be derived from the Clapeyron equation. The Clapeyron equation is stated for unit weight of the solution and solvent, as in Equations (6.11) and (6.12) respectively.

$$\frac{dp_s}{dT} = \frac{\lambda}{T\Delta V} \tag{6.11}$$

$$\frac{d(p_s)_W}{dT_W} = \frac{\lambda_W}{T_W\Delta V_W} \tag{6.12}$$

where T is the temperature in degrees Kelvin.

If the properties of the solutions and water are compared at constant pressure, that is $p_s = (p_s)_W$ and Equation (6.12) is divided by Equation (6.11) then,

$$\frac{dT}{dT_W} = \frac{\lambda_W}{\lambda}\frac{T\Delta V}{T_W\Delta V_W} = A \tag{6.13}$$

where T is the temperature in degrees Kelvin.

Since the differential of T in degrees Kelvin is identical to the differential of T in degrees Centigrade

$$\frac{dT}{dT_W} = \frac{\lambda_W T\Delta V}{\lambda T_W\Delta V_W} \tag{6.14}$$

The Duhring relation, in this case, can be represented by Equation (6.15)

$$T = AT_W + B \tag{6.15}$$

Differentiating Equation (6.15) yields

$$\frac{dT}{dT_W} = A \tag{6.16}$$

By comparing Equations (6.13), (6.14) and (6.16) it is clear that the constant A in them is the same as the constant A in the Duhring equation, i.e. Equation (6.15), if the data plots as a straight line.

In this work, it was considered that the liquid volume is significant compared with the vapour volume in Equations (6.11) to (6.13). McNeely ["Thermodynamic diagrams of solutions of lithium bromide", McNeely, L.A., ASHRAE Transactions, 85(1), 413-434 (1979)] assumed that the liquid volume is negligible in comparison with its volume in the vapour phase. The validity for the assumption is evident from the ratio of the volume of water in the vapour phase to its volume in the liquid phase (VR) presented in Figures (4.9) to (4.12).

Equation (6.15) is used to determine the dew point temperatures T_W of solutions of lithium bromide at different known concentrations and temperatures. If the graph of dew point temperatures and corresponding solution temperatures is a straight line, then the slope is A in the relation between the Clapeyron and the empirical Duhring equations.

6.3 VAPOUR PRESSURE DATA

The determination of the true value of the Duhring equation is important in the determination of the precise value of the enthalpy of solutions of lithium bromide. It is therefore necessary to use accurate vapour pressure data to obtain dew point temperatures of the solutions.

The vapour pressure-concentration-temperature data of Boryta, Maas and Grant ["Vapour pressure-temperature-concentration relationship for system lithium bromide and water (40-70 per cent lithium bromide), Boryta, D.A., Maas, A.J. and Grant, C.B., Journal of Chemical and Engineering Data, 20(3) (1975)] cover the widest ranges of concentration and temperatures among those available in the literature. Experimentally determined pressure-concentration-temperature data of Boryta, Maas and Grant are in the concentration and temperature ranges of 40-70 per cent lithium bromide and 25-180^{o}C respectively. The experimentally determined pressure-concentration-temperature data of Uemura and Hasaba ["Studies on the lithium bromide-water absorption refrigerating machine", Uemura, T. and Hasaba, S., Technical Report of Kansai University, Japan, 6, 31-35 (1964)] cover the ranges of concentrations and temperatures 34-65 per cent lithium bromide and 20-160^{o}C respectively. The latter data rank next in ranges of concentrations and temperatures, to those of Boryta, Maas and Grant. Other reported pressure-concentration-temperature data are within narrower ranges of concentrations and temperatures of the solutions. Boryta, Maas and Grant showed that their pressure-concentration-temperature data and those of Urmura and Hasaba agree in the ranges where both reported experimental data. However, they differ in the ranges where the extrapolated data of Uemura and Hasaba are compared with the

experimental data of Boryta, Maas and Grant. Thus, it is clear that the pressure-concentration-temperature data for lithium bromide solutions (being nonideal salt solutions) may not be safely extrapolated beyond the range of experimental data.

For the purpose of the calculations in this thesis, the pressure-concentration-temperature data of Boryta, Maas and Grant were fitted with polynomial Equations (6.17) to (6.20).

$$\ln p = A + B/T + C/T \qquad (6.17)$$

where T is the temperature in degrees Kelvin, for $40 < X < 70$ per cent, $333.15 < T < 493.15$ K

$$A = 22.34 - 2.207E\text{-}1X + 2.464E\text{-}3X^3 \qquad (6.18)$$

$$B = -5.403E3 + 98.42X - 1.290X^2 \qquad (6.19)$$

$$C = -3.272E5 + 3.809E3X - 58.01X^2 \qquad (6.20)$$

The average deviation of the observed data from Equations (6.17) to (6.20) was about 0.3 per cent.

For the purpose of determining the dew point temperature of a lithium bromide solution exerting a vapour pressure determined from Equations (6.17) to (6.20), the vapour pressure-temperature data of Keenan, Keys, Hill and Moore ["Thermodynamic properties of water including vapour, liquid and solid phases", Keenan, J.H., Keyes, F.G. and Moore, J.G., John Wiley and Sons, New York, (1969)] for water between 4 and 220^{o}C were fitted with Equation (6.21).

$$\ln p = 11.5923 - 3.6699E3/T_W - 2.4309E5/T_W^2 \qquad (6.21)$$

where T is the temperature in degrees Kelvin for $277.15 < T_W < 493.15$ K. The average deviation of the original data from Equation (6.21) was about 0.2 per cent. The vapour pressure of a solution of lithium bromide at a given concentration and temperature obtained from Equations (6.17) to (6.20) was substituted into Equation (6.21) to obtain the dew points of the solutions.

6.4 DETERMINATION OF THE ENTHALPY-CONCENTRATION-TEMPERATURE DATA

The enthalpy-concentration-temperature data were obtained from the relation derived by Haltenberger ["Enthalpy-concentration charts from vapour pressure data", Haltenberger, W. (Jr), Industrial and Engineering Chemistry, 31(6), 783-786 (June 1939)] using the heat capacity values of the solution at one concentration and values of heat of dilution over the entire concentration and temperature ranges. In the process of foregoing equations, others which are given below, and the heat capacity values obtained from the literature were used. A Fortran 77 computer programme was developed and used to determine enthalpy-concentration-temperature data for aqueous solutions of lithium bromide in the range of concentrations 50 and 68 per cent lithium bromide and temperatures 60 and 220^{o}C. The enthalpy-concentration-temperature of solutions data were fitted with a bivariate polynomial which was to the second degree in temperature and the fourth degree in concentration of the solutions. Similarly, the temperature of solutions-concentration-dew point temperature data were fitted with a bivariate polynomial which was to the first degree in temperature and the third degree in concentration of the solutions. The polynomials were

represented in double Chevyshev series form.

6.4.1 The Haltenberger's relation

From a heat and material balance of the isothermal evaporation of water from a base concentration solution, the equation derived by Haltenberger can be used in the form

$$H = \frac{H_o - \int_{X_o}^{X} \bar{H}\, d(1 - X_o/X)}{X_o/X} \qquad (6.22)$$

6.4.2 Reference state

The base concentration is taken as 50 per cent lithium bromide solution. The reference state for zero enthalpy was set at 0^oC for convenience for each of the two constituents - 50 per cent lithium bromide solution and water. The enthalpy values from the steam table of Keenan, Keyes, Hill and Moore were used directly where required, since the enthalpy reference state was also 0^oC.

6.4.3 Determination of the enthalpy of the base concentration solution

The enthalpy of the base concentration solution was obtained from Equation (6.23)

$$H_o = \int_0^T C_p\, dT \qquad (6.23)$$

6.4.4 Heat capacity data

The heat capacity of the 50 per cent lithium bromide solution was obtained for each isotherm from Equations (6.24) to (6.27).

$$C_p = A + BT + CT^2 \qquad (6.24)$$

for $10 < X < 66$ per cent, $25 < T < 130^{o}C$

$$A = 1.098 - 1.529E\text{-}2X + 6.220E\text{-}5X^2 \qquad (6.25)$$

$$B = -3.651E\text{-}3 + 4.204E\text{-}5X \qquad (6.26)$$

$$C = 3.576E\text{-}5 - 4.238E\text{-}7X \qquad (6.27)$$

Equations (6.24) to (6.27) were those obtained by Uemura and Hasaba. These equations have been applied in this exercise in concentration and temperature ranges $50 < X < 68$ per cent and $60 < T < 220^{o}C$ respectively. These ranges are wider than those from which they were derived. However, of those obtainable in the literature they cover the widest ranges. Moreover, they should give more realistic heat capacity values than the supposed temperature independent value which McNeely used in his calculations.

6.4.5 The partial enthalpy of water in the solutions

The partial enthalpy H of water in solution defined as the difference between the enthalpy of the vapour and its latent heat, was obtained from Equation (6.28)

$$\bar{H} = H_V - \lambda \qquad (6.28)$$

6.5 COMPUTER PROGRAMME

A computer programme has been developed to obtain enthalpy-concentration-temperature correlations starting with a basic pressure-concentration-temperature equation for solutions of aqueous lithium bromide. The programme was written to solve Equation (6.22) using all the relevant equations given before. The latent heat of vaporisation of water, volumes of saturated water and water vapour were obtained from the simplified steam table equations presented below:

$$\lambda_W = (H_V)_W - H_\ell \qquad (6.29)$$

$$H_W = 4.1910T_W - 0.0419 \qquad (6.30)$$

$$(H_V)_W = (0.16381T_W - 30.44969)P + (1.88163T_W + 2500.87) \qquad (6.31)$$

$$H_V = (0.16381T - 30.44969)P + (1.88163T + 2500.87) \qquad (6.32)$$

$$V_W = (-2.6295E\text{-}6(T_W)^2 + 8.6144E\text{-}4T_W - 0.07968 + (4.614E\text{-}3T_W + 1.260734)/P \qquad (6.33)$$

$$V = (-2.6295E\text{-}6T^2 + 8.6144E\text{-}4T - 0.07968) + (4.614E\text{-}3 + 1.260734)/P \qquad (6.34)$$

$$V_W = \frac{V_C + a(T_C-T_W)^{\frac{1}{3}} + b(T_C-T_W) + c(T_C-T_W)^4}{1 + d(T_C-T_W)^{\frac{1}{3}} + e(T_C-T_W)} \qquad (6.35)$$

$$
\left.\begin{array}{lcl}
V_C & = & 3.1975E\text{-}3 \\
T_C & = & 374.11^{o}C \\
a & = & -3.151548E\text{-}4 \\
b & = & -1.203374E\text{-}6 \\
c & = & 7.48908E\text{-}16 \\
d & = & 1.342489E\text{-}1 \\
e & = & -3.946263E\text{-}3
\end{array}\right\} \qquad (6.36)
$$

Equations (6.29) to (6.34) were adopted from McNeely ["Thermodynamic properties of aqueous solutions of lithium bromide", McNeely, L.A., ASHRAE Transactions, 85(1), 413-434 (1979)]. Equations (6.35) and (6.36) were taken from Keenan and Keyes ["Thermodynamic properties of water including vapour, liquid and solid phases", Keenan, J.H. and Keyes, F.G., John Wiley and Sons, New York, 21, (1939)].

The programme has been written in Fortran 77. A computer listing of the programme is presented in Appendix I. The listing includes detailed comments explaining the sequence of the programme.

6.6 ACCURACY

According to Haltenberger ["Enthalpy-concentration charts from vapour pressure data", Haltenberger, W. (Jr), Industrial and Engineering Chemistry, 31(6), 783-786 (1939)], the main source of errors in using his method for the determination of the enthalpy of solutions lies in the determination of the slope of the Duhring line. Such an error will introduce error in the computed value of the latent heat of vaporisation of the solution. This error will in turn be numerically transferred to the partial enthalpy of water in the

solution. The resultant error in the value of the enthalpy of solution is a function of the concentration at which the errors occur. From Equation (6.22) for an average error E kJ in λ_W between concentration X_o and X, the error in the enthalpy H of the solution is $E(1 - X/D_o)$ kJ.

Table (6.3) shows the order of magnitude of errors in H due to errors of one-thousandth and one-hundredth in the slope of the Duhring line A over a 10 per cent change in concentration.

These errors become cumulative as the integration in Equation (6.22) is carried out from low to high concentrations. Thus, larger errors are incurred at higher concentrations. This type of error is caused by the use of incorrect vapour pressure data.

6.7 RESULTS AND DISCUSSION

The plots of the temperatures of solutions of lithium bromide and the corresponding saturation temperatures of water produced straight lines for all the concentrations considered in this work.

The correlations for the enthalpy-concentration-saturation temperature data of solutions, and the saturation temperature of water-concentration-saturation temperature of solutions data obtained in this thesis have been presented in Equations (6.9) and (6.10), and Tables (6.1) and (6.2) respectively.

Table (6.3) shows possible errors in the calculated enthalpy per unit mass due to some errors in the Duhring constant values over a 10 per cent range of concentration.

The maximum and minimum errors of the Duhring lines fitted by the least square method were -4.3E-2 per cent with a standard deviation of 0.397 per cent and 8.7E-3 per cent with a standard deviation of 8.06E2 per cent respectively. The correlation coefficients of the Duhring lines were between 0.99997 and 1.00000. The values of the Duhring constants for concentrations of aqueous lithium bromide solutions of 50 per cent, 55 per cent, 60 per cent and 65 per cent weight of lithium bromide are given in Table (6.4). In addition, Table (6.4) gives the corresponding values of the correlation coefficients of the Duhring curves, the mean errors and the standard deviations of the errors.

The correlations of the enthalpy-concentration-saturation temperature data of solutions, and the saturation temperature of solutions-concentration-saturation temperature of water data obtained in this exercise, have been presented in Equations (6.9) and (6.10), and Tables (6.1) and (6.2) respectively.

Table (6.5) gives the mean errors and standard deviations of the mean errors for the enthalpy-concentration fit for a range of concentrations of solutions 50 to 68 per cent.

Table (6.6) shows the mean errors and standard deviations of the mean errors for the concentration-saturation temperature of water fit for saturation temperatures of water 50^{o}C, 70^{o}C, 90^{o}C, 110^{o}C and 130^{o}C over the range of concentrations 50 to 68 per cent.

Table (6.7) is a presentation of the saturation temperatures of water from the report of McNeely ["Thermodynamic diagrams of solutions of lithium bromide", McNeely, L.A., ASHRAE Transactions, 85(1), 413-434,

(1969)] and from calculations in this exercise for lithium bromide solutions in the range where data in both exercises exist for the same temperatures of solutions.

(Table 6.8) gives the saturation temperatures of water obtained from the correlations derived in this exercise and from the experimentally obtained absorption data for the lithium bromide solutions.

Table (6.9) shows the enthalpy per unit mass reported by McNeely, and those obtained from the correlations derived in this exercise for the solutions of lithium bromide in the range of temperatures for which data are available in both cases.

The errors in the Duhring constants shown in Table (6.4) are reflected in the correlations for the enthalpy-concentration-temperature data according to the predictions presented in Table (6.3). However, it could be seen in Table (6.9) that the deviations between the values of the enthalpies obtained from the correlation developed in this exercise and the enthalpies obtained from the correlations of McNeely reduce progressively as the temperatures of the solutions increase. It is expected that the data from both sources would agree at higher solution temperatures if they existed.

Tables (6.7) and (6.8) show that the saturation temperatures obtained from the correlations in this exercise agree with the observed data and the results of the correlation developed by McNeely.

The correlations in this exercise are therefore recommended for use at high temperatures.

Figure (6.1) shows the enthalpy-concentration-saturation temperature of solutions for solution concentrations in the range

50 to 68 per cent weight of lithium bromide for saturation temperatures of solutions in the range 60°C to 220°C.

Figure (6.2) gives the saturation temperature of water-concentration-saturation temperatures of solutions for solution concentrations in the range 50 to 68 per cent weight of lithium bromide for saturation temperatures of solutions in the range 60°C to 220°C.

Figures (6.1) and (6.2) together with Figures (6.3), which is a plot of pressure against enthalpy per unit mass for water, and data for superheated vapour from tables ["Thermodynamic properties of water including vapour, liquid and solid phases", Keenan, J.H., Keyes, F.G. and Moore, J.G., John Wiley and Sons, New York, (1969)] could be used to evaluate absorption heat pump systems using water-lithium bromide solutions. Furthermore, the data could be used in conjunction with the thermal properties of aqueous solutions of lithium bromide available in the literature ["Lithium bromide", Boryta, D.A., Technical Data, Bulletin 145, Foote Mineral Co., Extan, U.S.A.] to design absorption heat pump systems using the water-lithium bromide mixture.

j \ i	0	1	2
0	1.173E3	3.405E2	2.898E1
1	1.688E1	-2.503E1	-2.248
2	2.287E1	-1.673	2.237E-3
3	9.226E-1	-2.044E-1	9.655E-3
4	4.120E-2	-1.304E-3	-2.132E-3

TABLE 6.1 CHEBYSHEV COEFFICIENTS OF THE POLYNOMIAL FOR THE ENTHALPY-CONCENTRATION-TEMPERATURE DATA FOR SOLUTIONS OF LITHIUM BROMIDE

j \ i	0	1
0	5.682E2	9.335E1
1	4.222E1	2.953E-1
2	1.311	-2.986E-1
3	-2.033E-1	-7.368E-3

TABLE 6.2 CHEBYSHEV COEFFICIENTS OF THE CHEBYSHEV POLYNOMIAL FOR THE TEMPERATURE OF SOLUTIONS-CONCENTRATION-SATURATION TEMPERATURE OF WATER DATA FOR SOLUTIONS OF LITHIUM BROMIDE

X_o, per cent	X, per cent	error in enthalpy per unit mass	
		0.001 error	0.01 error
40	50	0.565	5.65
50	60	0.452	4.52
60	70	0.3777	3.77

TABLE 6.3 ERRORS IN ENTHALPY PER UNIT MASS DUE TO SPECIFIED ERRORS IN THE DUHRING LINE SLOPE OVER A 10 PER CENT RANGE OF CONCENTRATIONS

concentration (per cent)	Duhring constant (dimen-sionless)	correlation coefficient (dimen-sionless)	mean error of the Duhring constant (per cent)	standard deviation of the mean error (per cent)
50	1.15970	0.99997	-4.3E-2	0.397
55	1.17033	0.99998	-3.1E-2	0.290
60	1.17466	1.00000	-1.4E-2	0.128
65	1.17421	1.00000	8.7E-3	8.06E-2

TABLE 6.4 DUHRING CONSTANT, CORRELATION COEFFICIENT OF THE DUHRING CURVE, MEAN ERROR OF THE DUHRING CONSTANT AND STANDARD DEVIATION OF THE MEAN ERROR FOR TEMPERATURE OF SOLUTIONS 60-220^{o}C AND A RANGE OF CONCENTRATIONS OF AQUEOUS SOLUTIONS OF LITHIUM BROMIDE

temperature of solution (^{o}C)	mean error (per cent)	standard deviation of the mean error (per cent)
60.0	1.23	0.999
100.0	-0.47	0.415
140.0	0.18	0.106
180.0	0.60	0.318
220.0	0.003	0.429

TABLE 6.5 ERROR IN THE ENTHALPY-CONCENTRATION CORRELATION FOR CONCENTRATIONS OF LITHIUM BROMIDE 50 TO 68 PER CENT IN AQUEOUS SOLUTIONS OF LITHIUM BROMIDE

temperature of solution (^{o}C)	mean error (per cent)	standard deviation of the mean error (per cent)
50.0	-0.095	0.1280
70.0	0.021	0.0284
90.0	0.043	0.0596
110.0	0.015	0.0206
130.0	-0.079	0.1682

TABLE 6.6 ERROR IN THE CONCENTRATION SATURATION TEMPERATURE OF WATER CORRELATION FOR CONCENTRATIONS OF LITHIUM BROMIDE 50 TO 68 PER CENT IN AQUEOUS SOLUTIONS OF LITHIUM BROMIDE

temperature of solution °C	concentration of solutions X, per cent											
	50			55			60			65		
	this exercise °C	McNeely °C	dev. per cent	this exercise °C	McNeely °C	dev. per cent	this exercise °C	McNeely °C	dev. per cent	this exercise °C	McNeely °C	dev. per cent
60	36.0	35.5	1.3	27.7	27.3	1.4	18.4	18.4	0	8.3	9.5	-14.3
80	53.7	53.4	0.6	45.1	44.8	0.7	35.5	35.6	-0.3	25.2	26.0	-3.2
100	71.2	71.3	-0.1	62.4	62.4	0	52.7	52.7	0	42.2	42.4	0
120	88.6	89.2	-0.7	79.6	79.9	-0.4	69.8	69.8	0	59.2	58.9	0.5
140	105.9	107.1	-1.1	96.8	97.4	-0.6	86.8	87.0	-0.2	76.2	75.3	1.2
160	123.1	125.0	-1.5	113.8	115.0	-1.0	103.8	104.1	-0.3	93.2	91.8	1.5

TABLE 6.7 SATURATION TEMPERATURE OF WATER FROM DATA DERIVED IN THIS EXERCISE AND THOSE REPORTED BY McNEELY FOR A RANGE OF TEMPERATURES AND CONCENTRATIONS FOR SOLUTIONS OF LITHIUM BROMIDE

temperature of solution °C	concentration of solutions X, per cent											
	54.0			52.9			50.5			50.7		
	Observed value °C	this exercise °C	dev. per cent	Observed value °C	this exercise °C	dev. per cent	Observed value °C	this exercise °C	dev. per cent	Observed value °C	this exercise °C	dev. per cent
197.3	147.5	147.9	-0.3									
171.8				127.0	127.2	-0.2						
110.7							82.0	80.5	1.8			
100.5										71.1	69.5	2.2
110.7												

TABLE 6.8 OBSERVED SATURATION TEMPERATURE OF WATER AND THOSE REPORTED BY McNEELY FOR A RANGE OF TEMPERATURES AND CONCENTRATIONS FOR SOLUTIONS OF LITHIUM BROMIDE

temperature of solution °C	concentration of solutions X, per cent											
	50			55			60			65		
	this exercise kJ kg^{-1}	McNeely kJ kg^{-1}	dev. per cent	this exercise kJ kg^{-1}	McNeely kJ kg^{-1}	dev. per cent	this exercise kJ kg^{-1}	McNeely kJ kg^{-1}	dev. per cent	this exercise kJ kg^{-1}	McNeely kJ kg^{-1}	dev. per cent
60	119.0	125.8	-5.7	116.3	134.7	-15.8	127.8	153.7	-20.3	156.4	181.4	-16.0
100	190.4	214.6	-12.7	184.3	218.2	-18.4	191.3	231.5	-21.0	213.9	253.5	-18.5
140	278.9	303.2	-8.7	267.7	301.1	-12.5	268.9	308.1	-14.6	284.3	324.7	-14.7
180	384.2	293.1	-2.1	366.5	383.4	-4.6	360.5	384.3	-6.6	367.8	395.8	-7.6

TABLE 6.9 ENTHALPY PER UNIT MASS FROM DATA DERIVED IN THIS EXERCISE AND THOSE REPORTED BY McNEELY FOR A RANGE OF TEMPERATURES AND CONCENTRATIONS FOR SOLUTIONS OF LITHIUM BROMIDE

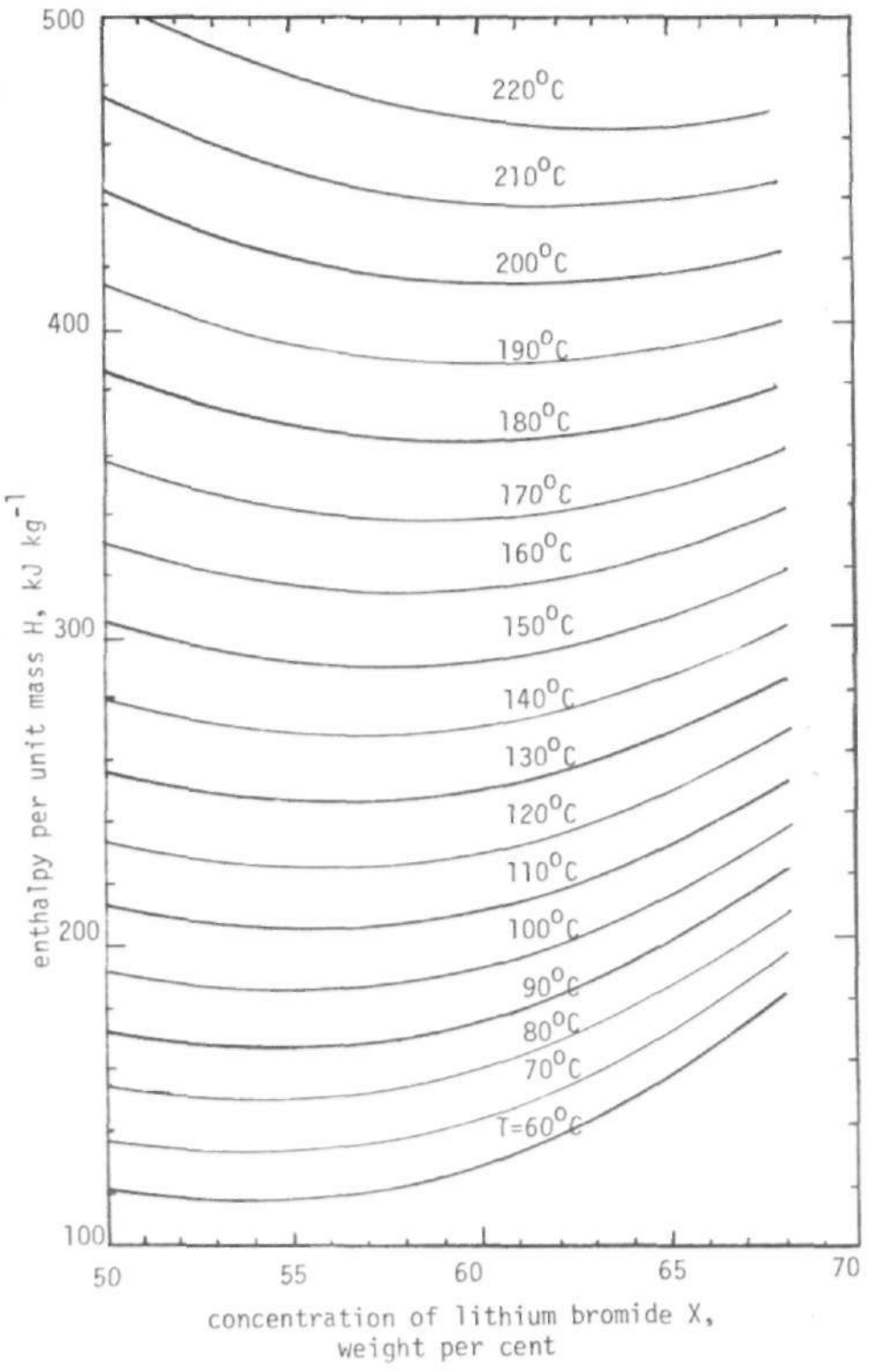


FIGURE (6.1) ENTHALPY PER UNIT MASS OF AQUEOUS SOLUTIONS OF LITHIUM BROMIDE AGAINST CONCENTRATION FOR VARIOUS SATURATION TEMPERATURES

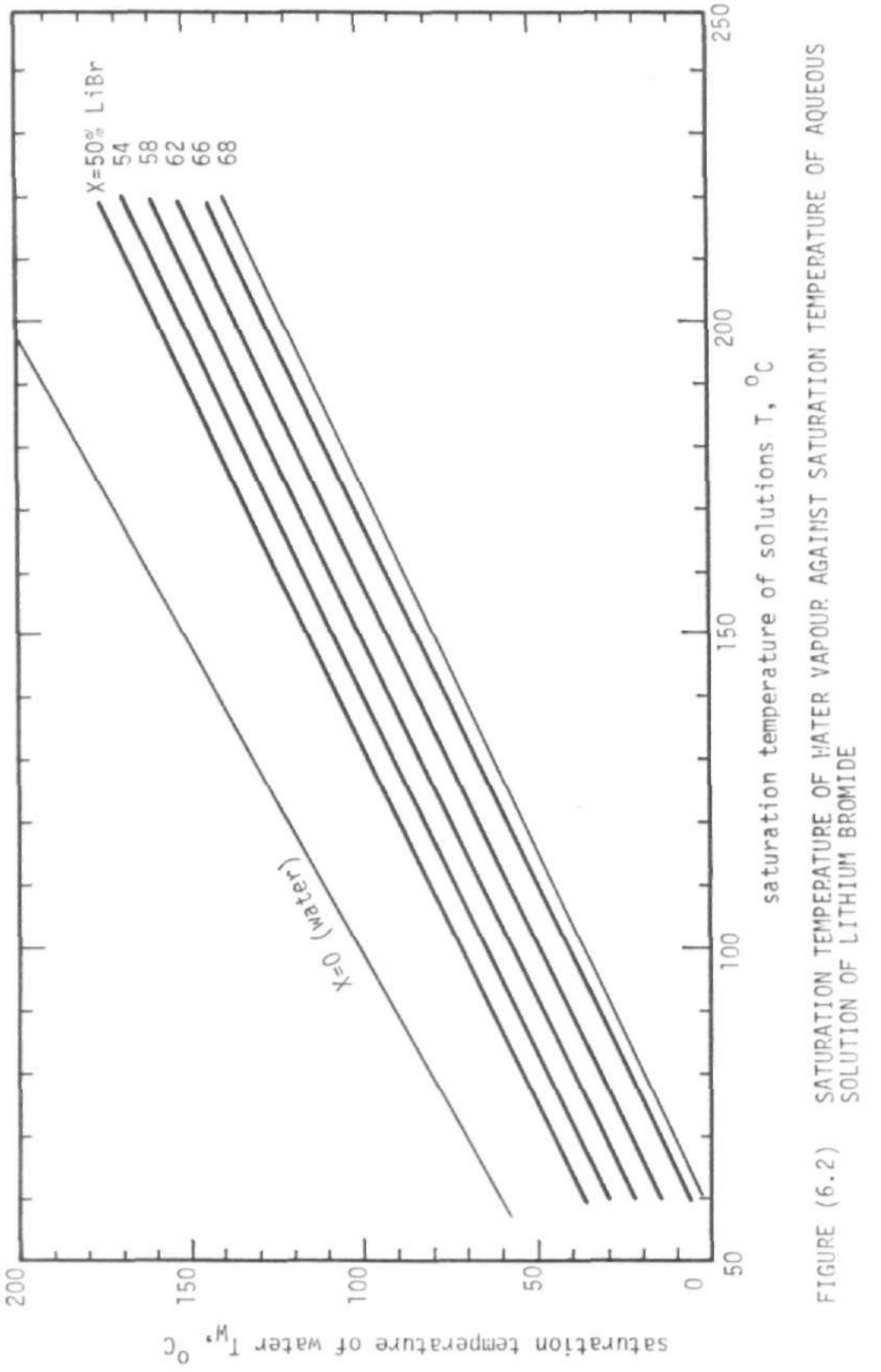


FIGURE (6.2) SATURATION TEMPERATURE OF WATER VAPOUR AGAINST SATURATION TEMPERATURE OF AQUEOUS SOLUTION OF LITHIUM BROMIDE

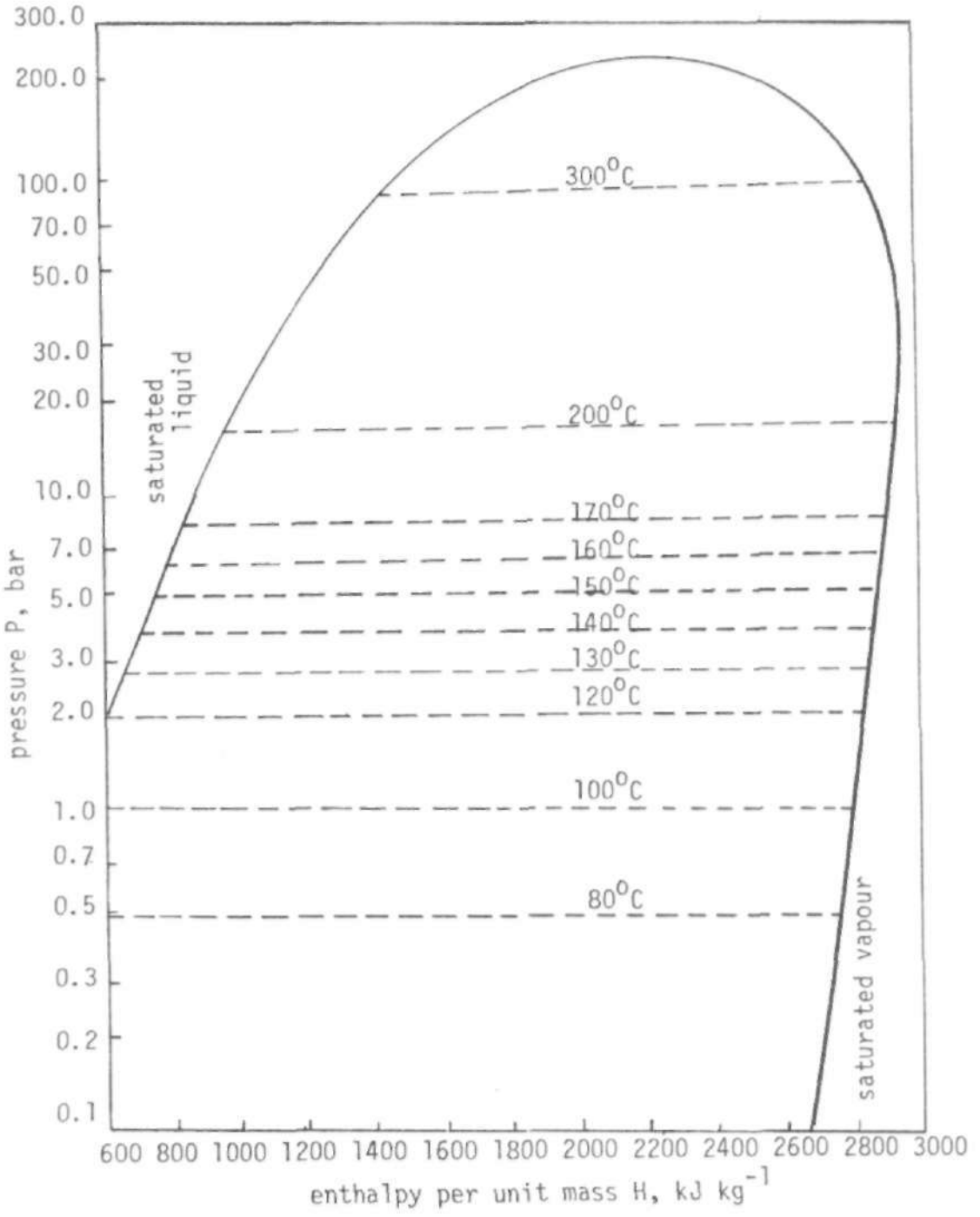


FIGURE (6.3) SATURATION PRESSURE AGAINST ENTHALPY PER UNIT MASS FOR WATER (R718)

CHAPTER 7

THERMODYNAMIC ANALYSIS OF A CONVENTIONAL WATER-LITHIUM BROMIDE ABSORPTION HEAT PUMP SYSTEM

CHAPTER 7

THERMODYNAMIC ANALYSIS OF A CONVENTIONAL WATER-LITHIUM BROMIDE ABSORPTION HEAT PUMP SYSTEM

7.1 INTRODUCTION

A thermodynamic analysis of a conventional water-lithium bromide absorption heat pump for the delivery of heat at high temperatures above 100°C is required since it is not available in the literature.

A thermodynamic analysis for evaporator temperatures T_{EV} between 90°C and 140°C, generator temperatures T_{GE} between 160°C and 220°C, and absorber temperature T_{AB} up to 190°C has been made for a conventional water-lithium bromide absorption heat pump system. The thermodynamic data used were those developed in Chapter 6.

7.2 THEORY OF ABSORPTION HEAT PUMPS

The theory of absorption heat pumps is based on the thermodynamics of solution mixtures. In binary mixtures, as against simple substances, each condition of state is determined by three parameters: pressure p, temperature T and solution concentration X_w in weight fraction of working fluid.

The second law of thermodynamics states that if heat is transferred reversibly, the change in entropy will be zero. Moreover, if heat can be transferred reversibly down a temperature gradient it should also be possible to transfer it up a temperature gradient.

Evaporation followed by condensation is a reversible process. However, pure substances evaporate and condense at the same temperature.

In a solution mixture, the absorbing material causes the solvent to evaporate at a higher temperature than that at which it condenses. This is because the interaction between the absorbent and the solvent causes the lowering of the vapour pressure of the solvent. Thus the heat energy necessary to evaporate the solvent from the mixture will have to be supplied at a higher temperature than the temperature at which the solvent condenses.

In a conventional absorption heat pump, heat energy is supplied for the evaporation of the pure solvent at a lower temperature than that at which it is released when condensation takes place.

7.3 CONVENTIONAL ABSORPTION HEAT PUMP CYCLE

Figure (7.1) shows a simplified conventional absorption heat pump system. Figure (7.2) presents the cycle on a three-dimensional pressure-enthalpy-concentration diagram. The composite diagrams are those presented in Figures (6.1), (6.2) and (6.3).

Referring to Figures (7.1) and (7.2) the working fluid leaving the generator (1) at high pressure, condenses in the condenser. A quantity of heat Q_{CO}, consisting of heat of desuperheat and latent heat of condensation, is rejected by the condenser into a heat sink. The liquid working fluid (2) expands, isentropically, across a valve to yield a mixture of liquid and vapour (3). Subsequently, the remaining liquid vaporises in the evaporator by abstracting a quantity of heat Q_{EV} from a heat source. The vapour (4) produced in the

evaporator then flows into the absorber. In the absorber, working fluid-poor solution (7) absorbs the vapour. The heats of solution and condensation produced during the process are rejected into a heat sink. A pump transfers the working fluid-rich solution (8) at low pressure from the absorber through the economiser where it gains heat from the working fluid-poor solution, returning from the generator through a pressure reducing valve into the absorber. The working fluid-rich solution (10), leaving the economiser then enters the generator where it absorbs a quantity of heat Q_{GE} from a heat source to effect evaporation at a high pressure. The value of Q_{GE} consists of sensible heat and heat of desorption. The resulting vapour (1) flows into the condenser to continue the cycle.

7.4 EXPRESSIONS FOR COEFFICIENT OF PERFORMANCE

The coefficient of performance (COP) for the conventional absorption heat pump is defined by the expression

$$(COP)_{AH} = \frac{Q_{AB} + Q_{CO}}{Q_{GE}} \qquad (7.1)$$

It is possible to distinguish three forms of $(COP)_{AH}$ in absorption heating systems; $(COP)_{AHC}$ based on the Carnot cycle, $(COP)_{AHMO}$ (maximum obtainable coefficient of performance) based on the validity of certain assumptions and $(COP)_{AHA}$ (actual coefficient of performance) based on the actual values of Q_{AB}, Q_{CO} and Q_{GE}.

7.4.1 $(COP)_{AHC}$

The coefficient of performance for a completely reversible

process, $(COP)_{AHC}$, is defined through the concept of Carnot engine. A heat balance over the heat pump yields

$$Q_{EV} + Q_{GE} = Q_{CO} + Q_{AB} \tag{7.2}$$

For no entropy change

$$\frac{Q_{EV}}{T_{EV}} + \frac{Q_{GE}}{T_{GE}} = \frac{Q_{CO}}{T_{CO}} + \frac{Q_{AB}}{T_{AB}} \tag{7.3}$$

Assuming

$$T_{CO} = T_{AB} \tag{7.4}$$

and writing

$$Q'_{CO} = Q_{CO} + Q_{AB} \tag{7.5}$$

Then

$$\frac{Q_{EV}}{T_{EV}} + \frac{Q_{GE}}{T_{GE}} = \frac{Q'_{CO}}{T_{CO}} \tag{7.6}$$

Therefore

$$Q_{EV} = Q'_{CO'} - Q_{GE} \tag{7.7}$$

and

$$\frac{Q'_{CO} - Q_{GE}}{T_{EV}} + \frac{Q_{GE}}{T_{GE}} = \frac{Q'_{CO}}{T_{CO}} \tag{7.8}$$

from which it follows that

$$Q'_{CO}\left[\frac{1}{T_{EV}} - \frac{1}{T_{CO}}\right] = Q_{GE}\left[\frac{1}{T_{EV}} - \frac{1}{T_{GE}}\right] \tag{7.9}$$

or

$$Q'_{CO}\left[\frac{T_{CO} - T_{EV}}{T_{EV}\ T_{CO}}\right] = Q_{GE}\left[\frac{T_{GE} - T_{EV}}{T_{EV}\ T_{GE}}\right] \tag{7.10}$$

Therefore

$$\frac{Q'_{CO}}{Q_{GE}} = \left[1 - \frac{T_{EV}}{T_{GE}}\right]\left[\frac{T_{CO}}{T_{CO} - T_{EV}}\right] \tag{7.11}$$

and hence

$$(COP)_{AHC} = \left[1 - \frac{T_{EV}}{T_{GE}}\right]\left[\frac{T_{CO}}{T_{CO} - T_{EV}}\right] \tag{7.12}$$

or

$$(COP)_{AHC} = \frac{T_{CO}}{T_{GE}}\left[\frac{T_{GE} - T_{EV}}{T_{CO} - T_{EV}}\right] \tag{7.13}$$

7.4.2 $(COP)_{AHMO}$

The maximum obtainable coefficient of performance is defined on the basis of the validity of some assumptions on the behaviour of the hardware and the fluids in the system. These assumptions are as follows:

(i) The temperatures (and pressures) of the fluids in the

various components are uniform at the stated values.

(ii) The fluids in the generator, condenser, absorber and evaporator are in respective equilibrium conditions.

(iii) The pressure in the condenser and generator is the saturation pressure corresponding to the temperature in the condenser.

(iv) The pressure in the evaporator and absorber is the saturation pressure corresponding to the temperature in the evaporator.

(v) The enthalpy of the non-equilibrium state is the same as the equilibrium enthalpy of the state with the same temperature and concentration.

(vi) Heat exchange with the environment other than prescribed by the heat transfer to the generator, evaporator or from the condenser and absorber, does not occur.

(vii) Pressure drops due to friction do not occur within the system.

The $(COP)_{AH}$ of the system that satisfies the foregoing assumptions is defined as the maximum obtainable coefficient of performance $(COP)_{AHMO}$. The mathematical relation between $(COP)_{AHMO}$ and the solutions and working fluid in the system is found through mass and energy balances. Referring to Figure (7.1), Table (7.1) gives a summary of the mass and energy balances. From Equation (7.1) and Table (7.1) the relation for $(COP)_{AHMO}$ is

$$(COP)_{AHMO} = \frac{H_4-H_7+(FR)(H_7-H_8)+H_1-H_2}{(FR)(H_5-H_{10})+H_1-H_5} \qquad (7.14)$$

where

$$(FR) = \frac{1 - (X_W)_5}{(X_W)_{10}-(X_W)_5} = \frac{X_{GE}}{X_{GE} - X_{AB}}$$

7.4.3 $(COP)_{AHA}$

The practical coefficient of performance $(COP)_{AHA}$ is obtained from the actual values of Q_{AB}, Q_{CO} and Q_{GE} for the practical system.

7.5 COMPUTER PROGRAMME

A computer programme has been developed to give $(COP)_{AHMO}$ from Equation (7.14). The relations from which the relevant thermodynamic properties were obtained were taken from Chapter 6. The relevant equations are:

$$\ell n\ p_s = A + B/T + C/T \qquad (6.17)$$

for $40 < X < 70$ per cent, $293.15 < T < 493.15$ K, where T is the temperature in degrees Kelvin.

$$A = 22.34 - 2.207E-1X + 2.464E-3X^2 \qquad (6.18)$$

$$B = -5.043E3 + 98.42X - 1.290X^2 \qquad (6.19)$$

$$C = -3.273E5 + 3.809E3X - 58.01X^2 \qquad (6.20)$$

$$H_W = 4.1910\ T_W - 0.0419 \qquad (6.30)$$

$$H_V = (0.16381T_W - 30.44969)P + 1.88163T_W + 2500.87 \quad (6.32)$$

$$T = ((-2*2.4309E5)/(-3.6699E3+(-3.6699E3**2 -4*-2.4309E5*(11.5923-\ell n\ p_s))**0.5)) -273.15 \quad (6.21)$$

and

$$H = \sum_{i=0}^{4} \sum_{j=0}^{2} A_{i,j}\ T_i(XCAP)\ T_j(tCAP) \quad (6.9)$$

where $A_{i,j}$ are:

j \ i	0	1	2
0	1.173E3	3.405E2	2.898E1
1	1.688E1	-2.503E1	-2.248
2	2.287E1	-1.673	2.237E-1
3	9.226E-1	-2.044E-1	9.655E-3
4	4.120E-2	-1.304E-3	-2.132E-3

These equations are for H_2O/LiBr solutions. The programme can be used to evaluate $(COP)_{AHMO}$ for any system when appropriate thermodynamic equations are provided.

The programme has been written in Fortran 77 and consists of a main programme and four sub-programmes. The flow chart for the main programme is presented in Figure (7.3). The main programme consists mainly of the calculations for the $(COP)_{AHMO}$. The calculations of the required thermodynamic properties are performed by the sub-

programmes.

Overall, six input variables are required.

The programme can be used to incorporate sensitivity analyses on $(COP)_{AHMO}$ based on a typical pressure drop within the system due to friction, concentration changes due to entrainment and partial loading.

A computer listing of the programme is presented in Appendix (A.I.3).

7.6 DISCUSSION OF DERIVED DATA

Figure (7.4) shows the influence of the generator temperature T_{GE} on the plot of the Carnot absorption coefficient of performance $(COP)_{AHC}$ against the gross condenser temperature lift $(T_{CO} - T_{EV})$. The plots are for an evaporator temperature T_{EV} of $100^{o}C$ and an absorber temperature T_{AB} equal to the condenser temperature T_{CO}. Similarly, Figure (7.5) shows the effect of T_{GE} on the plot of the maximum obtainable coefficient of performance $(COP)_{AHMO}$ against $(T_{CO}-T_{EV})$ for $T_{CO}=T_{AB}$ and T_{EV} of $100^{o}C$. It should be noted that the absolute values of $(COP)_{AHC}$ are higher than the absolute values of $(COP)_{AHMO}$ for corresponding values of T_{GE} and $(T_{CO}-T_{EV})$. Furthermore, $(COP)_{AHC}$ is independent of the concentration of the lithium bromide solution. However, $(COP)_{AHMO}$ is inter alia a function of the concentration of the lithium bromide solution. A comparison of parameters and derivatives from Figures (7.4) and (7.5) could give ideas about the effectiveness of a conventional absorption heat pump system. A comparison of the ratio $(COP)_{AHMO}/(COP)_{AHC}$ at generator

temperatures T_{GE} of 190°C and 210°C, presented in Table (7.2), shows that the maximum obtainable absorption heat pump effectiveness $(HPE)_{AHMO}$ [which is the ratio of $(COP)_{AHA}$ to $(COP)_{AHMO}$] increases as T_{GE} increases. Both Figures (7.4) and (7.5) show that some high values of $(T_{CO}-T_{EV})$ could be obtained only at higher values of T_{GE}.

Figure (7.6) shows that $(COP)_{AHMO}$ is not very sensitive to T_{GE}. Furthermore, for a given T_{EV} and concentration of water in the absorber $(X_W)_{AB}$, only a narrow range of $(T_{CO}-T_{EV})$ values may be obtained for a given T_{GE}. Higher $(T_{CO}-T_{EV})$ values are obtainable at higher T_{GE} values. A comparison of Figures (7.5) and (7.6) shows that higher $(COP)_{AHMO}$ values are possible when $T_{CO} \neq T_{AB}$ than when $T_{CO} = T_{AB}$ for given values of $(X_W)_{AB}$ and T_{GE}. In practice, it is more desirable to have $T_{CO} \neq T_{AB}$ than $T_{CO} = T_{AB}$. This is because, apart from higher $(COP)_{AHMO}$ values, the stream with the lower temperature could be used to preheat the cooling water before it withdraws heat from the stream with the higher temperature. Alternatively, two different temperature levels of heat may be obtained simultaneously.

Figure (7.7) shows that $(COP)_{AHMO}$ is not very sensitive to the ratio of the flow rate of the water-rich lithium bromide solution to the flow rate of the pure water (FR). However, higher gross condenser temperature lifts are obtainable at higher values of (FR). As the gross condenser temperature lift increases the corresponding absorber temperature decreases.

A comparison of Figures (7.6) to (7.8) shows that for a given $(COP)_{AHMO}$ and gross temperature lift, different concentrations of solution are required in the absorber and generator. Therefore, the

concentration furthest away from the crystallisation line should be selected for the required (COP) and gross temperature lift. Figure (7.9) is a solubility curve of lithium bromide in water as compiled by Boryta ["Solubility of lithium bromide in water between -50^{o} and 100^{o}C (45 to 70% lithium bromide), Boryta, D.A., Journal of Chemical Engineering Data, 15(1), 142-144, (1970)].

Figure (7.10) shows that the compression ratio (CR) is proportional to (T_{CO}-T_{EV}). This implies that $(COP)_{AHMO}$ is also not sensitive to (CR). For this reason absorption heat pump systems are better alternatives to vapour compression heat pump systems when high temperature lifts are required.

Figure (7.11) shows that for a given set of T_{GE} and T_{EV} values higher $(COP)_{AHMO}$ values are possible for a lower temperature approach (TA) in the absorber end of the economiser heat exchanger. It implies that very low values of (COP) would be obtained with an absorption heat pump system without an economiser heat exchanger. On the other hand, improved values of (COP) would be obtained by using very efficient, and costly, economiser heat exchangers.

Comparison of Figures (7.4) to (7.8) and (7.11) showsthat a family of curves which are plots of $(COP)_{AHMO}$ against (T_{CO}-T_{EV}) for various values of T_{GE} emerge. It was also shown that for a given T_{GE}, (T_{CO}-T_{EV}) depends on the (FR). The data of $(COP)_{AHMO}$, (T_{CO}-T_{EV}), T_{GE} and (FR) were reduced to Equations (7.15) to (7.18) using the NONLINEAR REGRESSION SPSS subroutine obtained from the University of Manchester Regional Computer Centre, Manchester, U.K.

$$(T_{CO}-T_{EV}) = A_1 + A_2\ T_{GE} \qquad (7.15)$$

where

$$A_1 = -1.4750E2 + 3.2658(FR) - 9.3214E\text{-}2(FR)^2 \quad (7.16)$$

$$A_2 = 0.8594 - 2.8268E\text{-}3(FR) + 1.0268E\text{-}4(FR)^2 \quad (7.17)$$

with root mean square residual = 0.1937

$$(COP)_{AHMO} = 0.11646(T_{GE})^{0.5534} - 8.6748E\text{-}3(T_{CO}-T_{EV})^{0.9707} \quad (7.18)$$

with root mean square residual = 6.6995E-3

The ranges of application of Equations (7.15) to (7.18) are for solution concentrations between 50 per cent and 68 per cent, and solution temperatures between $160^{o}C$ and $220^{o}C$.

Equations (7.15) to (7.18) together with Table (7.1) and typical values of $(HPE)_{AHMO}$ can be used to design a conventional absorption heat pump using water-lithium bromide solutions.

equipment	equations	
	mass balance	energy balance
condenser	(1) $M_1 = M_2$ $M_1/M_1 = m_1 = 1 = M_2/M_1 = m_2$	(2) $Q_{CO} + M_2H_2 = M_1H_1$ $q_{CO} = H_1-H_2$
absorber	(3) $M_4 + M_7 = M_8$ $m_7 = m_8 - 1 = (FR) - 1$ with $M_4 = M_1$	(4) $Q_{AB} + M_8H_8 = M_4H_4 + M_7H_7$ $q_{AB} = H_4+(m_8-1)H_7 - m_8H_8$ $= H_4 + m_8(H_7-H_8) - H_7$
economiser	(5) $m_5 = m_6 = m_7$ (6) $m_8 = m_9 = m_{10} = (FR)$ (7) $m_5(1-X_W)_5) = m_{10}(1-(X_W)_{10})$	(8) $m_5H_5 + m_9H_9 = m_{10}H_{10} + m_6H_6$ $(m_{10}-1)H_5+m_{10}H_9 = m_{10}H_{10}+(m_{10}-1)H_6$ $H_{10} = (1-1/m_{10})(H_5-H_6) + H_9$
generator	(9) $m_{10} = m_5 + 1 = (FR)$	(10) $q_{GE} + m_{10}H_{10} = m_5H_5 + H_1$ $q_{GE} = H_1 + (m_{10}-1)H_5 - m_{10}H_{10}$ $= m_{10}(H_5-H_{10}) + H_1-H_5$

TABLE (7.1) MASS AND ENERGY BALANCES OVER A CONVENTIONAL ABSORPTION HEAT PUMP SYSTEM

T_{GE} ^{o}C	$T_{GE}-T_{EV}$	$(COP)_{AHC}$	$(COP)_{AHMO}$	$(COP)_{AHMO}/(COP)_{AHC}$
190	40	2.007	1.2125	0.604
210	40	2.3516	1.5812	0.6724

TABLE (7.2) HEAT PUMP EFFECTIVENESS FACTORS AT A GROSS CONDENSER TEMPERATURE LIFT OF $40^{o}C$ AND GENERATOR TEMPERATURES OF $190^{o}C$ and $210^{o}C$

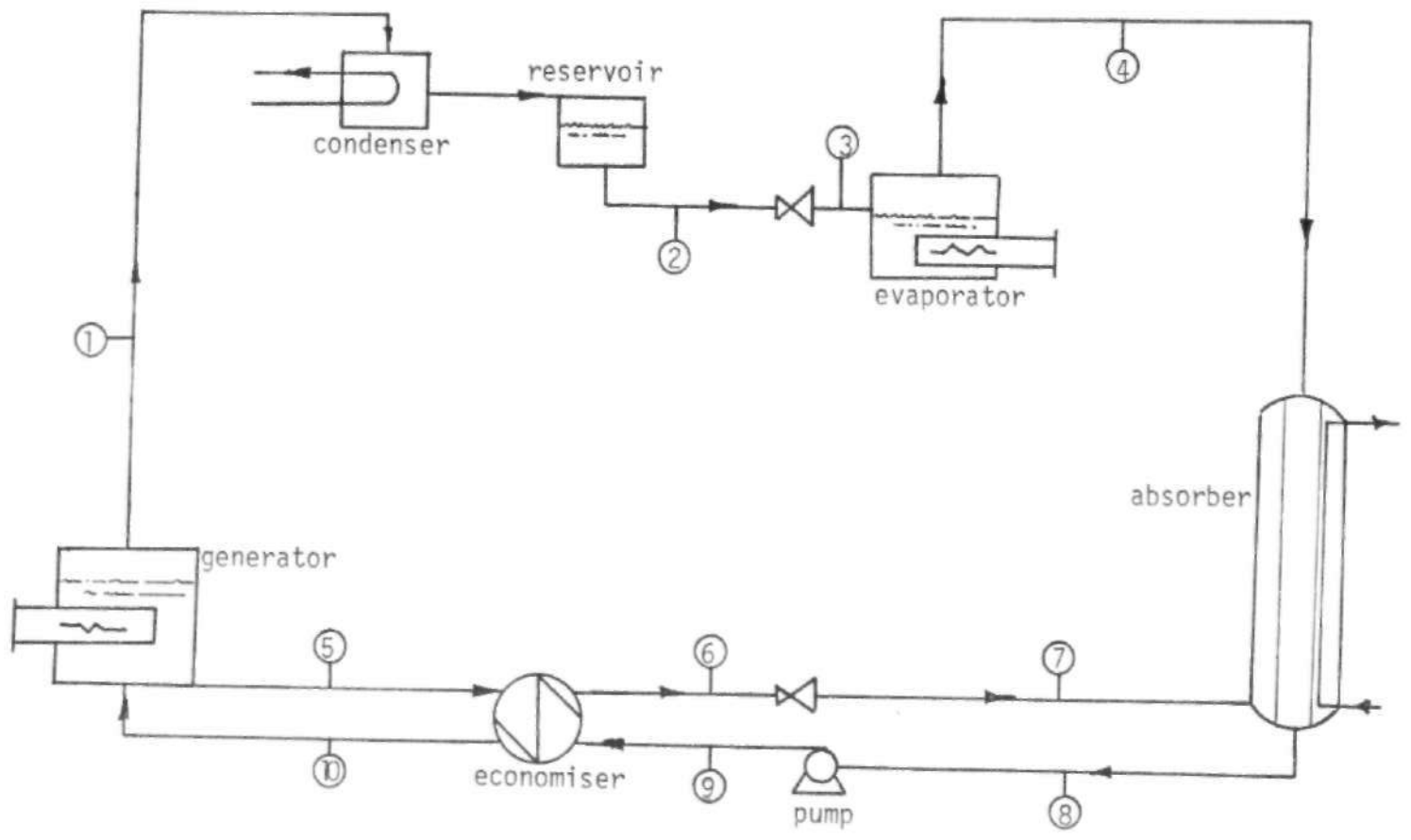


FIGURE (7.1) CONVENTIONAL ABSORPTION HEAT PUMP UNIT

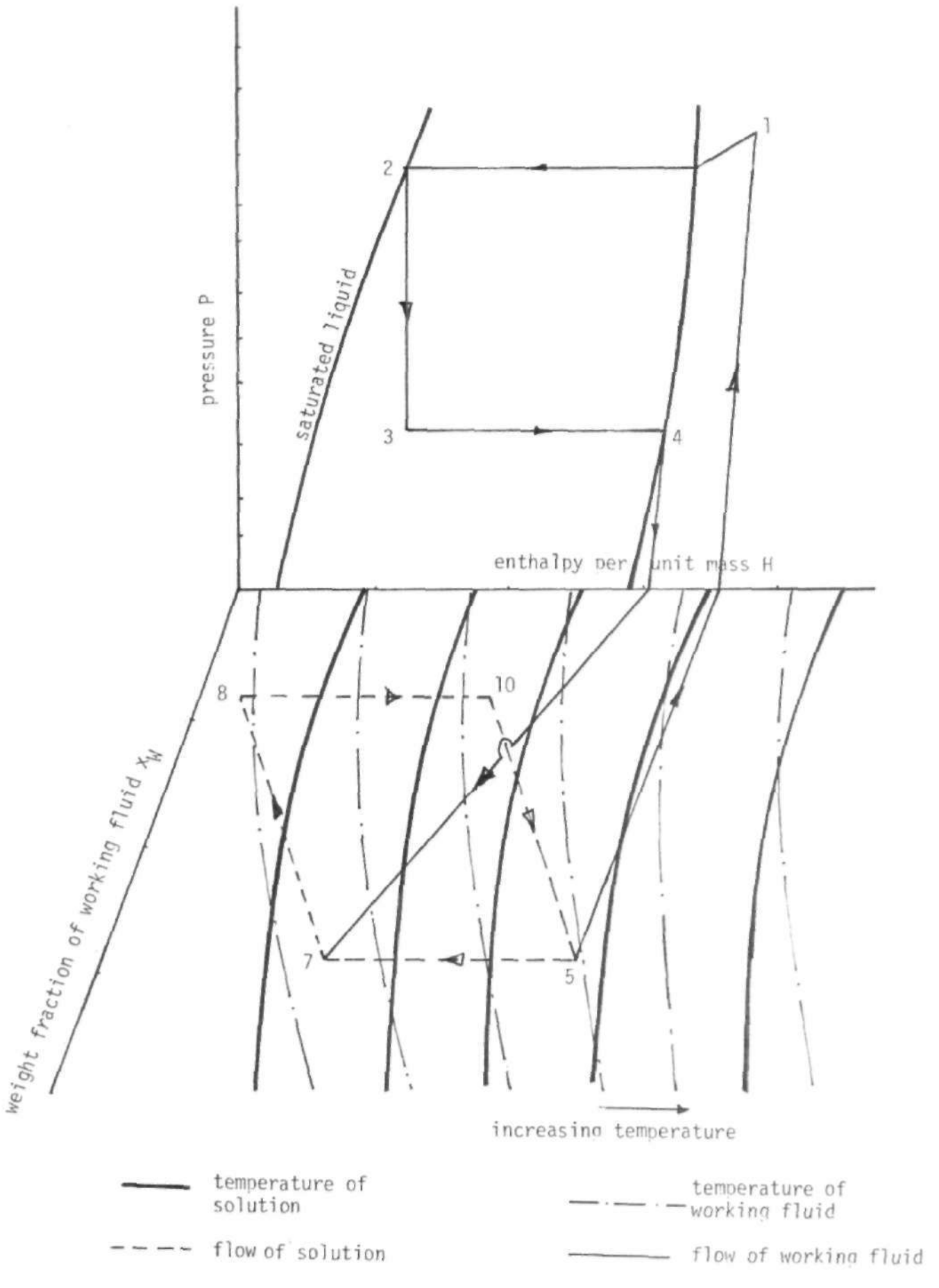


FIGURE (7.2) CYCLE OF A CONVENTIONAL ABSORPTION HEAT PUMP

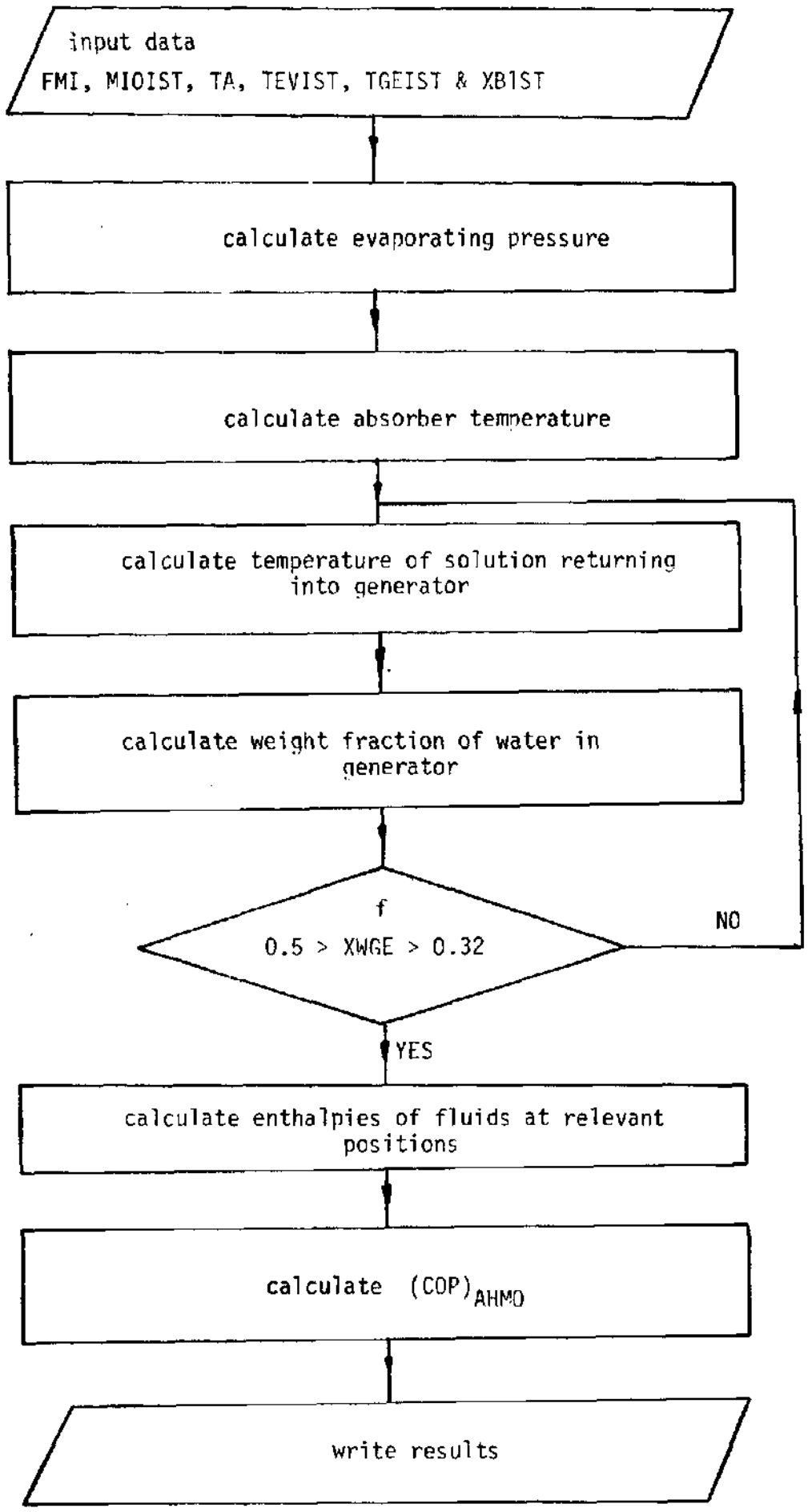


FIGURE (7.3) FLOW CHART FOR THE MAIN COMPUTER PROGRAMME FOR CALCULATING $(COP)_{AHMO}$ FOR A CONVENTIONAL ABSORPTION HEAT PUMP

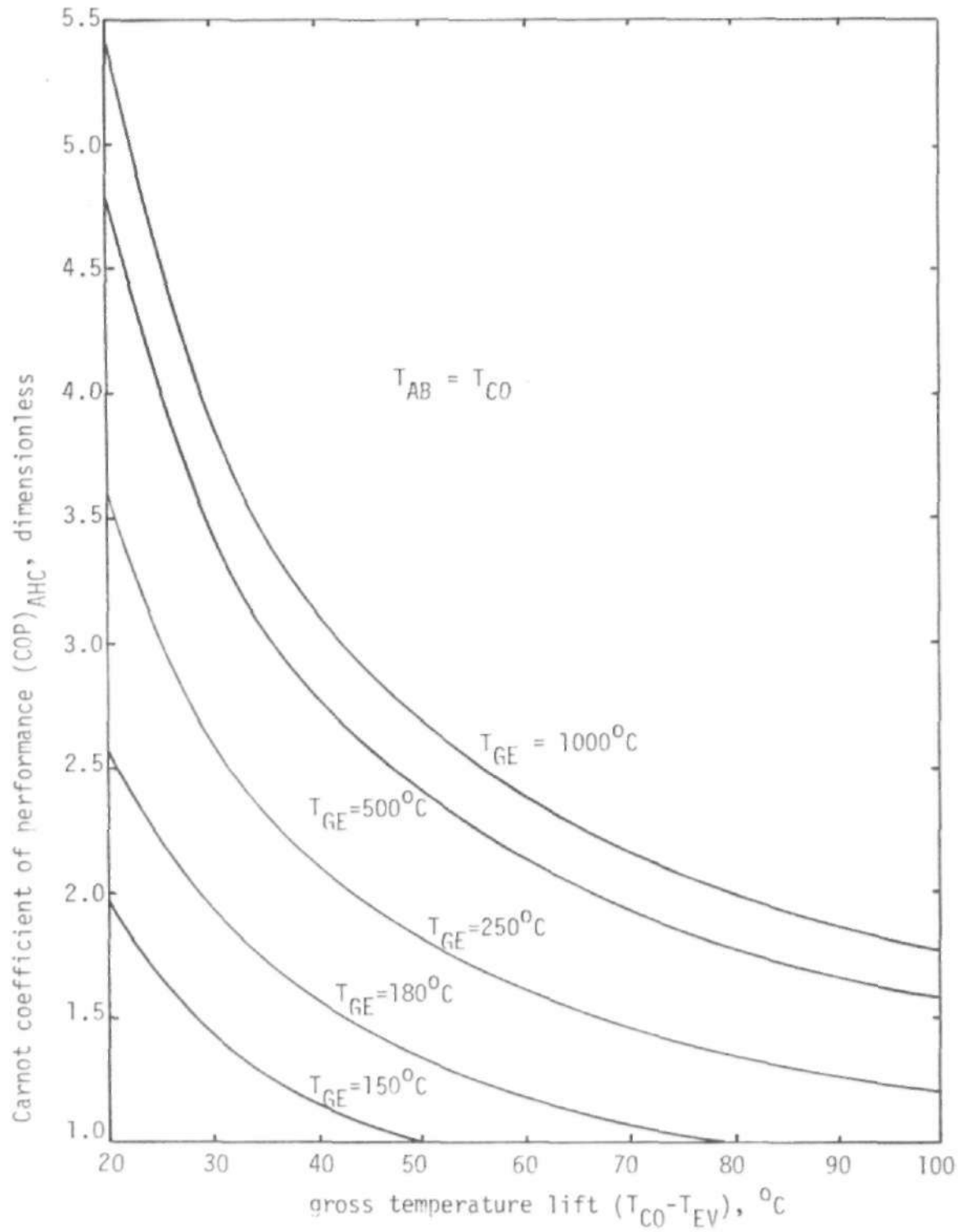


FIGURE (7.4) CARNOT COEFFICIENT OF PERFORMANCE AGAINST GROSS TEMPERATURE LIFT FOR AN EVAPORATOR TEMPERATURE OF 100°C AND A RANGE OF GENERATOR TEMPERATURES FOR A CONVENTIONAL ABSORPTION HEAT PUMP SYSTEM

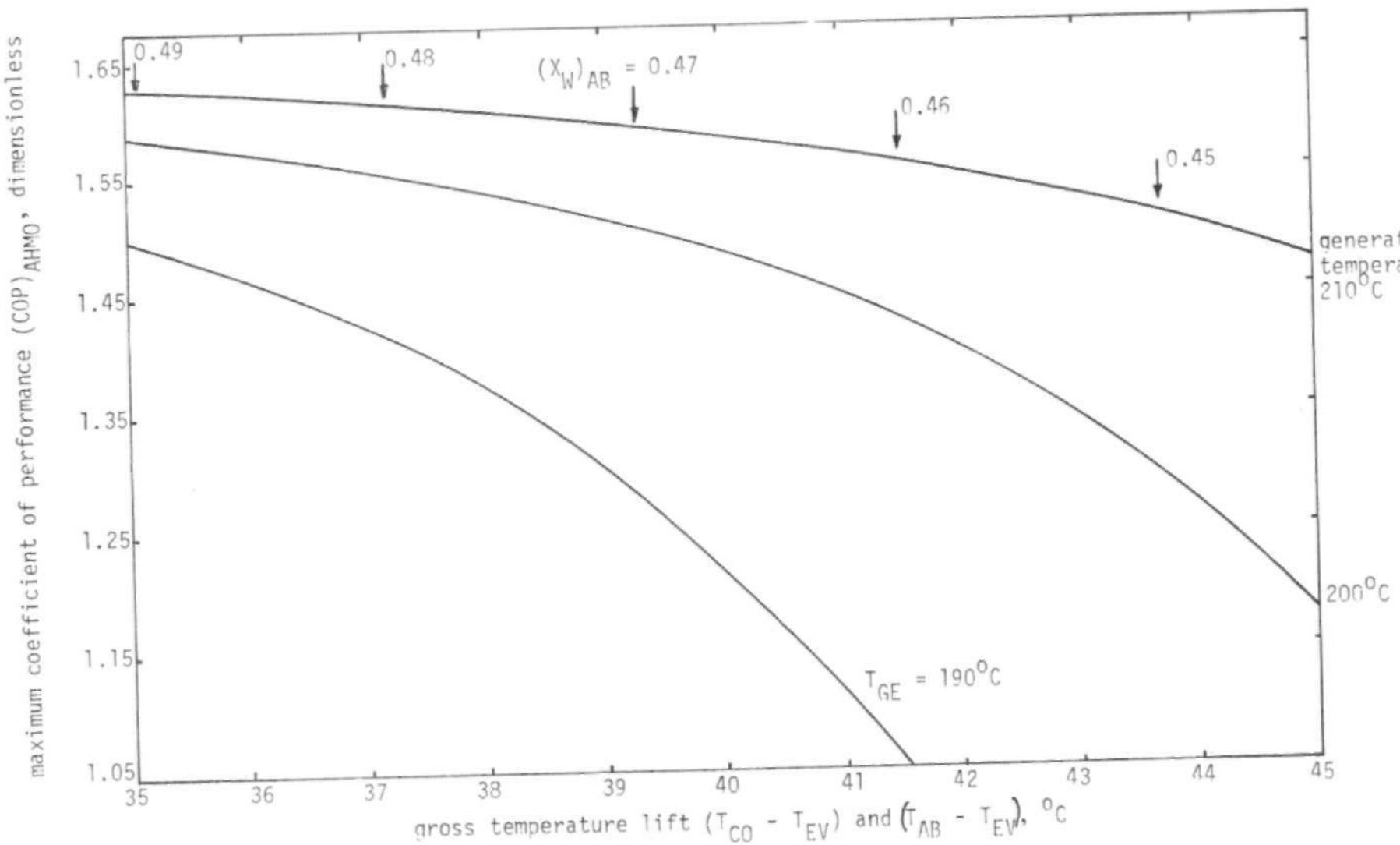


FIGURE (7.5) MAXIMUM OBTAINABLE COEFFICIENT OF PERFORMANCE AGAINST GROSS TEMPERATURE LIFT FOR EQUAL CONDENSER AND ABSORBER TEMPERATURES FOR EVAPORATOR TEMPERATURE OF 100°C AND A RANGE OF GENERATOR TEMPERATURES FOR THE WATER-LITHIUM BROMIDE SYSTEM

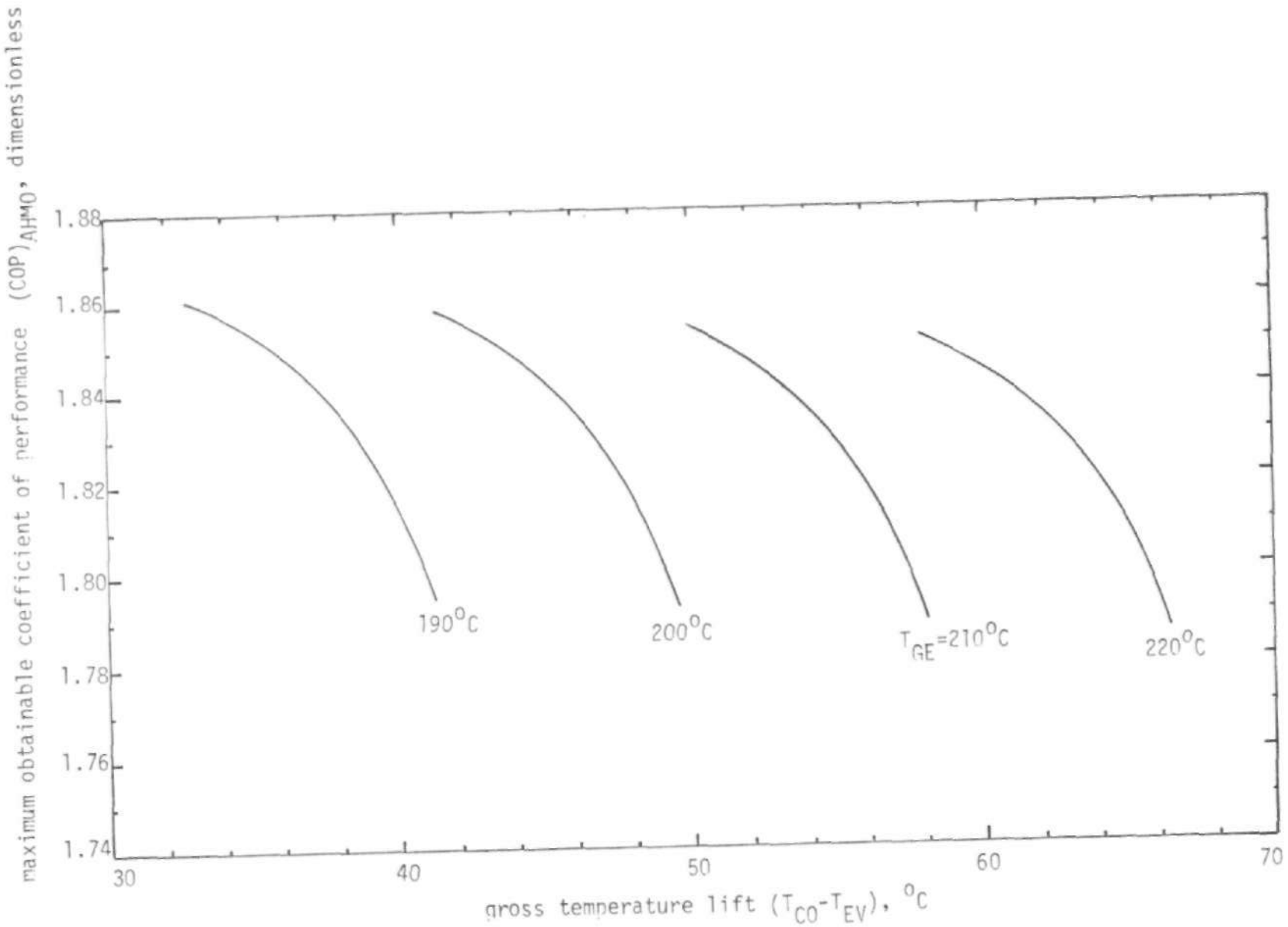


FIGURE (7.6) MAXIMUM OBTAINABLE COEFFICIENT OF PERFORMANCE AGAINST GROSS TEMPERATURE LIFT SHOWING THE INFLUENCE OF GENERATOR TEMPERATURE FOR AN ABSORBER TEMPERATURE LIFT OF 35.1°C, AN EVAPORATOR TEMPERATURE OF 100°C AND A WEIGHT FRACTION OF WATER IN THE ABOSRBER OF 0.49 FOR THE WATER-LITHIUM BROMIDE SYSTEM.

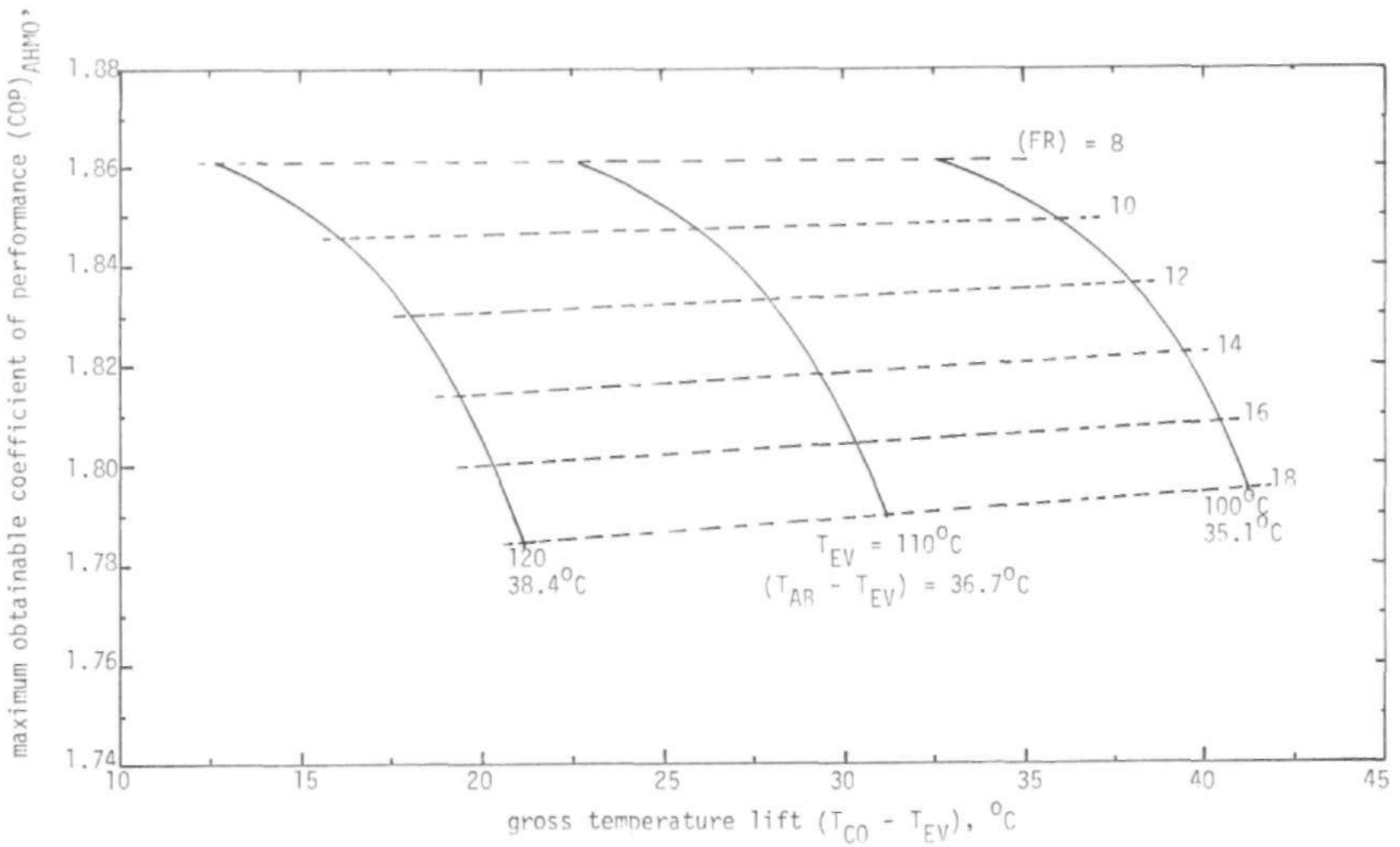


FIGURE (7.7) MAXIMUM OBTAINABLE COEFFICIENT OF PERFORMANCE AGAINST GROSS TEMPERATURE LIFT SHOWING THE INFLUENCE OF WATER-RICH SOLUTION FLOW RATE TO UNIT FLOW RATE OF VAPOUR (FR) FOR A RANGE OF EVAPORATOR TEMPERATURES, A GENERATOR TEMPERATURE 190°C AND A WEIGHT FRACTION OF WATER IN THE ABSORBER OF 0.49 FOR THE WATER-LITHIUM BROMIDE SYSTEM.

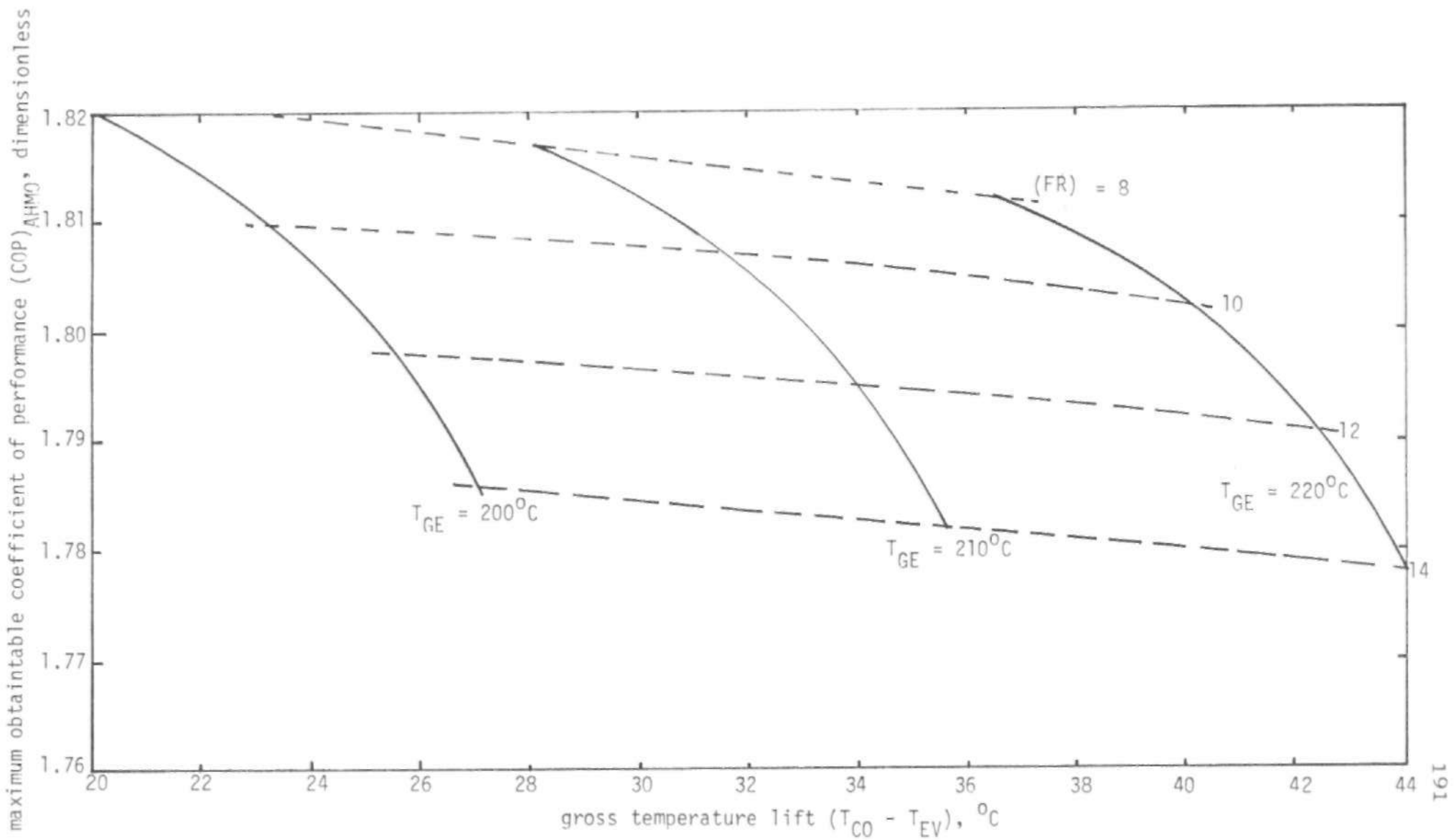


FIGURE (7.8) MAXIMUM OBTAINABLE COEFFICIENT OF PERFORMANCE AGAINST GROSS TEMPERATURE LIFT SHOWING THE INFLUENCE OF GENERATOR TEMPERATURE FOR A GROSS ABSORBER TEMPERATURE LIFT OF 47.8°C AND EVAPORATOR TEMPERATURE OF 110°C AND A WEIGHT FRACTION OF WATER IN THE ABSORBER OF 0.44 FOR THE WATER-LITHIUM BROMIDE SYSTEM

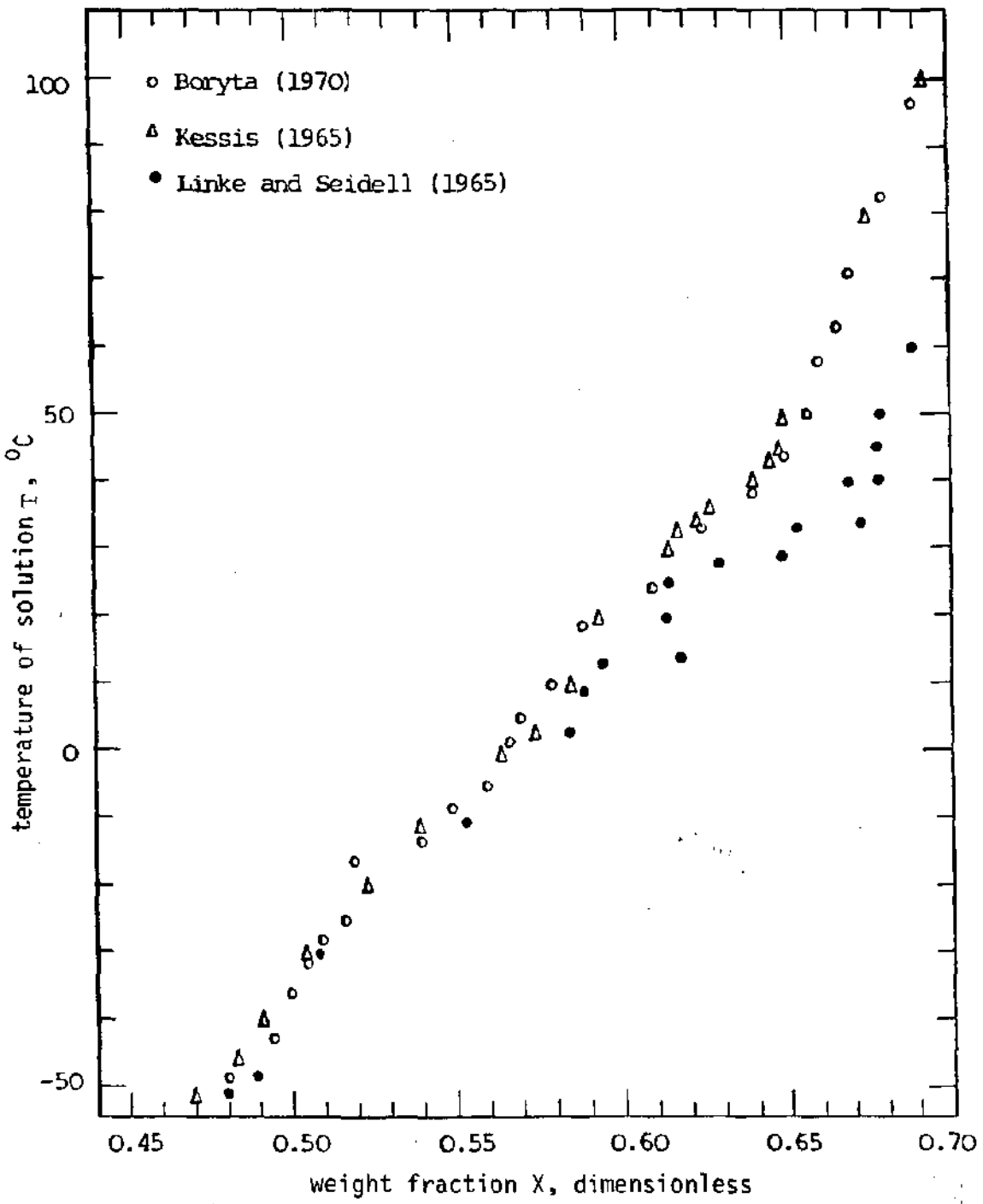


FIGURE (7.9) SOLUBILITY OF LITHIUM BROMIDE IN WATER

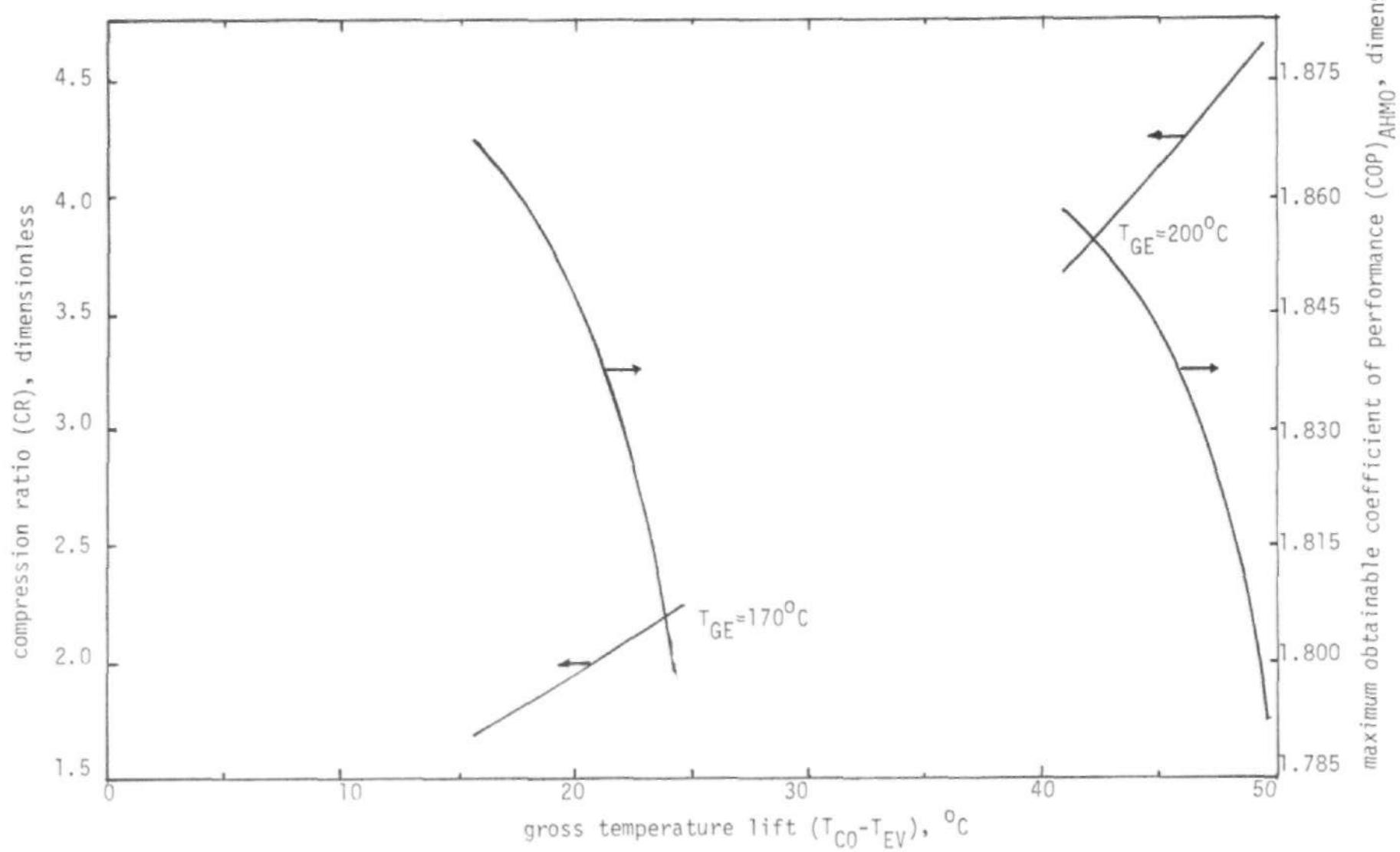


FIGURE (7.10) COMPRESSION RATIO AND MAXIMUM OBTAINABLE COEFFICIENT OF PERFORMANCE AGAINST GROSS TEMPERATURE LIFT FOR A GROSS ABSORBER TEMPERATURE LIFT OF $35^{o}C$ AND A WEIGHT FRACTION OF WATER IN THE ABSORBER OF 0.49 FOR VARIOUS GENERATOR TEMPERATURES FOR THE WATER-LITHIUM BROMIDE SYSTEM.

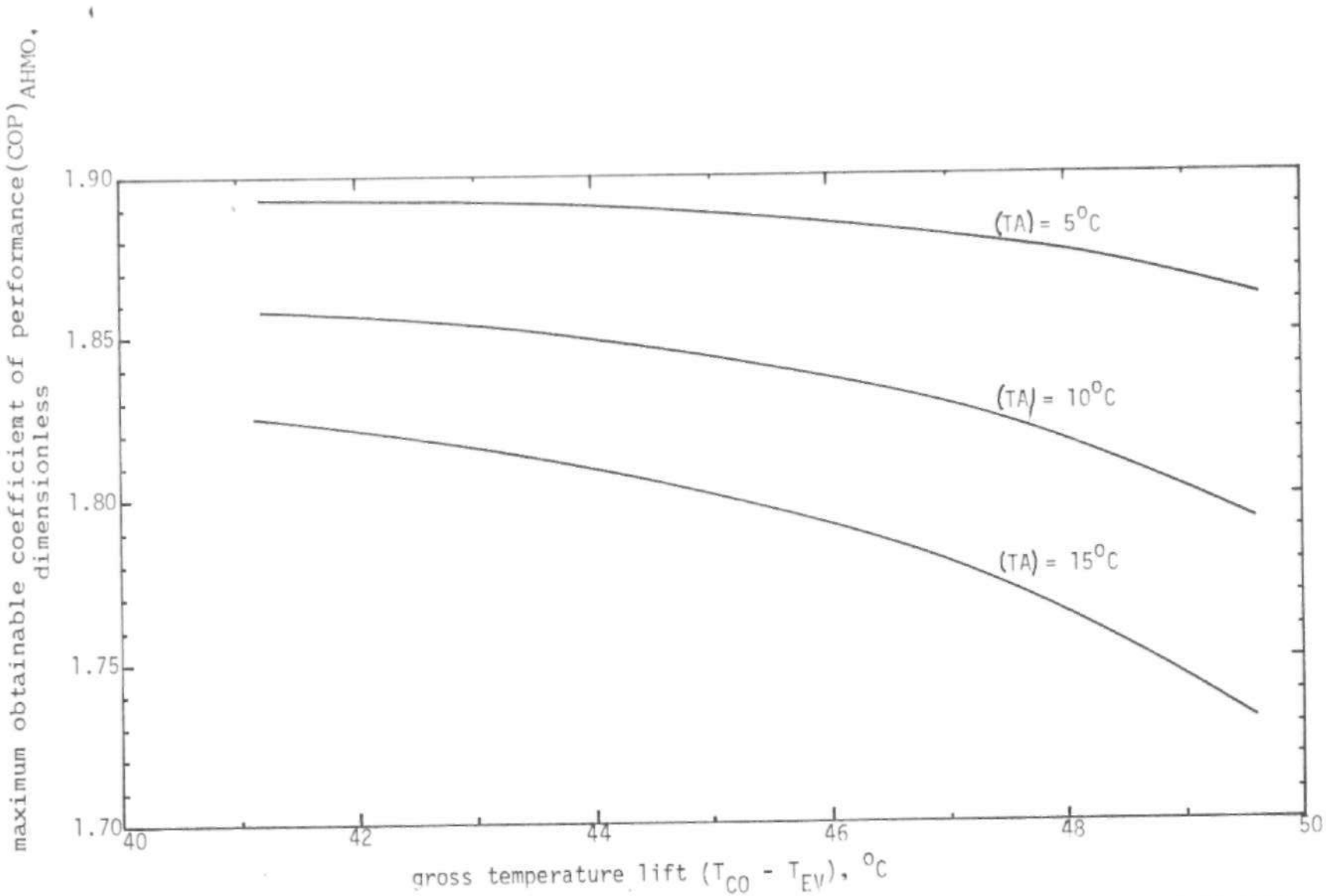


FIGURE (7.11) MAXIMUM OBTAINABLE COEFFICIENT OF PERFORMANCE AGAINST GROSS TEMPERATURE LIFT FOR VARIOUS TEMPERATURES (TA) IN THE ECONOMISER FOR AN EVAPORATOR TEMPERATURE OF 100°C, A GENERATOR TEMPERATURE OF 200°C AND A WEIGHT FRACTION OF WATER IN THE ABSORBER OF 0.49 FOR THE WATER-LITHIUM BROMIDE SYSTEM

CHAPTER 8

PERFORMANCE STUDIES USING WATER-LITHIUM BROMIDE SOLUTIONS IN CONVENTIONAL ABSORPTION HEAT PUMP SYSTEMS

CHAPTER 8

PERFORMANCE STUDIES USING WATER-LITHIUM BROMIDE SOLUTIONS IN CONVENTIONAL ABSORPTION HEAT PUMP SYSTEMS

8.1 INTRODUCTION

It has been shown in Chapter 7 that the insensitivity of the maximum obtainable coefficient of performance of a conventional absorption heat pump system $(COP)_{AHMO}$ to the compression ratio (CR) gives it an advantage over a vapour compression heat pump system, when high gross temperature lifts are required. This is particularly true when high temperature heat pump working fluids like water with characteristic high volume per unit enthalpy are the suitable candidates.

It has been shown in Chapter 4 that the high critical temperature of water, its high values of the theoretical Rankine coefficient of performance $(COP)_R$ and its stability, even at high temperatures, make it very attractive for use as a working fluid in heat pump systems required to deliver heat at temperatures up to 300°C. However, in Chapter 5 it was pointed out that its low enthalpy per unit volume $(\Delta H)_V$ was also responsible for the relative high heat losses leading to non-isentropic compression in the compressor. This resulted in low values of (COP) and gross temperature lift. This is because water vapour with a low heat load per unit volume passes through a compressor where it is likely

to lose a relatively high proportion of the heat it carries.

In an absorption heat pump system, the lift in pressure is achieved while the working fluid is essentially in the liquid state within the generator-expansion valve-absorber-solution pump unit. Figure (8.1) shows a simplified mechanical vapour compression heat pump and a simplified conventional absorption heat pump system. In the absorption heat pump system the equipment enclosed within the broken rectangle is essentially its 'compressor'. A notable advantage of the separate and simple units of the 'compressor' in the absorption heat pump system is that problems could be traced to separate units relatively more and solved easily than in the mechanical vapour compression system where the compressor, even in an open system, is always complex.

In most of the work reported on absorption processes using water as the working fluid, lithium bromide solutions are predominant. This is because of the relatively high affinity of lithium bromide for water resulting in relatively low pressures in the system. The first water-lithium bromide absorption system was reported by Berestneff ["Absorption refrigeration", Berestneff, A.A., Mechanical Engineering, 72, 216-220 (March 1950)]. It was built for cooling. Recently Boldrin, Bolzan and Lazarin ["Lithium bromide absorption cooling devices", Boldrin, B., Bolzan, M. and Lazarin, R., Tagunsbericht Internationales Sonneforum 2nd., Hamburg, West Germany, 127-136 (1978)] used a

lithium bromide chiller type Yazaki WFC 400S as a heat pump. They reported the following results:

temperature of solution in the generator, ^{o}C	90
temperature of evaporating fluid, ^{o}C	13
temperature of solution in the absorber, ^{o}C	47
temperature of condensing fluid, ^{o}C	47
coefficient of performance, dimensionless	1,31

There are no reports in the literature on the use of water-lithium bromide in conventional absorption heat pump systems to produce heat at high temperatures.

It is possible that the reasons why absorption heat pump systems using water-lithium bromide mixtures have not been developed are corrosion and crystallisation due to complete degassing at high temperatures. Mansoori and Patel ["Thermodynamic basis for the choice of working fluids for solar absorption cooling systems", Mansoori, G. A. and Patel, V., Solar Energy, 22(6), 483-91 (1979)] reported that the system water-lithium bromide is corrosive to steel at high temperatures. However, attempts had earlier been made by Kreuger ["Corrosion inhibitors for absorption refrigeration system", Kreuger, R.H., U.S. 4,019,992 (April 26 1977)] to overcome this disadvantage through the addition of anti-corrosion materials. The properties of hydrated salts of lithium bromide given by the manufacturers ["Technical data", Boryta, D.A., Bulletin 145, Foote Mineral Company, Exton, U.S.A.] and reproduced in Table (A.IV.2)

show that crystallisation of solutions of the salt could occur at temperatures above 156°C due to complete degassing.

The problem of corrosion is not expected to be so serious as to outweigh the other advantages of the water-lithium bromide system for use at high temperatures in absorption heat pump systems. If serious problems are observed, corrosion inhibitors could be used. Crystallisation due to complete degassin at high temperatures would be avoided by ensuring good mixing of the solutions particularly, in the generator.

The decision was made to design and develop an experimental conventional absorption heat pump system operating on water-lithium bromide solutions at high temperatures using stainless steel as the material of construction. In addition, it was decided to modify an equivalent system which was constructed mainly with glass, for use at medium temperatures. The glass system was originally used for investigations on the reversed absorption heat pump cycle.

8.2 PERFORMANCE STUDIES USING WATER-LITHIUM BROMIDE SOLUTIONS IN A METAL ABSORPTION HEAT PUMP SYSTEM

8.2.1 Equipment

The experimental equipment developed for investigations

using water-lithium mixture at high temperatures is presented in Figure (8.2). All the vessels were custom made using stainless steel AISI type 304 while all the pipes were stainless steel (seamless cast) AISI type 316. All the other parts were selected from well proven, reliable parts, readily available in the U.K.

The design of the equipment was based on the assumption of a thermal load in the evaporator Q_{EV} of 1.2kW at a temperature T_{EV} of 100°C, and lithium bromide concentrations in the absorber and in the generator of 50 per cent and 55 per cent respectively. The design procedure and calculations for the absorber are given in Appendix III.
The design of the other units are not reproduced here because the procedures are well known. Heat was removed from the absorber and condenser using pressurised water.

A brief description of the various parts of the equipment is given below.

Evaporator

A detailed drawing of the evaporator is shown in Figure (8.3). It was installed vertically.

The unit consisted of a main chamber and a side arm connected by two channels. The arrangement was conceived to effect mixing by natural circulation.

On the main chamber, the largest of the three openings

through the top cover served as outlet for vapour while the other two were used (one each) for pressure and temperature measuring probes. The pressure measuring probe also carried a high pressure cut off valve. An opening towards the top of the side wall was used as inlet for water from the condenser while an opening on the bottom cover served as the sampling point.

Four holes were placed on a vertical line directly opposite the side arm. Initially, holes number 1 and 3 (counting from the top) carried liquid level indicators. The liquid level indicators were made using the LM 1830 liquid detector supplied by Farnell Electronic Components, Leeds, U.K. The LM 1830 was a bipolar integrated circuit through which an AC signal was passed within the liquid. A detector determined the presence or absence of liquid by comparing the resistance of the fluid between the probes with the resistance internal to the integrated circuit. The liquid in the evaporator proved too conductive for the design of the probe and it was replaced with a sight glass supplied by Ashfords of Salford, Salford, U.K. The sight glass was connected to the lowest and uppermost holes on the vessel.

The use of a sight glass was avoided originally so that the equipment would be operable at high pressure (and temperature) levels. The maximum pressure recommended for the glass was 45 psig. The two extra holes on the vertical line were fitted with stainless steel rod intended to

monitor corrosion. The vessel was filled with stainless steel swarf to the level of the fluid inlet point. This was intended to prevent bumping during boiling and also to prevent entrainment of liquid droplets. A baffle, which was one third of the inner diameter of the vessel, was welded to the wall just below the fluid inlet point. The baffle tilted down at 10 degrees from the horizontal. It was intended to spread the incoming fluid in a thin layer.

The side arm of the unit carried an inner tube with an internal diameter of $\frac{3}{4}$in (0.01905m) to hold a 2kW cartridge heater. The sheath temperature of the heater at maximum load is 800°C. The heater was supplied by Cole Equipment Ltd., Sussex, U.K. It was $\frac{3}{4}$in. (0.01905m) in diameter and 8ins. (0.2032m) tall and was placed in the tube through the base. The inner tube was grooved externally to enhance heat transfer through its wall. A small hole at the top of the inner tube served as a point for the measurement of the temperature of the heater.

Generator

The generator was similar to the evaporator except in the supply of heat and the design of the outlet on the bottom cover.

Originally, heat was supplied to the generator using the same type of cartridge heater in the evaporator. However, the failure of the original liquid level probes

resulted in crystallisation of lithium bromide solutions due to local degassing, (lithium bromide solution is even more conductive than water) causing the burning of the heating element. Therefore, inspite of the replacement of the liquid level indicator, the heating system was replaced with two electric heating coils. The coils were wound in series, around the main chamber of the unit. Each of the elements, with a diameter of 0.250in. (0.006m) had overall and effective lengths of 115.75ins (2.94m) and 111.5ins. (2.83m) respectively. The overall capacity of the two elements was 1.5kW. The sheath temperature at maximum load is 400^{o}C. The heaters were supplied by Backer Electric Co. Ltd., Rotherham, U.K. The new arrangement of heating was designed to supply heat through a high surface area. This would prevent possible degassing of the lithium bromide solution in the vessel.

The hole on the bottom cover of the main chamber carried a T-joint to separate the solution outlet pass and the sampling point.

Absorber

The complex unit referred to here as the absorber consisted of a mixing vessel and an absorption tube within a cooling tube. The unit was installed vertically.

The mixing vessel was 0.17m tall and 0.14m wide. It admitted lithium bromide solution through a top opening while water vapour entered through the mid-point of the side.

The mixture of water vapour and the solution flowed into the absorber tube. A stainless steel guaze shaped into a series of three concentric cones was placed at the solution inlet of the mixer. The cone was 0.025m wide at the base and 0.15m long. It was secured with a pin placed horizontally through a T-joint above the mixer. The gauze was intended to effect distribution of the lithium bromide solution.

The absorber tube and the absorber cooler were made of two concentric tubes. The arrangement was designed to effect absorption and heat transfer simultaneously. Absorption took place in the inner tube which was 0.97m long and had a $\frac{3}{4}$in. (0.01905m) inside diameter. Stainless steel swarf was placed in the bottom of the inner tube to a depth of 0.05m. A strip of stainless steel gauze was installed above the swarf. The gauze was shaped into an helix with a nominal diameter of the tube. This packing was intended to effect mixing and enhance heat transfer. External fins on the tube were intended to further enhance heat transfer. The fins were spirally arranged. The inner diameter of the shell was 3ins. (0.076m). It was packed with $\frac{1}{8}$in (0.00317m) Raschig rings. Cooling water flowed through it co-currently with the mixture of water vapour and lithium bromide solution.

A cylindrical vessel was connected to the bottom of the absorber to receive water-rich lithium bromide solution. The receiver was 0.15m tall and 0.10m wide. A sight glass was installed on the receiver through two side openings. Pressure and temperature measuring points were also provided

on the side of the receiver. The sight glass replaced a liquid detector LM 1830 which was initially installed to monitor the solution level. The liquid detector was replaced because it failed like the ones in the generator and evaporator.

Economiser heat exchanger

The economiser was a double pipe heat exchanger positioned horizontally. It consisted of two passes with the cool and hot solutions flowing counter-currently through the tube and shell respectively. The inner tube with inside diameter of 0.01905m was 0.86m long per pass. The outer tube with an inside diameter of 0.005m was 0.76m long per pass. The centre to centre distance of the inner tubes was 0.2m. The shells were connected through a tube with $\frac{1}{2}$in. (0.00127m) inside diameter. Both the shells and the tubes were loosely filled with stainless steel swarf to enhance heat transfer.

Condenser

The condenser was made of double concentric pipes and it was positioned vertically. Water vapour entered the inner tube from the top. Cooling water was passed through the shell, counter-currently to the condensing water. Both the inner tube and the shell were filled with stainless steel swarf to enhance heat transfer.

The inner tube had an internal diameter of $\frac{3}{4}$in (1.9cm)

and was 0.51m long. The shell was 0.05m wide.

A condensate receiver which was a cylindrical shell 0.25m long and 0.18m wide, was installed horizontally by the side of the condenser. The centre line of the cylinder was positioned on the same level as the lowest end of the condenser shell. This arrangement allowed sub-cooling or otherwise of the condensate. Sub-cooling was achieved by raising the level of the condensate, in the cylinder and in the tube, above the level of cooling water entering the shell of the condenser. The inner tube of the condenser was connected to the condensate receiver at its base. The condensate outlet was also positioned at the base of the receiver. The outlet led to the evaporator and vent through a T-joint. An opening at the top of the receiver carried a pipe with a funnel at its end. Two holes at the side provided for the attachment of a sight glass with an extension on the lower arm for pressure point.

Pumps

The equipment was fitted with three gear pumps - a solution pump between the absorber and the economiser heat exchanger and one each on the cooling water lines into the absorber and condenser.

The solution pump was a P.Q.10 Morgan Pump supplied by Pump and General, Sussex, U.K. It was driven by a three-phase 0.375kW motor supplied by Allspeeds Ltd., Accrington, U.K.

The pump had a maximum capacity of 10 litres per minute at a pressure of 10 bar. It is capable of delivering 8.7 litres per minute at a pressure of 80 bar when driven by a 3kW motor. The other two pumps, supplied by Michael Smith Engineers Ltd., Surrey, U.K., were the 120-401-10A type. They are capable of providing flows up to 4.5 litres per minute or pressures up to 90 psig.

Valves

The flow control valves and the two pressure reducing valves were needle valves supplied by Kenmac Controls Ltd., Isle of Man, U.K. The packings in them were PTFE. The pressure relief valve on the generator was the spring load type supplied by Hoke International Ltd., Barnet, U.K. The pressure control valves used on the cooling water lines were the spring loaded relief valves supplied by Hale Hamilton (Valves) Ltd., Uxbridge, U.K. Three-way valves were used on the cooling water lines drains for the purpose of directing water into either the drain or for collection.

8.2.2 Instrumentation

Chromel-alumel thermocouples with digital read-out accurate to 0.1^{o}C were used for temperature measurements. The thermocouples measuring the temperatures in the generator, evaporator, generator solution outlet, water-rich solution into the economiser, water-poor solution from the economiser and the temperature of sub-cooled water from the condenser

were connected to a six point recorder. The recorder, Model 3020 was supplied by Chessel Ltd., Sussex, U.K.

Bourdon type guages were used for pressure measurements. Four guages were provided on the high pressure side and three on the low pressure side. The guages on the high pressure side ranged from 0 to 16 bar and were readable to 0.1 bar. The pressure guage on the evaporator ranged from 30ins. vacuum to 15psi and was readable to 0.2in and 0.2psi. The other two guages ranged from 0 to 6 bar and were readable to 0.02 bar. Atmospheric pressure was read from a Toricellian barometer and ambient temperature was read from a mercury in glass thermometer.

Standard ammeters and voltmeters were used for electrical measurements. The flow rates of cooling water through the absorber and condenser were obtained by direct weighing. The temperature of the cooling water was controlled using the LM 3911N temperature controller supplied by Farnell Electronic Components, Leeds, U.K. The temperature controller was connected to the cooling water heater.

The outlet pressure of the water was controlled using the spring loaded pressure relief valve with a manual control system.

The flow rate of the water-rich solution was read from a rotameter.

The levels of fluid in the generator, condenser,

absorber and evaporator were monitored using sight glasses supplied by Ashfords of Salford, Salford, U.K.

All instruments were calibrated before installation and checked in situ. Figure (8.2) shows the locations of the measurement positions.

8.2.3 Commissioning the equipment

After the initial setting up of the equipment it was tested for pressure and water tightness simultaneously. This was done by charging the equipment with water through one of the valves at the low levels. The procedure was preceeded with the shutting of all the other valves except the one at the topmost level on the equipment. This valve was closed when water began to flow out through it indicating that the system was purged of air. The pressure guages with the maximum range below the required test-pressure were isolated. The sight glasses were also isolated.

A pneumatically operated hydraulic pump supplied by Madan Fluid Power From Air Co. Ltd., Altrincham, U.K., was used for pressurisation. The pump, which was pneumatically operated, was capable of producing pressures up to 200 bars.

During the process of pressurisation, leaks were investigated and stopped. At this stage, the leaks were through the compression fittings on the pipes. The leaks were stopped by re-tightening the fittings. In some cases the rings on the fittings had to be replaced. In few cases

PTFE tapes had to be used in conjunction with the rings.

The equipment was certified to be capable of standing a pressure of 15 bar (guage). In addition, it was water-tight up to this pressure. The equipment should be capable of standing higher pressures but this was not investigated because it was not required.

After the high pressure testing, the pressure on the equipment was relieved to a pressure of 4 bar guage, by opening the pressure relief valve on the generator. Then the isolations on the sight glasses were removed.

After this procedure, the equipment was vacuum-tested. The vacuum was established using a Metrovac Rotary Vacuum Pump type GDP, manufactured by Associated Electrical Industries Ltd., U.K. The equipment withstood a vacuum of 758mmHg for three nights.

The equipment was cleaned by circulating hot water through all the units for periods of about four hours. The water was heated in the generator.

Initially, the equipment was lagged using a 0.01m thick fibrous insulating material. When the lagging material on the generator got burnt, it was replaced with two layers of fibrefrax over the heater and followed with the original lagging material.

The system was then charged with lithium bromide

solution and a trial operation was carried out. The operation was not successful because of the failure of the electronic liquid level probes.

The first operation after the installation of the sight glasses failed because of leakages of fluid through many joints on the equipment. The leaks were mainly through welded parts, some valves and connections where PTFE rings were used as packing. It was discovered that the leaks on the welded parts were due to the corrosion of left-over slag. The leaks through the valves and joints with PTFE rings were due to the contraction of the PTFE after the initial expansion during the first heating operation. The welds were remade and the joints were re-tightened all round, particularly where PTFE materials were present. In some cases, two valves (one after the other) were installed.

The system was pressure-tested and vacuum-tested again as described above. It was successful for both conditions.

Charging

The solution reservoir was filled with lithium bromide solution of the required concentration. Then solution from the reservoir was allowed to flow into the absorber receiver. When the liquid level reached a prescribed mark in the receiver, the pump was switched on. The flow rate of the solution into the generator was controlled by adjusting the speed of the pump and the valve immediately below the rotameter.

The main aim was to maintain the level of the solution in the absorber receiver. Meanwhile, a marked level of liquid in the solution reservoir was maintained by topping with more lithium bromide solution. These operations were continued until lithium bromide solution reached a marked level in the generator. The pump was switched off and the valve below the rotameter was closed to prevent back flow of solution into the absorber. It was observed that eight litres of lithium bromide solution were required to charge the economiser and generator.

The condensate receiver was charged with distilled water through a funnel which was installed above it. Referring to Figure (8.2) and Table (8.1), the condensate expansion valve was opened to let water flow into the evaporator. During this process the valve at the top of the evaporator was opened. This was required to prevent pressure build-up in the evaporator. When the water in the evaporator had reached a marked level the condensate expansion valve was closed. Six and half litres of water were required to charge the two vessels.

8.2.4 Experimental procedure

8.2.4.1 Preparation and standardisation of aqueous lithium bromide solution

The anhydrous lithium bromide used was supplied by Foote Mineral, U.K. The assay of the salt is presented in Table (A.IV.1). Since the salt was contaminated with

dirt, it had to be purified before use.

A stock solution of approximately 50 per cent by weight of lithium bromide was prepared by weighing known quantities of the anhydrous lithium bromide and distilled water into a plastic container and a stainless steel vessel respectively. The salt was sprinkled into the distilled water, while stirring vigorously. A stainless steel rod and a stainless steel spatula were used. The hot dirty solution was then left to cool down.

The solution was purified by filtering it through a double layered filter paper No. 44. The stock solution was stored in a plastic bottle.

About 250ml of the stock solution was heated in a beaker using a bunsen burner, until it crystallised. The crystallised salt was stored in an oven at 180^{o}C for twenty-four hours.

Known weights of the clean anhydrous salt and distilled water were placed in 20ml sample bottles. The weighing was done using an Oertling R41 Electric Balance type Mark II weighing balance, accurate to the fifth decimal place. The refractive indices of the solutions were obtained using a high precision ABBE '60' 60/ED refractometer. The refractometer was also accurate to the fifth decimal place. The light source was a 589.6nm sodium D-line.

The refractive indices of solutions between 40 per cent

and 65 per cent were measured at 30°C. The calibration curve is presented in Figure (A.IV.1).

8.2.4.2 Experimental technique

In order to establish steady state conditions in the system, it was necessary that the mass flow rate of the working fluid (water) leaving the generator and that absorbed into the absorber were exactly the same. At steady state the following balances hold

$$M_{AB} = M_{GE} + (M_W)_{EV} \qquad (8.1)$$

$$(M_W)_{CO} = (M_W)_{EV} \qquad (8.2)$$

Equations (8.1) and (8.2) imply that the levels of the liquids in the generator, absorber receiver and the evaporator should remain unchanged under steady state conditions. This was achieved by balancing

the rate of heat input to the generator Q_{GE}
the rate of heat input to the evaporator Q_{EV}
the circulation ratio (FR)
the reflux ratio (FRX)

with

the rate of cooling of the condenser Q_{CO}
the rate of cooling of the absorber Q_{AB}

The circulation ratio (FR) is the ratio of the mass flow rate of the water-rich lithium bromide solution M_{AB} to the mass flow rate of the pure water M_W. The reflux ratio (FRX) is the ratio of the mass flow rate of the water-rich lithium bromide recirculated through the absorber M_R to the mass flow rate of the water-rich lithium bromide solution pumped into the generator M_{AB}. Observations showed that the steady state conditions were significantly influenced by the reflux ratio. A constant flow rate of the working fluid (water) through the system was achieved by correct adjustments.

After a series of experimental runs, the pre-start, start-up, experimental investigations and shut-down routines for the heat pump system were established to be as follows:

(a) Pre-start

i) Plan the experimental investigations to be carried out.

ii) Determine roughly the condenser and absorber temperatures.

(b) Start-up

i) Switch on the cooling water tank heater.

ii) Switch on the cooling water temperature control heater. Set the temperature

controller based on the lowest possible temperature in (a) (ii).

iii) Ensure that the liquid levels in the generator, condensate receiver, evaporator and the absorber receiver correspond to the indicated marks.

iv) Switch on the solution pump and open the appropriate valves to ensure circulation of solution in the system. Adjust the pump speed controls and the appropriate valves to obtain the required flow rates of solution into and from the generator in order to maintain constant levels in the generator and absorber receiver.

v) Switch on the generator heater. When the generator temperature reaches a reasonable level [this is based on (a) (i)] switch on the generator heater. Control the heat input to the generator so that the generator temperature rises steadily. Control the heat input into the evaporator so that $(T_{AB}-T_{EV})$ is about $20^{o}C$. Vent air from the system through appropriate valves. When the solution in the generator starts to boil at its saturation temperature, shut the vent valve. When the water in the evaporator

starts to boil at its saturation temperature, shut the vent valve (if the boiling temperature is not reached before the required generator temperature is attained purge the evaporator-absorber with a vacuum pump).

(c) Experimental investigations

i) When the required generator temperature is attained, start reflux of solution through the absorber. Adjust the flow rate of the water-rich solution. Switch on the cooling water pump. Adjust the flow rate of the cooling water to the condenser and absorber. Reset the cooling water temperature controller if necessary. Adjust the cooling water pressure relief valve as required.

ii) When steady state is attained maintain it for thirty (30) minutes.

iii) Take temperature and pressure readings. Take the rotameter reading. Collect cooling water over a recorded time. Collect samples of solutions from the generator and absorber. Weigh the cooling water. Measure the refractive indices of the samples of solution.

iv) Alter the experimental conditions and establish a new steady state. The lithium bromide solution in the generator is diluted by reducing the rate of heat input into it. The heat input into the evaporator is maintained and the cooling of the condenser and absorber is maintained. The lithium bromide solution in the generator is concentrated by reducing the rate of heat input into the evaporator while increasing the rate of heat input to the generator. The cooling of the condenser is maintained while the absorber is by-passed.

(d) <u>Shut-down</u>

i) Switch off the generator heater and stop the flow of cooling water to the condenser. Continue the circulation of the solution through the system. Dilute the solution in the generator to a concentration sufficiently below the crystallisation limit at room temperature.

ii) Switch off the evaporator heater. Bring the level of solution in the absorber receiver to the indicated mark and switch off the solution pump. Switch off the cooling water pump and close all valves.

8.2.5 Results and discussion

The results of the three sets of experimental runs conducted at two different generator temperatures T_{GE} and two different evaporator temperatures T_{EV}, and a range of concentrations of lithium bromide solutions, are presented in Tables (8.2) to (8.4)

Graphs of observed coefficients of performance $(COP)_{AHA}$ and maximum obtainable coefficients of performance $(COP)_{AHMO}$ against gross condenser temperature lifts are presented in Figures (8.4) to (8.6).

The heat supplied to the evaporator Q_{EV} and the heat supplied to the generator Q_{GE} were taken as the product of the voltages and the currents read from the voltmeters and ammeters attached to the electric heaters on the units.

The heat delivered by the absorber Q_{AB} was computed as the product of the flow rate of cooling water $(M_{CW})_{AB}$ the heat capacity $(C_p)_{CW}$ at its bulk temperature and its temperature rise $(\Delta T)_{CW}$.

$$Q_{AB} = (M_{CW})_{AB} (C_p)_{CW} [(T_{CW})_{OUT} - (T_{CW})_{IN}] \qquad (8.3)$$

Similarly, the heat delivered by the condenser Q_{CO} was computed using Equation (8.4)

$$Q_{CO} = (M_{CW})_{CO} (C_p)_{CW} [(T_{CW})_{OUT} - (T_{CW})_{IN}] \qquad (8.4)$$

The total heat delivered was taken as the sum of Q_{AB} and Q_{CO}.

$$Q_D = Q_{AB} + Q_{CO} \tag{8.5}$$

The heat capacity per unit mass of water was obtained by interpolation from tables ["Chemical Engineers Handbook", Perry, R.H., Chilton, C.H. and Kirkpatrick, S.D., McGraw-Hill Book Company, Inc., 4th Edition, 3-123, (1963)].

Assuming there were no heat losses to the ambient, a perfect heat balance would be

$$Q_D = Q_{EV} + Q_{GE} \tag{8.6}$$

The heat balance error was computed with reference to the delivered heat Q_D as

$$\text{Percentage heat balance error} = \frac{Q_D - Q_{EV} - Q_{GE}}{Q_D} \frac{100}{1} \tag{8.7}$$

The actual coefficient of performance was evaluated using Equation (8.8)

$$(COP)_{AHA} = \frac{Q_{AB} + Q_{CO}}{Q_{GE}} \tag{8.8}$$

The maximum obtainable heat pump effectiveness factor was obtained using Equation (8.9)

$$(HPE)_{AHMO} = \frac{(COP)_{AHA}}{(COP)_{AHMO}} \tag{8.9}$$

The maximum obtainable coefficient of performance $(COP)_{AHMO}$ was evaluated using Equation (7.14)

$$(COP)_{AHMO} = \frac{H_4-H_7+(FR)(H_7-H_8)+H_1-H_2}{(FR)(H_5-H_{10})+H_1-H_5} \qquad (7.14)$$

The numbers in Equation (7.14) refer to those in Figure (7.1). The values of the enthalpies in Equation (7.14) were obtained by interpolation using Figures (6.1) to (6.3) and from tables ["Thermodynamic properties of water including vapour, liquid and solid phases", Keenan, J.H., Keyes, F.G. and Moore, J.G., John Wiley and Sons, New York, (1969)] using the values of some temperatures obtained experimentally. In order to avoid the dependence of the computed value of $(COP)_{AHMO}$ on heat losses from the equipment, the enthalpy per unit mass of the fluids leaving the generator, condenser, absorber and evaporator were obtained using the bulk temperatures in the respective unit of the equipment. The enthalpy per unit mass of the materials entering the generator, condenser, absorber and evaporator were taken at the conditions of the fluids in the units preceeding them. However, the enthalpy per unit mass of the solution of lithium bromide entering the absorber was determined at the temperature of the solution at the exit of the economiser heat exchanger so that the inefficiencies of the expansion valve and the piping between them are not reflected in the values of $(COP)_{AHMO}$.

The flow ratio (FR) was computed using Equation (8.10)

$$(FR) = \frac{X_{GE}}{X_{GE}-X_{AB}} \qquad (8.10)$$

The flow rate of the water-rich solution of lithium bromide from the absorber was determined using Equation (8.11)

$$M_{AB} = M_G \rho_{AB}/\rho_G \qquad (8.11)$$

where

M_G is the mass flow rate of the water-rich solution of lithium bromide, corresponding to the reading on the absorber rotameter, obtained using the calibration curve in Figure (A.IV.2).

ρ_{AB} is the density of the water-rich solution of lithium bromide at the conditions of the experiment.

ρ_G is the density of the solution of lithium bromide used for the calibration.

The density of solutions of lithium bromide was obtained using Equation (8.12)

$$\left.\begin{aligned} &\rho_{LiBr} = A + B/T \\ &A = 8.77067E\text{-}1 + 2.68857E\text{-}3X + 1.3494E\text{-}4X^2 \\ &B = 4.60172E1 + 3.94630E\text{-}1X - 3.5986E\text{-}3X^2 \\ &\text{root mean square residual} = 1.6488E\text{-}3 \end{aligned}\right\} (8.12)$$

where T is in degrees Kelvin.

Equation (8.12) was obtained using the NON-LINEAR REGRESSION SPSS Computer programme at the University of Manchester Regional Computer Centre, Manchester, U.K. The density-concentration-saturation temperature data of lithium bromide

solutions presented by Uemura ["Studies on the lithium bromide-water absorption refrigerating machine", Uemura, T., and Hasaba, S., Technical Report of Kansai University 6, 31-35 (1964)] were used.

The flow rates of water M_W and water-poor solution of lithium bromide were obtained using Equations (8.13) and (8.14)

$$M_W = M_{AB}/(FR) \tag{8.13}$$

$$M_{GE} = M_{AB} - M_W \tag{8.14}$$

The arithmetic mean of the pressures taken just before and after the condenser was considered to be more representative of the condensing pressure P_{CO}. The equilibrium condensing temperature T_{CO} was determined as the saturation temperature of water corresponding to P_{CO}. The observed evaporator temperature corresponded with the equilibrium saturation temperature of water.

The experimental values of T_{CO} varied between 123°C and 147°C while the values of T_{AB} varied between 129°C and 135°C. The heat removed from the system was delivered at temperatures between 124°C and 141°C. The highest temperature reached in the system was limited by the pressure in the generator at which the sight glass could be used safely. Gross temperature lifts varied between 24°C and 47°C. The experimental errors introduced into the results were relatively very small.

The measurements of temperatures with the NiCr/NiAl thermocouples coupled to the digital unit introduced an error of $\pm$ 0.1^{o}C. The values of the heat capacities of water and the enthalpy per unit mass lithium bromide solutions were obtained from the literature and from correlation in this thesis and are in themselves subject to experimental errors. However, for the purpose of analysing the performance of this equipment, the values of these heat capacities were assumed to be error free.

The mass flow rates of lithium bromide solutions were determined from the calibration curve in Figure (A.IV.2).

The curve was obtained by weighing samples of solutions collected during intervals of two (2) minutes. The weights were determinable to within $\pm$ 0.01gm under these conditions. The mass flow rate per hour was approximated to the nearest $\pm$ 0.1kg. For the average flow rate of 16kg h^{-1}, the error was 0.31 per cent.

The errors in the measurement of the temperature lifts and the temperature changes in the cooling fluid streams could be $\pm$ 0.2^{o}C. The maximum percentage error occurs with the smallest temperature change observed. For a minimum temperature lift of 24^{o}C and a minimum temperature change of about 16^{o}C for the cooling fluid, the maximum errors thus amounted to 0.8 per cent and 1.33 per cent respectively.

The values of Q_{AB} and Q_{CO} were obtained using Equations (8.3) and (8.4) respectively. The percentage error in Q_{AB} and Q_{CO} were the sum of the percentage errors in the individual

variables on the right hand sides of Equations (8.3) and (8.4). For a cooling water flow rate of 16kg h^{-1} and a temperature change of 15°C the maximum error in Q_{AB} and Q_{CO} was

$$0.31 + 1.33 = 1.64 \text{ per cent each}$$

The voltmeters and the ammeters could be read to the nearest $\pm$ 2volts and $\pm$ 0.1amps respectively. For the minimum rate of heat input into the generator Q_{GE} of 1100W the percentage error was 0.018 per cent.

The $(COP)_{AHA}$ was obtained using Equation (8.8). The maximum expected error in $(COP)_{AHA}$ was, therefore, the sum of the error, in Q_{AB}, Q_{CO} and Q_{GE} and would be

$$1.64 + 1.64 + 0.018 = 3.298 \text{ per cent}$$

Figures (8.4), (8.5) and (8.6) are plots of $(COP)_{AHA}$ and $(COP)_{AHMO}$ against gross temperature lifts $(T_{CO} - T_{EV})$ for T_{GE} of 172°C, 172°C and 197°C respectively. The experimental results were reproducible and consistent as born out by the three graphs.

'Best fit' curves were drawn through the experimental points. The correlations of the curves in Figures (8.4), (8.5) and (8.6) are given in Equations (8.15) to (8.17)

respectively.

$$(COP)_{AHA} = 4.1418E\text{-}2 + 2.9215(T_{CO}-T_{EV})^{-0.26179} \quad (8.15)$$

with root mean square residual = 3.0881E-3

$$(COP)_{AHA} = -2.9493E\text{-}2 + 3.6588(T_{CO}-T_{EV})^{-0.30297} \quad (8.16)$$

with root mean square residual = 2.3426E-3

$$(COP)_{AHA} = 1.5575 - 8.1879E\text{-}3(T_{CO}-T_{EV})^{0.97554} \quad (8.17)$$

with root mean square residual = 2.9129E-3

Figures (8.4), (8.5) and (8.6) show that $(COP)_{AHA}$ is not very sensitive to temperature lifts. This is in agreement with the theoretical thermodynamic analysis as already shown in Chapter 7 and also by the $(COP)_{AHMO}$ curves in Figures (8.4), (8.5) and (8.6). However, for a given T_{GE} and $(T_{AB}-T_{EV})$, $(COP)_{AHA}$ decreases as $(T_{CO}-T_{EV})$ increases. It also follows that $(COP)_{AHA}$ decreases as (FR) increases. This is evident from Tables (8.2) to (8.4).

A comparison of Figures (8.4) and (8.5) shows that higher values of $(COP)_{AHA}$ were obtained at higher values of T_{EV} when the system was operated at a constant T_{GE} and a similar gross absorber temperature lift $(T_{AB}-T_{EV})$.

Tables (8.2) to (8.4) show the heat balance errors for the three sets of experimental investigations. The heat balance errors ranged between -20.1 per cent and -21.3 per cent at T_{GE} is 172°C. The errors ranged between

-21.7 per cent and -22.6 per cent at T_{GE} is 197°C. Heat losses are relatively higher at the higher value of T_{GE}. This may be the reason for the relatively low values of $(COP)_{AHA}$ at the relatively low value of T_{GE}.

It is expected that the values of $(COP)_{AHA}$ would increase progressively as the values of T_{GE} decrease. However, this can not be investigated in the equipment because of design limitations. The equipment was designed to operate at T_{GE} of 180°C and T_{AB} of 130°C. The limitations on the equipment are the pipe sizes of the absorber and the evaporator. Relatively lower values of T_{GE} will require relatively lower values of T_{AB} and correspondingly lower values of T_{EV}. At values of T_{EV} much lower than 90°C the volume per unit enthalpy for water increases sharply as the temperature decreases. Therefore, progressively larger pipe sizes are required for a given heat intake capacity of the system.

The heat pump effectiveness factor related to the maximum obtainable coefficient of performance for the system $(HPE)_{AHMO}$ ranged between 0.83 and 0.86 at T_{GE} of 172°C. The values of $(HPE)_{AHMO}$ at T_{GE} of 197°C ranged between 0.82 and 0.85. The values of $(HPE)_{AHMO}$ at a given value of T_{GE} can be considered essentially constant.

The stainless steel rods which were used to monitor corrosion in the generator and absorber were withdrawn and checked. The rods in the generator showed no sign of

corrosion. They were in lithium bromide solution for a total operating time of 200 hours. The average temperature T_{GE} and concentration X_{GE} were 190°C and 53 per cent respectively.

However, a blackish-brown deposit was found on the rod in the absorber. The deposit was on the portion which got into contact with water vapour from the evaporator. The deposit could be easily removed and underneath,it, there was no general corrosion. However, there was evidence of localised attack. This took the form of small, round and shallow pits. Within the pits the metal was clean. Around each pit there were alternate rings of blackish-brown deposit. The rod was in the absorber for a total operating time of 200 hours. The average temperature and concentration on it were 130°C and 50 per cent respectively. The portion of the rod which did not get into contact with water vapour was perfectly clean and unattacked. The Figures in Plate(8.1) show the phenomena.

These observations suggest that stainless steel AISI 316 is suitable for use in lithium bromide solution with concentrations and temperatures T in the ranges 50 - 55 per cent and 120°C - 200°C respectively. Further corrosion studies would be required to confirm this.

8.3 PERFORMANCE STUDIES USING WATER-LITHIUM BROMIDE SOLUTIONS IN A GLASS ABSORPTION HEAT PUMP SYSTEM

8.3.1 Introduction

It has been indicated that relatively high values of

$(COP)_{AHA}$ could be obtained with an absorption heat pump when it is operated at relatively low values of T_{GE}. This led to the decision to carry out experiments at values of $T_{GE} \approx 100^{o}C$. An existing glass absorption heat pump system designed by Siddiq Mohamad ["Performance studies on a reversed absorption heat pump, Siddiq Mohamad, B.E., Ph.D. Thesis, University of Salford, Salford, U.K. (1982)] was used for this purpose. Originally, the equipment was developed and used as a reversed absorption heat pump. The system was modified and used as a conventional absorption heat pump.

8.3.2 Equipment

The diagram of the glass absorption heat pump is presented in Figure (8.7). A list of equipment parts is shown in Table (8.1)

The evaporator and the economiser heat exchangers were retained as in the original system. However, the generator, absorber and condenser were modified for easier control and better efficiency of the system.

The absorber was a modified Quickfit heat exchanger type C23/77/3. The original absorber receiver was replaced. The new receiver was 0.15m long and 0.07m wide. It carried a 0.008m wide tubing as sight glass. Another 0.008m tubing dipped in as thermocouple pocket. The new arrangement allowed for more space for absorption. Moreover, this extra space reduced the chance of back flow of lithium

bromide solution from the absorber into the evaporator. In addition, the absorber could be lagged very well since the level of the solution can be viewed through the sight glass. In the original arrangement, the absorber receiver was 0.05m long and 0.045m wide and the solution level was viewed through the wall of the absorber.

The original generator which was essentially a round bottomed flask (FR2L/5UM) was replaced. Figure (8.8) shows the plan and side view of the new generator. The tall neck was designed to effect disentrainment of droplets of liquid in the water vapour.

The condenser was a modified heat exchanger type C23/77/3. A socket (40/45) was attached to the mid-point of the side of the original heat exchanger. The modification was intended to allow super-heated vapour in the shell to rise. The vapour would be desuper-heated and fall. The saturated vapour would then condense and get sub-cooled as it fell to the lower portion of the condenser. The original condenser was the unmodified heat exchanger type C23/77/3. Super-heated vapour entered the condenser from the bottom. Heat would be removed from the rising vapour below the coils carrying cooling water. Therefore, this heat would not be accounted for in the heat removed by the cooling water. Rather, the heat would reduce the sub-cooling of the condensate. These effects would lead to lower values of $(COP)_{AHA}$. The condensate receiver was identical to the absorber receiver.

The economiser heat exchanger was a standard heat

exchanger type C23/77/3. Similarly, the evaporator was the standard evaporator type EF11/1/28.

The original lagging material over the whole equipment was one layer of polyurethane. It was 0.025m thick. One layer of fibrous lagging material was placed over the original insulation to reduce heat losses. The fibrous insulation was 0.025m thick.

Water-rich solution was returned into the generator with a 24W gear pump. The pump was manufactured by Micropump, California, U.S.A. The water-poor solution returned from the generator by gravity.

Separate cooling water lines were installed for the absorber and condenser. This was designed for easier control. On each line water was transferred with a centrigal pump. The pump (type 802 5836) was manufactured by Stuart Turner Ltd., U.K. The flow rate of the water in each line was measured by No.7 rotameters having a maximum capacity of $0.06m^3\ h^{-1}$.

The liquids in the generator and evaporator were heated with electrical immersion heater. Each of the heaters (EF 13C) was 0.44m long and was rated at 1kW. Heat input was controlled by means of a variac variable auto transformer, supplied by Claude Lyons, Ltd., U.K. Each of the heaters had a separate control.

The necessary vacuum was established with a Metrovac

Rotary Pump GDP. It was manufactured by Associated Electrical Industries Ltd., U.K. The manometers were type GML-590-J, manufactured by Griffin Ltd. U.K. One each was connected to the condenser and absorber. The ranges of the manometers were 500-0-500mmHg and 0-960mmHg for the condenser and absorber respectively.

The pipings were neoprene rubber hoses.

Hoffman Clips were used as control and stop valves. They were supplied by Gallenkamp Griffin, Wythenshawe, Manchester, U.K. The clips were more reliable than the Quickfit valves.

Silicone rubber (Silastic 9161 RTV) manufactured by DOW CORNING Ltd., Barry, U.K., was applied to joints. This was very effective in maintaining vacuum.

Temperatures were measured using 1mm NiCr/NiAl thermocouple. The thermocouple was type PKW 2N10 manufactured by BICC Pyrotenax, U.K.

8.3.3 Accuracy of instruments

Temperatures were read to the nearest $\pm$ 0.1°C using the R33CR/NIAL digital read out manufactured by Control and Read-out Ltd., U.K. Pressures were read to the nearest $\pm$ 2mmHg. Heat input measurements were made using standard ammeters and voltmeters appropriate to the required

ranges. The ammeters were readable to ± 0.1amps and the voltmeters were readable to ± 2volts. The atmospheric pressure was measured with a standard mercury Toricellian barometer to an accuracy of 1mmHg. Ambient temperature was measured with a mercury in glass thermometer to an accuracy of $0.5^{o}C$. The rotameters were readable to $\pm 0.0012 m^3 h^{-1}$. The weighing balance used for weighing water was accurate to 1gm.

8.3.4 Experimental technique

The experimental technique was as described in (8.2.4.2). However, since the glass system was always under vacuum, the equipment was evacuated at the beginning of the experiments. Moreover, the charging of liquids into the system was slightly different.

The whole system was evacuated and lithium bromide solution was sucked into the system through the absorber. It was then pumped into the generator. Similarly, water was charged into the system through the evaporator.

Experimental investigations were carried out by using the appropriate controls on the equipment similar to the description given in (8.2.4.3).

8.3.5 Results and discussion

The results of the two sets of experiments carried out at $T_{GE} = 100^{o}C$ and $T_{GE} = 110^{o}C$, and an average $T_{EV} = 47^{o}C$.

are presented in Tables (8.5) and (8.6).

The results were treated as described in (8.2.5). However, the equilibrium condensing pressure P_{CO} was taken as the observed condenser pressure. The equilibrium condensing temperature T_{CO} was assumed to correspond to the condenser pressure. The equilibrium evaporating temperature T_{EV} was taken as the observed evaporator temperature.

At T_{GE} = 100°C, the values of T_{CO} ranged between 67.2°C and 70.0°C. The values of T_{AB} and T_{EV} were 71°C and 47.6°C respectively. The condenser temperature lifts ($T_{CO}-T_{EV}$) ranged between 30.9°C and 34.4°C. The delivery temperatures ranged between 74.9°C and 81.2°C.

The errors in the computed values of $(COP)_{AHA}$ and gross temperature lifts were as presented in (8.2.5).

Figures (8.8) and (8.9) are plots of $(COP)_{AHA}$ and $(COP)_{AHMO}$ against $(T_{CO}-T_{EV})$ for the experimental investigations at T_{GE} = 100°C and 110°C respectively. 'Best fit' curves were drawn through the experimental points shown in Figures (8.9) and (8.10). The correlations of these curves are given in Equations (8.18) and (8.19) respectively.

$$(COP)_{AHA} = -16.829 + 19.921(T_{CO}-T_{EV})^{-0.02950} \qquad (8.18)$$

with root mean square residual = 7.8126E-3

$$(COP)_{AHA} = -0.083099 + 5.3905(T_{CO}-T_{EV})^{0.2597} \qquad (8.19)$$

with root mean square residual = 6.4487E-3

The following can be deduced from Figures (8.9) and (8.10) :

i) $(COP)_{AHA}$ is not sensitive to $(T_{CO}-T_{EV})$

ii) $(COP)_{AHA}$ values at $T_{GE} = 100^{o}C$ are higher than at $T_{GE} = 110^{o}C$.

iii) Gross temperature lifts at $T_{GE} = 110^{o}C$ are higher than at $T_{GE} = 100^{o}C$.

The average heat balance errors for $T_{GE} = 100^{o}C$, calculated from Tables (8.5) and (8.6) are -11.4 per cent and -12.0 per cent respectively. The higher values of heat losses at the higher $T_{GE} = 110^{o}C$ may be the reason for the lower $(COP)_{AHA}$ values at this temperature compared to those at the lower $T_{GE} = 100^{o}C$. The average heat loss reported by Siddig Mohamad ["Performance studies on a reversed absorption heat pump", Siddig Mohamad, B.E., Ph.D Thesis, University of Salford, Salford, U.K. (1982)] using essentially the same equipment as a heat transformer was -35 per cent in the temperature range $100^{o}C$ to $110^{o}C$. It should be remembered that he used relatively thin insulations on the equipment. Initial investigations carried out on the conventional heat pump using the thin insulations yielded an average $(COP)_{AHA}$ of about 1.1 at $T_{GE} = 100^{o}C$. These show that heat losses reduce the performance of heat pump systems.

The average values of $(HPE)_{AHMO}$ were 0.80 and 0.81

at T_{GE} = 100°C and T_{GE} = 110°C respectively.

8.4 SUMMARY OF EXPERIMENTAL RESULTS AND CONCLUSIONS

For comparison the 'best fit' curves representing the actual coefficients of performance against the condenser gross temperature lifts for the investigations carried out in the metal and glass systems are presented in Figure (8.11). It can be seen that the values of $(COP)_{AHA}$ decrease as the values of T_{GE} increase.

Tables (8.2) to (8.6) show that the values of $(HPE)_{AHMO}$ decrease as the values of T_{GE} decrease. This is in accordance with the theoretical observations made in Chapter 7. However, the values of $(HPE)_{AHMO}$ were essentially constant for a given value of T_{GE}. The values of $(HPE)_{AHMO}$ are recommendable for use in the design of absorption heat pump systems.

The range over which the metal equipment can be varied is limited by the size of the absorber. If a wider pipe is used in the absorber it should be possible to operate the system at values of T_{EV} lower than 90°C.

The range over which the glass equipment can operate is limited by the pressure which the glass can withstand. The glass equipment can be operated at super-atmospheric pressures if the neoprene rubber pipes are replaced with glass and if the inter-connections are better secured.

The range within which an absorption heat pump should be designed to operate, should depend mainly on the required temperature lifts.

part number	description
1	generator
2	condenser
2	condensate receiver
3	absorber
3	absorber mixer
3	absorber receiver
E(1-3)	economiser heat exchanger
4	evaporator
5	solution pump
6	cooling water pumps
7	electric heaters
8	sight glasses
V(1-3), V(2-8)	expansion valves
9	absorber rotameter
10	water reservoir
11	solution reservoir
12	cooling water heater
13	pressure relief valves

TABLE (8.1) LIST OF EQUIPMENT PARTS

run no	1	2	3	4
<u>generator data</u>				
temperature of bulk solution T_{GE}, ^{o}C	171.8	171.6	171.4	171.9
inlet temperature of solution, ^{o}C	147.3	147.5	147.1	147.3
temperature of super-heated vapour, ^{o}C	170.5	170.5	170.8	170.7
absolute pressure P_{GE}, bar	2.563	2.463	2.363	2.263
mass flow rate of water-poor solution M_{GE}, kg h^{-1}	17.88	16.08	14.17	13.62
concentration of water-poor solution X_{GE}, wt. per cent	52.9	53.2	53.6	53.8
heat load Q_{GE}, W	1128	1112	1081	1056
<u>condenser data</u>				
condenser temperature T_{CO}, ^{o}C	127.8	127.0	125.5	124.5
absolute pressure P_{CO}, bar	2.563	2.463	2.363	2.263
inlet temperature of cooling water $(T_{CW})_{IN}$, ^{o}C	87.7	89.5	88.7	91.0
outlet temperature of cooling water $(T_{CW})_{OUT}$, ^{o}C	103.2	104.5	104.3	106.1

TABLE (8.2) RAW EXPERIMENTAL DATA AND COMPUTED VALUES FOR THE WATER-LITHIUM BROMIDE SYSTEM FOR A GENERATOR TEMPERATURE OF 171.8^{o}C

run no	1	2	3	4
<u>condenser data (cont.)</u>				
temperature of sub-cooled condensate, ^{o}C	108.4	109.3	109.1	110.3
mass flow rate of cooling water M_{CW}, kg h^{-1}	28.68	30.17	29.81	31.29
heat load Q_{CO}, W	518	529	541	550
<u>evaporator data</u>				
evaporator temperature T_{EV}, ^{o}C	100.0	99.8	99.8	100.1
absolute pressure P_{EV}, bar	1.013	1.013	1.013	1.013
heat load Q_{EV}, W	589	589	607	607
<u>absorber data</u>				
inlet temperature of solution, ^{o}C	143.7	143.8	143.7	143.4
outlet temperature T_{AB}, ^{o}C	131.8	131.9	131.3	131.7
inlet temperature of cooling water $(T_{CW})_{IN}$, ^{o}C	99.1	101.0	101.2	103.2
outlet temperature of cooling water $(T_{CW})_{OUT}$, ^{o}C	126.2	126.2	125.8	125.9

TABLE (8.2)(continued) RAW EXPERIMENTAL DATA AND COMPUTED VALUES FOR THE WATER-LITHIUM BROMIDE SYSTEM FOR A GENERATOR TEMPERATURE OF 171.8^{o}C

run no	1	2	3	4
<u>absorber data (cont.)</u>				
mass flow rate of cooling water M_{CW}, kg h^{-1}	28.68	30.17	29.81	31.29
concentration of water-rich solution X_{AB}, wt. per cent	50.5	50.5	50.5	50.5
heat load Q_{AB}, W	917	887	856	829
<u>economiser heat exchanger data</u>				
inlet temperature of water-rich solution, °C	128.7	128.7	128.5	128.6
outlet temperature of water-rich solution, °C	147.3	147.4	147.1	147.3
inlet temperature of water-poor solution, °C	169.6	169.5	169.5	169.7
outlet temperature of water-poor solution, °C	148.2	148.6	148.3	147.9
<u>general data</u>				
condenser temperature lift (T_{CO}-T_{EV}), °C	27.8	27.2	25.7	24.4
absorber temperature lift (T_{AB}-T_{EV}), °C	31.8	32.1	31.5	31.6
circulation ratio (FR), dimensionless	22.04	19.70	17.29	16.30
actual coefficient of performance $(COP)_{AHA}$, dimensionless	1.263	1.273	1.292	1.306

TABLE (8.2)(continued) RAW EXPERIMENTAL DATA AND COMPUTED VALUES FOR THE WATER-LITHIUM BROMIDE SYSTEM FOR A GENERATOR TEMPERATURE OF 171.8°C

run no	1	2	3	4
<u>general data (cont.)</u>				
maximum obtainable coefficient of performance $(COP)_{AHMO}$, dimensionless	1.470	1.509	1.509	1.528
heat pump effectiveness $(HPE)_{AHMO}$, dimensionless	0.86	0.84	0.85	0.84
heat balance error per cent	-20.5	-20.1	-20.9	-20.6
barometric pressure, mm Hg	760	760	760	760

TABLE (8.2) (continued) RAW EXPERIMENTAL DATA AND COMPUTED VALUES FOR THE WATER-LITHIUM BROMIDE SYSTEM FOR A GENERATOR TEMPERATURE OF 171.8°C

run no	1	2	3	4
<u>generator data</u>				
temperature of bulk solution T_{GE}, ^{o}C	171.8	171.8	171.6	171.5
inlet temperature of solution, ^{o}C	146.5	146.2	146.4	146.3
temperature of super-heated vapour, ^{o}C	170.6	170.5	170.6	170.5
absolute pressure P_{GE}, bar	2.463	2.363	2.263	2.188
mass flow rate of water-poor solution M_{GE}, kg h^{-1}	17.22	15.75	15.05	13.68
concentration of water-poor solution X_{GE}, wt. per cent	55.0	55.3	55.5	55.8
heat load Q_{GE}, W	1145	1128	1108	1087
<u>condenser data</u>				
condenser temperature T_{CO}, ^{o}C	127.0	125.5	124.5	123.0
absolute pressure P_{CO}, bar	2.463	2.363	2.263	2.188
inlet temperature of cooling water $(T_{CW})_{IN}$, ^{o}C	85.6	86.5	87.1	88.7
outlet temperature of cooling water $(T_{CW})_{OUT}$, ^{o}C	100.5	101.1	102.0	103.2

TABLE (8.3) RAW EXPERIMENTAL DATA AND COMPUTED VALUES FOR THE WATER-LITHIUM BROMIDE SYSTEM FOR A GENERATOR TEMPERATURE OF 171.8°C

run no	1	2	3	4
<u>condenser data (cont.)</u>				
temperature of sub-cooled condensate, ^{o}C	107.9	109.1	108.2	109.3
mass flow rate of cooling water M_{CW}, kg h^{-1}	28.98	30.90	30.56	32.56
heat load Q_{CO}, W	504	523	535	551
<u>evaporator data</u>				
evaporator temperature T_{EV}, ^{o}C	94.2	94.2	94.2	94.2
absolute pressure P_{EV}, bar	0.810	0.810	0.810	0.810
heat load Q_{EV}, W	585	590	597	600
<u>absorber data</u>				
inlet temperature of solution, ^{o}C	143.1	143.0	144.8	143.1
outlet temperature T_{AB}, ^{o}C	129.5	129.1	129.3	129.0
inlet temperature of cooling water $(T_{CW})_{IN}$, ^{o}C	97.2	99.6	100.1	102.1
outlet temperature of cooling water $(T_{CW})_{OUT}$, ^{o}C	124.4	124.5	124.7	124.5

TABLE (8.3) (continued) RAW EXPERIMENTAL DATA AND COMPUTED VALUES FOR THE WATER-LITHIUM BROMIDE SYSTEM FOR A GENERATOR TEMPERATURE OF 171.8^{o}C

run no	1	2	3	4
<u>absorber data (cont.)</u>				
mass flow rate of cooling water M_{CW}, kg h^{-1}	28.98	30.90	30.56	32.56
concentration of water-rich solution X_{AB}, wt. per cent	52.5	52.5	52.5	52.5
heat load Q_{AB}, W	920	894	875	851
<u>economiser heat exchanger data</u>				
inlet temperature of water-rich solution, °C	126.6	126.4	126.4	126.2
outlet temperature of water-rich solution, °C	146.5	146.2	146.4	146.3
inlet temperature of water-poor solution, °C	169.7	169.5	169.6	169.5
outlet temperature of water-poor solution, °C	148.3	148.0	147.9	148.1
<u>general data</u>				
condenser temperature lift (T_{CO}-T_{EV}), °C	32.8	31.6	30.4	28.9
absorber temperature lift (T_{AB}-T_{EV}), °C	35.3	35.2	35.2	34.9
circulation ratio (FR), dimensionless	22.00	19.75	18.50	16.91
actual coefficient of performance $(COP)_{AHA}$, dimensionless	1.240	1.257	1.272	1.290

TABLE (8.3)(continued) RAW EXPERIMENTAL DATA AND COMPUTED VALUES FOR THE WATER-LITHIUM BROMIDE SYSTEM FOR A GENERATOR TEMPERATURE OF 171.8°C

run no	1	2	3	4
general data (cont.)				
maximum obtainable coefficient of performance $(COP)_{AHMO}$, dimensionless	1.487	1.518	1.534	1.561
heat pump effectiveness $(HPE)_{AHMO}$, dimensionless	0.83	0.83	0.83	0.83
heat balance error per cent	-21.5	-21.3	-21.0	-20.3
barometric pressure, mm Hg	760	760	760	760

TABLE (8.3)(continued) RAW EXPERIMENTAL DATA AND COMPUTED VALUES FOR THE WATER-LITHIUM BROMIDE SYSTEM FOR A GENERATOR TEMPERATURE OF 171.8°C

run no	1	2	3	4
<u>generator data</u>				
temperature of bulk solution T_{GE}, ^{o}C	197.3	197.1	197.2	197.1
inlet temperature of solution, ^{o}C	171.8	171.7	171.9	171.1
temperature of super-heated vapour, ^{o}C	196.8	196.2	196.9	196.3
absolute pressure P_{GE}, bar	4.463	4.363	4.263	4.163
mass flow rate of water-poor solution M_{GE}, kg h^{-1}	19.16	17.30	16.31	14.80
concentration of water-poor solution X_{GE}, wt. per cent	54.0	54.3	54.5	54.75
heat load Q_{GE}, W	1311	1288	1288	1260
<u>condenser data</u>				
condenser temperature T_{CO}, ^{o}C	147.5	146.7	145.8	145.0
absolute pressure P_{CO}, bar	4.463	4.363	4.263	4.163
inlet temperature of cooling water $(T_{CW})_{IN}$, ^{o}C	124.1	123.6	122.8	124.0
outlet temperature of cooling water $(T_{CW})_{OUT}$, ^{o}C	141.1	141.0	140.9	141.7

TABLE (8.4) RAW EXPERIMENTAL DATA AND COMPUTED VALUES FOR THE WATER-LITHIUM BROMIDE SYSTEM FOR A GENERATOR TEMPERATURE OF $197^{o}C$

run no	1	2	3	4
<u>condenser data (cont.)</u>				
temperature of sub-cooled condensate, ^{o}C	145.8	144.9	144.6	144.5
mass flow rate of cooling water M_{CW}, kg h^{-1}	27.90	27.81	27.54	28.74
heat load Q_{CO}, W	554	565	581	594
<u>evaporator data</u>				
evaporator temperature T_{EV}, ^{o}C	100.7	101.1	100.8	101.0
absolute pressure P_{EV}, bar	1.113	1.114	1.113	1.114
heat load Q_{EV}, W	618	630	630	637
<u>absorber data</u>				
inlet temperature of solution, ^{o}C	146.1	146.2	146.8	146.5
outlet temperature T_{AB}, ^{o}C	134.9	135.0	134.9	134.9
inlet temperature of cooling water $(T_{CW})_{IN}$, ^{o}C	124.1	123.6	122.8	124.0
outlet temperature of cooling water $(T_{CW})_{OUT}$, ^{o}C	141.1	141.0	140.9	141.7

TABLE (8.4) (continued) RAW EXPERIMENTAL DATA AND COMPUTED VALUES FOR THE WATER-LITHIUM BROMIDE SYSTEM FOR A GENERATOR TEMPERATURE OF 197^{o}C

run no	1	2	3	4
<u>absorber data (cont.)</u>				
mass flow rate of cooling water M_{CW}, kg h^{-1}	27.90	27.81	27.54	28.74
concentration of water-rich solution X_{AB}, wt. per cent	51.5	51.5	51.5	51.5
heat load Q_{AB}, W	1032	1000	994	958
<u>economiser heat exchanger data</u>				
inlet temperature of water-rich solution, ^{o}C	132.0	131.9	131.9	132.1
outlet temperature of water-rich solution, ^{o}C	171.8	171.7	171.9	171.1
inlet temperature of water-poor solution, ^{o}C	195.3	195.1	195.3	195.1
outlet temperature of water-poor solution, ^{o}C	154.1	153.9	153.2	153.4
<u>general data</u>				
condenser temperature lift (T_{CO}-T_{EV}), ^{o}C	46.8	45.6	45.0	44.0
absorber temperature lift (T_{AB}-T_{EV}), ^{o}C	34.2	34.9	34.9	33.9
circulation ratio (FR), dimensionless	21.6	19.4	18.17	16.85
actual coefficient of performance $(COP)_{AHA}$, dimensionless	1.210	1.215	1.222	1.230

TABLE (8.4)(continued) RAW EXPERIMENTAL DATA AND COMPUTED VALUES FOR THE WATER-LITHIUM BROMIDE SYSTEM FOR A GENERATOR TEMPERATURE OF 197^{o}C

run no	1	2	3	4
general data (cont.)				
maximum obtainable coefficient of performance $(COP)_{AHMO}$, dimensionless	1.430	1.460	1.479	1.503
heat pump effectiveness $(HPE)_{AHMO}$, dimensionless	0.85	0.83	0.83	0.82
heat balance error per cent	-21.7	-22.6	-21.8	-22.2
barometric pressure, mm Hg	758	758	758	758

TABLE (8.4)(continued) RAW EXPERIMENTAL DATA AND COMPUTED VALUES FOR THE WATER-LITHIUM BROMIDE SYSTEM FOR A GENERATOR TEMPERATURE OF 197°C

run no	1	2	3	4
<u>generator data</u>				
temperature of bulk solution T_{GE}, ^{o}C	100.5	100.0	100.3	100.1
inlet temperature of solution, ^{o}C	83.7	83.4	82.8	82.7
temperature of super-heated vapour, ^{o}C	99.1	98.6	99.2	99.1
absolute pressure P_{GE}, bar	0.312	0.298	0.286	0.273
mass flow rate of water-poor solution M_{GE}, kg h^{-1}	16.373	14.564	13.165	12.114
concentration of water-poor solution X_{GE}, wt. per cent	50.7	51.0	51.3	51.6
heat load Q_{GE}, W	922	896	876	850
<u>condenser data</u>				
condenser temperature T_{CO}, ^{o}C	70.0	69.0	68.2	67.2
absolute pressure P_{CO}, bar	0.312	0.298	0.286	0.273
inlet temperature of cooling water $(T_{CW})_{IN}$, ^{o}C	42.4	42.5	42.8	42.5
outlet temperature of cooling water $(T_{CW})_{OUT}$, ^{o}C	69.2	68.4	67.1	65.2

TABLE (8.5) RAW EXPERIMENTAL DATA AND COMPUTED VALUES FOR THE WATER-LITHIUM BROMIDE SYSTEM FOR A GENERATOR TEMPERATURE OF 100.5°C

run no	1	2	3	4
<u>condenser data (cont.)</u>				
temperature of sub-cooled condensate, ^{o}C	69.0	69.1	68.9	69.2
mass flow rate of cooling water M_{CW}, kg h^{-1}	12.89	13.88	15.17	16.93
heat load Q_{CO}, W	415	429	440	458
<u>evaporator data</u>				
evaporator temperature T_{EV}, ^{o}C	46.7	46.7	46.6	46.7
absolute pressure P_{EV}, bar	0.104	0.104	0.104	0.104
heat load Q_{EV}, W	431	447	459	478
<u>absorber data</u>				
inlet temperature of solution, ^{o}C	79.9	79.2	78.8	77.2
outlet temperature T_{AB}, ^{o}C	71.1	71.0	71.2	71.1
inlet temperature of cooling water $(T_{CW})_{IN}$, ^{o}C	30.3	30.5	30.1	30.4
outlet temperature of cooling water $(T_{CW})_{OUT}$, ^{o}C	74.1	74.4	73.2	71.4

TABLE (8.5) (continued) RAW EXPERIMENTAL DATA AND COMPUTED VALUES FOR THE WATER-LITHIUM BROMIDE SYSTEM FOR A GENERATOR TEMPERATURE OF 100,5^{o}C

run no	1	2	3	4
general data (cont.)				
maximum obtainable coefficient of performance $(COP)_{AHMO}$, dimensionless	1.694	1.700	1.718	1.738
heat pump effectiveness $(HPE)_{AHMO}$, dimensionless	0.78	0.80	0.80	0.80
heat balance error per cent	-11.1	-10.9	-11.3	-12.2
barometric pressure, mm Hg	742	742	742	742

TABLE (8.5)(continued) RAW EXPERIMENTAL DATA AND COMPUTED VALUES FOR THE WATER-LITHIUM BROMIDE SYSTEM FOR A GENERATOR TEMPERATURE OF 100.5°C

run no	1	2	3	4
<u>absorber data (cont.)</u>				
mass flow rate of cooling water M_{CW}, kg h^{-1}	15.41	15.00	14.80	14.85
concentration of water-rich solution X_{AB}, wt. per cent	48.8	48.8	48.8	48.8
heat load Q_{AB}, W	803	782	760	726
<u>economiser heat exchanger data</u>				
inlet temperature of water-rich solution, ^{o}C	69.4	69.1	68.9	68.8
outlet temperature of water-rich solution, ^{o}C	82.3	82.1	81.9	81.7
inlet temperature of water-poor solution, ^{o}C	98.7	98.1	97.9	97.7
outlet temperature of water-poor solution, ^{o}C	86.5	85.9	85.6	85.4
<u>general data</u>				
condenser temperature lift (T_{CO}-T_{EV}), ^{o}C	23.3	22.3	21.6	20.5
absorber temperature lift (T_{AB}-T_{EV}), ^{o}C	24.4	24.3	24.6	24.4
circulation ratio (FR), dimensionless	26.70	23.20	20.50	18.40
actual coefficient of performance $(COP)_{AHA}$, dimensionless	1.321	1.352	1.370	1.393

TABLE (8.5)(continued) RAW EXPERIMENTAL DATA AND COMPUTED VALUES FOR THE WATER-LITHIUM BROMIDE SYSTEM FOR A GENERATOR TEMPERATURE OF 100.5^{o}C

run no	1	2	3	4
<u>generator data</u>				
temperature of bulk solution T_{GE}, ^{o}C	110.7	109.7	110.4	110.7
inlet temperature of solution, ^{o}C	88.2	88.3	88.1	88.2
temperature of super-heated vapour, ^{o}C	110.3	109.0	110.0	109.9
absolute pressure P_{GE}, bar	0.526	0.487	0.479	0.465
mass flow rate of water-poor solution M_{GE}, kg h^{-1}	15.908	13.763	12.263	11.377
concentration of water-poor solution X_{GE}, wt. per cent	50.5	50.9	51.3	51.6
heat load Q_{GE}, W	954	935	908	870
<u>condenser data</u>				
condenser temperature T_{CO}, ^{o}C	82.0	80.8	79.5	78.5
absolute pressure P_{CO}, bar	0.526	0.487	0.479	0.465
inlet temperature of cooling water $(T_{CW})_{IN}$, ^{o}C	44.5	45.1	45.4	44.9
outlet temperature of cooling water $(T_{CW})_{OUT}$, ^{o}C	81.2	78.5	78.2	76.9

TABLE (8.6) RAW EXPERIMENTAL DATA AND COMPUTED VALUES FOR THE WATER-LITHIUM BROMIDE SYSTEM FOR A GENERATOR TEMPERATURE OF

run no	1	2	3	4
<u>condenser data (cont.)</u>				
temperature of sub-cooled condensate, ^{o}C	79.5	79.3	78.9	77.8
mass flow rate of cooling water M_{CW}, kg h^{-1}	9.90	11.32	11.92	12.53
heat load Q_{CO}, W	424	441	456	468
<u>evaporator data</u>				
evaporator temperature T_{EV}, ^{o}C	47.6	47.5	47.4	47.7
absolute pressure P_{EV}, bar	0.113	0.112	0.112	0.113
heat load Q_{EV}, W	441	467	478	482
<u>absorber data</u>				
inlet temperature of solution, ^{o}C	80.7	80.3	80.8	79.4
outlet temperature T_{AB}, ^{o}C	68.4	68.3	68.3	68.4
inlet temperature of cooling water $(T_{CW})_{IN}$, ^{o}C	31.3	31.5	31.4	31.6
outlet temperature of cooling water $(T_{CW})_{OUT}$, ^{o}C	75.3	74.8	75.1	74.9

TABLE (8.6) (continued) RAW EXPERIMENTAL DATA AND COMPUTED VALUES FOR THE WATER-LITHIUM BROMIDE SYSTEM FOR A GENERATOR TEMPERATURE OF 110.7^{o}C

run no	1	2	3	4
<u>absorber data (cont.)</u>				
mass flow rate of cooling water M_{CW}, kg h^{-1}	16.19	16.13	15.24	14.51
concentration of water-rich solution X_{AB}, wt. per cent	48.5	48.5	48.5	48.5
heat load Q_{AB}, W	831	815	777	733
<u>economiser heat exchanger data</u>				
inlet temperature of water-rich solution, ^{o}C	66.7	66.6	66.3	66.1
outlet temperature of water-rich solution, ^{o}C	87.7	87.7	87.1	87.4
inlet temperature of water-poor solution, ^{o}C	105.6	104.6	105.2	104.7
outlet temperature of water-poor solution, ^{o}C	90.3	89.1	89.3	87.9
<u>general data</u>				
condenser temperature lift (T_{CO}-T_{EV}), ^{o}C	34.4	33.3	32.1	30.8
absorber temperature lift (T_{AB}-T_{EV}), ^{o}C	20.8	20.8	20.9	20.7
circulation ratio (FR), dimensionless	25.25	21.21	18.32	16.65
actual coefficient of performance $(COP)_{AHA}$, dimensionless	1.316	1.343	1.358	1.381

TABLE (8.6)(continued) RAW EXPERIMENTAL DATA AND COMPUTED VALUES FOR THE WATER-LITHIUM BROMIDE SYSTEM FOR A GENERATOR TEMPERATURE OF 110.7^{o}C

run no	1	2	3	4
general data (cont.)				
maximum obtainable coefficient of performance $(COP)_{AHMO}$, dimensionless	1.622	1.660	1.682	1.700
heat pump effectiveness $(HPE)_{AHMO}$, dimensionless	0.81	0.81	0.81	0.81
heat balance error per cent	-11.2	-11.6	-12.4	-12.6
barometric pressure, mm Hg	742	742	742	742

TABLE (8.6)(continued) RAW EXPERIMENTAL DATA AND COMPUTED VALUES FOR THE WATER-LITHIUM BROMIDE SYSTEM FOR A GENERATOR TEMPERATURE OF 110.7°C

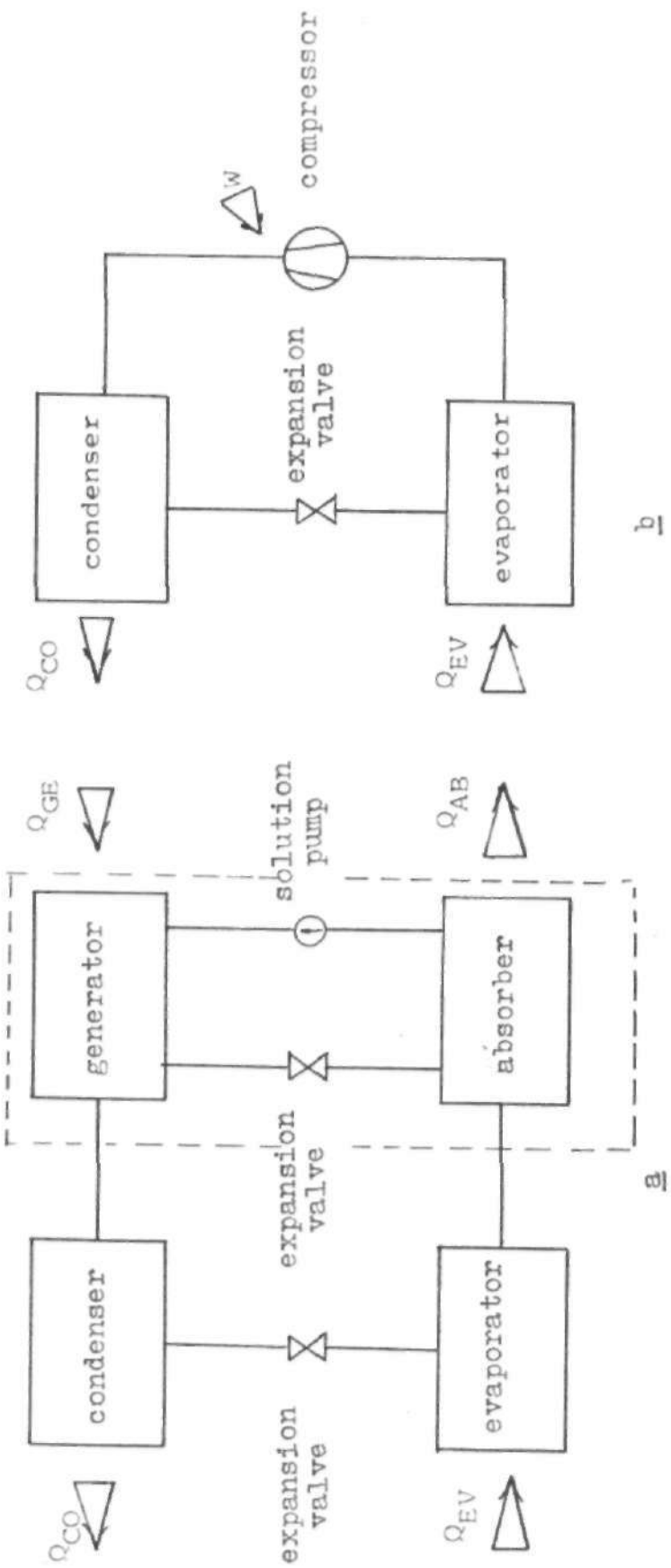


FIGURE (8.1) a) SIMPLIFIED ABSORPTION HEAT PUMP

b) SIMPLIFIED VAPOUR COMPRESSION HEAT PUMP

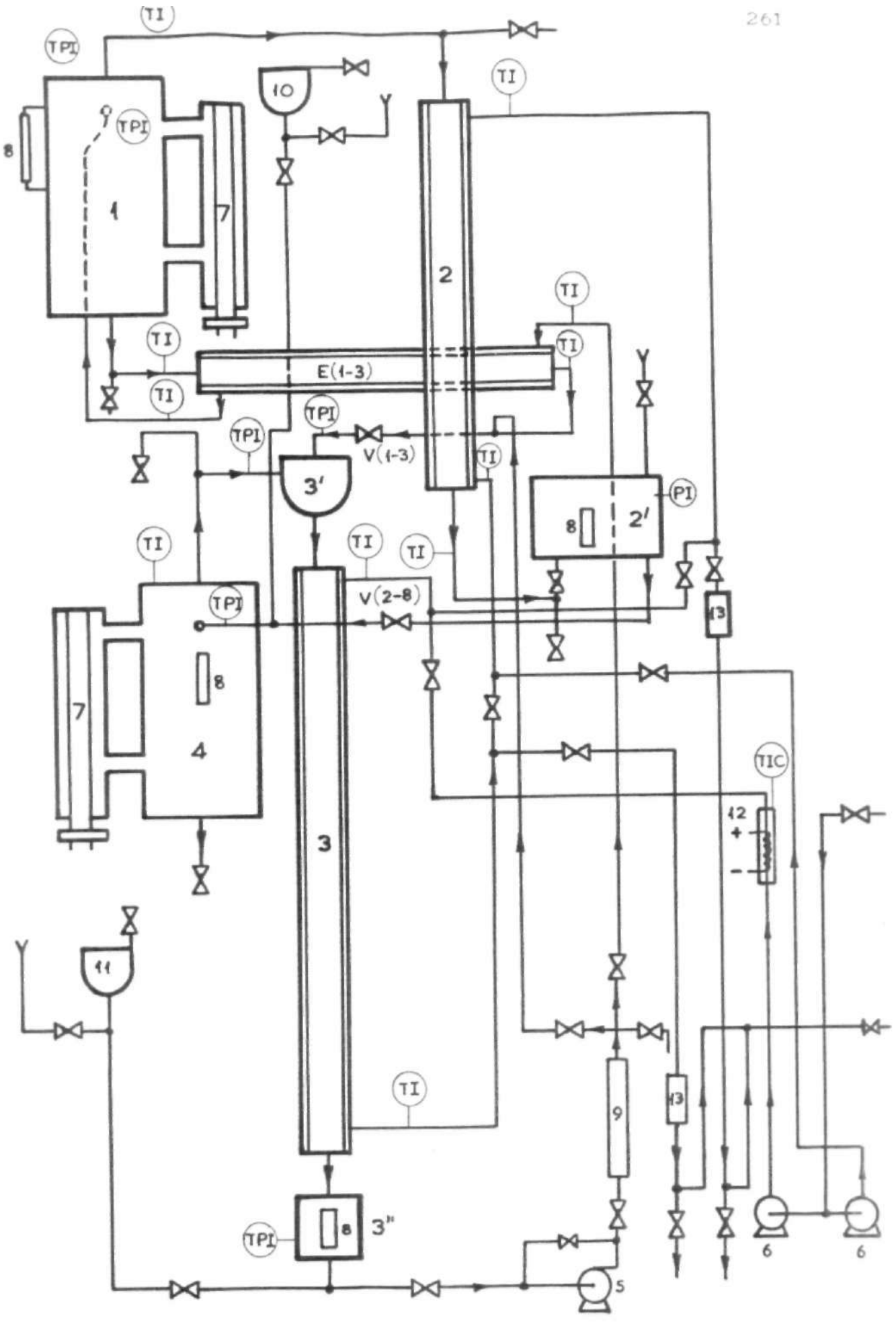
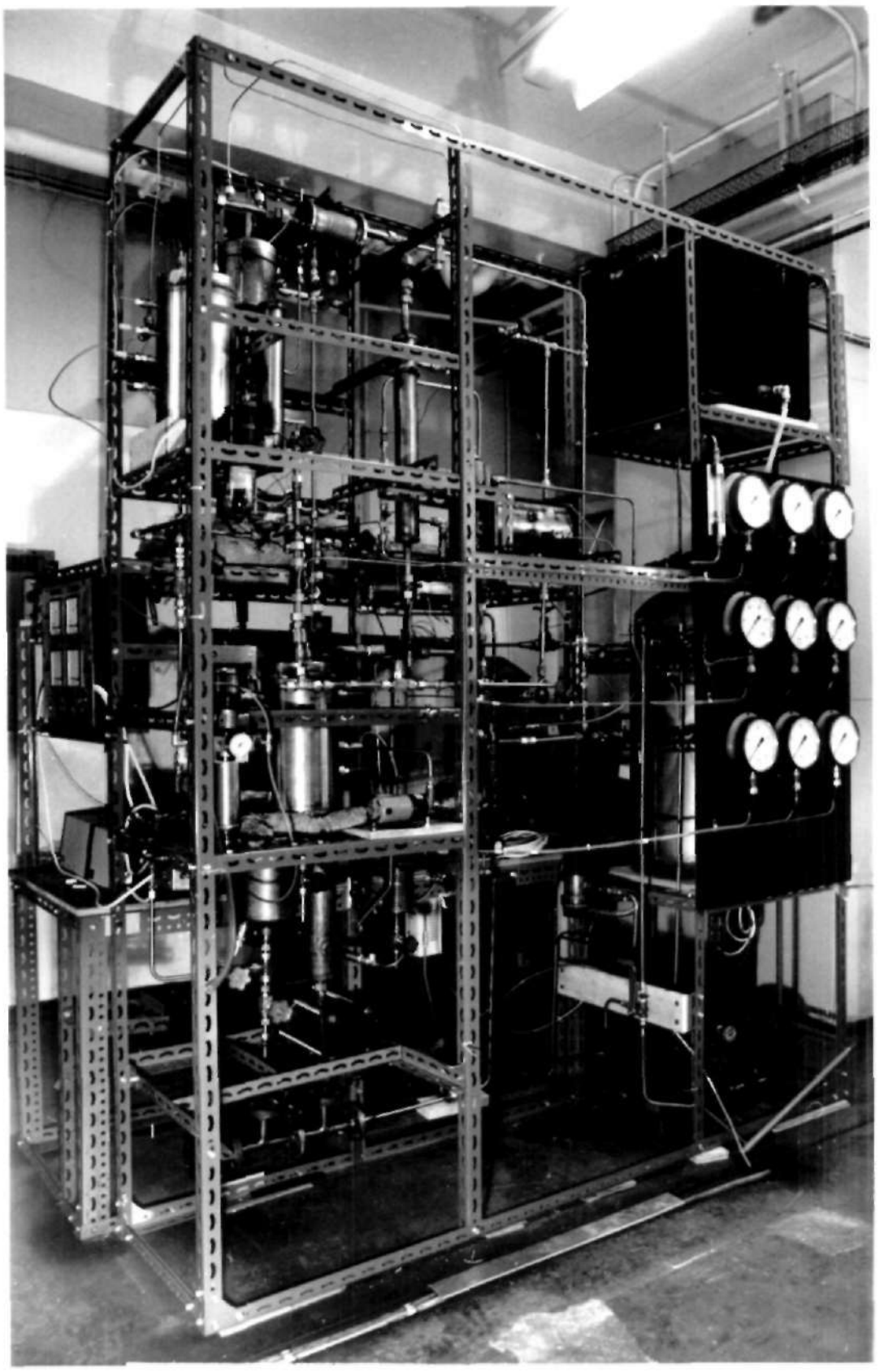
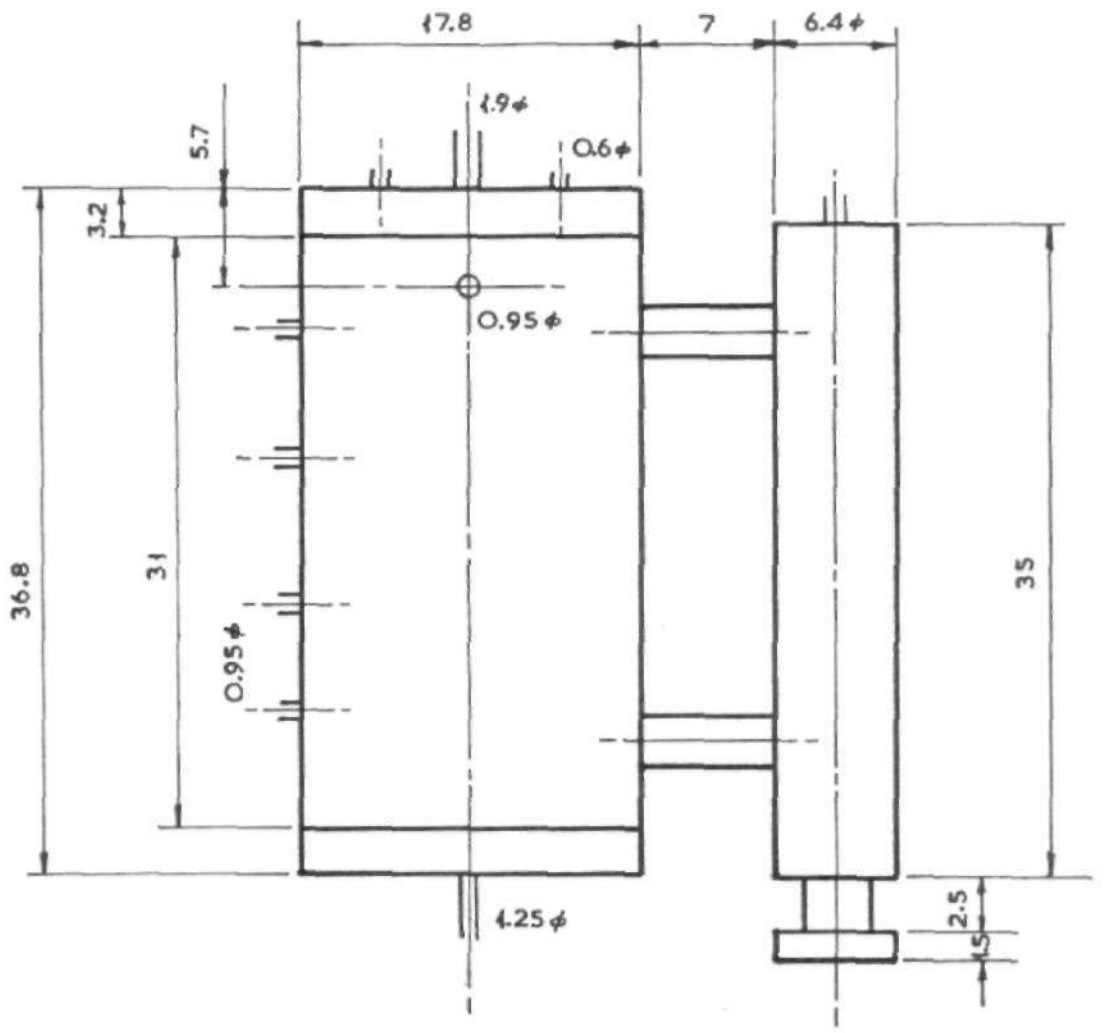


FIGURE 8.2 THE METAL CONVENTIONAL ABSORPTION HEAT PUMP.



THE METAL ABSORPTION HEAT PUMP SYSTEM



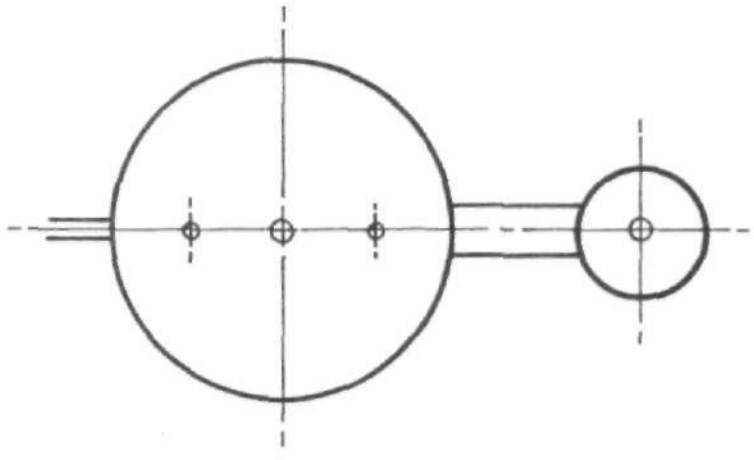


FIGURE 8.3 GENERATOR / EVAPORATOR OF THE METAL CONVENTIONAL HEAT PUMP SYSTEM.

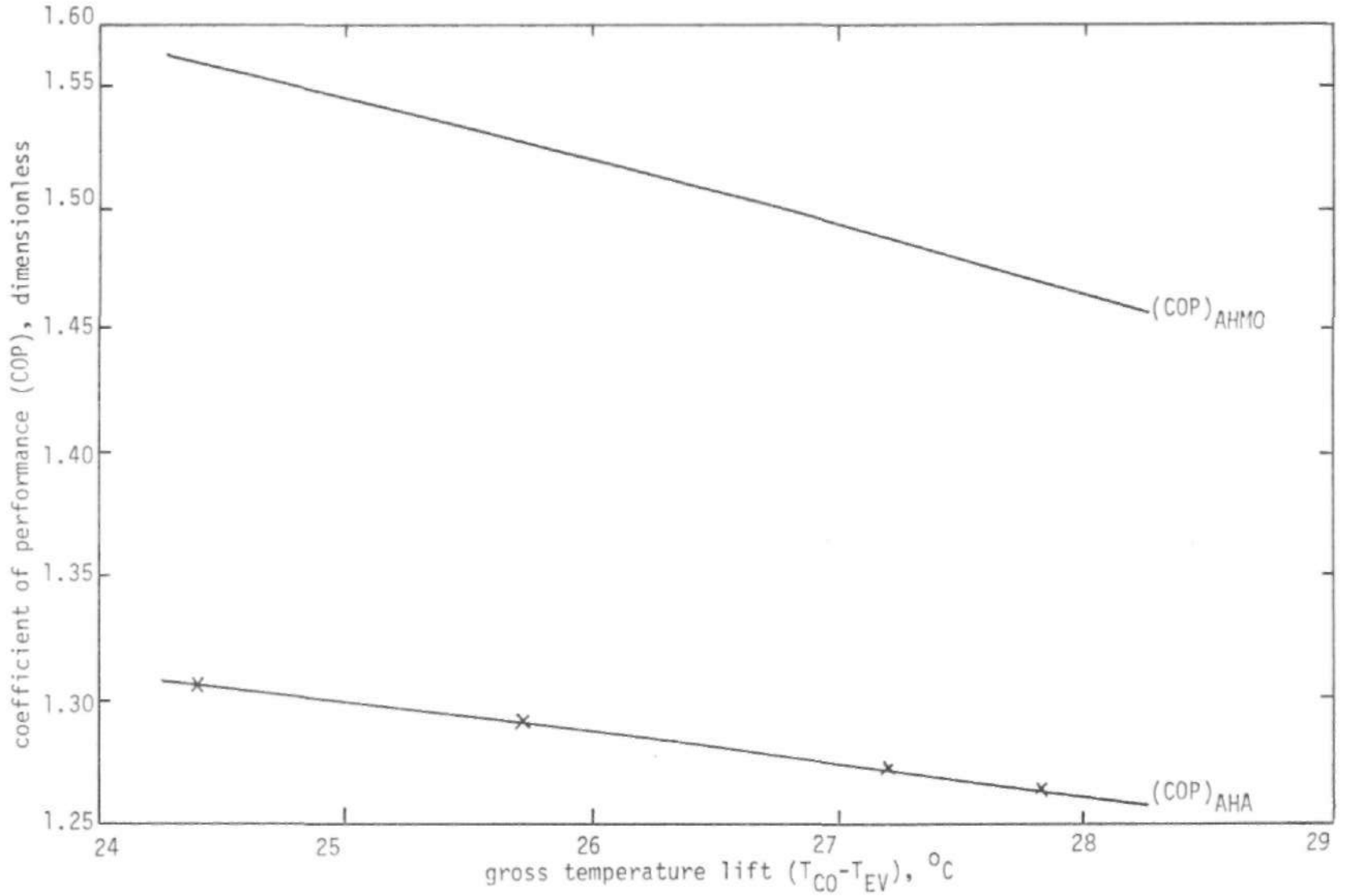


FIGURE (8.4) COEFFICIENT OF PERFORMANCE AGAINST GROSS CONDENSER TEMPERATURE LIFT FOR A GROSS ABSORBER TEMPERATURE LIFT OF 32°C, AN EVAPORATOR TEMPERATURE OF 100°C, A GENERATOR TEMPERATURE OF 172°C AND A CONCENTRATION OF LITHIUM-BROMIDE OF 50.5 WEIGHT PER CENT IN THE ABSORBER FOR THE WATER-LITHIUM BROMIDE SYSTEM

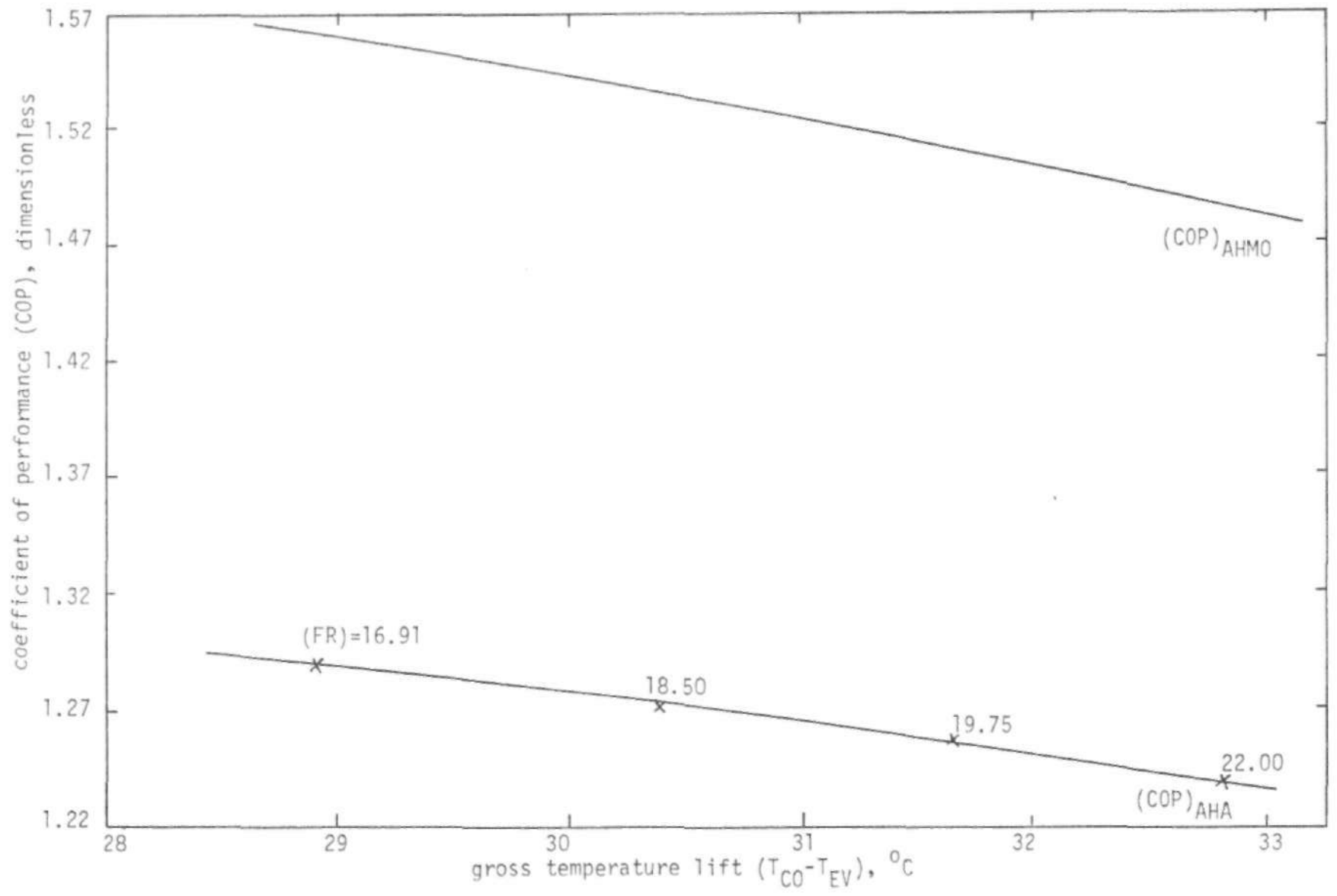


FIGURE (8.5) COEFFICIENT OF PERFORMANCE AGAINST GROSS CONDENSER TEMPERATURE LIFT FOR A GROSS ABSORBER TEMPERATURE LIFT OF 35°C, AN EVAPORATOR TEMPERATURE OF 94°C, A GENERATOR TEMPERATURE OF 172°C, AND A CONCENTRATION OF LITHIUM BROMIDE OF 52.5 WEIGHT PER CENT IN THE ABSORBER FOR THE WATER-LITHIUM BROMIDE SYSTEM

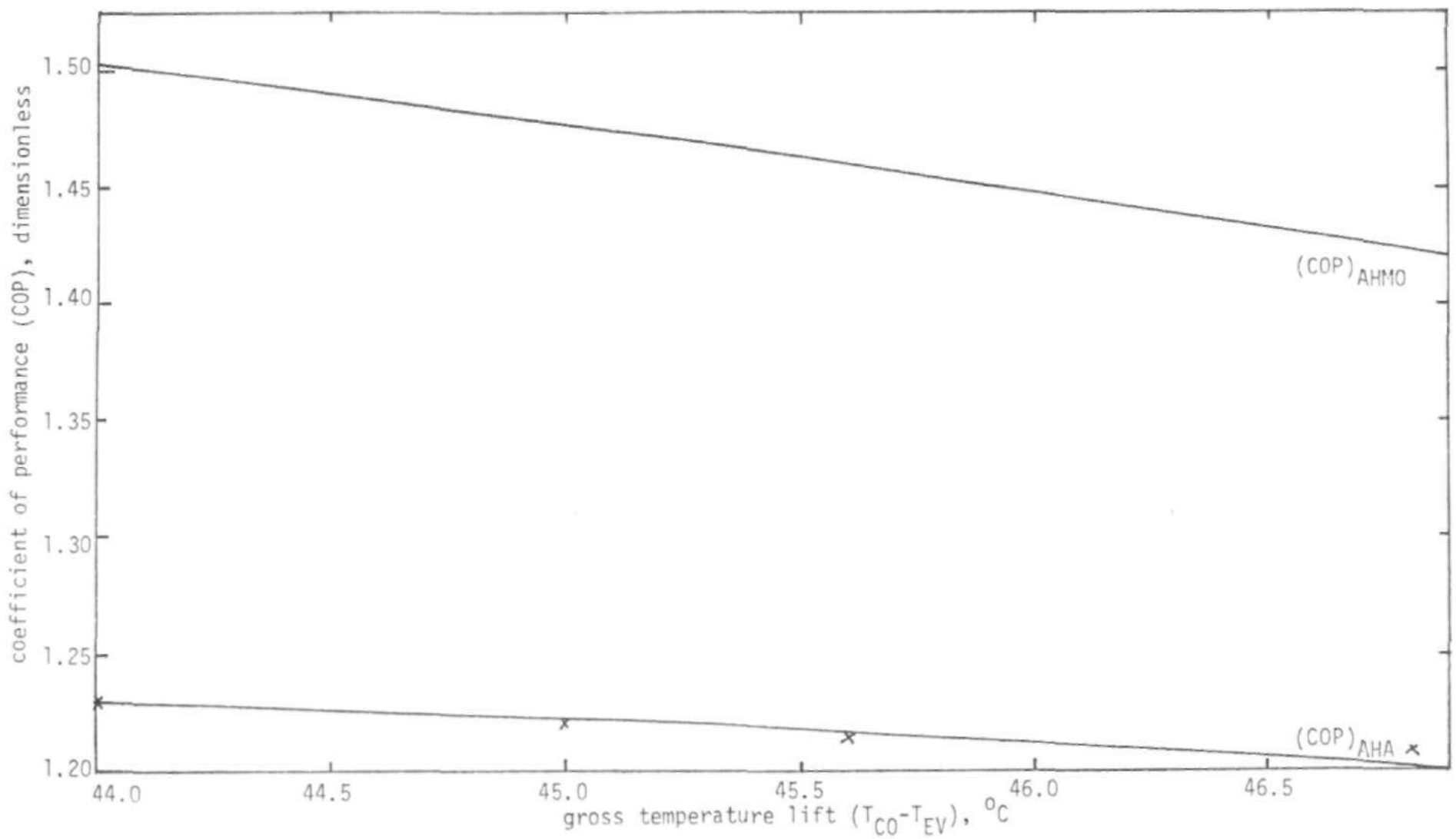


FIGURE (8.6) COEFFICIENT OF PERFORMANCE AGAINST GROSS CONDENSER TEMPERATURE LIFT FOR A GROSS ABSORBER TEMPERATURE LIFT OF 35°C, AN EVAPORATOR TEMPERATURE OF 101°C, A GENERATOR TEMPERATURE OF 197°C AND A CONCENTRATION OF LITHIUM BROMIDE OF 51.5 WEIGHT PER CENT IN THE ABSORBER FOR THE WATER-LITHIUM BROMIDE SYSTEM

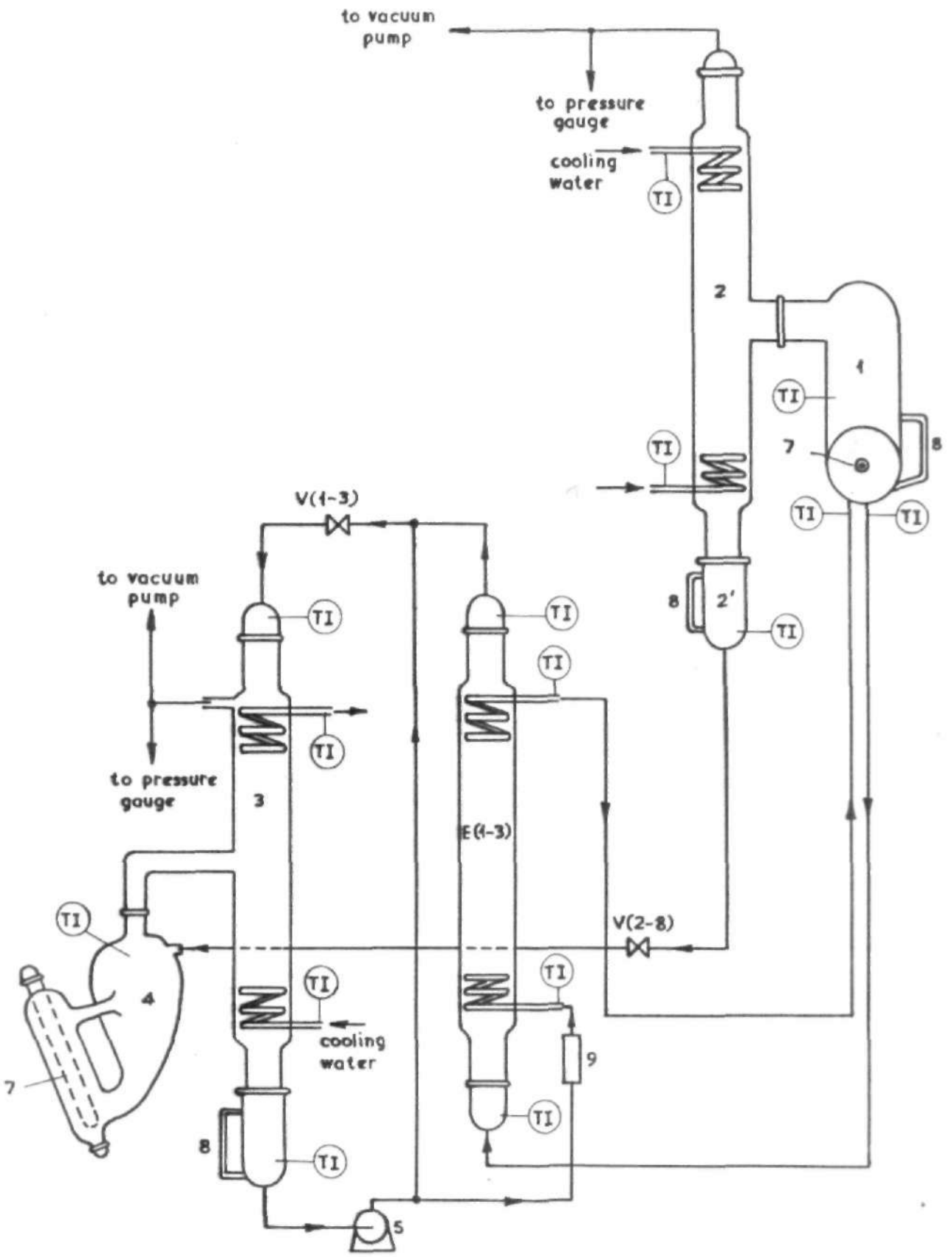


FIGURE 8.7 EXPERIMENTAL CONVENTIONAL ABSORPTION HEAT PUMP.

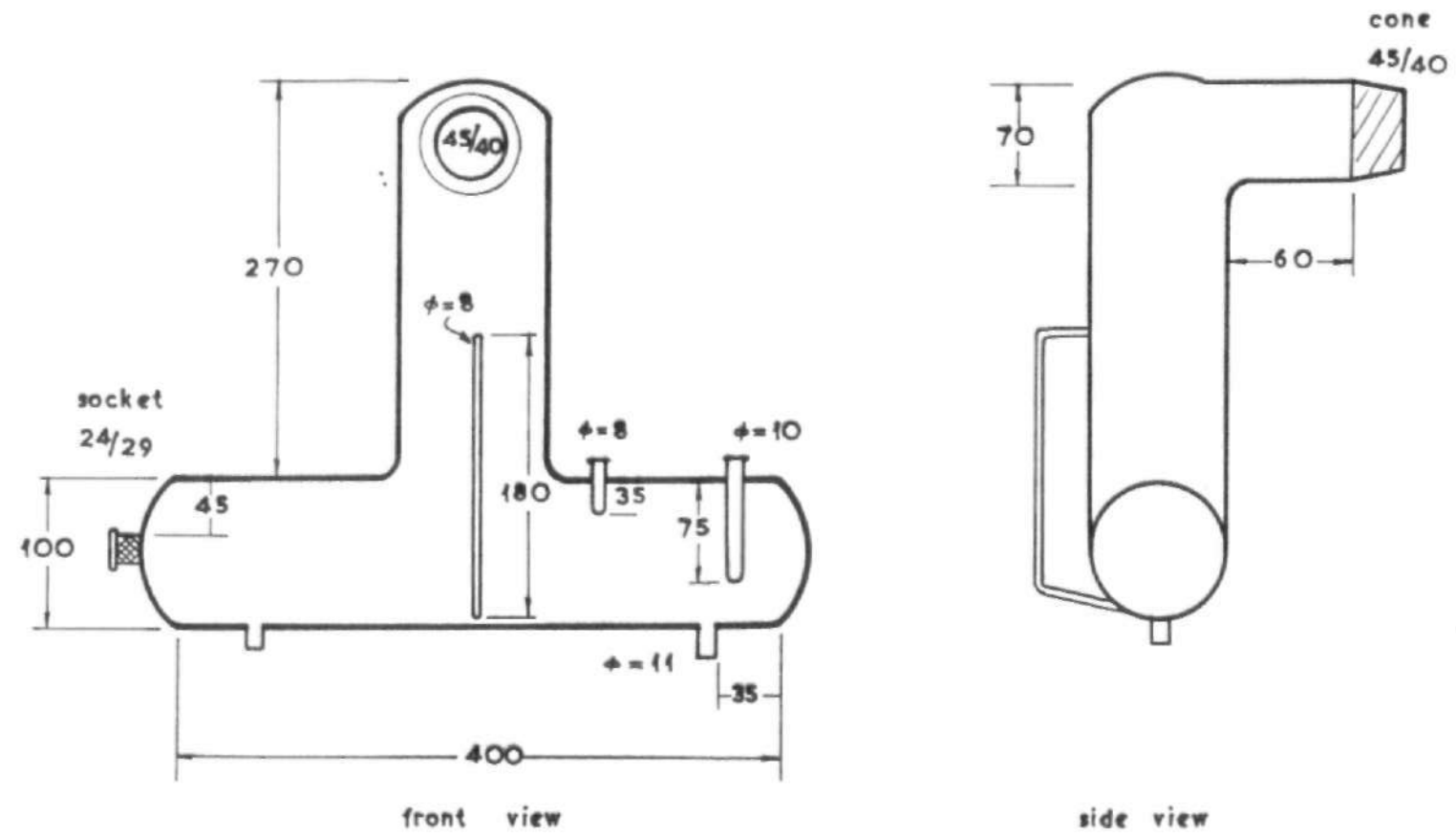


FIGURE 8.8 GENERATOR OF THE GLASS HEAT PUMP.

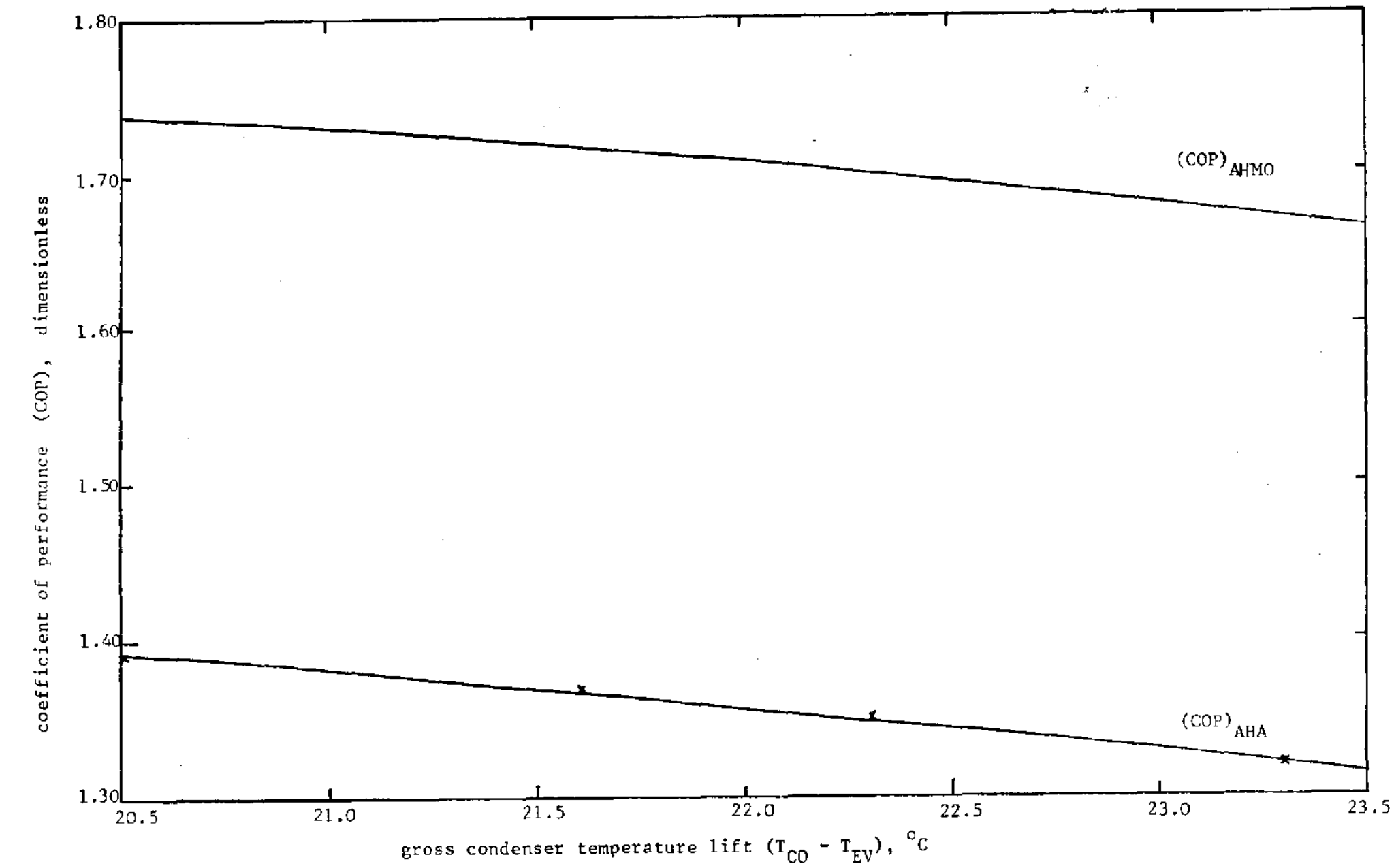


FIGURE (8.9) COEFFICIENT OF PERFORMANCE AGAINST GROSS CONDENSER TEMPERATURE LIFT FOR A GROSS ABSORBER TEMPERATURE LIFT OF 24.4°C AN EVAPORATOR TEMPERATURE OF 46.7°C A GENERATOR TEMPERATURE OF 100°C AND A CONCENTRATION OF LITHIUM BROMIDE OF 48.8 WEIGHT PER CENT IN THE ABSORBER FOR WATER-LITHIUM BROMIDE SYSTEM

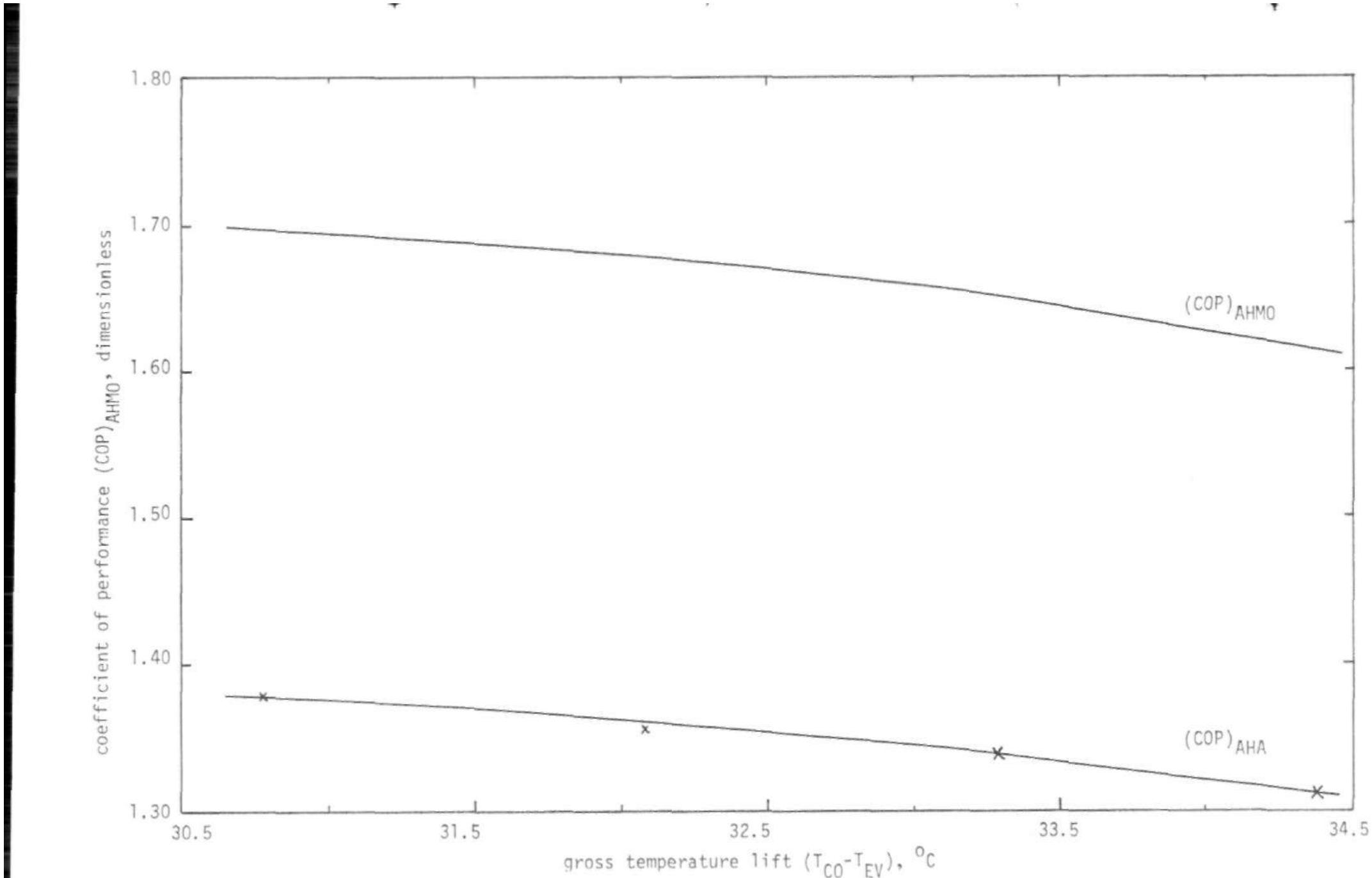


FIGURE (8.10) COEFFICIENT OF PERFORMANCE AGAINST GROSS CONDENSER TEMPERATURE LIFT FOR A GROSS ABSORBER TEMPERATURE LIFT OF 20.8°C AN EVAPORATOR TEMPERATURE LIFT OF 47.6°C A GENERATOR TEMPERATURE OF 110°C AND A CONCENTRATION OF LITHIUM BROMIDE OF 48.5 WEIGHT PER CENT IN THE ABSORBER FOR WATER-LITHIUM BROMIDE SYSTEM

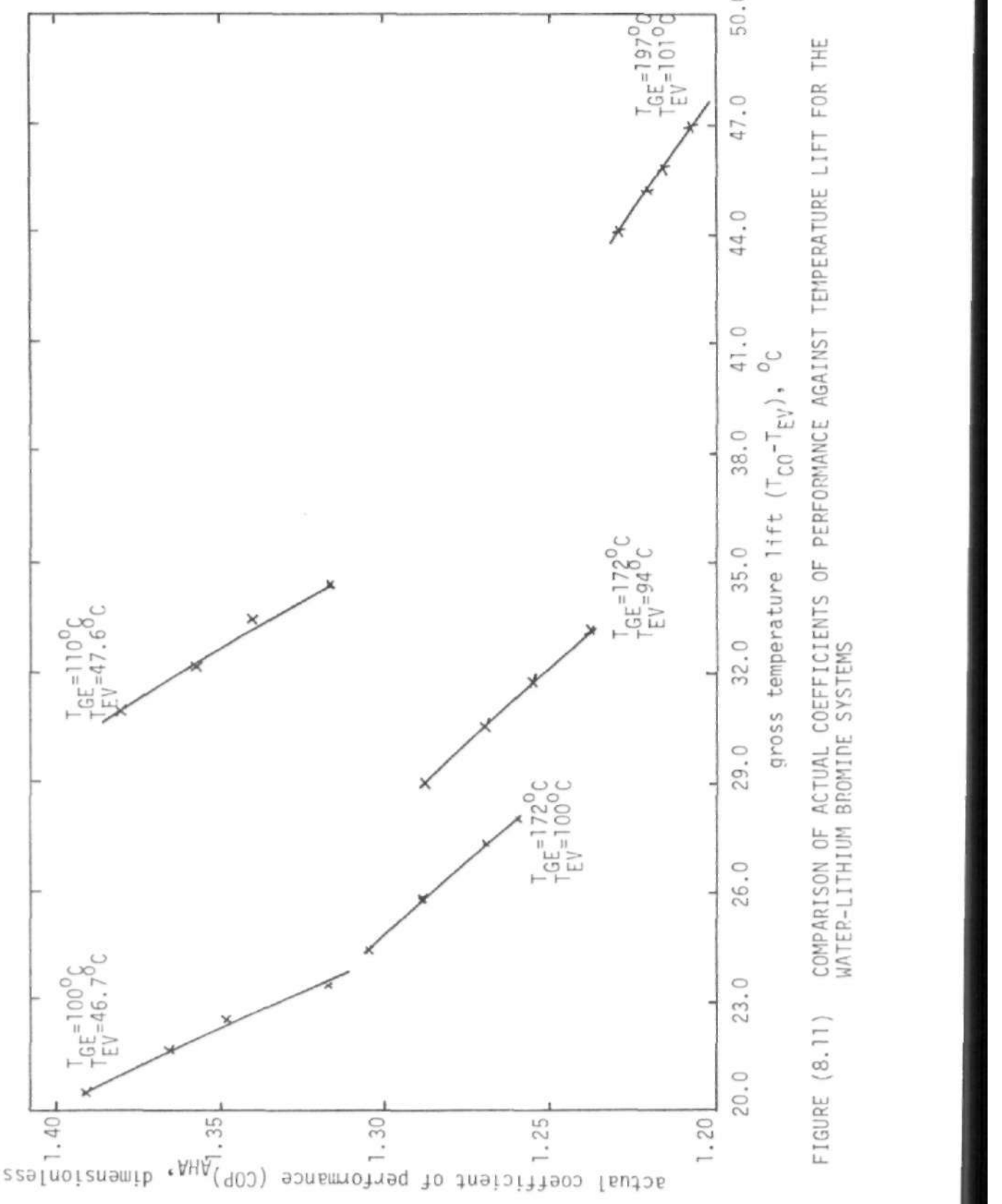


FIGURE (8.11) COMPARISON OF ACTUAL COEFFICIENTS OF PERFORMANCE AGAINST TEMPERATURE LIFT FOR THE WATER-LITHIUM BROMIDE SYSTEMS

CHAPTER 9

CONCLUSIONS AND RECOMMENDATIONS FOR FUTURE WORK

CHAPTER 9

CONCLUSIONS AND RECOMMENDATIONS FOR FUTURE WORK

9.1 CONCLUSIONS

Performance data were obtained for R113 and R718 (which are high temperature working fluids) in mechanical vapour compression heat pumps. Investigations were also carried out using R718 in conventional absorption heat pumps.

Experiments were carried out using an existing mechanical vapour compression water-to-water heat pump originally designed for R12. Performance data were obtained on the system using R113. Two vapour compression heat pump systems were constructed using different types of air compressors. Investigations were carried out on them using water as the working fluid. It was not possible to obtain a small compressor of the desired size designed for the compression of water vapour.

A conventional absorption heat pump system was constructed to operate on water-lithium bromide mixtures at relatively high temperatures. Performance data were obtained on this unit. In addition investigations were made at lower temperatures with an existing glass absorption heat pump using aqueous lithium bromide mixtures.

The conclusions drawn from the investigations carried out with the mechanical vapour compression heat pump systems and the conventional absorption machines are presented below.

9.1.1 Mechanical vapour compression systems

9.1.1.1 Water-to-water system operating on R113

The highest observed condensing temperature of 94.9°C was limited by back pressure in the cooling water line. Higher condensing temperatures could be obtained with a coolant having normal boiling temperature significantly higher than 100°C. The low values of actual coefficients of performance in the range 3.75 to 4.44 are attributable to heat losses. The average heat pump effectiveness factor was 0.37. The average heat load of the system ((about 2.5kW) was much lower than the average design heat load of 15kW.

9.1.1.2 Comparison of performance data for R12,R11,R114 and R113

The performance data for R113 were compared with those for R12 and R114 obtained by previous wokers. The analysis of the performance data of R12, R11,R114 and R113 indicated that the bulk of the heat lost in a heat pump may be through the compressor. The calculated values of the efficiency for the compressor,operating on different working fluids, are in good agreement with the corresponding values of the heat pump effectiveness factor. The performance data for a heat pump operating on a given working fluid could be used to predict the performance of the system when it is operated on another working fluid. This means that if the efficiency

of a compressor can be accurately determined it could be used to design a heat pump system.

9.1.1.3 Small heat pumps operating on air and water vapour

As would be expected the air compressors gave good performance for the compression of air. A compression ratio of 1.3 and gross temperature lift of only 8°C were obtained when operated on steam. The average efficiency of these compressors was about 0.2. The performance of the systems while operating on steam could be predicted using the data from the investigations on air. Small compressors are not adequate for use in heat pumps for steam. This may be due to its low latent heat of vaporisation per unit volume.

9.1.1.4 General conclusions concerning mechanical vapour compression heat pump systems

The compressor could be the major contributor to the inefficiency of a mechanical vapour compression heat pump. For a particular unit, lower performances were observed for high temperature working fluids. Special compressors will be required to obtain good performance with high temperature working fluids.

9.1.2 Conventional absorption heat pump systems

9.1.2.1 Metal absorption heat pump system

High delivery temperatures were obtained. The highest observed condensing temperature of 147.5^{o}C was limited by the maximum pressure which the sight glasses on the system could withstand. The highest condensing temperature was obtained at the highest operating temperature of the generator i.e 197^{o}C. Similarly, the highest gross temperature lift of 47^{o}C was obtained with the highest generator temperature. The actual coefficients of performance were higher at the lower generator temperatures. The lowest generator and evaporator temperatures at which investigations were carried out were 172^{o}C and 94^{o}C respectively. Lower temperatures were not possible because of the small sizes of the absorber and the pipes carrying the water vapour.

9.1.2.2 Glass absorption heat pump system

The system was operated at low generator and evaporator temperatures. The condenser temperature was 82^{o}C when the system was operated at a generator temperature of 110^{o}C. Higher gross temperature lifts were obtained at the higher generator temperature of 100^{o}C. The actual coefficients of performance were higher at the lower generator temperature.

9.1.2.3 General conclusions concerning the effect of varying operating parameters

1) The actual coefficients of performance were not very sensitive to gross temperature lifts. However, they decreased (slightly) as the gross temperature lifts increased.

2) The values of the coefficient of performance increased as the generator temperature increased. At generator temperatures of 197°C and 100°C, the highest values of the actual coefficient of performance were 1.230 and 1.393 respectively.

3) Heat losses were higher at the higher generator temperatures. The average heat losses at generator temperatures of 197°C and 100°C were -22 per cent and -11 per cent respectively. The average values of the heat pump effectiveness factor related to the maximum obtainable coefficient of performance at generator temperatures of 197°C and 100°C were 0.83 and 0.80 respectively.

4) At a given generator temperature, the actual coefficient of performance decreased as the gross temperature lift increased. The gross temperature lift increased as the circulation ratio increased. The gross temperature lifts could be varied only within a range of about 4°C for a given generator temperature.

5) The values of the coefficients of performance were not sensitive to the concentrations of the solutions.

6) Corrosion of the stainless steel equipment occured in lithium bromide solutions only in the presence of contaminants.

9.1.3 General conclusions concerning the mechanical vapour compression and conventional absorption heat pump systems

In terms of controllability, the absorption heat pump system is better than the mechanical vapour compression heat pump. A compressor is a complex unit. Usually, it has to be replaced if any major problems occur in it. Its speed is the major parameter which may be used to control the performance of the heat pump system. In an absorption heat pump system the generator, absorber, solution pump or the expansion valve may be used separately to control the performance of the system. Certainly, for small scale operations the heat losses in the the absorption heat pump system are minimised.

9.2 RECOMMENDATIONS FOR FUTURE WORK

Further investigations should be carried out using small

compressors with very adequate lagging in heat pumps operating on high temperature working fluids.Experiments should be conducted with high evaporating temperatures where the values of the latent heat of vaporisation per unit volume are high. Investigations should also be carried out using low temperature working fluids in heat pumps with small compressors. The results may be useful to assess the relationship between performance and the the latent heat of vaporisation per unit volume of working fluids.

The sight glasses on the metal absorption heat pump should be replaced by thicker walled glass. This would make it possible to carry out investigations at higher condenser temperatures(and pressures). Apart from obtaining heat at higher temperatures,investigations of the corrosion of stainless steel in lithium bromide solutions at higher temperatures could be made.

The diameter of the pipes carrying vapour from the generator to the condenser and from the evaporator to the absorber should be increased. Similarly,the absorber should be replaced by another with a larger pipe size. These changes would enable the equipment to be used for investigations at low temperatures without impairing its utility at high temperatures.

During the course of the experiments, reflux ratios were kept at optimum levels. Observations showed that the ratio had a significant effect on the performance of the system. This effect should be studied quantitatively. The

results would be useful in the design of heat pump systems.

It was observed that significant temperature drops took place across the expansion valve. Further investigations should be made with the view to specifying more efficient expansion valves. It should be noted that the expansion valve could be replaced by a turbine. This would be useful particularly on large scale systems.

Other forms of heating other than electric should be investigated. This could bring about a higher performance even with less lagging. Direct gas heating of the generator should be considered. The indirect heating of the evaporator using hot water or hot oil should also be considered.

Investigations should be carried out using other working fluid-absorbent mixtures. The aim should be to obtain performance data for design purposes and for assessing the utility of combinations.

REFERENCES

Ackroyd, K., "Refrigerants: properties, selection and hazards", The Chemical Engineer, 366-70, (May, 1978).

Aker, J.E., Squires, R.G. and Albright, L.F., "An evaluation of alcohol-salt mixtures as absorption refrigeration solution", ASHRAE Journal, 7, 90-92,(1965).

Albright, L.F., Shannon, P.T., Terrier, F. and Chueh, P.L., "Solubility of chlorofluoromethane in non-volatile polar organic solvents", A.I.Ch.E. Journal, 8, 668-72, (November, 1962).

Albright, L.F., Shannon, P.T., Yu. S.N. and Chueh, P.L., "Solubility of sulphur dioxide in polar organic solvents", Chemical Engineering Progress Symposium Series, 59(44), 66-74, (1963).

Alefeld, G., "New approaches to energy conversion by alternative working fluids", Festkoerper probleme, 18, 53-76, (1978).

Altenkirch, E., "Reversible absorption machines", Zeitschrift Gezamte Kalteindustrie, 20, 114 and 150, (1913).

Altenkirch, E., "Reversible absorption machines", Zeitschrift Gezamte Kalteindustrie, 21, 7 and 21, (1914).

American Conference of Government Industrial Hygienists, "Threshold limit values for chemical substances and physical agents in work-room environment", 1-2, (1977).

American Society of Heating, Refrigerating and Air Conditioning Engineers, "Enthalpy-concentration Diagram for Lithium Bromide-water Combination", ASHRAE Handbook, (1977). Fundamentals and Product Directory, New York, 16.81-16.82, (1977).

Anonymous, "An absorption heat pump heats the federal criminal court building", Sanitaer-und Heizungstechnik, 46(3), 308-310, (March, 1981).

Awnis, A. "OPEC oil for Western Europe", The Challenge of Energy-policies in the Making, Edited by Khouja, M.W., Longman Group Ltd., Essex, 81, (1981).

Bach, R.O. and Boardman, W.W., "Vapour pressure of aqueous lithium iodide solutions", ASHRAE Journal, 9(11), 33-6 (1967).

Berestneff, A.A., "Absorption refrigeration, Mechanical Engineering, 72, 216-220, (March, 1950).

Bier, K. and Gorenflo, D., "Universal representation of the thermophysical properties of boiling liquids", Bull. Inst. Ind. Froid, Annexe (4), 135-41, (1973).

Bjurstrom, H. and Raldow, W., "The absorption process for heating, cooling and energy storage - an historical survey", Energy Research, 5, 43-59, (1981).

Blytas, G.C. and Daniels, F., "Concentrated solutions of sodium thiocyanate in liquid ammonia: solubility, density, vapour pressure, viscosity, thermal conductance, heat of solution and heat capacity", Journal of American Chemical Society, 84(7), 1075-1083, (1962).

Bogatykh, S.A. and Evnovich, I.D., "A study of the viscosities of aqueous solutions of lithium chloride, lithium bromide and calcium chloride applicable to the normal drying of gases", Journal of the Applied Chemistry of the U.S.S.R., 36(8), 1808-1809, (1963).

Bogatykh, S.A. and Evnovich, I.D., "Investigation of densities of aqueous lithium bromide, lithium chloride and calcium chloride solutions in relation to conditions of gas drying", Journal of Applied Chemistry of the U.S.S.R., 38(4), 932-933, (1965).

Boldrin, B., Bolzan, M. and Lazzarin, R., "Lithium bromide absorption cooling devices as heat pumps", Tagunsbericht Internationales Sonnen forum 2nd, Hamburg, West Germany, 127-136 (1978).

Boryta, D.A., Maas, A.J. and Grant, C.B., "Vapour pressure-temperature-concentration relationship for system lithium bromide and water (40-70 per cent lithium bromide), Journal of Chemical Engineering Data, 20(3), 316-319, (1975).

Bresin, A., "Emploi de la machine a absorption comme pompe a chaleur", Revue, Gen. du Froid, 30, 1089, (1953).

Carré, F., "Appareils et procédés propres à produire du froid et fabriquer de la glance", French Patent 41958, (1859).

Chapman, P., "How we use fuels", Fuel's Paradise, Energy Options for Britain, Penguin Books, 40-57, (1979).

Cohen, G., Salvat, J. and Rojey, A., "A new absorption-cycle process for up-grading waste heat", Proceedings of the 14th Inter-society Energy Conversion Engineering Conference, Boston, U.S.A., 2, 1720-1724, (1979).

Cohen, G., Salvat, J. and Rojey, A., "Absorption heat pump developments", International Advanced Course on Heat Pump Fundamentals, Espinho, Portugal, (NATO advanced study institutes programme), (September, 1980).

Cohen, G., Salvat, J. and Rojey, A., Personal communication from Allied Chemical, International Advanced Course on Heat Pump Fundamentals, Espinho, Portugal, (NATO advanced study institutes programme), (September, 1980).

Copley, M.J., Zellhoefer, G.F. and Marvel, C.S., "Hydrogen bonds involving the C-H link. IV. The effect of solvent association on solubility", Journal of the American Chemical Society, 60, 2666-2673, (1938).

Department of Energy, London, "Energy conservation for new measures and long term strategy", Energy Paper No.33, Department of Energy, H.M.S.O., London, 34-35, (February, 1979).

Dolotov, A.G., "Method of determination of thermodynamic properties of hydrocarbons for design calculation of processes in a cycle of absorption refrigeration machine", Kholodilnye I. Ustroistva, 116-121, (1976).

Dosat, R.J., Principles of Refrigeration, John Wiley and Sons, New York, (1961).

Dow Chemical Company, ACG Data Book, A-10-5.

Dunkerly, J., Ramsay, L.G. and Cecelski, E., "Energy strategies for developing nations", John Hopkins University Press, London, 1st Edition, (1981).

Downing, R.C., "Refrigerant equations", ASHRAE Transactions, 80(2), 158-169, (1974).

Ellington, R.T., Kunst, G. and Peck, R.E. "Absorption cooling process", Institute of Gas Technology, Illinois, Research Bulletin 14, (1957).

Farnham, R.S., "Peat resources-classification, properties and geographical distribution", Symposium on Management and Assessment of Peats as an Energy Resource, Arlington, Va, (July, 1979), (June, 1980).

George, J.H.B. and Birkett, J.D., "A study of a liquid ammonia-salt system and their potential application to the absorption cooling process", Projects ZF-72 and 72(a), Library of Congress No.65-19567, (1965).

Gibbard, H.F. and Scatchard, G., "Liquid vapour equilibrium of aqueous lithium chloride from 25^{o}C to 100^{o}C and from 1.0 to 18.5 molal, and related

properties", Journal of Chemical Engineering Data, 18(3), 293-297, (1973).

Grosman, E.R. and Zhuravelenko, V. Ya., "Absorption refrigeration machine operating with a solution of methanol and lithium bromide", Kholodilnaya Tekhnika, 45(1), 4-6, (1968).

Grosman, E.R., "Properties of a solution of methanol and lithium bromide studied as working substances of absorption refrigeration machines", Kholodilnaya Tekhnika Teknol., 11, 84-86, (1971).

Grosman, E.R., Zhuravlenko, W.I., Kremniev, O.A., Kurilow, G.W. and Ryzhow, S.I., "Wykorzystanie ciepla procesow hutniczych do wytwarzania Zimna technicznego i klimatyzacji, Wiad. Hutn., 32, 369, (1976).

Haltenberger, W. (Jr.), "Enthalpy-concentration charts from vapour pressure data", Industrial and Engineering Chemistry 31(6), 783-786, (1939).

Hensel, W.E. and Harlowe, W.W., "Lithium bromide-lithium iodide composition for absorption refrigeration system", U.S. 3,524,3151 patented, (August 18, 1970), U.S. Cl. 252-269.

Hildebrand, J.H., Prausmitz, J.M. and Scott, R.L., "Regular and related solutions", Van Nostrand Reinhold

Company, New York, (1970).

Holland, F.A., "Heat pumps: Part 1, the potential for heat pump in India",Indian Chemical Engineer, XXI, 2(3), (1979).

Holland, F.A., "What is a heat pump", Symposium Papers (3), Institution of Chemical Engineers, North Western Branch, (3), 1.1-1.15, (April, 1981).

Holland, F.A., Watson, F.A. and Devotta, S., "Thermodynamic Design Data For Heat Pump Systems, Pergamon Press, Oxford, (1982).

Hornick, J.R., "Wood fuel resources in the United States, ASHRAE Annual Meeting, (June, 1982).

Hundermann, A.S., "Heat pumps. Volume 2. 1978 - February, 1980", NTIS/PB80-805815/EES, (1980).

Imperial Chemical Industries, "Thermodynamic properties of Arcton 12 SI units", Imperial Chemical House, Millbank. London.

Imperial Chemical Industries, "Thermodynamic properties of Arcton 113 SI units", Imperial Chemical House, Millbank, London.

Ingra, O., "Compact shrouds for wind turbines", Energy Conservation, 16, 149-157, (1977).

Isshiki, N., "Storage and generation of power and heat by aqueous solution of salts", Proceedings from the International Seminar on Thermochemical Energy Storage, Stockholm, 301-339, (1980).

Iyoki, S. and Uemura, T., "Studies on corrosion inhibitors in water-lithium bromide absorption refrigerating machines", Reito, 53(614), 1101-1105, (1978).

Janben, H.A. and Oelert, G., "Development of a primary driven absorption heat pump for domestic heating", New ways to save energy - Commission of the European Communities, D. Reidel Publishing Company, 198-220, (1979).

Jelink, M., Borde, J. and Yaron, I., "Enthalpy-concentration diagram of the system R22-dimethyl formamide and performance characteristics of refrigeration cycle operating with this system", ASHRAE Transactions, 84(2), 60-67, (1978).

Jenssen, P.F. and Johnston, I.W. "Some thoughts on the domestic, gas-fired heat pump", Gas Engineering and Management, 553-557, (November, 1979).

Keenan, J.H. and Keyes, F.G., "Thermodynamic properties of water including vapour, liquid and solid phases", John Wiley and Sons, New York, 21, (1939).

Keenan, J.H., Keyes, F.G. and Moore, J.G., "Thermodynamic properties of water including vapour, liquid and solid phases", John Wiley and Sons, New York, (1969).

Kessis, J.J., Le systeme eau-bromure de lithium", Bulletin Societe Chemique, No.7, 48-52, (1965).

Khadurdyev, A. and Daikhanov, S., "Phase diagram for lithium chloride and calcium chloride aqueous solutions", Izvestiya Academic Nauk Turkmenskot S.S.R. Seriya, Fiziko-Tekhnich. Khim. Geolog. Nauk, 5, 41-44, (1977).

Koenemann, E., "Ein neus zweistoffverfahren zur krafterzeugung", 2nd World Power Conference, (1930), 5(10), Rep.15, VDI-Verlag, (1930).

Kribel, M. and Löffler, H.J., "Thermodynamische Eigenschaftern des binären Systems Difluoromonochloromethane (R22) - Tetraäthylen glykoldimethyläther (E181)", Kältetechnik, 17(9), 266-271, (1965).

Kruse, H. and Jakobs, R., "Significance of the non-azoetropic binary refrigerants, when used in heat pumps and refrigeration plants", Klima Kalte Inginieur 5(7-8), 253-260, (1977).

Latyschev, V.P., "Enthalpy-concentration diagrams for freon 22-dibutylphthalate and freon 22-dimethyl ether of tetraethylene glycol", Kholodilnaya Tekhnika, 46(7), 61-62, (1969).

Latyschev, V.P., "Experimental investigation of thermal capacity of dimethyl phthalate, of tetraethylene glycol dimethyl ether and heat of their mixing", Kholodilnaya Tekhnika, 46(8), 31-34, (1969).

Latyschev, V.P., "Temperature-concentration diagram for a solution of freon 22 in dibutyl phthalate and dimetyl formamide", Kholodilnaya Tekhnika, 47(11), 61, (November, 1970).

Leslie, J., "Professor Leslie's process for making ice", Mechanics Magazine, 1, 311-314,and 322-323, (1824).

Linke, W.F. and Scidell, A., "Solubilities of inorganic and metal organic compounds", American Chemical Society, Vol.2, 4th Edition, Washington, D.C., (1965).

Lower, H., "Thermodynamic and physical properties of aqueous lithium bromide solutions", Kaltetechnik, 13(5), 178-183, (1961).

Lower, H., "Sorption heat pumps as heating machines", Klima and Kalte Inginieur, 5(12), (1977).

Lower, H., "Technical potentiality and development of the absorption heat pumps", Ki Klima Kaelte Heizungstechnik, 9(5), 225-262, (May, 1981).

Macriss, R.A. and Rush, W.F., "Lithium bromide-lithium thiocyanate-water composition for an absorbent-refrigeration system", U.S. 3,541,013, (November 17, 1970).

Malhotra, K.S., Nahar, N.M. and Ramana, B.V., "An improved solar cooker", Internatinal Journal of Energy Research, 6(3), 227, (July - September, 1982).

Mastranglo, S.V.R., "Solubility of some chlorofluoro hydrocarbons in E181, ASHRAE Journal, 64-67, (October, 1959).

McCornick, W.T., Kalishi, R.B. and Wonder, T.J., "The future of world natural gas supply", World Energy Resources, 1985-2020, World Energy Conference 1978, IPC Science and Technology Press, 50-51, (1978).

McNeely, L.A., "Thermodynamic properties of aqueous solutions of lithium bromide", ASHRAE Transactions, 85(1), 413-434, (1979).

Nakanishi, T., Furukawa, T., Sata, N., Shibamoto, N. and Baba, H., "Industrial high-temperature heat pump", Hitachi Zosen Technical Review, 42(1), 7-13, (March, 1981).

Nesselmann, K., "The theory of heat transformer", Wissensch. Verroffentl. Siemens-Konzern, 12, 89-100, (1933).

Niebergall, W., "Die Absorptions-Kalteanlagen in der Braueritechnik", Die Kalte, 4, 237, (1951).

Niebergall, W., "Absorptionsheizanlgen", Kaltetechnik, 9, 239, (1957).

Odell, P.R., "Oil and World Power", Pelican Books, 6th Edition, 272, (1981).

Ovcharenko, V.A., "Natural gas prospects in developing countries and the role of LNG transportation", Natural Resources Forum, 4(3), 277-290, (1980).

Pechatnikov, M.Z. and D'Yachenko, Yu. I., "Selection of thermodynamic optimum pair for hydrocarbon absorption refrigerating machines", Tr. Vsesoyuznoi Nauchno - Tekhnicheskoi Konf Termodin. Sbornik Dokladov, Sektisii Novye Tepl., 379-386, (1968).

Pennington, W., "How to find accurate vapour pressure of lithium bromide solutions", Refrigeration Engineering, 57-61, (May, 1955).

Perelshtein, I.I. and Parushin, E.B., "Method to determine the thermodynamic properties of principal coolants from experimental data", Kholodilnaya Tekhnika No.1, 27-30, (1976).

Perry, R.H., Chilton, C.H. and Kirkpatrick, S.D., "Chemical Engineers Handbook", 4th Edition, McGraw-Hill, New York, (1969).

Pinevitsh, G., "Viscosities of ammonia-water mixtures and liquid ammonia", Kholodilnaya Tekhnika, 20(3), 30-37, (1948).

Praires, Pierre Des, "World petroleum supply limits", World Energy Resources, 1985 - 2020, World Energy Conference 1978, IPC Science and Technology Press, 2-14, (1978).

Qasrawi, A.M.S., "Absorption heat pump generators", Lucas Group Services Limited, Lucas Research Centre, West Midlands, U.K., (August, 1980).

Radermacher, R. and Alefeld, G., "Working fluid combinations for absorption heat pumps", Proceedings from the International Seminar on Thermochemical Energy Storage, Stockholm, 341-347, (1980).

Rashkovskaya, E.A. and Chernen'kaya, E.I., "Densities of solutions of ammonium bicarbonate, sodium bicarbonate, ammonium chloride and ammonia in the 20-100°C range", Journal of the applied Chemistry of the U.S.S.R., 40(2), 289-295, (1967).

Reay, D.A., "Industrial energy conservation", Pergamon Press Ltd., Oxford, 296, (1977).

Renz, M., "Solubility of working fluid pairs for absorption heat pump processes", Vulkanverlag, (1978).

Roberson, J.P., Lee, Ch. Y., Squires, R.G. and Albright, L.F., "Vapour pressure of ammonia and methylamines in solutions for absorption refrigeration systems", ASHRAE Transactions, 72(1), 198-208, (1966).

Rohsenow, B.M., "A method of correlating heat-transfer data for surface boiling of liquids", Transactions of the ASME, 970-976, (August, 1951).

Royal Society, The, "British say coal reserves over-stated", Coal Age, 85(5), 52, (May, 1980).

Royal Society, The, "West German plans project large coal imports before 1995, Coal Age, 85(5), 45, (May, 1980).

Rozenfeld, L.M. and Karnaukh, M.S., "Dynamic heating by means of a reversed absorption lithium bromide machine", Journal of Technical Physics (U.S.S.R.), 28(7), 1460-1465, (1958).

Salem, B. and van Nao, T., "Fuel-wood production in traditional farming systems", Food and agricultural Organisation of United Nations, Rome, 33(131), (1981).

Salter, S.H., "Wave power", Nature, 249, (June, 1974).

Salter, S.H., "Characteristics of a rocking wave power device", Nature, 254, 504-506, (1975).

Sarkes, L.A., Nicholis, J.A. and Menzer, M.S., "Gas-fired heat pumps: an emerging technology", ASHRAE Journal, 19(3), S.36-41, (1977).

Sax, N.I., "Dangerous properties of industrial material", Van Nostrand Reinhold, 5th, (1979).

Schmitt, K., "Gas heat pumps using the absorption principle", VDI-Berichte, 353, 79-86, (1980).

Schwartz, F. and Lange, E., "Lösung-und Verdünnungswärmer von Salzen von der äussersten Verdünnung bis zur Sättigung", Zeitschrift fur Physikalische Chemie, 133, 129-149, (1928).

Scrosati, B. and Vincent, C.A., "Solubility data series, Vol.II: solubility of solids in liquids", Pergamon Press, Oxford, (1960).

Seliverstov, V.M., "Enthalpy-concentration diagrams for solutions Freon 22-dibutyl phthalate", Kholodilnaya Tekhnika, 43(4), 36-38, (1966).

Seliverstov, V.M., "Solubility of Freon22 in a mixture of dibutyl phthalate and dimethyl formamide", Kholodilnaya Tekhnika, 47(11), 34-36, (November, 1970).

Sellerio, V., "Absorption - Kaltemaschine mit Isobutylazetat - R22", Kaltetechnik, 18(1), 2-3, (1966).

Siddig Mohamad, B.E., "Performance studies on a reversed absorption heat pump", Ph.D. Thesis, University of Salford, Salford, U.K. (1982).

Siddig Mohammed, B.E., Watson, F.A. and Holland, F.A., "A study of the operating characteristics of a reversed absorption heat pump (heat transformer)", Transactions of the Institution of Chemical Engineers (accepted for publication).

Smith, I.E. and El-Shamarka, S.E., "Absorption heat pumps for space heating", 3rd International Conference on Future Energy Concepts, Electrical Engineers' Conference, London, (192), 232-237, (1981).

Smith, I.E. and El-Shamarka, S.E., "Absorption heat pumps for space heating", 3rd International Conference on Future Energy Concepts, London, 232-237, (1981).

Smith, I.E. and Carey, C.O.B., "Thermal transformers for up-grading industrial waste heat", International Symposium on the Industrial Application of Heat Pumps, Coventry, England, 251-253, (1982).

Smith, I.E., "Heat pump absorbers", School of Mechanical Engineering, Cranfield Institute of Technology, Bedford, U.K. (1980).

Smith, I.K., "The use of the Lee and Kesler equations of state for estimation of common refrigerant properties", Department of Mechanical Engineering, City University, London, EC1V 4PB.

Togam, N., Enokizalea, T., Iide, T. and Okamoto, M., "Fluorohydrocarbon Composition", Japan. Kokai Tokyo Koho, 7906881, (January 19, 1979).

Uemura, T., "Methanol-lithium iodide-bromide absorption refrigerating machine", Reito, 50(568), 95-101, (1975).

Uemura, T. "Studies on the methanol-zinc bromide refrigerating machine", Reito, 51, 1027-1036, (1976).

Uemura, T. and Hasaba, S., "Studies on the lithium bromide-water absorption refrigerating machine", Technology Report of Kansai University, 6(6), 31-55, (1964).

Uemura, T., "Physical properties of refrigerant absorbent systems for absorption refrigerants", Reito, 53(600), 929-940, (1977).

United Nations, "Energy production and consumption", United Nations Statistical Year Book 1978, 389-392, (1979).

Uri, N.D., "Estimating undiscovered oil resources: an engineering approach, Energy Sources, 5(3), 197, (1980).

Usyukin, I.P., "Thermodynamic diagrams of solution lithium bromide-water", Kholodilnaya Tekhnika, 46(1), 25-29, (1969).

Smith, N., "Societies can no longer afford to harvest forests just for lumber or fuel", World-watch Paper-wood: an ancient fuel with a new future, World-watch Institute, Washington, 9, (January, 1981).

Soave, G., "Equilibrium constants from a modified Redlich-Kwong equation of state", Chemical Engineering Science, 27, 1197-1203, (197).

Stephan, K., "Working substances for absorption heat pumps and transformers", Institut für Technische Thermodynamik und Thermische Verfahrenstechnik, Univ. Stuttgart, F.R. Germany, (1980).

Stephan, K. and Seher, D., "Heating with two-stage absorption heat pumps", Kaelte Heizungstechnik, 9(9), 431-438, (September, 1981).

Stephen, H. and Stephen, T., "Solubilities of Inorganic and Organic Compounds", Vol.1, Vol.2, Pergamon Press, Oxford, (1963).

Stingel, D.E., "A new energy emphasis for the United States: transferring energy-intensive industry from the United States to developing countries", Natural Resources Forum, United Nations, New York, 4(3), 260, (July, 1980).

van Looveren, A., Verelst, J., Berghmans, J. and Gelders, L., "Determining the capital cost of industrial heat pumps by correlation", International Symposium On the Industrial Application of Heat Pumps, BHRA Fluid Engineering, Cranfield, England, (March, 1982).

Vielvoye, R., "West African crude suddenly is crucial", Oil and Gas Journal, 47, (January, 1981).

Vielvoye, R., "Vast gas program looms in Nigeria", Oil and Gas Journal, 61, (January, 1981).

Williams, D.A. and Tiedmann, J.B., "A heat pump powered by natural thermal gradients", Proceedings of the Inter-society Energy Conversion Engineering Conference 9th, California, U.S.A., 538-540, (August, 1974).

Zellhoefer, G.F., Copley, M.J. and Marvel, C.S., "Hydrogen bonds involving the C-H link. The solubility of halogens in donor solvents", Journal of the American Chemical Society, 60, 1337-4, (1938).

APPENDIX I

COMPUTER PROGRAMMES AND RESULTS

APPENDIX I

A.I.1 ENTHALPY-CONCENTRATION-TEMPERATURE RELATION FOR WATER-LITHIUM BROMIDE SOLUTIONS

```
      CHECK EVERYTHING
      LIBRARY 'NAG77'
*  THIS PROGRAM WAS WRITTEN TO DO THE FOLLOWING:
*
*  1  CALCULATE THE DEW POINT TEMPERATURE AND ENTHALPY PER UNIT MASS OF
*     AQUEOUS SALT SOLUTIONS FROM THE VAPOUR PRESSURE-TEMPERATURE
*     RELATION AT PRESCRIBED TEMPERATURES OF SOLUTIONS
*  2  DURING THE COURSE OF THE ABOVE ,PERFORM A SIMPLE LINEAR REGRESSIO
*     USING THE TEMPERATURE OF THE SOLUTION AS THE DEPENDENT VARIABLE
*     AND THE DEW POINT TEMPERATURE AS THE INDEPENDENT VARIABLE
*  3  USING THE RESULTS FROM (2) CALCULATE THE TEMPERATURE OF THE SOLUTION
*     AT PRESCRIBED DEW POINT TEMPERATURE
*  4  FIT THE ENTHALPY-CONCENTRATION DATA WITH A POLYNOMIAL WITH
*     APPROPRIATE DEGREE IN THE CONCENTRATION AND TEMPERATURE OF THE
*     SOLUTION USING THE LEAST-SQUARE CHEBYSHEV SERIES AND GIVING THE
*     CHEBYSHEV COEFFICIENTS
*  5  FIT THE TEMPERATURE OF SOLUTIONS-CONCENTRATION-DEW POINT TEMPERATURE
*     DATA AS IN (4)
*
*                          NOMENCLATURE
*
*   A,B,C          CONSTANTS FOR THE VAPOUR PRESURE
*                  EQUATION OF WATER                      DIMENSIONLESS
*   AA,BB,CC       CONSTANTS FOR THE VAPOUR EQUATI-
*                  ON OF WATER                            DIMENSIONLESS
*   ACP,BCP,CCP    CONSTANTS FOR ENTHALPY PER UNIT
*                  MASS EQUATION FOR THE SOLUTION         DIMENSIONLESS
*   FMNERR          MEAN  OF  THE  PERCENTAGE ERROR
*                   IN THE TEMPERATURE OF THE SOLUT-
*                   ION                                   PER CENT
*   H              INTEGRAL OF HPARTW D(1-WT(1)/WT(J))
*                  BETWEEN WT(1) AND WT(J)                KJ PER KG
*   HO             ENTHALPY OF BASE CONCENTRATION         KJ PER KG
*   HPARTW         PARTIAL ENTHALPY OF WATER IN
*                  SOLUTION                               KJ PER KG
*   HSOLVL         LATENT HEAT OF THE SOLUTION            KJ PER KG
*   HSWL           ENTHALPY OF WATER AT TDEW              KJ PER KG
*   HSUPV          ENTHALPY OF SUPERHEATED WATER
*                  VAPOUR                                 KJ PER KG
*   HWT            ENTHALPY OF SOLUTION                   KJ PER KG
*   HWVAP          ENTHALPY OF SATURATED WATER VAPOUR
*                  AT TDEW                                KJ PER KG
*   HWVL           LATENT HEAT OF VAPOURISATION OF
*                  WATER                                  KJ PER KG
*   LP             PRESSURE                               PSI,MM HG
*   NDEW           NUMBER OF STEPS OF DEW POINT
*                  TEMPERATURE REQUIRED                   DIMENSIONLESS
*   NKEND          NUMBER OF STEPS OF SOLUTION TEMPER-
*                  ATURE REQUIRED                         DIMENSIONLESS
*   PSI            PRESSURE                               PSI
*   RESULT(1)      THE MEAN VALUE OF THE DEW POINT
*                  TEMPERATURE                            DEG. CENT.
*   RESULT(2)      THE MEAN VALUE OF THE TEMPERATURE
*                  OF SOLUTION                            DEG. CENT.
*   RESULT(3)      THE STANDARD DEVIATION OF THE DEW
*                  POINT TEMPERATURE                      DEG. CENT.
*   RESULT(4)      THE STANDARD DEVIATION OF THE
```

```
*                TEMPERATURE OF SOLUTION                DEG. CENT.
*   RESULT(5)    THE PEARSON PRODUCT-MOMENT CORRELATION
*                BETWEEN THE TEMPERATURE OF SOLUTION
*                AND THE DEW POINT TEMPERATURE          DIMENSIONLESS
*   RESULT(6)    THE REGRESSION COEFFICIENT             DIMENSIONLESS
*   RESULT(7)    THE REGRESSION CONSTANT                 DIMENSIONLESS
*   RESULT(8)    THE STANDARD ERROR OF THE REGRESSION
*                COEFFICIENT                            DIMENSIONLESS
*   RESULT(9)    THE STANDARD ERROR OF THE REGRESSION   DIMENSIONLESS
*   RESULT(10)   THE T-VALUE FOR THE REGRESSION
*                COEFFICIENT                            DIMENSIONLESS
*   RESULT(11)   THE T-VALUE FOR THE REGRESSION
*                CONSTANT                               DIMENSIONLESS
*   RESULT(12)   THE SUM OF SQUARES ATTRIBUTABLE TO
*                THE REGRESSION                         DIMENSIONLESS
*   RESULT(13)   THE DEGREES OF FREEDOM ATTRIBUTABLE
*                TO THE REGRESSION                      DIMENSIONLESS
*   RESULT(14)   THE MEAN SQUARE ATTRIBUTABLE TO
*                THE REGRESSION                         DIMENSIONLESS
*   RESULT(15)   THE F-VALUE FOR THE ANALYSIS OF
*                VARIABLE                               DIMENSIONLESS
*   RESULT(16)   THE SUM OF SQUARES OF DEVIATIONS
*                ABOUT THE REGRESSION                   DIMENSIONLESS
*   RESULT(17)   THE DEGREES OF FREEDOM OF DEVIATIONS
*                ABOUT THE REGRESSION                   DIMENSIONLESS
*   RESULT(18)   THE MEAN SQUARES OF DEVIATIONS ABOUT
*                THE REGRESSION                         DIMENSIONLESS
*   RESULT(19)   THE TOTAL SUM OF SQUARES               DIMENSIONLESS
*   RESULT(20)   THE TOTAL DEGREES OF FREEDOM           DIMENSIONLESS
*   SDMNER       STANDARD DEVIATION OF PERCENTAGE ERROR
*                IN THE TENPERATURE OF THE SOLUTION     DIMENSIONLESS
*   SMSDER       SUM OF THE SQUARES OF THE DIFFERENCE
*                BETWEEN THE ERROR IN SOLUTION TEMPERATURE
*                AND THE MEAN ERROR                     DEG. CENT.
*   SMTEER       SUM OF THE ERRORS IN THE TEMPERATURE
*                OF THE SOLUTION BASED ON THE TEMPERATURE
*                OBTAINED FROM THE FIT                  DEG. CENT.
*   TDEW,TFDEW   DEW POINT TEMPERATURE                  DEG.CENT.
*   TE,TEI,TSL   TEMPERATURE OF SOLUTION                DEG.CENT.
*   TEER         PERCENTAGE ERROR IN THE TEMPERATURE
*                OF THE SOLUTION BASED ON THE TEMPERATURE
*                OBTAINED FROM THE FIT                  PER. CENT.
*   TER          TEMPERATURE OF SOLUTION                RANKINE
*   TEFIT        TEMPERATURE OF SOLUTION OBTAINED FROM
*                FIT                                    DEG. CENT.
*   VSATG        VOLUME OF SATURATED WATER VAPOUR       CUB. M. PER KG
*   VSATS        VOLUME OF SATTURATED SOLUTION          CUB. M. PER KG
*   VSATW        VOLUME OF SATURATED WATER AT TDEW      CUB. M. PER KG
*   VSUPG        VOLUME OF SUPERHEATED WATER VAPOUR     CUB. M. PER KG
*   WT           CONCENTRATION OF SOLUTION              KG LIBR PER KG SOLTN
*   WI           TOTAL WEIGHT OF WATER EVAPORATED AS
*                CONCENTRATION VARIES                   KG
*
*                        THE PROGRAMME
*
C     INITIALISATION
      DIMENSION TEI(20,20),WI(19),DELW(19),TDEWK(18),
```

```
     1A(19),B(19),C(19),PBAR(18),PSI(18),HWVL(18),
     1HSVAP(18),VSATG(18),TCW(18),TCS(18),HSWL(18),
     1VSATW(18),VSATS(18),VSUPG(18),HSUPV(18),HSOLVL(18),
     1TEK(19),HAV(19),HDEL(19),HWT(19,18),TSL(19,18),
     1HO(19,18),XOX1(19),HPARTW(19,18),H(19,18),HWVAP(18),
     1TFDEW(18),PWBAR(18)
      COMMON/BLK1/TE(18),TDEW(18)
      COMMON/BLK2/RESULT(400)
      COMMON/BLK3/WT(19),W(350),XMIN(18),XMAX(18)
      COMMON/BLK4/M(20),WT1(350),A0(15)
      INTEGER NW,NWORK,MI
*
*    FOR BORYTA'S AND UEMURA'S DATA
       DIMENSION TK(18)
*
*    FOR PENNINGTON'S DATA
*      DIMENSION TER(18)
*
       REAL LP(18),LPN(18)
*
*   CONSTANTS FOR PENNINGTON'S VAPOUR PRESSURE EQUATION
*      READ(1,100)(WT(J),A(J),B(J),C(J),J=1,19)
*  100 FORMAT(1X,F4.1,F12.5,F12.2,F13.1)
*
*   CONSTANTS FOR THE VAPOUR PRESSURE-TEMPERATURE
*                  EQUATION FOR WATER
       AA=11.5923
       BA=-3.66989E3
       CA=-2.43093E5
*
*   DETERMINATION OF THE REQUIRED CONCENTRATION OF SOLUTION
       DO 1 J=1,19
       WT(J)=50.+(J-1)
       WRITE(2,200)WT(J)
   200 FORMAT(1X,F4.1)
*
*   DETERMINATION OF THE REQUIRED TEMPERATURE OF SOLUTION
       DO 2 NP=1,17
       TE(NP)=60+(NP-1)*10
*
*   FOR PENNINGTON'S DATA
*      TER(NP)=TE(NP)*1.8+491.7
*
       TK(NP)=TE(NP)+273.15
*
*   CONSTANTS FOR DETERMINING VAPOUR PRESSURE FROM THE
*   VAPOUR PRESSURE-CONCENTRATION EQUATION OF UEMURA
*      A(J)=4.0686+.13292*WT(J)-.0014278*WT(J)**2
*      B(J)=1.0575E3-94.632*WT(J)+.9816*WT(J)**2
*      C(J)=-6.0135E5+1.9734E4*WT(J)-2.3701E2*WT(J)**2
*
*   CONSTANTS FOR DETERMINING VAPOUR PRESSURE FROM THE
*   VAPOUR PRESSURE-CONCENTRATION EQUATION OF BORYTA
       A(J)=.2234E2-.2207*WT(J)+.2464E-2*WT(J)**2
       B(J)=-.5403E4+.9842E2*WT(J)-1.29*WT(J)**2
       C(J)=-.3273E6+.3809E4*WT(J)-.5801E2*WT(J)**2
*
```

```
*  GENERAL VAPOUR PRESSURE EQUATION OF UEMURA AND BORYTA
      LP(NP)=(C(J)/TK(NP)**2)+B(J)/TK(NP)+A(J)
*
*  VAPOUR PRESSURE EQUATION OF PENNINGTON
*     LP(NP)=(C(J)/TER(NP)**2)+B(J)/TER(NP)+A(J)
*
*  CHANGE OF UNITS FOR VAPOUR PRESSURE TO POUNDS PER SQUARE INCH
*
*  FOR UEMURA'S DATA
*     PSI(NP)=(10.**LP(NP))*.0193203
*
*   FOR PENNINGTON'S DATA
*     PSI(NP)=10.**LP(NP)
*
*  FOR BORYTA'S DATA
      PSI(NP)=EXP(LP(NP))*.0193203
*
*  COMPUTATION OF ENTHALPY-CONCENTRATION DATA
      PBAR(NP)=PSI(NP)*.06895
      LPN(NP)=ALOG(PBAR(NP))
      TDEW(NP)=((-2*CA)/(BA+(BA**2-4*CA*(AA-LPN(NP)))
     1**.5))-273.15
      TDEWK(NP)=(TDEW(NP)+273.15)
      TEI(J,NP)=TE(NP)
      HWVAP(NP)=(.1638*TDEW(NP)-30.44969)*PBAR(NP)
     1+(1.88163*TDEW(NP)+2500.87)
      HSWL(NP)=4.19*TDEW(NP)-.0419
      HWVL(NP)=HWVAP(NP)-HSWL(NP)
      VSATG(NP)=-2.6295E-6*TDEW(NP)**2+8.6144E-4*TDEW(NP)
     1-.07968+(4.614E-3*TDEW(NP)+1.260734)/PBAR(NP)
      TCW(NP)=374.11-TDEW(NP)
      TCS(NP)=374.11-TE(NP)
      VSATW(NP)=(3.1975E-3-(3.151548E-4*TCW(NP)**.3333)
     1-1.203374E-6*TCW(NP)+7.48908E-16*TCW(NP)**4.)/
     1(1.+.1342489*TCW(NP)**.3333-3.946263E-3*TCW(NP))
      VSATS(NP)=(3.1975E-3-(3.151548E-4*TCS(NP)**.3333)
     1-1.203374E-6*TCS(NP)+7.48908E-16*TCS(NP)**4.)/
     1(1.+.1342489*TCS(NP)**.3333-3.946263E-3*TCS(NP))
      VSUPG(NP)=-2.6295E-6*TE(NP)**2+8.6144E-4*TE(NP)
     1-.07968+(4.614E-3*TE(NP)+1.260734)/PBAR(NP)
      HSUPV(NP)=(.16381*TE(NP)-30.44969)*PBAR(NP)
     1+(1.88163*TE(NP)+2500.87)
    2 CONTINUE
      IFAIL=0
*
*  G02CAF IS THE SUBROUTINE FROM THE NAG LIBRARY WHICH PERFORMS
*  A SIMPLE LINEAR REGRESION WITH TEMPERATURE OF SOLUTIONS AS
*  DEPENDENT VARIABLE AND DEW POINT TEMPERATURE OF WATER AS
*  INDEPENDENT VARIABLE
*
      CALL G02CAF(17,TDEW,TE,RESULT,IFAIL)
C TEST IFAIL
      IF(IFAIL)60,65,75
   60 WRITE(2,203)IFAIL
  203 FORMAT('ROUTINE FAILS IFAIL=',I2)
   65 CONTINUE
      WRITE(2,8001)RESULT(1)
```

```
      WRITE(2,8002)RESULT(2)
      WRITE(2,8003)RESULT(3)
      WRITE(2,8004)RESULT(4)
      WRITE(2,8005)RESULT(5)
      WRITE(2,8006)RESULT(6)
      WRITE(2,8007)RESULT(7)
      WRITE(2,8008)RESULT(8)
      WRITE(2,8009)RESULT(9)
      WRITE(2,8010)RESULT(10)
      WRITE(2,8011)RESULT(11)
      WRITE(2,8012)RESULT(12)
      WRITE(2,8013)RESULT(13)
      WRITE(2,8014)RESULT(14)
      WRITE(2,8015)RESULT(15)
      WRITE(2,8016)RESULT(16)
      WRITE(2,8017)RESULT(17)
      WRITE(2,8018)RESULT(18)
      WRITE(2,8019)RESULT(19)
      WRITE(2,8020)RESULT(20)
 8001 FORMAT(15X,'MEAN OF DEW PNT.                =',F10.1)
 8002 FORMAT(15X,'MEAN OF SOLTN. TEMP.            =',F10.1)
 8003 FORMAT(15X,'S.D. OF DEW PNT.                =',F12.3)
 8004 FORMAT(15X,'S.D. OF SOLTN. TEMP.            =',F12.3)
 8005 FORMAT(15X,'CORR. COFT.                     =',F14.5)
 8006 FORMAT(15X,'REGR.COEFT. OF (B)              =',F14.5)
 8007 FORMAT(15X,'REGR. CONST.OF (A)              =',F14.5)
 8008 FORMAT(15X,'S.E. OF (B)                     =',F14.5)
 8009 FORMAT(15X,'S.E. OF (A)                     =',F14.5)
 8010 FORMAT(15X,'T OF (B)                        =',F14.5)
 8011 FORMAT(15X,'T OF (A)                        =',F14.5)
 8012 FORMAT(15X,'SUM OF SQS. FOR REGR.           =',F12.3)
 8013 FORMAT(15X,'DEG. OF FRED. FOR REGR.         =',F10.1)
 8014 FORMAT(15X,'MEAN SQ. FOR REGR.              =',F14.5)
 8015 FORMAT(15X,'F-VAL. FOR ANAL. OF VAR.        =',F14.5)
 8016 FORMAT(15X,'SUM OF SQS. OF EEV. ABT. REGR.  =',F14.5)
 8017 FORMAT(15X,'DEG. OF FRED. OF DEV. ABT. REGR.=',F10.1)
 8018 FORMAT(15X,'MEAN SQ. OF DEV. ABT. REGR.     =',F14.5)
 8019 FORMAT(15X,'TOT. SUM. OF SQS.               =',F12.3)
 8020 FORMAT(15X,'TOT. DEGR. OF FRED.             =',F10.1)
      CALL FITER1(FMNERR,SDMNER,17)
      DO 3 NP=1,17
      HSOLVL(NP)=((HWVL(NP)*(VSUPG(NP)-VSATS(NP)))*(TE(NP)+273.15
     1))/((RESULT(6)*TDEWK(NP))*(VSATG(NP)-VSATW(NP)))
      HPARTW(J,NP)=HSUPV(NP)-HSOLVL(NP)
      WRITE(2,204)TE(NP),TDEW(NP),HSOLVL(NP),HPARTW(J,NP)
  204 FORMAT(5X,2F7.1,2F8.1)
    3 CONTINUE
   75 CONTINUE
*
*  FITTING THE ENTHALPY-CONCENTRATION DATA
*
      W1(1)=0
      XOX1(1)=1
      ACP=0.489
      BCP=-1.549E-3
      CCP=1.457E-5
      DO 4 NP=1,17
```

```
      H(1,NP)=0
      HO(J,NP)=((ACP*TE(NP))+(BCP*TE(NP)**2)/2.
     1+(CCP*TE(NP)**3)/3.)*4.1868
      IF(J.EQ.1)GO TO 90
      XOX1(J)=50./WT(J)
      W1(J)=1-XOX1(J)
      J1=J-1
      DELW(J)=W1(J)-W1(J1)
      HAV(J)=(HPARTW(J,NP)+HPARTW(J1,NP))/2.
      HDEL(J)=HAV(J)*DELW(J)
      H(J,NP)=HDEL(J)+H(J1,NP)
   90 CONTINUE
      HWT(J,NP)=(HO(J,NP)-H(J,NP))/XOX1(J)
      WRITE(2,205)TE(NP),HPARTW(J,NP),H(J,NP),HO(J,NP),HWT(J,NP)
  205 FORMAT(4X,F7.1,4F8.1)
    4 CONTINUE
    1 CONTINUE
      NDEW=9
      DO 44 ND=1,NDEW
      TFDEW(ND)=50.+(ND-1)*10.
      PWBAR(ND)=(EXP(AA+BA/(TFDEW(ND)+273.15)+CA/((TFDEW(ND)+273.15
     1)**2)))*750.
      DO 45 J=1,19
      TSL(J,ND)=((-2*C(J))/(B(J)+(B(J)**2-4*C(J)*(A(J)-ALOG(PWBAR(ND))
     1))**.5))-273.15
   45 CONTINUE
   44 CONTINUE
*  FITTING THE ENTHALPY-CONCENTRATION DATA
      CALL FITEQ(17,HWT,TE,1,360,15,4,2,900)
*     CALL FITEQ(NDEW,TSL,TFDEW,1,360,15,3,1,900)
      STOP
      END
*  SUBROUTINE FOR DETERMINING THE MEAN ERROR AND STANDARD DEVIATION
*  OF ERRORS FOR THE ABOVE SOLUTION TEMPERATURE-DEW POINT TEMPERATURE
*  FIT FOR SOME RANGES OF CONCENTRATIONS AND TEMPERATURES
*
      SUBROUTINE FITER1(FMNERR,SDMNER,NKEND)
      COMMON/BLK1/TE(18),TDEW(18)
      COMMON/BLK2/RESULT(400)
      REAL TEFIT(18),TEER(18),SMTEER(18),SDER(18),SMSDER(18)
      DO 876 NK=1,NKEND
      TEFIT(NK)=RESULT(7)+TDEW(NK)*RESULT(6)
      TEER(NK)=((TEFIT(NK)-TE(NK))/TEFIT(NK))*100.
      PRINT*,TE(NK),TEFIT(NK),TEER(NK)
      SMTEER(1)=TEER(1)
      IF(NK.NE.1) SMTEER(NK)=SMTEER(NK-1)+TEER(NK)
  876 CONTINUE
      FMNERR=SMTEER(NKEND)/NKEND
      DO 8765 NJ=1,NKEND
      SDER(NJ)=(TEER(NJ)-FMNERR)**2
      SMSDER(1)=SDER(1)
      IF(NJ.NE.1) SMSDER(NJ)=SMSDER(NJ-1)+SDER(NJ)
 8765 CONTINUE
      SDMNER=(SMSDER(NKEND)/(NKEND-1))**0.5
      PRINT*,FMNERR,SDMNER
      RETURN
      END
```

```
*
*  SUBROUTINE FOR FITTING THE ENTHALPY-CONCENTRATION DATA, USING THE
*  FIT TO GENERATE ENTHALPY-CONCENTRATION DATA AT REQUIRED CONDITIONS
*  AND DETERMINING THE ERRORS BETWEEN THE ORIGINAL DATA AND THE FIT
*
      SUBROUTINE FITEQ(NPLAST,Q,TDUM,IFL,NX1,NA1,K1,L1,NW1)
      COMMON/BLK3/WT(19),W(350),XMIN(18),XMAX(18)
      COMMON/BLK4/M(20),WT1(350),A0(15)
      INTEGER R,T
      REAL Q(19,18),Q1(350),TSB(18),FF(350),TDUM(18),WRK(10),WORK(900)
      MTOT=0
      DO 8 NP=1,NPLAST
      TSB(NP)=TDUM(NP)
*     PRINT*, TSB(NP)
      DO 101 J=1,19
      MTOT=MTOT+1
      Q1(MTOT)=Q(J,NP)
      WT1(MTOT)=WT(J)
      W(MTOT)=1
  101 CONTINUE
      M(NP)=19
      XMIN(NP)=50
      XMAX(NP)=68
*     PRINT*, M(NP),XMIN(NP),XMAX(NP)
    8 CONTINUE
      IFAIL=IFL
      NX=NX1
      NA=NA1
      K=K1
      L=L1
      NW=NW1
      KP1=K+1
*     PRINT*, NX,NA,K,KP1,L,NW,NPLAST,MTOT
*     DO 811 MT=1,MTOT
*     PRINT*, Q1(MT),WT1(MT),W(MT)
* 811 CONTINUE
*
*
*  SUBROUTINE FROM THE NAG LIBRARY FOR FITTING ENTHALPY-CONCENTRATION
*  DATA
*
      CALL E02CAF(M,NPLAST,K,L,WT1,TSB,Q1,W,NX,A0,NA,
     1XMIN,XMAX,TSB,1,TSB,1,WORK,NW,IFAIL)
      IF(IFAIL.EQ.0) GO TO 79
      PRINT*, IFAIL
   79 MI=0
*     WRITE(2,9015)
      DO 199 R=1,NPLAST
      IFAIL=1
      T=MI+1
      MI=MI+M(R)
      YR=TSB(R)
      YMAX=TSB(NPLAST)
      NWORK=10
*
*  SUBROUTINE FROM THE NAG LIBRARY FOR EVALUATING ENTHALPY-CONCENTRATION
*  DATA  FROM THE ABOVE FIT
```

```
*
      CALL E02CBF(T,MI,K,L,WT1,XMIN(R),XMAX(R),YR,TSB(1),
     1YMAX,FF,AO,NA,WRK,NWORK,IFAIL)
      IF(IFAIL.EQ.0) GO TO 1000
*  OUTPUT THE DATA AND FITTED VALUES ON
*  THE LINE Y=Y(R)
 1000 DO 102 I=T,MI
      RESID=FF(I)-Q1(I)
      PRESID=(RESID/FF(I))*100.
      PRINT*,YR,WT1(I),Q1(I),FF(I),RESID,PRESID
  102 CONTINUE
*     WRITE(2,9111)
  199 CONTINUE
*  OUTPUT THE CHEBYSHEV COEFFICIENTS OF
*  THE FIT
*     WRITE(2,9998)
      T=0
      DO 103 JK=1,KP1
      R=T+1
      T=R+L
      WRITE(2,9988)(AO(I),I=R,T)
  103 CONTINUE
*9015 FORMAT(6X,' Y(R)              WT                Q1
*    1 FITT          RESIDUAL       %RESIDUAL')
*9998 FORMAT(2X,'CHEBYSHEV COEFFICIENTS OF
*    1 THE FIT')
 9988 FORMAT(5X,3E15.4)
*9111 FORMAT(1X)
      RETURN
      END
```

A.I.2 ANALYSIS OF THE H_2O/LiBr SYSTEM

```
*  THIS PROGRAMME WAS DESIGNED TO CALCULATE THE MAXIMUM OBTAINABLE COP
*  FOR A RANGE OF CONCENTRATION OF AQUEOUS SALT SOLUTIONS AND A RANGE
*  OF TEMPERATURE APPROACH BETWEEN THE HOT SOLUTION LEAVING THE
*  ECONOMISER FOR THE ABSOBER VIA THE EXPANSION VALVE, AND THE WARM
*  SOLUTION ENTERING THE ECONOMISER FROM THE ABSOBER.
*
*  THE NUMBERING OF THE FLOW OF STREAMS OF FLUIDS IN THE ABSORPTION
*  HEAT PUMP SYSTEM IS AS FOLLOWS:
*
*  (1)  WATER VAPOUR FROM THE GENERATOR INTO THE CONDENSER
*  (2)  CONDENSED WATER LEAVING THE CONDENSER INTO THE EVAPORATOR VIA
*       THE EXPANSION VALVE
*  (3)  STREAM (2) AFTER THE EXPANSION VALVE
*  (4)  WATER VAPOUR FROM THE EVAPORATOR INTO THE ABSORBER
*  (5)  SOLUTION LEAVING THE GENERATOR FOR THE ECONOMISER
*  (6)  SOLUTION LEAVING THE ECONOMISER FOR THE ABSOBER VIA THE
*       EXPANSION VALVE
*  (7)  STREAM (6) AFTER THE EXPANSION VALVE
*  (8)   LEAVING THE ABSOBER INTO THE ECONOMISER VIA THE SOLUTION
*       SOLUTION PUMP
*  (9)  STREAM (8) AFTER THE SOLUTION PUMP
* (10)  SOLUTION FROM THE ECONOMISER INTO THE GENERATOR
*
*                    NOMENCLATURE
*
*
*
*  COP     COEFFICIENT OF PERFORMANCE  (DIMENSIONLESS)
*  CR      COMPRESSION RATIO  (DIMENSIONLESS)
*  FM1     RATE OF FLOW OF WATER IN THE CONDENSER AND EVAPORATOR
*          (DIMENSIONLESS)
*  HX      ENTHALPY PER UNIT WEIGHT OF FLUID AT FLOW STREAM POSITION
*  (X)     (KJ PER KG)
*  M101ST  LOWEST CIRCULATION RATIO (RATE OF FLOW OF WATER-RICH
*          AQUEOUS SOLUTION OF LITHIUM BROMIDE TO THE RATE OF FLOW OF WATER
*          IN THE CONDENSER AND EVAPORATOR)   (DIMENSIONLESS)
*  MX      CIRCULATION RATIO AT FLOW POSITION (X)   (DIMENSIONLESS)
*  PCO     CONDENSING PRESSURE OF WATER IN THE CONDENSER  (BAR)
*  PEV     EVAPORATING PRESSURE OF WATER IN THE EVAPORATOR   (BAR)
*  QAB     HEAT RATE FROM THE ABSORBER    (KW)
*  QCO     HEAT RATE FROM THE CONDENSER   (KW)
*  QEV     HEAT RATE INTO THE EVAPORATOR  (KW)
*  QGE     HEAT RATE INTO THE GENERATOR   (KW)
*  TA      TEMPERATURE APPROACH AT ABSORBER END OF THE ECONOMISER
*          (DEG  C)
*  TAB     TEMPERATURE OF SOLUTION IN THE ABSORBER  (DEG  C)
*  TBMTV   ABSORBER TEMPERATURE LIFT  (DEG  C)
*  TCMTV   CONDENSER TEMPERATURE LIFT  (DEG  C)
*  TCO     CONDENSING TEMPERATURE OF WATER IN THE CONDENSER  (DEG  C)
*  TEV     EVAPORATING TEMPERATURE OF WATER IN THE EVAPORATOR  (DEG  C)
*  TEV1ST  LOWEST EVAPORATING TEMPERATURE OF WATER  (DEG  C)
*  TGE     TEMPERATURE OF SOLUTION IN THE GENERATOR  (DEG  C)
*  TGE1ST  HIGHEST TEMPERATURE IN THE GENERATOR  (DEG  C)
*  TGMTB   GENERATOR TEMPERATURE LIFT  (DEG  C)
*  TX      TEMPERATURE OF FLUID AT FLOW STREAM POSITION (X)  (DEG  C)
*  XB      PERCENT WEIGHT OF LITHIUM BROMIDE IN WATER-RICH AQUEOUS
*          SOLUTION  OF LITHIUM BROMIDE  (PERCENT)
*  XB1ST   LOWEST PERCENT WEIGHT OF LITHIUM BROMIDE IN WATER-RICH
```

```
*          AQUEOUS SOLUTION OF LITHIUM BROMIDE  (PERCENT)
*  XWAB    WEIGHT FRACTION OF WATER IN WATER-RICH AQUEOUS SOLUTION OF
*          LITHIUM BROMIDE   (DIMENSIONLESS)
*  XWGE    WEIGHT FRACTION OF WATER IN WATER-RICH AQUEOUS SOLUTION OF
*          LITHIUM BROMIDE  (DIMENSIONLESS)
*
*                          THE PROGRAMME
*
*                      INITIALISATION
*
      DIMENSION XWAB(10,10),TAB(10,10),TB(10),PEV(10),
     *T7(10,10),H8(10,10),TEV(10),TGE5(10),TGE7(10),H7(10),
     *TGE(10,10,10),XGE(10),XB(10),PCO(10),TBMTV(10,10),
     *H4(10,10),H10(10),M10(10),XWGE(10),H5(10),TCO(10),
     *CR(10),XBMXG(10),TCMTV(10),H1(10),H2(10),COP(10)
      REAL TGE1ST,M101ST,XB1ST,X,P,TEV1ST,T,XG,TG5,TG7,FM10,
     *TGMTB
*
      COMMON/BLK1/F(10)
      COMMON/BLK2/P
      COMMON/BLK3/T
      COMMON/BLK4/XW
*
      FM1=1.2
      TA=10
      TGE1ST=200
      M101ST=8
      XB1ST=51.
      TEV1ST=80
      IAL=5
      DO 1 I=1,IAL
      TEV(I)=TEV1ST+(I-1)*10
      T=TEV(I)
      CALL PRESW
      PEV(I)=P
*
      JAL=8
      DO 2 J=1,JAL
      X=XB1ST+(J-1)
      P=PEV(I)
      CALL SOLTEP(X)
      TAB(I,J)=T
      XB(J)=X
      TBMTV(I,J)=TAB(I,J)-TEV(I)
      H4(I,J)=(0.16381*TEV(I)-30.44969)*PEV(I)+1.88163*
     *TEV(I)+2500.87
      T=TAB(I,J)
      XWAB(I,J)=1-(XB(J)/100.)
      XW=XWAB(I,J)
      IF(XW.GT.0.5.OR.XW.LT.0.32) GO TO 2
      T7(I,J)=TAB(I,J)+TA
      TB(J)=TAB(I,J)
      CALL SOLVEQ(J,XB,TB(J),4,2,15)
      H8(I,J)=F(J)
*
      KAL=6
      DO 3 KO=1,KAL
```

```
      TGE(I,J,KO)=TGE1ST-(KO-1)*10
      TGMTB=TGE(I,J,KO)-TAB(I,J)
      IF(TGMTB.LT.20)GO TO 3
      WRITE(2,100) TGE(I,J,KO),TAB(I,J),XWAB(I,J)
*
      MAL=6
      DO 4 MN=1,MAL
      M10(MN)=M101ST+(MN-1)*2
      XWGE(MN)=(M10(MN)*XWAB(I,J)-1)/(M10(MN)-1)
      IF(XWGE(MN).GT.0.5.OR.XWGE(MN).LT.0.32) GO TO 3
      XGE(MN)=(1-XWGE(MN))*100
      XG=XGE(MN)
      TGE7(MN)=T7(I,J)
      TGE5(MN)=TGE(I,J,KO)
      TG7=TGE7(MN)
      TG5=TGE5(MN)
      CALL SOLVEQ(MN,XGE,TGE7(MN),4,2,15)
       H7(MN)=F(MN)
      CALL SOLVEQ(MN,XGE,TGE5(MN),4,2,15)
      H5(MN)=F(MN)
      H10(MN)=H8(I,J)+(H5(MN)-H7(MN))*(1-(1/M10(MN)))
      XG=XGE(MN)
      CALL RUTPRS(XG,TG5)
      PCO(MN)=P
      CALL RUTEMP
       TCO(MN)=T
       TCMTV(MN)=TCO(MN)-TEV(I)
       IF(TCMTV(MN).LE.0.0) GO TO 4
       CR(MN)=PCO(MN)/PEV(I)
       XBMXG(MN)=XWAB(I,J)-XWGE(MN)
       H1(MN)=(0.16381*TGE5(MN)-30.44969)*PCO(MN)+(1.88163*TGE5
     *(MN)+2500.87)
       H2(MN)=4.191*TCO(MN)-0.0419
*      QEV=((H4(I,J)-H2(MN))*FM1)/3600.
*      QCO=((H1(MN)-H2(MN))*FM1)/3600.
*      QAB=((H4(I,J)+M10(MN)*(H7(MN)-H8(I,J))-H7(MN))*FM1)/3600.
*      QGE=((M10(MN)*(H5(MN)-H10(MN))+H1(MN)-H5(MN))*FM1)/3600.
*      FM10=M10(MN)*FM1
       COP(MN)=(H4(I,J)-H7(MN)+M10(MN)*(H7(MN)-H8(I,J))+(H1(MN)-
     *H2(MN)))/(M10(MN)*(H5(MN)-H10(MN))+H1(MN)-H5(MN))
*
       IF(COP(MN).GT.2) GO TO 4
       WRITE(2,101)M10(MN),XWGE(MN),XBMXG(MN),PCO(MN),PEV(I),
     *CR(MN),TCO(MN),TEV(I),TCMTV(MN),TBMTV(I,J),COP(MN)
*
*      WRITE(2,103)FM10,QEV,QCO,QAB,QGE
*
    4 CONTINUE
    3 CONTINUE
    2 CONTINUE
    1 CONTINUE
*
  100 FORMAT(35X,2F7.1,F8.4//)
  101 FORMAT(2X,I4,2F9.4,F7.2,2F8.3,4F9.1,F9.3/)
* 103 FORMAT(4X,5F11.2/)
*
*
```

```
*  CASES FOR ABSORBER TEMPERATURE EQUALS CONDENSER
*  TEMPERATURE
*
      DO 5 IQ=1,IAL
      DO 6 JQ=1,JAL
      T=TAB(IQ,JQ)
      CALL PRESW
      PCO(JQ)=P
      XW=XWAB(IQ,JQ)
      IF(XW.GT.0.5.OR.XW.LT.0.32)GO TO 6
      DO 7 KQ=1,KAL
      WRITE(2,100) TGE(IQ,JQ,KQ),TAB(IQ,JQ),XWAB(IQ,JQ)
      T=TGE(IQ,JQ,KQ)
      TGMTB=TGE(IQ,JQ,KQ)-TAB(IQ,JQ)
      IF(TGMTB.LE.15)GO TO 7
      P=PCO(JQ)
      CALL XCONC
      XWGE(KQ)=XW
      IF(XWGE(KQ).GT.0.5.OR.XWGE(KQ).LT.0.32)GO TO 7
      IF(XWGE(KQ).GE.XWAB(IQ,JQ))GO TO 7
      XGE(KQ)=(1-XWGE(KQ))*100
      CALL SOLVEQ(KQ,XGE,TGE7(KQ),4,2,15)
      H7(KQ)=F(KQ)
      FM10=(1-XWGE(KQ))/(XWAB(IQ,JQ)-XWGE(KQ))
      CALL SOLVEQ(KQ,XGE,TGE5(KQ),4,2,15)
      H5(KQ)=F(KQ)
      H10(KQ)=H8(IQ,JQ)+(H5(KQ)-H7(KQ))*(1-(1/FM10))
      TCMTV(KQ)=TAB(IQ,JQ)-TEV(IQ)
      IF(TCMTV(KQ).LE.0.0)GO TO 7
      CR(KQ)=PCO(JQ)/PEV(IQ)
      XBMXG(KQ)=XWAB(IQ,JQ)-XWGE(KQ)
      H1(KQ)=(0.16381*TGE5(KQ)-30.44969)*PCO(KQ)+(1.88163*TGE5(KQ)
     *+2500.87)
      H2(KQ)=4.191*TCO(KQ)-0.0419
      COP(KQ)=(H4(IQ,JQ)-H7(KQ)+FM10*(H7(KQ)-H8(IQ,JQ))+(H1(KQ)-
     *H2(KQ)))/(FM10*(H5(KQ)-H10(KQ))+H1(KQ)-H5(KQ))
*
*  PRINT TABLE
      IF(COP(KQ).GT.2)GO TO 7
      WRITE(2,102)FM10,XWGE(KQ),XBMXG(KQ),PCO(JQ),PEV(IQ),
     *CR(KQ),TEV(IQ),TCMTV(KQ),COP(KQ)
*
    7 CONTINUE
    6 CONTINUE
    5 CONTINUE
  102 FORMAT(12X,F5.2,2F9.4,F7.2,2F8.3,2F9.1,F9.3/)
*
      STOP
      END
*  SUBROUTINE FOR DETERMINING THE FRACTIONAL CONCENTRATION
*  OF LIBR IN H2O/LIBR SOLUTIONS
*
*
* SUBROUTINE FOR DETERMINING THE TEMPERRATURE OF H2O/LIBR
*  SOLUTIONS
*
*  INPUT: X (PER CENT)
```

```
*       :  P  (BAR)
*
      SUBROUTINE SOLTEP(X)
      REAL A,B,C,PX
      COMMON/BLK2/PX
      COMMON/BLK3/T
      A=22.34-.2207*X+(2.464E-3*X**2)
      B=-5.403E3+98.42*X-(1.29*X**2)
      C=-3.273E5+3.809E3*X-(58.01*X**2)
      T=((B-((-B)**2-4*(ALOG(PX*750)-A)*(-C))**.5)/(2*(ALOG(PX*750)-A
     *)))-273.15
      RETURN
      END
*
*  SUBROUTINE FOR DETERMINING WEIGHT FRACTION OF H2O IN H2O/LIBR
*  SOLUTIONS
*  INPUT:  P  (BAR)
*          T  (DEGREE CENTIGRADE)
*
      SUBROUTINE XCONC
      COMMON/BLK2/PR
      COMMON/BLK3/T
      COMMON/BLK4/XW
      REAL AA,BB,CC
*
      CC=22.34-ALOG(PR*750)-5.403E3/(T+273.15)-3.273E5/(T+273.15)**2
      BB=-2.207E-1+98.42/(T+273.15)+3.809E3/(T+273.15)**2
      AA=2.464E-3-1.290/(T+273.15)-58.01/(T+273.15)**2
      XW=1-(((-BB-(BB**2-4*AA*CC)**0.5)/(2*AA))/100)
      RETURN
      END
*
*  SUBROUTINE FOR DETERMINING PRESSURE OF CONDENSED WATER
*
      SUBROUTINE PRESW
      COMMON/BLK2/PR
      COMMON/BLK3/T
      REAL PR,A,B,C
      A=11.5923
      B=-3.6699E3
      C=-2.4309E5
      PR=EXP(A+B/(T+273.15)+C/(T+273.15)**2)
      RETURN
      END
*
*
*  SUBROUTINE FOR DETERMINING ENTHALPY PER UNIT MASS FOR AQUEOUS
*  SOLUTIONS OF SALT
      SUBROUTINE SOLVEQ(MDUM,XDUM,TDUM,K1,L1,NA1)
      COMMON/BLK1/F(10)
*
      REAL XDUM(*),TDUM(*),WK(10),A0(15)
      DATA A0(1),A0(2),A0(3)/1173,340.5,28.98/
      DATA A0(4),A0(5),A0(6)/16.88,-25.03,-2.248/
      DATA A0(7),A0(8),A0(9)/22.87,-1.673,.2237/
      DATA A0(10),A0(11),A0(12)/.9226,-.2044,.9655E-2/
      DATA A0(13),A0(14),A0(15)/-.4120E-1,-.1304E-2,-.2132E-2/
```

```
*
      NA=NA1
      K=K1
      L=L1
      IFAIL=1
      XMIN=50
      XMAX=68
      YMIN=60
      YMAX=220
      NWK=10
*
*  SUBROUTINE FROM THE NAG LIBRARY
*
      CALL E02CBF(MDUM,MDUM,K,L,XDUM,XMIN,XMAX,TDUM,YMIN,YMAX,
     *F,A0,NA,WK,NWK,IFAIL)
*
      RETURN
      END
*
*
*  SUBROUTINE FOR DETERMINING THE PRESSURE OF AQUEOUS SOLUTIONS
*  OF SALT
*
      SUBROUTINE RUTPRS(X,TE)
*
      COMMON/BLK2/P
      REAL X,TE
*
      P=(EXP((22.34-(2.207E-1*X)+(2.464E-3*X**2))
     1+(((-5.403E3)+98.42*X-(1.290*X**2))/(TE+273.15))
     1+(((-3.273E5)+3.809E3*X-(58.01*X**2))/((TE+273.15)**2))))/750.
*
      RETURN
      END
*
*
*  SUBROUTINE FOR DETERMINING THE TEMPERATURE OF WATER GIVEN THE
*  PRESSURE
*
      SUBROUTINE RUTEMP
      COMMON/BLK2/PR
      COMMON/BLK3/T
      REAL PR,A,B,C
*
      C=-2.4309E5
      B=-3.6699E3
      A=11.5923
      T=((-2*C)/(B+(B**2-4*C*(A-
     *ALOG(PR)))**.5))-273.15
*
      RETURN
      END
```

A.I.3 VOLUMETRIC FLOW RATE INTO COMPRESSORS

```
*  THIS PROGRAMME EVALUATES THE VOLUME RATE OF GAS INTO A COMPRESSOR
*  AT A GIVEN CONDENSING TEMPERATURE AND GROSS TEMPERATURE LIFT
*
*                    NOMENCLATURE
*
*  TCO       CONDENSING TEMPERATURE              DEG. CENT.
*  PCO       CONDENSING PRESSURE                 BAR
*  FMJM3V    ENTHALPY PER UNIT VOLUME            MJ PER CUB. M.
*  FM3VIN    FLOW RATE OF VAPOUR INTO
*            THE COMPRESSOR                      CUB. M. PER SEC.
*
*                    THE PROGRAM
*
      CHECK EVERYTHING
      DIMENSION TCO(25,100),PCO(25,100),FMJM3V(25,100),TCOI(25,100),
     *PCOI(25,100),TCMTV(100,20),FM3VIN(100,20)
      CHARACTER*88 BUF
      INTEGER NDAL,NPTCO,M,N,ND,NP,NQ
      DO  100 J=1,21
      READ*, NDAL,NPTCO
      DO 200 I=1,NDAL
      READ*,TCO(J,I),PCO(J,I),FMJM3V(J,I)
  200 CONTINUE
      ND=NDAL-(NPTCO-1)
      DO 300 K=1,ND
      NP=NPTCO+(K-1)
      TCOI(J,K)=TCO(J,NP)
      PCOI(J,K)=PCO(J,NP)
      DO 400 L=1,14
      TCMTV(K,L)=10+(L-1)*5
      N=2+(L-1)
      NQ=NP-N
      IF(NQ.LE.0)GO TO 101
      FM3VIN(K,L)=1/FMJM3V(J,NQ)
      GO TO 400
  101 FM3VIN(K,L)=0
  400 CONTINUE
  300 CONTINUE
      M=ND/10
      DO 500 JT=1,M
      IF(JT.EQ.1) THEN
      IBEG=1
      IEND=11
      ELSE
      IBEG=IEND
      IEND=IEND+10
      CONTINUE
      ENDIF
      WRITE(2,501)(TCOI(J,K),K=IBEG,IEND)
  501 FORMAT(1X,1H1//////10X,11F8.1/)
      WRITE(2,502)(PCOI(J,K),K=IBEG,IEND)
  502 FORMAT(12X,11F8.3)
      BUF(1:88)=' '
      DO 10 L=1,14
      K=1
      JR=8
      DO 11 N=IBEG,IEND
```

```
      IF(FM3VIN(N,L).EQ.0) THEN
      BUF(K:JR)='     -    '
                     ELSE
      WRITE(BUF(K:JR),30)FM3VIN(N,L)
   30 FORMAT(F8.4)
                     ENDIF
      K=K+8
      JR=JR+8
   11 CONTINUE
      WRITE(2,504)TCHTV(1,L),BUF
   10 CONTINUE
  504 FORMAT(2X/1X,F5.1,6X,A)
  500 CONTINUE
  100 CONTINUE
      STOP
      END
```

T_{CO} °C / P_{CO} bar / $(T_{CO}-T_{EV})$ °C	100.0	105.0	110.0	115.0	120.0	125.0	130.0	135.0	140.0	145.0	150.0
	1.013	1.208	1.433	1.690	1.985	2.321	2.701	3.130	3.614	4.155	4.760
10.0	1.0347	0.8732	0.7413	0.6327	0.5426	0.4675	0.4051	0.3521	0.3075	0.2696	0.2371
15.0	1.2323	1.0347	0.8732	0.7413	0.6327	0.5426	0.4675	0.4051	0.3521	0.3075	0.2696
20.0	1.4767	1.2323	1.0347	0.8732	0.7413	0.6327	0.5426	0.4675	0.4051	0.3521	0.3075
25.0	1.7804	1.4767	1.2323	1.0347	0.8732	0.7413	0.6327	0.5426	0.4675	0.4051	0.3521
30.0	2.1626	1.7804	1.4767	1.2323	1.0347	0.8732	0.7413	0.6327	0.5426	0.4675	0.4051
35.0	2.6438	2.1626	1.7804	1.4767	1.2323	1.0347	0.8732	0.7413	0.6327	0.5426	0.4675
40.0	3.2572	2.6438	2.1626	1.7804	1.4767	1.2323	1.0347	0.8732	0.7413	0.6327	0.5426
45.0	4.0415	3.2572	2.6438	2.1626	1.7804	1.4767	1.2323	1.0347	0.8732	0.7413	0.6327
50.0	5.0523	4.0415	3.2572	2.6438	2.1626	1.7804	1.4767	1.2323	1.0347	0.8732	0.7413
55.0	6.3845	5.0523	4.0415	3.2572	2.6438	2.1626	1.7804	1.4767	1.2323	1.0347	0.8732
60.0	8.1255	6.3845	5.0523	4.0415	3.2572	2.6438	2.1626	1.7804	1.4767	1.2323	1.0347
65.0	10.4384	8.1255	6.3845	5.0523	4.0415	3.2572	2.6438	2.1626	1.7804	1.4767	1.2323
70.0	13.5501	10.4384	8.1255	6.3845	5.0523	4.0415	3.2572	2.6438	2.1626	1.7804	1.4767
75.0	17.7809	13.5501	10.4384	8.1255	6.3845	5.0523	4.0415	3.2572	2.6438	2.1626	1.7804

TABLE A.I.1 THEORETICAL VOLUME FLOWRATE AT T_{EV} FOR A HEAT INTAKE RATE OF 1 MW FOR A RANGE OF LIFTS AND CONDENSING TEMPERATURES FOR R718

T_{CO} °C / P_{CO} bar / $(T_{CO}-T_{EV})$ °C	150.0	155.0	160.0	165.0	170.0	175.0	180.0	185.0	190.0	195.0	200.0
	4.760	5.433	6.180	7.008	7.920	8.925	10.027	11.234	12.553	13.989	15.551
10.0	0.2371	0.2094	0.1857	0.1651	0.1474	0.1319	0.1183	0.1066	0.0962	0.0871	0.0790
15.0	0.2696	0.2371	0.2094	0.1857	0.1651	0.1474	0.1319	0.1183	0.1066	0.0962	0.0871
20.0	0.3075	0.2696	0.2371	0.2094	0.1857	0.1651	0.1474	0.1319	0.1183	0.1066	0.0962
25.0	0.3521	0.3075	0.2696	0.2371	0.2094	0.1857	0.1651	0.1474	0.1319	0.1183	0.1066
30.0	0.4051	0.3521	0.3075	0.2696	0.2371	0.2094	0.1857	0.1651	0.1474	0.1319	0.1183
35.0	0.4675	0.4051	0.3521	0.3075	0.2696	0.2371	0.2094	0.1857	0.1651	0.1474	0.1319
40.0	0.5426	0.4675	0.4051	0.3521	0.3075	0.2696	0.2371	0.2094	0.1857	0.1651	0.1474
45.0	0.6327	0.5426	0.4675	0.4051	0.3521	0.3075	0.2696	0.2371	0.2094	0.1857	0.1651
50.0	0.7413	0.6327	0.5426	0.4675	0.4051	0.3521	0.3075	0.2696	0.2371	0.2094	0.1857
55.0	0.8732	0.7413	0.6327	0.5426	0.4675	0.4051	0.3521	0.3075	0.2696	0.2371	0.2094
60.0	1.0347	0.8732	0.7413	0.6327	0.5426	0.4675	0.4051	0.3521	0.3075	0.2696	0.2371
65.0	1.2323	1.0347	0.8732	0.7413	0.6327	0.5426	0.4675	0.4051	0.3521	0.3075	0.2696
70.0	1.4767	1.2323	1.0347	0.8732	0.7413	0.6327	0.5426	0.4675	0.4051	0.3521	0.3075
75.0	1.7804	1.4767	1.2323	1.0347	0.8732	0.7413	0.6327	0.5426	0.4675	0.4051	0.3521

TABLE A.I.1 (continued) THEORETICAL VOLUME FLOWRATE AT T_{EV} FOR A HEAT INTAKE RATE OF 1 MW FOR A RANGE OF LIFTS AND CONDENSING TEMPERATURES FOR R718

T_{CO} °C / P_{CO} bar / $(T_{CO}-T_{EV})$ °C	200.0	205.0	210.0	215.0	220.0	225.0	230.0	235.0	240.0	245.0	250.0
	15.551	17.245	19.080	21.062	23.201	25.504	27.979	30.635	33.480	36.524	39.776
10.0	0.0790	0.0775	0.0655	0.0599	0.0549	0.0504	0.0463	0.0427	0.0394	0.0365	0.0338
15.0	0.0871	0.0790	0.0775	0.0655	0.0599	0.0549	0.0504	0.0463	0.0427	0.0394	0.0365
20.0	0.0962	0.0871	0.0790	0.0775	0.0655	0.0599	0.0549	0.0504	0.0463	0.0427	0.0394
25.0	0.1066	0.0962	0.0871	0.0790	0.0775	0.0655	0.0599	0.0549	0.0504	0.0463	0.0427
30.0	0.1183	0.1066	0.0962	0.0871	0.0790	0.0775	0.0655	0.0599	0.0549	0.0504	0.0463
35.0	0.1319	0.1183	0.1066	0.0962	0.0871	0.0790	0.0775	0.0655	0.0599	0.0549	0.0504
40.0	0.1474	0.1319	0.1183	0.1066	0.0962	0.0871	0.0790	0.0775	0.0655	0.0599	0.0549
45.0	0.1651	0.1474	0.1319	0.1183	0.1066	0.0962	0.0871	0.0790	0.0775	0.0655	0.0599
50.0	0.1857	0.1651	0.1474	0.1319	0.1183	0.1066	0.0962	0.0871	0.0790	0.0775	0.0655
55.0	0.2094	0.1857	0.1651	0.1474	0.1319	0.1183	0.1066	0.0962	0.0871	0.0790	0.0775
60.0	0.2371	0.2094	0.1857	0.1651	0.1474	0.1319	0.1183	0.1066	0.0962	0.0871	0.0790
65.0	0.2696	0.2371	0.2094	0.1857	0.1651	0.1474	0.1319	0.1183	0.1066	0.0962	0.0871
70.0	0.3075	0.2696	0.2371	0.2094	0.1857	0.1651	0.1474	0.1319	0.1183	0.1066	0.0962
75.0	0.3521	0.3075	0.2696	0.2371	0.2094	0.1857	0.1651	0.1474	0.1319	0.1183	0.1066

TABLE A.I.1 (continued) THEORETICAL VOLUME FLOWRATE AT T_{EV} FOR A HEAT INTAKE RATE OF 1 MW FOR A RANGE OF LIFTS AND CONDENSING TEMPERATURES FOR R718

T_{CO} °C / P_{CO} bar / $(T_{CO}-T_{EV})$ °C	250.0	255.0	260.0	265.0	270.0	275.0	280.0	285.0	290.0	295.0	300.0
	39.776	43.250	46.940	50.870	55.050	59.490	64.190	69.180	74.450	80.020	85.920
10.0	0.0338	0.0314	0.0297	0.0272	0.0254	0.0237	0.0222	0.0208	0.0195	0.0184	0.0173
15.0	0.0365	0.0338	0.0314	0.0297	0.0272	0.0254	0.0237	0.0222	0.0208	0.0195	0.0184
20.0	0.0394	0.0365	0.0338	0.0314	0.0297	0.0272	0.0254	0.0237	0.0222	0.0208	0.0195
25.0	0.0427	0.0394	0.0365	0.0338	0.0314	0.0297	0.0272	0.0254	0.0237	0.0222	0.0208
30.0	0.0463	0.0427	0.0394	0.0365	0.0338	0.0314	0.0297	0.0272	0.0254	0.0237	0.0222
35.0	0.0504	0.0463	0.0427	0.0394	0.0365	0.0338	0.0314	0.0297	0.0272	0.0254	0.0237
40.0	0.0549	0.0504	0.0463	0.0427	0.0394	0.0365	0.0338	0.0314	0.0297	0.0272	0.0254
45.0	0.0599	0.0549	0.0504	0.0463	0.0427	0.0394	0.0365	0.0338	0.0314	0.0297	0.0272
50.0	0.0655	0.0599	0.0549	0.0504	0.0463	0.0427	0.0394	0.0365	0.0338	0.0314	0.0297
55.0	0.0775	0.0655	0.0599	0.0549	0.0504	0.0463	0.0427	0.0394	0.0365	0.0338	0.0314
60.0	0.0790	0.0775	0.0655	0.0599	0.0549	0.0504	0.0463	0.0427	0.0394	0.0365	0.0338
65.0	0.0871	0.0790	0.0775	0.0655	0.0599	0.0549	0.0504	0.0463	0.0427	0.0394	0.0365
70.0	0.0962	0.0871	0.0790	0.0775	0.0655	0.0599	0.0549	0.0504	0.0463	0.0427	0.0394
75.0	0.1066	0.0962	0.0871	0.0790	0.0775	0.0655	0.0599	0.0549	0.0504	0.0463	0.0427

TABLE A.I.1 (continued) THEORETICAL VOLUME FLOWRATE AT T_{EV} FOR A HEAT INTAKE RATE OF 1 MW FOR A RANGE OF LIFTS AND CONDENSING TEMPERATURES FOR R718

T_{CO} °C / P_{CO} bar / $(T_{CO}-T_{EV})$ °C	300.0	305.0	310.0	315.0	320.0	325.0	330.0	335.0	340.0	345.0	350.0
	85.920	92.140	98.700	105.610	112.900	120.570	128.650	137.140	146.080	155.480	165.370
10.0	0.0173	0.0163	0.0154	0.0146	0.0138	0.0131	0.0125	0.0119	0.0114	0.0109	0.0105
15.0	0.0184	0.0173	0.0163	0.0154	0.0146	0.0138	0.0131	0.0125	0.0119	0.0114	0.0109
20.0	0.0195	0.0184	0.0173	0.0163	0.0154	0.0146	0.0138	0.0131	0.0125	0.0119	0.0114
25.0	0.0208	0.0195	0.0184	0.0173	0.0163	0.0154	0.0146	0.0138	0.0131	0.0125	0.0119
30.0	0.0222	0.0208	0.0195	0.0184	0.0173	0.0163	0.0154	0.0146	0.0138	0.0131	0.0125
35.0	0.0237	0.0222	0.0208	0.0195	0.0184	0.0173	0.0163	0.0154	0.0146	0.0138	0.0131
40.0	0.0254	0.0237	0.0222	0.0208	0.0195	0.0184	0.0173	0.0163	0.0154	0.0146	0.0138
45.0	0.0272	0.0254	0.0237	0.0222	0.0208	0.0195	0.0184	0.0173	0.0163	0.0154	0.0146
50.0	0.0297	0.0272	0.0254	0.0237	0.0222	0.0208	0.0195	0.0184	0.0173	0.0163	0.0154
55.0	0.0314	0.0297	0.0272	0.0254	0.0237	0.0222	0.0208	0.0195	0.0184	0.0173	0.0163
60.0	0.0338	0.0314	0.0297	0.0272	0.0254	0.0237	0.0222	0.0208	0.0195	0.0184	0.0173
65.0	0.0365	0.0338	0.0314	0.0297	0.0272	0.0254	0.0237	0.0222	0.0208	0.0195	0.0184
70.0	0.0394	0.0365	0.0338	0.0314	0.0297	0.0272	0.0254	0.0237	0.0222	0.0208	0.0195
75.0	0.0427	0.0394	0.0365	0.0338	0.0314	0.0297	0.0272	0.0254	0.0237	0.0222	0.0208

TABLE A.I.1 (continued) THEORETICAL VOLUME FLOWRATE AT T_{EV} FOR A HEAT INTAKE RATE OF 1 MW FOR A RANGE OF LIFTS AND CONDENSING TEMPERATURES FOR R718

T_{CO} °C / P_{CO} bar / $(T_{CO}-T_{EV})$ °C	50.0	55.0	60.0	65.0	70.0	75.0	80.0	85.0	90.0	95.0	100.0
	1.113	1.305	1.520	1.763	2.035	2.337	2.673	3.044	3.453	3.902	4.393
10.0	1.1623	1.0007	0.8666	0.7544	0.6603	0.5808	0.5133	0.4557	0.4063	0.3638	0.3271
15.0	1.3581	1.1623	1.0007	0.8666	0.7544	0.6603	0.5808	0.5133	0.4557	0.4063	0.3638
20.0	1.5969	1.3581	1.1623	1.0007	0.8666	0.7544	0.6603	0.5808	0.5133	0.4557	0.4063
25.0	1.8904	1.5969	1.3581	1.1623	1.0007	0.8666	0.7544	0.6603	0.5808	0.5133	0.4557
30.0	2.2533	1.8904	1.5969	1.3581	1.1623	1.0007	0.8666	0.7544	0.6603	0.5808	0.5133
35.0	2.7049	2.2533	1.8904	1.5969	1.3581	1.1623	1.0007	0.8666	0.7544	0.6603	0.5808
40.0	3.2733	2.7049	2.2533	1.8904	1.5969	1.3581	1.1623	1.0007	0.8666	0.7544	0.6603
45.0	3.9936	3.2733	2.7049	2.2533	1.8904	1.5969	1.3581	1.1623	1.0007	0.8666	0.7544
50.0	4.9140	3.9936	3.2733	2.7049	2.2533	1.8904	1.5969	1.3581	1.1623	1.0007	0.8666
55.0	-	4.9140	3.9936	3.2733	2.7049	2.2533	1.8904	1.5969	1.3581	1.1623	1.0007
60.0	-	-	4.9140	3.9936	3.2733	2.7049	2.2533	1.8904	1.5969	1.3581	1.1623
65.0	-	-	-	4.9140	3.9936	3.2733	2.7049	2.2533	1.8904	1.5969	1.3581
70.0	-	-	-	-	4.9140	3.9936	3.2733	2.7049	2.2533	1.8904	1.5969
75.0	-	-	-	-	-	4.9140	3.9936	3.2733	2.7049	2.2533	1.8904

TABLE A.I.2 THEORETICAL VOLUME FLOWRATE AT T_{EV} FOR A HEAT INTAKE RATE OF 1 MW FOR A RANGE OF LIFTS AND CONDENSING TEMPERATURES FOR R114B2

T_{CO} °C / $(T_{CO}-T_{EV})$ °C — P_{CO} bar	100.0	105.0	110.0	115.0	120.0	125.0	130.0	135.0	140.0	145.0	150.0
	4.393	4.928	5.510	6.141	6.824	7.560	8.353	9.204	10.117	11.094	12.138
10.0	0.3271	0.2958	0.2673	0.2430	0.2216	0.2028	0.1861	0.1713	0.1582	0.1465	0.1360
15.0	0.3638	0.3271	0.2958	0.2673	0.2430	0.2216	0.2028	0.1861	0.1713	0.1582	0.1465
20.0	0.4063	0.3638	0.3271	0.2958	0.2673	0.2430	0.2216	0.2028	0.1861	0.1713	0.1582
25.0	0.4557	0.4063	0.3638	0.3271	0.2958	0.2673	0.2430	0.2216	0.2028	0.1861	0.1713
30.0	0.5133	0.4557	0.4063	0.3638	0.3271	0.2958	0.2673	0.2430	0.2216	0.2028	0.1861
35.0	0.5808	0.5133	0.4557	0.4063	0.3638	0.3271	0.2958	0.2673	0.2430	0.2216	0.2028
40.0	0.6603	0.5808	0.5133	0.4557	0.4063	0.3638	0.3271	0.2958	0.2673	0.2430	0.2216
45.0	0.7544	0.6603	0.5808	0.5133	0.4557	0.4063	0.3638	0.3271	0.2958	0.2673	0.2430
50.0	0.8666	0.7544	0.6603	0.5808	0.5133	0.4557	0.4063	0.3638	0.3271	0.2958	0.2673
55.0	1.0007	0.8666	0.7544	0.6603	0.5808	0.5133	0.4557	0.4063	0.3638	0.3271	0.2958
60.0	1.1623	1.0007	0.8666	0.7544	0.6603	0.5808	0.5133	0.4557	0.4063	0.3638	0.3271
65.0	1.3581	1.1623	1.0007	0.8666	0.7544	0.6603	0.5808	0.5133	0.4557	0.4063	0.3638
70.0	1.5969	1.3581	1.1623	1.0007	0.8666	0.7544	0.6603	0.5808	0.5133	0.4557	0.4063
75.0	1.8904	1.5969	1.3581	1.1623	1.0007	0.8666	0.7544	0.6603	0.5808	0.5133	0.4557

TABLE A.I.2 (continued) THEORETICAL VOLUME FLOWRATE AT T_{EV} FOR A HEAT INTAKE RATE OF 1 MW FOR A RANGE OF LIFTS AND CONDENSING TEMPERATURES FOR R114B2

T_{CO} °C / P_{CO} bar / $(T_{CO}-T_{EV})$	150.0	155.0	160.0	165.0	170.0	175.0	180.0	185.0	190.0	195.0	200.0
	12.138	13.252	14.441	15.706	17.053	18.487	20.013	21.637	23.367	25.212	27.182
10.0	0.1360	0.1265	0.1181	0.1104	0.1035	0.0973	0.0916	0.0866	0.0820	0.0781	0.0747
15.0	0.1465	0.1360	0.1265	0.1181	0.1104	0.1035	0.0973	0.0916	0.0866	0.0820	0.0781
20.0	0.1582	0.1465	0.1360	0.1265	0.1181	0.1104	0.1035	0.0973	0.0916	0.0866	0.0820
25.0	0.1713	0.1582	0.1465	0.1360	0.1265	0.1181	0.1104	0.1035	0.0973	0.0916	0.0866
30.0	0.1861	0.1713	0.1582	0.1465	0.1360	0.1265	0.1181	0.1104	0.1035	0.0973	0.0916
35.0	0.2028	0.1861	0.1713	0.1582	0.1465	0.1360	0.1265	0.1181	0.1104	0.1035	0.0973
40.0	0.2216	0.2028	0.1861	0.1713	0.1582	0.1465	0.1360	0.1265	0.1181	0.1104	0.1035
45.0	0.2430	0.2216	0.2028	0.1861	0.1713	0.1582	0.1465	0.1360	0.1265	0.1181	0.1104
50.0	0.2673	0.2430	0.2216	0.2028	0.1861	0.1713	0.1582	0.1465	0.1360	0.1265	0.1181
55.0	0.2958	0.2673	0.2430	0.2216	0.2028	0.1861	0.1713	0.1582	0.1465	0.1360	0.1265
60.0	0.3271	0.2958	0.2673	0.2430	0.2216	0.2028	0.1861	0.1713	0.1582	0.1465	0.1360
65.0	0.3638	0.3271	0.2958	0.2673	0.2430	0.2216	0.2028	0.1861	0.1713	0.1582	0.1465
70.0	0.4063	0.3638	0.3271	0.2958	0.2673	0.2430	0.2216	0.2028	0.1861	0.1713	0.1582
75.0	0.4557	0.4063	0.3638	0.3271	0.2958	0.2673	0.2430	0.2216	0.2028	0.1861	0.1713

TABLE A.I.2 (continued) THEORETICAL VOLUME FLOWRATE AT T_{EV} FOR A HEAT INTAKE RATE OF 1 MW FOR A RANGE OF LIFTS AND CONDENSING TEMPERATURES FOR R114B2

T_{CO} °C / $(T_{CO}-T_{EV})$ °C — P_{CO} bar	50.0	55.0	60.0	65.0	70.0	75.0	80.0	85.0	90.0	95.0	100.0
	1.096	1.288	1.505	1.749	2.022	2.327	2.666	3.041	3.453	3.908	4.405
10.0	1.1650	1.0009	0.8649	0.7518	0.6569	0.5770	0.5094	0.4517	0.4018	0.3595	0.3230
15.0	1.3646	1.1650	1.0009	0.8649	0.7518	0.6569	0.5770	0.5094	0.4517	0.4018	0.3595
20.0	1.6095	1.3646	1.1650	1.0009	0.8649	0.7518	0.6569	0.5770	0.5094	0.4517	0.4018
25.0	1.9113	1.6095	1.3646	1.1650	1.0009	0.8649	0.7518	0.6569	0.5770	0.5094	0.4517
30.0	2.2862	1.9113	1.6095	1.3646	1.1650	1.0009	0.8649	0.7518	0.6569	0.5770	0.5094
35.0	2.7563	2.2862	1.9113	1.6095	1.3646	1.1650	1.0009	0.8649	0.7518	0.6569	0.5770
40.0	3.3501	2.7563	2.2862	1.9113	1.6095	1.3646	1.1650	1.0009	0.8649	0.7518	0.6569
45.0	4.1051	3.3501	2.7563	2.2862	1.9113	1.6095	1.3646	1.1650	1.0009	0.8649	0.7518
50.0	5.0813	4.1051	3.3501	2.7563	2.2862	1.9113	1.6095	1.3646	1.1650	1.0009	0.8649
55.0	-	5.0813	4.1051	3.3501	2.7563	2.2862	1.9113	1.6095	1.3646	1.1650	1.0009
60.0	-	-	5.0813	4.1051	3.3501	2.7563	2.2862	1.9113	1.6095	1.3646	1.1650
65.0	-	-	-	5.0813	4.1051	3.3501	2.7563	2.2862	1.9113	1.6095	1.3646
70.0	-	-	-	-	5.0813	4.1051	3.3501	2.7563	2.2862	1.9113	1.6095
75.0	-	-	-	-	-	5.0813	4.1051	3.3501	2.7563	2.2862	1.9113

TABLE A.I.3 THEORETICAL VOLUME FLOWRATE AT T_{EV} FOR A HEAT INTAKE RATE OF 1 MW FOR A RANGE OF LIFTS AND CONDENSING TEMPERATURES FOR R113

T_{CO} °C / P_{CO} bar / $(T_{CO}-T_{EV})$ °C	100.0	105.0	110.0	115.0	120.0	125.0	130.0	135.0	140.0	145.0	150.0
	4.405	4.947	5.537	6.177	6.870	7.619	8.426	9.292	10.224	11.222	12.290
10.0	0.3230	0.2912	0.2636	0.2430	0.2182	0.1994	0.1830	0.1682	0.1551	0.1434	0.1330
15.0	0.3595	0.3230	0.2912	0.2636	0.2430	0.2182	0.1994	0.1830	0.1682	0.1551	0.1434
20.0	0.4018	0.3595	0.3230	0.2912	0.2636	0.2430	0.2182	0.1994	0.1830	0.1682	0.1551
25.0	0.4517	0.4018	0.3595	0.3230	0.2912	0.2636	0.2430	0.2182	0.1994	0.1830	0.1682
30.0	0.5094	0.4517	0.4018	0.3595	0.3230	0.2912	0.2636	0.2430	0.2182	0.1994	0.1830
35.0	0.5770	0.5094	0.4517	0.4018	0.3595	0.3230	0.2912	0.2636	0.2430	0.2182	0.1994
40.0	0.6569	0.5770	0.5094	0.4517	0.4018	0.3595	0.3230	0.2912	0.2636	0.2430	0.2182
45.0	0.7518	0.6569	0.5770	0.5094	0.4517	0.4018	0.3595	0.3230	0.2912	0.2636	0.2430
50.0	0.8649	0.7518	0.6569	0.5770	0.5094	0.4517	0.4018	0.3595	0.3230	0.2912	0.2636
55.0	1.0009	0.8649	0.7518	0.6569	0.5770	0.5094	0.4517	0.4018	0.3595	0.3230	0.2912
60.0	1.1650	1.0009	0.8649	0.7518	0.6569	0.5770	0.5094	0.4517	0.4018	0.3595	0.3230
65.0	1.3646	1.1650	1.0009	0.8649	0.7518	0.6569	0.5770	0.5094	0.4517	0.4018	0.3595
70.0	1.6095	1.3646	1.1650	1.0009	0.8649	0.7518	0.6569	0.5770	0.5094	0.4517	0.4018
75.0	1.9113	1.6095	1.3646	1.1650	1.0009	0.8649	0.7518	0.6569	0.5770	0.5094	0.4517

TABLE A.I.3 (continued) THEORETICAL VOLUME FLOWRATE AT T_{EV} FOR A HEAT INTAKE RATE OF 1 MW FOR A RANGE OF LIFTS AND CONDENSING TEMPERATURES FOR R113

T_{CO} °C / P_{CO} bar / $(T_{CO}-T_{EV})$ °C	150.0	155.0	160.0	165.0	170.0	175.0	180.0	185.0	190.0	195.0	200.0
	12.290	13.431	14.649	15.946	17.331	18.804	20.370	22.037	23.811	25.699	27.724
10.0	0.1330	0.1236	0.1152	0.1076	0.1008	0.0947	0.0892	0.0843	0.0801	0.0764	0.0733
15.0	0.1434	0.1330	0.1236	0.1152	0.1076	0.1008	0.0947	0.0892	0.0843	0.0801	0.0764
20.0	0.1551	0.1434	0.1330	0.1236	0.1152	0.1076	0.1008	0.0947	0.0892	0.0843	0.0801
25.0	0.1682	0.1551	0.1434	0.1330	0.1236	0.1152	0.1076	0.1008	0.0947	0.0892	0.0843
30.0	0.1830	0.1682	0.1551	0.1434	0.1330	0.1236	0.1152	0.1076	0.1008	0.0947	0.0892
35.0	0.1994	0.1830	0.1682	0.1551	0.1434	0.1330	0.1236	0.1152	0.1076	0.1008	0.0947
40.0	0.2182	0.1994	0.1830	0.1682	0.1551	0.1434	0.1330	0.1236	0.1152	0.1076	0.1008
45.0	0.2430	0.2182	0.1994	0.1830	0.1682	0.1551	0.1434	0.1330	0.1236	0.1152	0.1076
50.0	0.2636	0.2430	0.2182	0.1994	0.1830	0.1682	0.1551	0.1434	0.1330	0.1236	0.1152
55.0	0.2912	0.2636	0.2430	0.2182	0.1994	0.1830	0.1682	0.1551	0.1434	0.1330	0.1236
60.0	0.3230	0.2912	0.2636	0.2430	0.2182	0.1994	0.1830	0.1682	0.1551	0.1434	0.1330
65.0	0.3595	0.3230	0.2912	0.2636	0.2430	0.2182	0.1994	0.1830	0.1682	0.1551	0.1434
70.0	0.4018	0.3595	0.3230	0.2912	0.2636	0.2430	0.2182	0.1994	0.1830	0.1682	0.1551
75.0	0.4517	0.4018	0.3595	0.3230	0.2912	0.2636	0.2430	0.2182	0.1994	0.1830	0.1682

TABLE A.I.3 (continued) THEORETICAL VOLUME FLOWRATE AT T_{EV} FOR A HEAT INTAKE RATE OF 1 MW FOR A RANGE OF LIFTS AND CONDENSING TEMPERATURES FOR R113

T_{CO} °C / P_{CO} bar / $(T_{CO}-T_{EV})$ °C	20.0	25.0	30.0	35.0	40.0	45.0	50.0	55.0	60.0	65.0	70.0
	0.883	1.055	1.252	1.476	1.731	2.018	2.340	2.701	2.103	3.547	4.039
10.0	1.4888	1.2569	1.0687	0.9147	0.7878	0.6825	0.5945	0.5205	0.4580	0.4049	0.3596
15.0	1.7768	1.4888	1.2569	1.0687	0.9147	0.7878	0.6825	0.5945	0.5205	0.4580	0.4049
20.0	2.1372	1.7768	1.4888	1.2569	1.0687	0.9147	0.7878	0.6825	0.5945	0.5205	0.4580
25.0	-	2.1372	1.7768	1.4888	1.2569	1.0687	0.9147	0.7878	0.6825	0.5945	0.5205
30.0	-	-	2.1372	1.7768	1.4888	1.2569	1.0687	0.9147	0.7878	0.6825	0.5945
35.0	-	-	-	2.1372	1.7768	1.4888	1.2569	1.0687	0.9147	0.7878	0.6825
40.0	-	-	-	-	2.1372	1.7768	1.4888	1.2569	1.0687	0.9147	0.7878
45.0	-	-	-	-	-	2.1372	1.7768	1.4888	1.2569	1.0687	0.9147
50.0	-	-	-	-	-	-	2.1372	1.7768	1.4888	1.2569	1.0687
55.0	-	-	-	-	-	-	-	2.1372	1.7768	1.4888	1.2569
60.0	-	-	-	-	-	-	-	-	2.1372	1.7768	1.4888
65.0	-	-	-	-	-	-	-	-	-	2.1372	1.7768
70.0	-	-	-	-	-	-	-	-	-	-	2.1372
75.0	-	-	-	-	-	-	-	-	-	-	-

TABLE A.I.4 THEORETICAL VOLUME FLOWRATE AT T_{EV} FOR A HEAT INTAKE RATE OF 1 MW FOR A RANGE OF LIFTS AND CONDENSING TEMPERATURES FOR R11

T_{CO} °C / P_{CO} bar / $(T_{CO}-T_{EV})$ °C	70.0 4.039	75.0 4.581	80.0 5.175	85.0 5.826	90.0 6.537	95.0 7.310	100.0 8.150	105.0 9.060	110.0 10.044	115.0 11.105	120.0 12.248
10.0	0.3596	0.3206	0.2870	0.2579	0.2325	0.2103	0.1909	0.1738	0.1587	0.1453	0.1335
15.0	0.4049	0.3596	0.3206	0.2870	0.2579	0.2325	0.2103	0.1909	0.1738	0.1587	0.1453
20.0	0.4580	0.4049	0.3596	0.3206	0.2870	0.2579	0.2325	0.2103	0.1909	0.1738	0.1587
25.0	0.5205	0.4580	0.4049	0.3596	0.3206	0.2870	0.2579	0.2325	0.2103	0.1909	0.1738
30.0	0.5945	0.5205	0.4580	0.4049	0.3596	0.3206	0.2870	0.2579	0.2325	0.2103	0.1909
35.0	0.6825	0.5945	0.5205	0.4580	0.4049	0.3596	0.3206	0.2870	0.2579	0.2325	0.2103
40.0	0.7878	0.6825	0.5945	0.5205	0.4580	0.4049	0.3596	0.3206	0.2870	0.2579	0.2325
45.0	0.9147	0.7878	0.6825	0.5945	0.5205	0.4580	0.4049	0.3596	0.3206	0.2870	0.2579
50.0	1.0687	0.9147	0.7878	0.6825	0.5945	0.5205	0.4580	0.4049	0.3596	0.3206	0.2870
55.0	1.2569	1.0687	0.9147	0.7878	0.6825	0.5945	0.5205	0.4580	0.4049	0.3596	0.3206
60.0	1.4888	1.2569	1.0687	0.9147	0.7878	0.6825	0.5945	0.5205	0.4580	0.4049	0.3596
65.0	1.7768	1.4888	1.2569	1.0687	0.9147	0.7878	0.6825	0.5945	0.5205	0.4580	0.4049
70.0	2.1372	1.7768	1.4888	1.2569	1.0687	0.9147	0.7878	0.6825	0.5945	0.5205	0.4580
75.0	-	2.1372	1.7768	1.4888	1.2569	1.0687	0.9147	0.7878	0.6825	0.5945	0.5205

TABLE A.I.4 THEORETICAL VOLUME FLOWRATE AT T_{EV} FOR A HEAT INTAKE RATE OF I MW FOR A RANGE OF LIFTS AND CONDENSING TEMPERATURES FOR R216

T_{CO} °C / $(T_{CO}-T_{EV})$ °C — P_{CO} bar	40.0	45.0	50.0	55.0	60.0	65.0	70.0	75.0	80.0	85.0	90.0
	1.174	1.385	1.624	1.894	2.196	2.533	2.908	3.324	3.783	4.288	4.843
10.0	1.0999	0.9430	0.8133	0.7058	0.6160	0.5405	0.4764	0.4220	0.3755	0.3354	0.3009
15.0	1.2918	1.0999	0.9430	0.8133	0.7058	0.6160	0.5405	0.4764	0.4220	0.3755	0.3354
20.0	1.5279	1.2918	1.0999	0.9430	0.8133	0.7058	0.6160	0.5405	0.4764	0.4220	0.3755
25.0	1.8215	1.5279	1.2918	1.0999	0.9430	0.8133	0.7058	0.6160	0.5405	0.4764	0.4220
30.0	2.1911	1.8215	1.5279	1.2918	1.0999	0.9430	0.8133	0.7058	0.6160	0.5405	0.4764
35.0	2.6575	2.1911	1.8215	1.5279	1.2918	1.0999	0.9430	0.8133	0.7058	0.6160	0.5405
40.0	3.2541	2.6575	2.1911	1.8215	1.5279	1.2918	1.0999	0.9430	0.8133	0.7058	0.6160
45.0	-	3.2541	2.6575	2.1911	1.8215	1.5279	1.2918	1.0999	0.9430	0.8133	0.7058
50.0	-	-	3.2541	2.6575	2.1911	1.8215	1.5279	1.2918	1.0999	0.9430	0.8133
55.0	-	-	-	3.2541	2.6575	2.1911	1.8215	1.5279	1.2918	1.0999	0.9430
60.0	-	-	-	-	3.2541	2.6575	2.1911	1.8215	1.5279	1.2918	1.0999
65.0	-	-	-	-	-	3.2541	2.6575	2.1911	1.8215	1.5279	1.2918
70.0	-	-	-	-	-	-	3.2541	2.6575	2.1911	1.8215	1.5279
75.0	-	-	-	-	-	-	-	3.2541	2.6575	2.1911	1.8215

TABLE A.I.5 THEORETICAL VOLUME FLOWRATE AT T_{EV} FOR A HEAT INTAKE RATE OF 1 MW FOR A RANGE OF LIFTS AND CONDENSING TEMPERATURES FOR R216

T_{CO} °C / P_{CO} bar / $(T_{CO}-T_{EV})$ °C	90.0	95.0	100.0	105.0	110.0	115.0	120.0	125.0	130.0	135.0	140.0
	4.843	5.450	6.113	6.834	7.611	8.462	9.378	10.372	11.439	12.591	13.821
10.0	0.3009	0.2709	0.2448	0.2219	0.2015	0.1871	0.1688	0.1551	0.1429	0.1321	0.1225
15.0	0.3354	0.3009	0.2709	0.2448	0.2219	0.2015	0.1871	0.1688	0.1551	0.1429	0.1321
20.0	0.3755	0.3354	0.3009	0.2709	0.2448	0.2219	0.2015	0.1871	0.1688	0.1551	0.1429
25.0	0.4220	0.3755	0.3354	0.3009	0.2709	0.2448	0.2219	0.2015	0.1871	0.1688	0.1551
30.0	0.4764	0.4220	0.3755	0.3354	0.3009	0.2709	0.2448	0.2219	0.2015	0.1871	0.1688
35.0	0.5405	0.4764	0.4220	0.3755	0.3354	0.3009	0.2709	0.2448	0.2219	0.2015	0.1871
40.0	0.6160	0.5405	0.4764	0.4220	0.3755	0.3354	0.3009	0.2709	0.2448	0.2219	0.2015
45.0	0.7058	0.6160	0.5405	0.4764	0.4220	0.3755	0.3354	0.3009	0.2709	0.2448	0.2219
50.0	0.8133	0.7058	0.6160	0.5405	0.4764	0.4220	0.3755	0.3354	0.3009	0.2709	0.2448
55.0	0.9430	0.8133	0.7058	0.6160	0.5405	0.4764	0.4220	0.3755	0.3354	0.3009	0.2709
60.0	1.0999	0.9430	0.8133	0.7058	0.6160	0.5405	0.4764	0.4220	0.3755	0.3354	0.3009
65.0	1.2918	1.0999	0.9430	0.8133	0.7058	0.6160	0.5405	0.4764	0.4220	0.3755	0.3354
70.0	1.5279	1.2918	1.0999	0.9430	0.8133	0.7058	0.6160	0.5405	0.4764	0.4220	0.3755
75.0	1.8215	1.5279	1.2918	1.0999	0.9430	0.8133	0.7058	0.6160	0.5405	0.4764	0.4220

TABLE A.I.5 (continued) THEORETICAL VOLUME FLOWRATE AT T_{EV} FOR A HEAT INTAKE RATE OF 1 MW FOR A RANGE OF LIFTS AND CONDENSING TEMPERATURES FOR R216

T_{CO} °C / P_{CO} bar / $(T_{CO}-T_{EV})$ °C	20.0	25.0	30.0	35.0	40.0	45.0	50.0	55.0	60.0	65.0	70.0
	1.535	1.826	2.159	2.535	2.959	3.435	3.966	4.556	5.210	5.929	6.720
10.0	0.8675	0.7363	0.6295	0.5419	0.4694	0.4092	0.3587	0.3160	0.2799	0.2491	0.2226
15.0	1.0300	0.8675	0.7363	0.6295	0.5419	0.4694	0.4092	0.3587	0.3160	0.2799	0.2491
20.0	1.2330	1.0300	0.8675	0.7363	0.6295	0.5419	0.4694	0.4092	0.3587	0.3160	0.2799
25.0	-	1.2330	1.0300	0.8675	0.7363	0.6295	0.5419	0.4694	0.4092	0.3587	0.3160
30.0	-	-	1.2330	1.0300	0.8675	0.7363	0.6295	0.5419	0.4694	0.4092	0.3587
35.0	-	-	-	1.2330	1.0300	0.8675	0.7363	0.6295	0.5419	0.4694	0.4092
40.0	-	-	-	-	1.2330	1.0300	0.8675	0.7363	0.6295	0.5419	0.4694
45.0	-	-	-	-	-	1.2330	1.0300	0.8675	0.7363	0.6295	0.5419
50.0	-	-	-	-	-	-	1.2330	1.0300	0.8675	0.7363	0.6295
55.0	-	-	-	-	-	-	-	1.2330	1.0300	0.8675	0.7363
60.0	-	-	-	-	-	-	-	-	1.2330	1.0300	0.8675
65.0	-	-	-	-	-	-	-	-	-	1.2330	1.0300
70.0	-	-	-	-	-	-	-	-	-	-	1.2330
75.0	-	-	-	-	-	-	-	-	-	-	-

TABLE A.I.6 THEORETICAL VOLUME FLOWRATE AT T_{EV} FOR A HEAT INTAKE RATE OF 1 MW FOR A RANGE OF LIFTS AND CONDENSING TEMPERATURES FOR R21

T_{CO} °C / P_{CO} bar / $(T_{CO}-T_{EV})$ °C	70.0	75.0	80.0	85.0	90.0	95.0	100.0	105.0	110.0	115.0	120.0
	6.720	7.586	8.533	9.561	10.679	11.889	13.197	14.609	16.129	17.762	19.518
10.0	0.2226	0.1998	0.1800	0.1628	0.1472	0.1345	0.1228	0.1126	0.1034	0.0953	0.0880
15.0	0.2491	0.2226	0.1998	0.1800	0.1628	0.1472	0.1345	0.1228	0.1126	0.1034	0.0953
20.0	0.2799	0.2491	0.2226	0.1998	0.1800	0.1628	0.1472	0.1345	0.1228	0.1126	0.1034
25.0	0.3160	0.2799	0.2491	0.2226	0.1998	0.1800	0.1628	0.1472	0.1345	0.1228	0.1126
30.0	0.3587	0.3160	0.2799	0.2491	0.2226	0.1998	0.1800	0.1628	0.1472	0.1345	0.1228
35.0	0.4092	0.3587	0.3160	0.2799	0.2491	0.2226	0.1998	0.1800	0.1628	0.1472	0.1345
40.0	0.4694	0.4092	0.3587	0.3160	0.2799	0.2491	0.2226	0.1998	0.1800	0.1628	0.1472
45.0	0.5419	0.4694	0.4092	0.3587	0.3160	0.2799	0.2491	0.2226	0.1998	0.1800	0.1628
50.0	0.6295	0.5419	0.4694	0.4092	0.3587	0.3160	0.2799	0.2491	0.2226	0.1998	0.1800
55.0	0.7363	0.6295	0.5419	0.4694	0.4092	0.3587	0.3160	0.2799	0.2491	0.2226	0.1998
60.0	0.8675	0.7363	0.6295	0.5419	0.4694	0.4092	0.3587	0.3160	0.2799	0.2491	0.2226
65.0	1.0300	0.8675	0.7363	0.6295	0.5419	0.4694	0.4092	0.3587	0.3160	0.2799	0.2491
70.0	1.2330	1.0300	0.8675	0.7363	0.6295	0.5419	0.4694	0.4092	0.3587	0.3160	0.2799
75.0	–	1.2330	1.0300	0.8675	0.7363	0.6295	0.5419	0.4694	0.4092	0.3587	0.3160

TABLE A.I.6 (continued) THEORETICAL VOLUME FLOWRATE AT T_{EV} FOR A HEAT INTAKE RATE OF 1 MW FOR A RANGE OF LIFTS AND CONDENSING TEMPERATURES FOR R21

T_{CO} °C / P_{CO} bar / $(T_{CO}-T_{EV})$ °C	20.0	25.0	30.0	35.0	40.0	45.0	50.0	55.0	60.0	65.0	70.0
	2.076	2.429	2.839	3.271	3.779	4.349	4.967	5.656	6.408	7.226	8.126
10.0	0.6870	0.5927	0.5146	0.4492	0.3925	0.3460	0.3061	0.2720	0.2432	0.2185	0.1969
15.0	0.8049	0.6870	0.5927	0.5146	0.4492	0.3925	0.3460	0.3061	0.2720	0.2432	0.2185
20.0	0.9424	0.8049	0.6870	0.5927	0.5146	0.4492	0.3925	0.3460	0.3061	0.2720	0.2432
25.0	-	0.9424	0.8049	0.6870	0.5927	0.5146	0.4492	0.3925	0.3460	0.3061	0.2720
30.0	-	-	0.9424	0.8049	0.6870	0.5927	0.5146	0.4492	0.3925	0.3460	0.3061
35.0	-	-	-	0.9424	0.8049	0.6870	0.5927	0.5146	0.4492	0.3925	0.3460
40.0	-	-	-	-	0.9424	0.8049	0.6870	0.5927	0.5146	0.4492	0.3925
45.0	-	-	-	-	-	0.9424	0.8049	0.6870	0.5927	0.5146	0.4492
50.0	-	-	-	-	-	-	0.9424	0.8049	0.6870	0.5927	0.5146
55.0	-	-	-	-	-	-	-	0.9424	0.8049	0.6870	0.5927
60.0	-	-	-	-	-	-	-	-	0.9424	0.8049	0.6870
65.0	-	-	-	-	-	-	-	-	-	0.9424	0.8049
70.0	-	-	-	-	-	-	-	-	-	-	0.9424
75.0	-	-	-	-	-	-	-	-	-	-	-

TABLE A.I.7 THEORETICAL VOLUME FLOWRATE AT T_{EV} FOR A HEAT INTAKE RATE OF 1 MW FOR A RANGE OF LIFTS AND CONDENSING TEMPERATURES FOR R600

T_{CO} °C / P_{CO} bar / $(T_{CO}-T_{EV})$ °C	70.0	75.0	80.0	85.0	90.0	95.0	100.0	105.0	110.0	115.0	120.0
	8.126	9.099	10.168	11.309	12.544	13.883	15.310	16.834	18.491	20.283	22.195
10.0	0.1969	0.1782	0.1620	0.1476	0.1350	0.1242	0.1147	0.1060	0.0984	0.0916	0.0857
15.0	0.2185	0.1969	0.1782	0.1620	0.1476	0.1350	0.1242	0.1147	0.1060	0.0984	0.0916
20.0	0.2432	0.2185	0.1969	0.1782	0.1620	0.1476	0.1350	0.1242	0.1147	0.1060	0.0984
25.0	0.2720	0.2432	0.2185	0.1969	0.1782	0.1620	0.1476	0.1350	0.1242	0.1147	0.1060
30.0	0.3061	0.2720	0.2432	0.2185	0.1969	0.1782	0.1620	0.1476	0.1350	0.1242	0.1147
35.0	0.3460	0.3061	0.2720	0.2432	0.2185	0.1969	0.1782	0.1620	0.1476	0.1350	0.1242
40.0	0.3925	0.3460	0.3061	0.2720	0.2432	0.2185	0.1969	0.1782	0.1620	0.1476	0.1350
45.0	0.4492	0.3925	0.3460	0.3061	0.2720	0.2432	0.2185	0.1969	0.1782	0.1620	0.1476
50.0	0.5146	0.4492	0.3925	0.3460	0.3061	0.2720	0.2432	0.2185	0.1969	0.1782	0.1620
55.0	0.5927	0.5146	0.4492	0.3925	0.3460	0.3061	0.2720	0.2432	0.2185	0.1969	0.1782
60.0	0.6870	0.5927	0.5146	0.4492	0.3925	0.3460	0.3061	0.2720	0.2432	0.2185	0.1969
65.0	0.8049	0.6870	0.5927	0.5146	0.4492	0.3925	0.3460	0.3061	0.2720	0.2432	0.2185
70.0	0.9424	0.8049	0.6870	0.5927	0.5146	0.4492	0.3925	0.3460	0.3061	0.2720	0.2432
75.0	-	0.9424	0.8049	0.6870	0.5927	0.5146	0.4492	0.3925	0.3460	0.3061	0.2720

TABLE A.I. 7 (continued) THEORETICAL VOLUME FLOWRATE AT T_{EV} FOR A HEAT INTAKE RATE OF 1 MW FOR A RANGE OF LIFTS AND CONDENSING TEMPERATURES FOR R600

T_{CO} °C / $(T_{CO}-T_{EV})$ °C — P_{CO} bar	20.0	25.0	30.0	35.0	40.0	45.0	50.0	55.0	60.0	65.0	70.0
	2.364	2.767	3.220	3.726	4.291	4.916	5.606	6.366	7.198	8.106	9.094
10.0	-	0.5230	0.4543	0.3970	0.3488	0.3082	0.2736	0.2441	0.2188	0.1969	0.1781
15.0	-	-	0.5230	0.4543	0.3970	0.3488	0.3082	0.2736	0.2441	0.2188	0.1969
20.0	-	-	-	0.5230	0.4543	0.3970	0.3488	0.3082	0.2736	0.2441	0.2188
25.0	-	-	-	-	0.5230	0.4543	0.3970	0.3488	0.3082	0.2736	0.2441
30.0	-	-	-	-	-	0.5230	0.4543	0.3970	0.3488	0.3082	0.2736
35.0	-	-	-	-	-	-	0.5230	0.4543	0.3970	0.3488	0.3082
40.0	-	-	-	-	-	-	-	0.5230	0.4543	0.3970	0.3488
45.0	-	-	-	-	-	-	-	-	0.5230	0.4543	0.3970
50.0	-	-	-	-	-	-	-	-	-	0.5230	0.4543
55.0	-	-	-	-	-	-	-	-	-	-	0.5230
60.0	-	-	-	-	-	-	-	-	-	-	-
65.0	-	-	-	-	-	-	-	-	-	-	-
70.0	-	-	-	-	-	-	-	-	-	-	-
75.0	-	-	-	-	-	-	-	-	-	-	-

TABLE A.I.8 THEORETICAL VOLUME FLOWRATE AT T_{EV} FOR A HEAT INTAKE RATE OF 1 MW FOR A RANGE OF LIFTS AND CONDENSING TEMPERATURES FOR R12B1

T_{CO} °C / P_{CO} bar / $(T_{CO}-T_{EV})$ °C	70.0	75.0	80.0	85.0	90.0	95.0	100.0	105.0	110.0	115.0	120.0
	9.094	10.166	11.337	12.588	13.933	15.376	16.921	18.570	20.327	22.128	24.176
10.0	0.1781	0.1617	0.1474	0.1349	0.1237	0.1141	0.1056	0.0982	0.0916	0.0859	0.0807
15.0	0.1969	0.1781	0.1617	0.1474	0.1349	0.1237	0.1141	0.1056	0.0982	0.0916	0.0859
20.0	0.2188	0.1969	0.1781	0.1617	0.1474	0.1349	0.1237	0.1141	0.1056	0.0982	0.0916
25.0	0.2441	0.2188	0.1969	0.1781	0.1617	0.1474	0.1349	0.1237	0.1141	0.1056	0.0982
30.0	0.2736	0.2441	0.2188	0.1969	0.1781	0.1617	0.1474	0.1349	0.1237	0.1141	0.1056
35.0	0.3082	0.2736	0.2441	0.2188	0.1969	0.1781	0.1617	0.1474	0.1349	0.1237	0.1141
40.0	0.3488	0.3082	0.2736	0.2441	0.2188	0.1969	0.1781	0.1617	0.1474	0.1349	0.1237
45.0	0.3970	0.3488	0.3082	0.2736	0.2441	0.2188	0.1969	0.1781	0.1617	0.1474	0.1349
50.0	0.4543	0.3970	0.3488	0.3082	0.2736	0.2441	0.2188	0.1969	0.1781	0.1617	0.1474
55.0	0.5230	0.4543	0.3970	0.3488	0.3082	0.2736	0.2441	0.2188	0.1969	0.1781	0.1617
60.0	-	0.5230	0.4543	0.3970	0.3488	0.3082	0.2736	0.2441	0.2188	0.1969	0.1781
65.0	-	-	0.5230	0.4543	0.3970	0.3488	0.3082	0.2736	0.2441	0.2188	0.1969
70.0	-	-	-	0.5230	0.4543	0.3970	0.3488	0.3082	0.2736	0.2441	0.2188
75.0	-	-	-	-	0.5230	0.4543	0.3970	0.3488	0.3082	0.2736	0.2441

TABLE A.I.8 (continued) THEORETICAL VOLUME FLOWRATE AT T_{EV} FOR A HEAT INTAKE RATE OF 1 MW FOR A RANGE OF LIFTS AND CONDENSING TEMPERATURES FOR R12B1

T_{CO} °C / P_{CO} bar / $(T_{CO}-T_{EV})$ °C	20.0	25.0	30.0	35.0	40.0	45.0	50.0	55.0	60.0	65.0	70.0
	1.805	2.130	2.497	2.910	3.372	3.887	4.458	5.088	5.780	6.539	7.370
10.0	-	0.6553	0.5653	0.4907	0.4286	0.3768	0.3330	0.2959	0.2642	0.2370	0.2092
15.0	-	-	0.6553	0.5653	0.4907	0.4286	0.3768	0.3330	0.2959	0.2642	0.2370
20.0	-	-	-	0.6553	0.5653	0.4907	0.4286	0.3768	0.3330	0.2959	0.2642
25.0	-	-	-	-	0.6553	0.5653	0.4907	0.4286	0.3768	0.3330	0.2959
30.0	-	-	-	-	-	0.6553	0.5653	0.4907	0.4286	0.3768	0.3330
35.0	-	-	-	-	-	-	0.6553	0.5653	0.4907	0.4286	0.3768
40.0	-	-	-	-	-	-	-	0.6553	0.5653	0.4907	0.4286
45.0	-	-	-	-	-	-	-	-	0.6553	0.5653	0.4907
50.0	-	-	-	-	-	-	-	-	-	0.6553	0.5653
55.0	-	-	-	-	-	-	-	-	-	-	0.6553
60.0	-	-	-	-	-	-	-	-	-	-	-
65.0	-	-	-	-	-	-	-	-	-	-	-
70.0	-	-	-	-	-	-	-	-	-	-	-
75.0	-	-	-	-	-	-	-	-	-	-	-

TABLE A.I.9 THEORETICAL VOLUME FLOWRATE AT T_{EV} FOR A HEAT INTAKE RATE OF 1 MW FOR A RANGE OF LIFTS AND CONDENSING TEMPERATURES FOR R114

T_{CO} °C / P_{CO} bar / $(T_{CO}-T_{EV})$ °C	70.0	75.0	80.0	85.0	90.0	95.0	100.0	105.0	110.0	115.0	120.0
	7.370	8.270	9.255	10.317	11.471	12.713	14.058	15.505	17.071	18.753	20.575
10.0	0.2092	0.1933	0.1765	0.1601	0.1464	0.1344	0.1237	0.1143	0.1058	0.0984	0.0918
15.0	0.2370	0.2092	0.1933	0.1765	0.1601	0.1464	0.1344	0.1237	0.1143	0.1058	0.0984
20.0	0.2642	0.2370	0.2092	0.1933	0.1765	0.1601	0.1464	0.1344	0.1237	0.1143	0.1058
25.0	0.2959	0.2642	0.2370	0.2092	0.1933	0.1765	0.1601	0.1464	0.1344	0.1237	0.1143
30.0	0.3330	0.2959	0.2642	0.2370	0.2092	0.1933	0.1765	0.1601	0.1464	0.1344	0.1237
35.0	0.3768	0.3330	0.2959	0.2642	0.2370	0.2092	0.1933	0.1765	0.1601	0.1464	0.1344
40.0	0.4286	0.3768	0.3330	0.2959	0.2642	0.2370	0.2092	0.1933	0.1765	0.1601	0.1464
45.0	0.4907	0.4286	0.3768	0.3330	0.2959	0.2642	0.2370	0.2092	0.1933	0.1765	0.1601
50.0	0.5653	0.4907	0.4286	0.3768	0.3330	0.2959	0.2642	0.2370	0.2092	0.1933	0.1765
55.0	0.6553	0.5653	0.4907	0.4286	0.3768	0.3330	0.2959	0.2642	0.2370	0.2092	0.1933
60.0	-	0.6553	0.5653	0.4907	0.4286	0.3768	0.3330	0.2959	0.2642	0.2370	0.2092
65.0	-	-	0.6553	0.5653	0.4907	0.4286	0.3768	0.3330	0.2959	0.2642	0.2370
70.0	-	-	-	0.6553	0.5653	0.4907	0.4286	0.3768	0.3330	0.2959	0.2642
75.0	-	-	-	-	0.6553	0.5653	0.4907	0.4286	0.3768	0.3330	0.2959

TABLE A.I. 9 (continued) THEORETICAL VOLUME FLOWRATE AT T_{EV} FOR A HEAT INTAKE RATE OF 1 MW FOR A RANGE OF LIFTS AND CONDENSING TEMPERATURES FOR R114

T_{CO} °C / P_{CO} bar / $(T_{CO}-T_{EV})$ °C	20.0	25.0	30.0	35.0	40.0	45.0	50.0	55.0	60.0	65.0	70.0
	3.294	3.854	4.486	5.193	5.981	6.860	7.832	8.902	10.080	11.373	12.789
10.0	0.4368	0.3770	0.3273	0.2855	0.2506	0.2210	0.1959	0.1743	0.1558	0.1399	0.1261
15.0	0.5094	0.4368	0.3770	0.3273	0.2855	0.2506	0.2210	0.1959	0.1743	0.1558	0.1399
20.0	0.5981	0.5094	0.4368	0.3770	0.3273	0.2855	0.2506	0.2210	0.1959	0.1743	0.1558
25.0	-	0.5981	0.5094	0.4368	0.3770	0.3273	0.2855	0.2506	0.2210	0.1959	0.1743
30.0	-	-	0.5981	0.5094	0.4368	0.3770	0.3273	0.2855	0.2506	0.2210	0.1959
35.0	-	-	-	0.5981	0.5094	0.4368	0.3770	0.3273	0.2855	0.2506	0.2210
40.0	-	-	-	-	0.5981	0.5094	0.4368	0.3770	0.3273	0.2855	0.2506
45.0	-	-	-	-	-	0.5981	0.5094	0.4368	0.3770	0.3273	0.2855
50.0	-	-	-	-	-	-	0.5981	0.5094	0.4368	0.3770	0.3273
55.0	-	-	-	-	-	-	-	0.5981	0.5094	0.4368	0.3770
60.0	-	-	-	-	-	-	-	-	0.5981	0.5094	0.4368
65.0	-	-	-	-	-	-	-	-	-	0.5981	0.5094
70.0	-	-	-	-	-	-	-	-	-	-	0.5981
75.0	-	-	-	-	-	-	-	-	-	-	-

TABLE A.I.10 THEORETICAL VOLUME FLOWRATE AT T_{EV} FOR A HEAT INTAKE RATE OF 1 MW FOR A RANGE OF LIFTS AND CONDENSING TEMPERATURES FOR R506

T_{CO} °C / P_{CO} bar / $(T_{CO}-T_{EV})$ °C	70.0	75.0	80.0	85.0	90.0	95.0	100.0	105.0	110.0	115.0	120.0
	12.789	14.325	16.001	17.823	19.793	21.920	24.217	26.690	29.350	32.212	35.275
10.0	0.1261	0.1140	0.1036	0.0944	0.0863	0.0793	0.0731	0.0676	0.0628	0.0586	0.0551
15.0	0.1399	0.1261	0.1140	0.1036	0.0944	0.0863	0.0793	0.0731	0.0676	0.0628	0.0586
20.0	0.1558	0.1399	0.1261	0.1140	0.1036	0.0944	0.0863	0.0793	0.0731	0.0676	0.0628
25.0	0.1743	0.1558	0.1399	0.1261	0.1140	0.1036	0.0944	0.0863	0.0793	0.0731	0.0676
30.0	0.1959	0.1743	0.1558	0.1399	0.1261	0.1140	0.1036	0.0944	0.0863	0.0793	0.0731
35.0	0.2210	0.1959	0.1743	0.1558	0.1399	0.1261	0.1140	0.1036	0.0944	0.0863	0.0793
40.0	0.2506	0.2210	0.1959	0.1743	0.1558	0.1399	0.1261	0.1140	0.1036	0.0944	0.0863
45.0	0.2855	0.2506	0.2210	0.1959	0.1743	0.1558	0.1399	0.1261	0.1140	0.1036	0.0944
50.0	0.3273	0.2855	0.2506	0.2210	0.1959	0.1743	0.1558	0.1399	0.1261	0.1140	0.1036
55.0	0.3770	0.3273	0.2855	0.2506	0.2210	0.1959	0.1743	0.1558	0.1399	0.1261	0.1140
60.0	0.4368	0.3770	0.3273	0.2855	0.2506	0.2210	0.1959	0.1743	0.1558	0.1399	0.1261
65.0	0.5094	0.4368	0.3770	0.3273	0.2855	0.2506	0.2210	0.1959	0.1743	0.1558	0.1399
70.0	0.5981	0.5094	0.4368	0.3770	0.3273	0.2855	0.2506	0.2210	0.1959	0.1743	0.1558
75.0	-	0.5981	0.5094	0.4368	0.3770	0.3273	0.2855	0.2506	0.2210	0.1959	0.1743

TABLE A.I.10 (continued) THEORETICAL VOLUME FLOWRATE AT T_{EV} FOR A HEAT INTAKE RATE OF 1 MW FOR A RANGE OF LIFTS AND CONDENSING TEMPERATURES FOR R506

T_{CO} °C / P_{CO} bar / $(T_{CO}-T_{EV})$ °C	20.0	25.0	30.0	35.0	40.0	45.0	50.0	55.0	60.0	65.0	70.0
	2.898	3.387	3.939	4.558	5.249	6.019	6.873	7.818	8.854	9.994	11.245
10.0	0.5018	0.4327	0.3753	0.3273	0.2869	0.2527	0.2237	0.1989	0.1777	0.1595	0.1437
15.0	0.5855	0.5018	0.4327	0.3753	0.3273	0.2869	0.2527	0.2237	0.1989	0.1777	0.1595
20.0	0.6872	0.5855	0.5018	0.4327	0.3753	0.3273	0.2869	0.2527	0.2237	0.1989	0.1777
25.0	-	0.6872	0.5855	0.5018	0.4327	0.3753	0.3273	0.2869	0.2527	0.2237	0.1989
30.0	-	-	0.6872	0.5855	0.5018	0.4327	0.3753	0.3273	0.2869	0.2527	0.2237
35.0	-	-	-	0.6872	0.5855	0.5018	0.4327	0.3753	0.3273	0.2869	0.2527
40.0	-	-	-	-	0.6872	0.5855	0.5018	0.4327	0.3753	0.3273	0.2869
45.0	-	-	-	-	-	0.6872	0.5855	0.5018	0.4327	0.3753	0.3273
50.0	-	-	-	-	-	-	0.6872	0.5855	0.5018	0.4327	0.3753
55.0	-	-	-	-	-	-	-	0.6872	0.5855	0.5018	0.4327
60.0	-	-	-	-	-	-	-	-	0.6872	0.5855	0.5018
65.0	-	-	-	-	-	-	-	-	-	0.6872	0.5855
70.0	-	-	-	-	-	-	-	-	-	-	0.6872
75.0	-	-	-	-	-	-	-	-	-	-	-

TABLE A.I.11 THEORETICAL VOLUME FLOWRATE AT T_{EV} FOR A HEAT INTAKE RATE OF 1 MW FOR A RANGE OF LIFTS AND CONDENSING TEMPERATURES FOR R142B

T_{CO} °C / P_{CO} bar / $(T_{CO}-T_{EV})$ °C	70.0	75.0	80.0	85.0	90.0	95.0	100.0	105.0	110.0	115.0	120.0
	11.245	12.599	14.078	15.679	17.413	19.283	21.296	23.457	25.771	28.245	30.766
10.0	0.1437	0.1300	0.1182	0.1079	0.0990	0.0911	0.0844	0.0785	0.0735	0.0692	0.0658
15.0	0.1595	0.1437	0.1300	0.1182	0.1079	0.0990	0.0911	0.0844	0.0785	0.0735	0.0692
20.0	0.1777	0.1595	0.1437	0.1300	0.1182	0.1079	0.0990	0.0911	0.0844	0.0785	0.0735
25.0	0.1989	0.1777	0.1595	0.1437	0.1300	0.1182	0.1079	0.0990	0.0911	0.0844	0.0785
30.0	0.2237	0.1989	0.1777	0.1595	0.1437	0.1300	0.1182	0.1079	0.0990	0.0911	0.0844
35.0	0.2527	0.2237	0.1989	0.1777	0.1595	0.1437	0.1300	0.1182	0.1079	0.0990	0.0911
40.0	0.2869	0.2527	0.2237	0.1989	0.1777	0.1595	0.1437	0.1300	0.1182	0.1079	0.0990
45.0	0.3273	0.2869	0.2527	0.2237	0.1989	0.1777	0.1595	0.1437	0.1300	0.1182	0.1079
50.0	0.3753	0.3273	0.2869	0.2527	0.2237	0.1989	0.1777	0.1595	0.1437	0.1300	0.1182
55.0	0.4327	0.3753	0.3273	0.2869	0.2527	0.2237	0.1989	0.1777	0.1595	0.1437	0.1300
60.0	0.5018	0.4327	0.3753	0.3273	0.2869	0.2527	0.2237	0.1989	0.1777	0.1595	0.1437
65.0	0.5855	0.5018	0.4327	0.3753	0.3273	0.2869	0.2527	0.2237	0.1989	0.1777	0.1595
70.0	0.6872	0.5855	0.5018	0.4327	0.3753	0.3273	0.2869	0.2527	0.2237	0.1989	0.1777
75.0	-	0.6872	0.5855	0.5018	0.4327	0.3753	0.3273	0.2869	0.2527	0.2237	0.1989

TABLE A.I.11 THEORETICAL VOLUME FLOWRATE AT T_{EV} FOR A HEAT INTAKE RATE OF 1 MW FOR A RANGE OF LIFTS AND CONDENSING TEMPERATURES FOR R142B

T_{CO} °C / P_{CO} bar / $(T_{CO}-T_{EV})$ °C	20.0	25.0	30.0	35.0	40.0	45.0	50.0	55.0	60.0	65.0	70.0
	3.005	3.482	4.148	4.610	5.265	5.986	6.785	7.667	8.630	9.669	10.803
10.0	0.4997	0.4365	0.3827	0.3383	0.3003	0.2679	0.2399	0.2158	0.1949	0.1765	0.1606
15.0	0.5761	0.4997	0.4365	0.3827	0.3383	0.3003	0.2679	0.2399	0.2158	0.1949	0.1765
20.0	0.6685	0.5761	0.4997	0.4365	0.3827	0.3383	0.3003	0.2679	0.2399	0.2158	0.1949
25.0	-	0.6685	0.5761	0.4997	0.4365	0.3827	0.3383	0.3003	0.2679	0.2399	0.2158
30.0	-	-	0.6685	0.5761	0.4997	0.4365	0.3827	0.3383	0.3003	0.2679	0.2399
35.0	-	-	-	0.6685	0.5761	0.4997	0.4365	0.3827	0.3383	0.3003	0.2679
40.0	-	-	-	-	0.6685	0.5761	0.4997	0.4365	0.3827	0.3383	0.3003
45.0	-	-	-	-	-	0.6685	0.5761	0.4997	0.4365	0.3827	0.3383
50.0	-	-	-	-	-	-	0.6685	0.5761	0.4997	0.4365	0.3827
55.0	-	-	-	-	-	-	-	0.6685	0.5761	0.4997	0.4365
60.0	-	-	-	-	-	-	-	-	0.6685	0.5761	0.4997
65.0	-	-	-	-	-	-	-	-	-	0.6685	0.5761
70.0	-	-	-	-	-	-	-	-	-	-	0.6685
75.0	-	-	-	-	-	-	-	-	-	-	-

TABLE A.I.12 THEORETICAL VOLUME FLOWRATE AT T_{EV} FOR A HEAT INTAKE RATE OF 1 MW FOR A RANGE OF LIFTS AND CONDENSING TEMPERATURES FOR R600a

T_{CO} °C / $(T_{CO}-T_{EV})$ °C, P_{CO} bar	70.0	75.0	80.0	85.0	90.0	95.0	100.0	105.0	110.0	115.0	120.0
	10.803	12.038	13.372	14.814	16.369	18.044	19.844	21.774	23.842	26.053	28.418
10.0	0.1606	0.1471	0.1350	0.1243	0.1149	0.1067	0.0994	0.0932	0.0878	0.0833	0.0796
15.0	0.1765	0.1606	0.1471	0.1350	0.1243	0.1149	0.1067	0.0994	0.0932	0.0878	0.0833
20.0	0.1949	0.1765	0.1606	0.1471	0.1350	0.1243	0.1149	0.1067	0.0994	0.0932	0.0878
25.0	0.2158	0.1949	0.1765	0.1606	0.1471	0.1350	0.1243	0.1149	0.1067	0.0994	0.0932
30.0	0.2399	0.2158	0.1949	0.1765	0.1606	0.1471	0.1350	0.1243	0.1149	0.1067	0.0994
35.0	0.2679	0.2399	0.2158	0.1949	0.1765	0.1606	0.1471	0.1350	0.1243	0.1149	0.1067
40.0	0.3003	0.2679	0.2399	0.2158	0.1949	0.1765	0.1606	0.1471	0.1350	0.1243	0.1149
45.0	0.3383	0.3003	0.2679	0.2399	0.2158	0.1949	0.1765	0.1606	0.1471	0.1350	0.1243
50.0	0.3827	0.3383	0.3003	0.2679	0.2399	0.2158	0.1949	0.1765	0.1606	0.1471	0.1350
55.0	0.4365	0.3827	0.3383	0.3003	0.2679	0.2399	0.2158	0.1949	0.1765	0.1606	0.1471
60.0	0.4997	0.4365	0.3827	0.3383	0.3003	0.2679	0.2399	0.2158	0.1949	0.1765	0.1606
65.0	0.5761	0.4997	0.4365	0.3827	0.3383	0.3003	0.2679	0.2399	0.2158	0.1949	0.1765
70.0	0.6685	0.5761	0.4997	0.4365	0.3827	0.3383	0.3003	0.2679	0.2399	0.2158	0.1949
75.0	-	0.6685	0.5761	0.4997	0.4365	0.3827	0.3383	0.3003	0.2679	0.2399	0.2158

TABLE A.I.12 (continued) THEORETICAL VOLUME FLOWRATE AT T_{EV} FOR A HEAT INTAKE RATE OF 1 MW FOR A RANGE OF LIFTS AND CONDENSING TEMPERATURES FOR R600A

T_{CO} °C / P_{CO} bar / $(T_{CO}-T_{EV})$ °C	20.0	25.0	30.0	35.0	40.0	45.0	50.0	55.0	60.0	65.0	70.0
	8.584	10.040	11.680	13.517	15.564	17.835	20.348	23.122	26.172	29.512	33.160
10.0	0.1445	0.1445	0.1257	0.1098	0.0964	0.0851	0.0754	0.0672	0.0602	0.0539	0.0486
15.0	0.1950	0.1445	0.1445	0.1257	0.1098	0.0964	0.0851	0.0754	0.0672	0.0602	0.0539
20.0	0.2289	0.1950	0.1445	0.1445	0.1257	0.1098	0.0964	0.0851	0.0754	0.0672	0.0602
25.0	-	0.2289	0.1950	0.1445	0.1445	0.1257	0.1098	0.0964	0.0851	0.0754	0.0672
30.0	-	-	0.2289	0.1950	0.1445	0.1445	0.1257	0.1098	0.0964	0.0851	0.0754
35.0	-	-	-	0.2289	0.1950	0.1445	0.1445	0.1257	0.1098	0.0964	0.0851
40.0	-	-	-	-	0.2289	0.1950	0.1445	0.1445	0.1257	0.1098	0.0964
45.0	-	-	-	-	-	0.2289	0.1950	0.1445	0.1445	0.1257	0.1098
50.0	-	-	-	-	-	-	0.2289	0.1950	0.1445	0.1445	0.1257
55.0	-	-	-	-	-	-	-	0.2289	0.1950	0.1445	0.1445
60.0	-	-	-	-	-	-	-	-	0.2289	0.1950	0.1445
65.0	-	-	-	-	-	-	-	-	-	0.2289	0.1950
70.0	-	-	-	-	-	-	-	-	-	-	0.2289
75.0	-	-	-	-	-	-	-	-	-	-	-

TABLE A.I.13 THEORETICAL VOLUME FLOWRATE AT T_{EV} FOR A HEAT INTAKE RATE OF 1 MW FOR A RANGE OF LIFTS AND CONDENSING TEMPERATURES FOR R717

T_{CO} °C / P_{CO} bar / $(T_{CO}-T_{EV})$ °C	70.0	75.0	80.0	85.0	90.0	95.0	100.0	105.0	110.0	115.0	120.0
	33.160	37.137	41.475	46.189	51.286	56.777	62.688	69.059	75.915	83.245	91.025
10.0	0.0486	0.0440	0.0400	0.0365	0.0334	0.0307	0.0283	0.0262	0.0245	0.0230	0.0218
15.0	0.0539	0.0486	0.0440	0.0400	0.0365	0.0334	0.0307	0.0283	0.0262	0.0245	0.0230
20.0	0.0602	0.0539	0.0486	0.0440	0.0400	0.0365	0.0334	0.0307	0.0283	0.0262	0.0245
25.0	0.0672	0.0602	0.0539	0.0486	0.0440	0.0400	0.0365	0.0334	0.0307	0.0283	0.0262
30.0	0.0754	0.0672	0.0602	0.0539	0.0486	0.0440	0.0400	0.0365	0.0334	0.0307	0.0283
35.0	0.0851	0.0754	0.0672	0.0602	0.0539	0.0486	0.0440	0.0400	0.0365	0.0334	0.0307
40.0	0.0964	0.0851	0.0754	0.0672	0.0602	0.0539	0.0486	0.0440	0.0400	0.0365	0.0334
45.0	0.1098	0.0964	0.0851	0.0754	0.0672	0.0602	0.0539	0.0486	0.0440	0.0400	0.0365
50.0	0.1257	0.1098	0.0964	0.0851	0.0754	0.0672	0.0602	0.0539	0.0486	0.0440	0.0400
55.0	0.1445	0.1257	0.1098	0.0964	0.0851	0.0754	0.0672	0.0602	0.0539	0.0486	0.0440
60.0	0.1445	0.1445	0.1257	0.1098	0.0964	0.0851	0.0754	0.0672	0.0602	0.0539	0.0486
65.0	0.1950	0.1445	0.1445	0.1257	0.1098	0.0964	0.0851	0.0754	0.0672	0.0602	0.0539
70.0	0.2289	0.1950	0.1445	0.1445	0.1257	0.1098	0.0964	0.0851	0.0754	0.0672	0.0602
75.0	-	0.2289	0.1950	0.1445	0.1445	0.1257	0.1098	0.0964	0.0851	0.0754	0.0672

TABLE A.I.13 (continued) THEORETICAL VOLUME FLOWRATE AT T_{EV} FOR A HEAT INTAKE RATE OF 1 MW FOR A RANGE OF LIFTS AND CONDENSING TEMPERATURES FOR R717

T_{CO} °C / P_{CO} bar / $(T_{CO}-T_{EV})$ °C	20.0	25.0	30.0	35.0	40.0	45.0	50.0	55.0	60.0	65.0	70.0
	5.723	6.585	7.536	8.590	9.749	11.020	12.410	13.923	15.568	17.352	19.282
10.0	0.2741	0.2412	0.2133	0.1897	0.1694	0.1520	0.1369	0.1209	0.1125	0.1026	0.0939
15.0	0.3131	0.2741	0.2412	0.2133	0.1897	0.1694	0.1520	0.1369	0.1209	0.1125	0.1026
20.0	0.2301	0.3131	0.2741	0.2412	0.2133	0.1897	0.1694	0.1520	0.1369	0.1209	0.1125
25.0	-	0.2301	0.3131	0.2741	0.2412	0.2133	0.1897	0.1694	0.1520	0.1369	0.1209
30.0	-	-	0.2301	0.3131	0.2741	0.2412	0.2133	0.1897	0.1694	0.1520	0.1369
35.0	-	-	-	0.2301	0.3131	0.2741	0.2412	0.2133	0.1897	0.1694	0.1520
40.0	-	-	-	-	0.2301	0.3131	0.2741	0.2412	0.2133	0.1897	0.1694
45.0	-	-	-	-	-	0.2301	0.3131	0.2741	0.2412	0.2133	0.1897
50.0	-	-	-	-	-	-	0.2301	0.3131	0.2741	0.2412	0.2133
55.0	-	-	-	-	-	-	-	0.2301	0.3131	0.2741	0.2412
60.0	-	-	-	-	-	-	-	-	0.2301	0.3131	0.2741
65.0	-	-	-	-	-	-	-	-	-	0.2301	0.3131
70.0	-	-	-	-	-	-	-	-	-	-	0.2301
75.0	-	-	-	-	-	-	-	-	-	-	-

TABLE A.I.14 THEORETICAL VOLUME FLOWRATE AT T_{EV} FOR A HEAT INTAKE RATE OF 1 MW FOR A RANGE OF LIFTS AND CONDENSING TEMPERATURES FOR R505

T_{CO} °C / P_{CO} bar / $(T_{CO}-T_{EV})$ °C	20.0	25.0	30.0	35.0	40.0	45.0	50.0	55.0	60.0	65.0	70.0
	2.662	3.137	3.675	4.280	4.956	5.708	6.542	7.463	8.475	9.584	10.795
10.0	0.5233	0.4492	0.3883	0.3378	0.2959	0.2607	0.2310	0.2059	0.1845	0.1662	0.1504
15.0	0.6143	0.5233	0.4492	0.3883	0.3378	0.2959	0.2607	0.2310	0.2059	0.1845	0.1662
20.0	0.7266	0.6143	0.5233	0.4492	0.3883	0.3378	0.2959	0.2607	0.2310	0.2059	0.1845
25.0	-	0.7266	0.6143	0.5233	0.4492	0.3883	0.3378	0.2959	0.2607	0.2310	0.2059
30.0	-	-	0.7266	0.6143	0.5233	0.4492	0.3883	0.3378	0.2959	0.2607	0.2310
35.0	-	-	-	0.7266	0.6143	0.5233	0.4492	0.3883	0.3378	0.2959	0.2607
40.0	-	-	-	-	0.7266	0.6143	0.5233	0.4492	0.3883	0.3378	0.2959
45.0	-	-	-	-	-	0.7266	0.6143	0.5233	0.4492	0.3883	0.3378
50.0	-	-	-	-	-	-	0.7266	0.6143	0.5233	0.4492	0.3883
55.0	-	-	-	-	-	-	-	0.7266	0.6143	0.5233	0.4492
60.0	-	-	-	-	-	-	-	-	0.7266	0.6143	0.5233
65.0	-	-	-	-	-	-	-	-	-	0.7266	0.6143
70.0	-	-	-	-	-	-	-	-	-	-	0.7266
75.0	-	-	-	-	-	-	-	-	-	-	-

TABLE A.I.15 THEORETICAL VOLUME FLOWRATE AT T_{EV} FOR A HEAT INTAKE RATE OF 1 MW FOR A RANGE OF LIFTS AND CONDENSING TEMPERATURES FOR RC318

T_{CO} °C / P_{CO} bar / $(T_{CO}-T_{EV})$ °C	20.0	25.0	30.0	35.0	40.0	45.0	50.0	55.0	60.0	65.0	70.0
	5.673	6.516	7.449	8.477	9.606	10.843	12.193	13.663	15.259	16.988	18.858
10.0	0.2795	0.2465	0.2184	0.1946	0.1732	0.1565	0.1413	0.1281	0.1166	0.1066	0.0979
15.0	0.3188	0.2795	0.2465	0.2184	0.1946	0.1732	0.1565	0.1413	0.1281	0.1166	0.1066
20.0	0.3656	0.3188	0.2795	0.2465	0.2184	0.1946	0.1732	0.1565	0.1413	0.1281	0.1166
25.0	-	0.3656	0.3188	0.2795	0.2465	0.2184	0.1946	0.1732	0.1565	0.1413	0.1281
30.0	-	-	0.3656	0.3188	0.2795	0.2465	0.2184	0.1946	0.1732	0.1565	0.1413
35.0	-	-	-	0.3656	0.3188	0.2795	0.2465	0.2184	0.1946	0.1732	0.1565
40.0	-	-	-	-	0.3656	0.3188	0.2795	0.2465	0.2184	0.1946	0.1732
45.0	-	-	-	-	-	0.3656	0.3188	0.2795	0.2465	0.2184	0.1946
50.0	-	-	-	-	-	-	0.3656	0.3188	0.2795	0.2465	0.2184
55.0	-	-	-	-	-	-	-	0.3656	0.3188	0.2795	0.2465
60.0	-	-	-	-	-	-	-	-	0.3656	0.3188	0.2795
65.0	-	-	-	-	-	-	-	-	-	0.3656	0.3188
70.0	-	-	-	-	-	-	-	-	-	-	0.3656
75.0	-	-	-	-	-	-	-	-	-	-	-

TABLE A.I.16 THEORETICAL VOLUME FLOWRATE AT T_{EV} FOR A HEAT INTAKE RATE OF 1 MW FOR A RANGE OF LIFTS AND CONDENSING TEMPERATURES FOR R12

T_{CO} °C / P_{CO} bar	20.0	25.0	30.0	35.0	40.0	45.0	50.0	55.0	60.0	65.0	70.0
$(T_{CO}-T_{EV})$ °C	6.688	7.688	8.796	10.017	11.359	12.829	14.434	16.182	18.080	20.139	22.366
10.0	0.2367	0.2086	0.1848	0.1645	0.1473	0.1324	0.1196	0.1086	0.0990	0.0906	0.0833
15.0	0.2702	0.2367	0.2086	0.1848	0.1645	0.1473	0.1324	0.1196	0.1086	0.0990	0.0906
20.0	0.3103	0.2702	0.2367	0.2086	0.1848	0.1645	0.1473	0.1324	0.1196	0.1086	0.0990
25.0	-	0.3103	0.2702	0.2367	0.2086	0.1848	0.1645	0.1473	0.1324	0.1196	0.1086
30.0	-	-	0.3103	0.2702	0.2367	0.2086	0.1848	0.1645	0.1473	0.1324	0.1196
35.0	-	-	-	0.3103	0.2702	0.2367	0.2086	0.1848	0.1645	0.1473	0.1324
40.0	-	-	-	-	0.3103	0.2702	0.2367	0.2086	0.1848	0.1645	0.1473
45.0	-	-	-	-	-	0.3103	0.2702	0.2367	0.2086	0.1848	0.1645
50.0	-	-	-	-	-	-	0.3103	0.2702	0.2367	0.2086	0.1848
55.0	-	-	-	-	-	-	-	0.3103	0.2702	0.2367	0.2086
60.0	-	-	-	-	-	-	-	-	0.3103	0.2702	0.2367
65.0	-	-	-	-	-	-	-	-	-	0.3103	0.2702
70.0	-	-	-	-	-	-	-	-	-	-	0.3103
75.0	-	-	-	-	-	-	-	-	-	-	-

TABLE A.I.17 THEORETICAL VOLUME FLOWRATE AT T_{EV} FOR A HEAT INTAKE RATE OF 1 MW FOR A RANGE OF LIFTS AND CONDENSING TEMPERATURES FOR R500

T_{CO} °C / $(T_{CO}-T_{EV})$ °C — P_{CO} bar	20.0	25.0	30.0	35.0	40.0	45.0	50.0	55.0	60.0	65.0	70.0
	8.350	9.503	10.769	12.155	13.668	15.314	17.103	19.041	21.137	23.401	25.843
10.0	0.2020	0.1799	0.1611	0.1449	0.1309	0.1187	0.1082	0.0990	0.0909	0.0839	0.0779
15.0	0.2278	0.2020	0.1799	0.1611	0.1449	0.1309	0.1187	0.1082	0.0990	0.0909	0.0839
20.0	0.2584	0.2278	0.2020	0.1799	0.1611	0.1449	0.1309	0.1187	0.1082	0.0990	0.0909
25.0	-	0.2584	0.2278	0.2020	0.1799	0.1611	0.1449	0.1309	0.1187	0.1082	0.0990
30.0	-	-	0.2584	0.2278	0.2020	0.1799	0.1611	0.1449	0.1309	0.1187	0.1082
35.0	-	-	-	0.2584	0.2278	0.2020	0.1799	0.1611	0.1449	0.1309	0.1187
40.0	-	-	-	-	0.2584	0.2278	0.2020	0.1799	0.1611	0.1449	0.1309
45.0	-	-	-	-	-	0.2584	0.2278	0.2020	0.1799	0.1611	0.1449
50.0	-	-	-	-	-	-	0.2584	0.2278	0.2020	0.1799	0.1611
55.0	-	-	-	-	-	-	-	0.2584	0.2278	0.2020	0.1799
60.0	-	-	-	-	-	-	-	-	0.2584	0.2278	0.2020
65.0	-	-	-	-	-	-	-	-	-	0.2584	0.2278
70.0	-	-	-	-	-	-	-	-	-	-	0.2584
75.0	-	-	-	-	-	-	-	-	-	-	-

TABLE A.I.18 THEORETICAL VOLUME FLOWRATE AT T_{EV} FOR A HEAT INTAKE RATE OF 1 MW FOR A RANGE OF LIFTS AND CONDENSING TEMPERATURES FOR R290

T_{CO} °C / P_{CO} bar / $(T_{CO}-T_{EV})$ °C	20.0	25.0	30.0	35.0	40.0	45.0	50.0	55.0	60.0	65.0	70.0
	9.087	10.432	11.921	13.562	15.365	17.341	19.499	21.851	24.407	27.178	30.176
10.0	0.1762	0.1555	0.1380	0.1231	0.1103	0.0993	0.0898	0.0816	0.0746	0.0685	0.0632
15.0	0.2008	0.1762	0.1555	0.1380	0.1231	0.1103	0.0993	0.0898	0.0816	0.0746	0.0685
20.0	0.2301	0.2008	0.1762	0.1555	0.1380	0.1231	0.1103	0.0993	0.0898	0.0816	0.0746
25.0	-	0.2301	0.2008	0.1762	0.1555	0.1380	0.1231	0.1103	0.0993	0.0898	0.0816
30.0	-	-	0.2301	0.2008	0.1762	0.1555	0.1380	0.1231	0.1103	0.0993	0.0898
35.0	-	-	-	0.2301	0.2008	0.1762	0.1555	0.1380	0.1231	0.1103	0.0993
40.0	-	-	-	-	0.2301	0.2008	0.1762	0.1555	0.1380	0.1231	0.1103
45.0	-	-	-	-	-	0.2301	0.2008	0.1762	0.1555	0.1380	0.1231
50.0	-	-	-	-	-	-	0.2301	0.2008	0.1762	0.1555	0.1380
55.0	-	-	-	-	-	-	-	0.2301	0.2008	0.1762	0.1555
60.0	-	-	-	-	-	-	-	-	0.2301	0.2008	0.1762
65.0	-	-	-	-	-	-	-	-	-	0.2301	0.2008
70.0	-	-	-	-	-	-	-	-	-	-	0.2301
75.0	-	-	-	-	-	-	-	-	-	-	-

TABLE A.I.19 THEORETICAL VOLUME FLOWRATE AT T_{EV} FOR A HEAT INTAKE RATE OF 1 MW FOR A RANGE OF LIFTS AND CONDENSING TEMPERATURES FOR R22

T_{CO} °C / P_{CO} bar / $(T_{CO}-T_{EV})$ °C	20.0	25.0	30.0	35.0	40.0	45.0	50.0	55.0	60.0	65.0	70.0
	7.920	9.047	10.293	11.659	13.166	14.813	16.622	18.596	20.762	23.123	25.716
10.0	0.2106	0.1872	0.1672	0.1501	0.1260	0.1225	0.1114	0.1018	0.0935	0.0865	0.0807
15.0	0.2380	0.2106	0.1872	0.1672	0.1501	0.1260	0.1225	0.1114	0.1018	0.0935	0.0865
20.0	0.2705	0.2380	0.2106	0.1872	0.1672	0.1501	0.1260	0.1225	0.1114	0.1018	0.0935
25.0	-	0.2705	0.2380	0.2106	0.1872	0.1672	0.1501	0.1260	0.1225	0.1114	0.1018
30.0	-	-	0.2705	0.2380	0.2106	0.1872	0.1672	0.1501	0.1260	0.1225	0.1114
35.0	-	-	-	0.2705	0.2380	0.2106	0.1872	0.1672	0.1501	0.1260	0.1225
40.0	-	-	-	-	0.2705	0.2380	0.2106	0.1872	0.1672	0.1501	0.1260
45.0	-	-	-	-	-	0.2705	0.2380	0.2106	0.1872	0.1672	0.1501
50.0	-	-	-	-	-	-	0.2705	0.2380	0.2106	0.1872	0.1672
55.0	-	-	-	-	-	-	-	0.2705	0.2380	0.2106	0.1872
60.0	-	-	-	-	-	-	-	-	0.2705	0.2380	0.2106
65.0	-	-	-	-	-	-	-	-	-	0.2705	0.2380
70.0	-	-	-	-	-	-	-	-	-	-	0.2705
75.0	-	-	-	-	-	-	-	-	-	-	-

TABLE A.I.20 THEORETICAL VOLUME FLOWRATE AT T_{EV} FOR A HEAT INTAKE RATE OF 1 MW FOR A RANGE OF LIFTS AND CONDENSING TEMPERATURES FOR R115

APPENDIX II

DESCRIPTION OF ICE1

APPENDIX II

DESCRIPTION OF ICE1

Figure(A.II.1) shows ICE1 schematically. The system was designed originally for operation with R12. It was assembled using very reliable equipment readily available in the U.K.

The Dunham-Bush condenser and evaporator,model CSTC-B548 and CH-324A respectively, had a safe working pressure of 21.7 bar(300psig). In the condenser R113 flowed through the shell and water through the tubes, whereas in the evaporator, R113 flowed through the shell. The evaporator was provided with a safety device to shut down the unit if the exit water temperature fell below $4^{o}C$.

The Frigidare compressor, model EP4, was an open type model capable of producing pressures up to 22 bar. The open type model was flexible in that its prime mover could be changed. In addition it permitted easy inspection. The compressor was driven by a 2.2 kW, 240/415V, 8.1/4.7A, 1420rpm, 3 phase 50Hz General Electric induction motor conforming to British Standard 2613. The compressor was provided with a safety device to shut it down if the delivery pressure exceeded 22 bar.

A manually operated needle valve, manufactured by Ashford Controls, was used as the expansion valve. This valve bypassed a Danfoss TEF2, expansion valve which was

used during unattended periods.

An auxilliary heat exchanger with bypass lines was provided in order to superheat the vapour leaving the evaporator by extracting heat from the vapour leaving the compressor.

The equipment included other items like solenoid valves, stop valves, sight glass, filling points and, in particular, a drying unit, model EK164, supplied by Alco Controls Ltd.. Two tanks, each with a capacity of 680 litres(150 gallons) provided with steam heating were provided for supplying the source water for the evaporator and condenser.

Instrumentation

Chromel-alumel thermocouples with digital readout accurate to 0.1^{o}C were used for temperature measurements. Bourdon type guages were used for pressure measurements. Three guages were provided on the high pressure side and three on the low pressure side.

The pressure guages used for measuring the pressure at the condenser outlet P3, and at the evaporator outlet P7, ranged from 0 to 200psig(1 to 14.8 bar) and 0 to 160 psig (1 to 14.0 bar) respectively by 1 psi divisions in both cases. The pressures P1 and P4 were measured with guages ranging from 0 to 300 psig(1 to 21.7 bar) by 10 psi divisions and the pressures P2 and P6 were measured using guages ranging from 30 inch Hg vacuum to 100psig(0 to 7.9 bar)

by 2 psi divisions. Atmospheric pressure was read from a standard Toricellian barometer and ambient temperature from a mercury in glass thermometer. Standard ammeters, voltmeters and wattmeters were used for electrical measurements. The water flow rates through the evaporator and condenser were measured using standard rotameters.

All instruments were calibrated before installation and checked in situ. Figure(A.II.2) shows the locations of the measurement points.

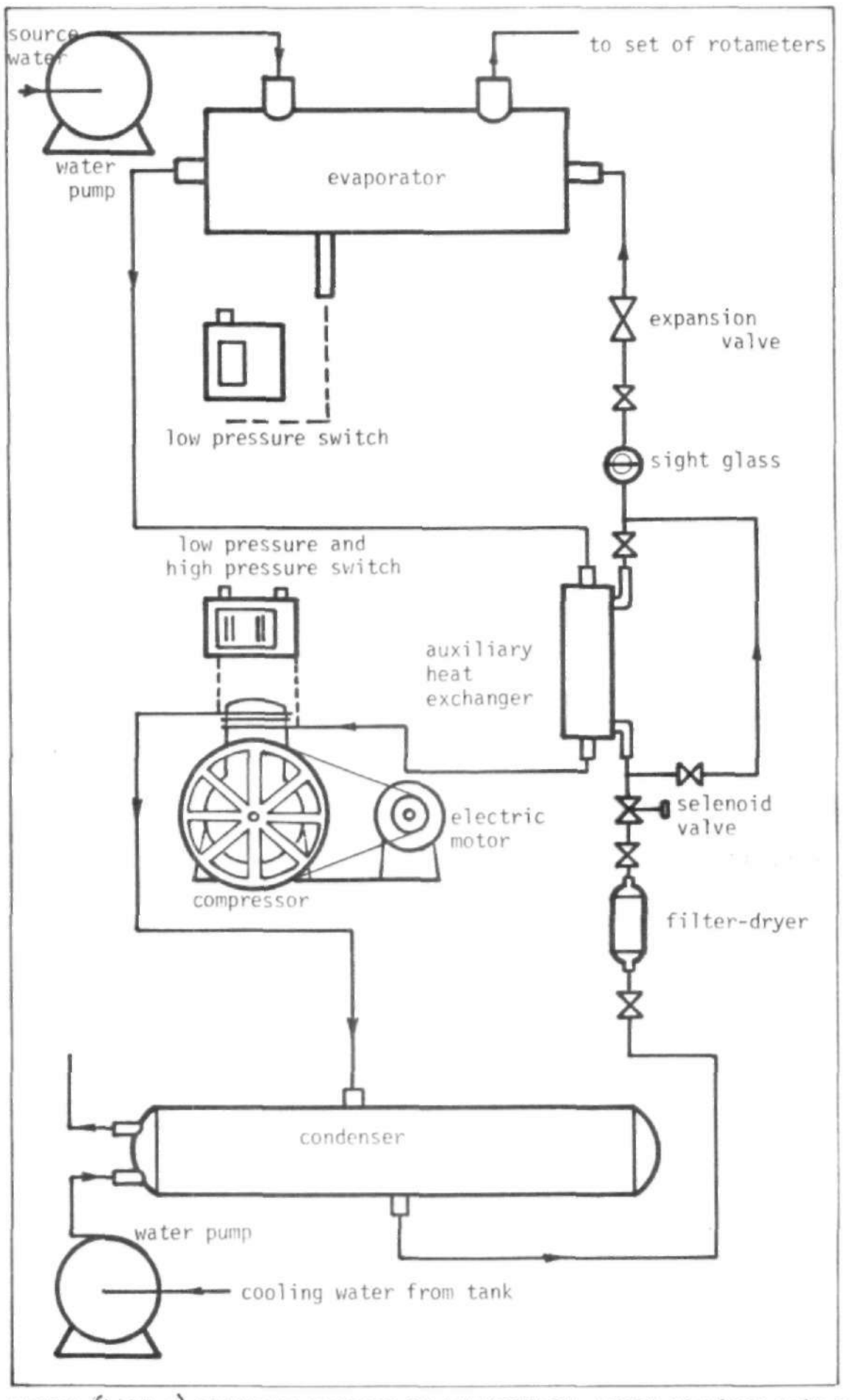


FIGURE (A.II.1) SCHEMATIC DIAGRAM OF EXPERIMENTAL WATER TO WATER HEAT PUMP

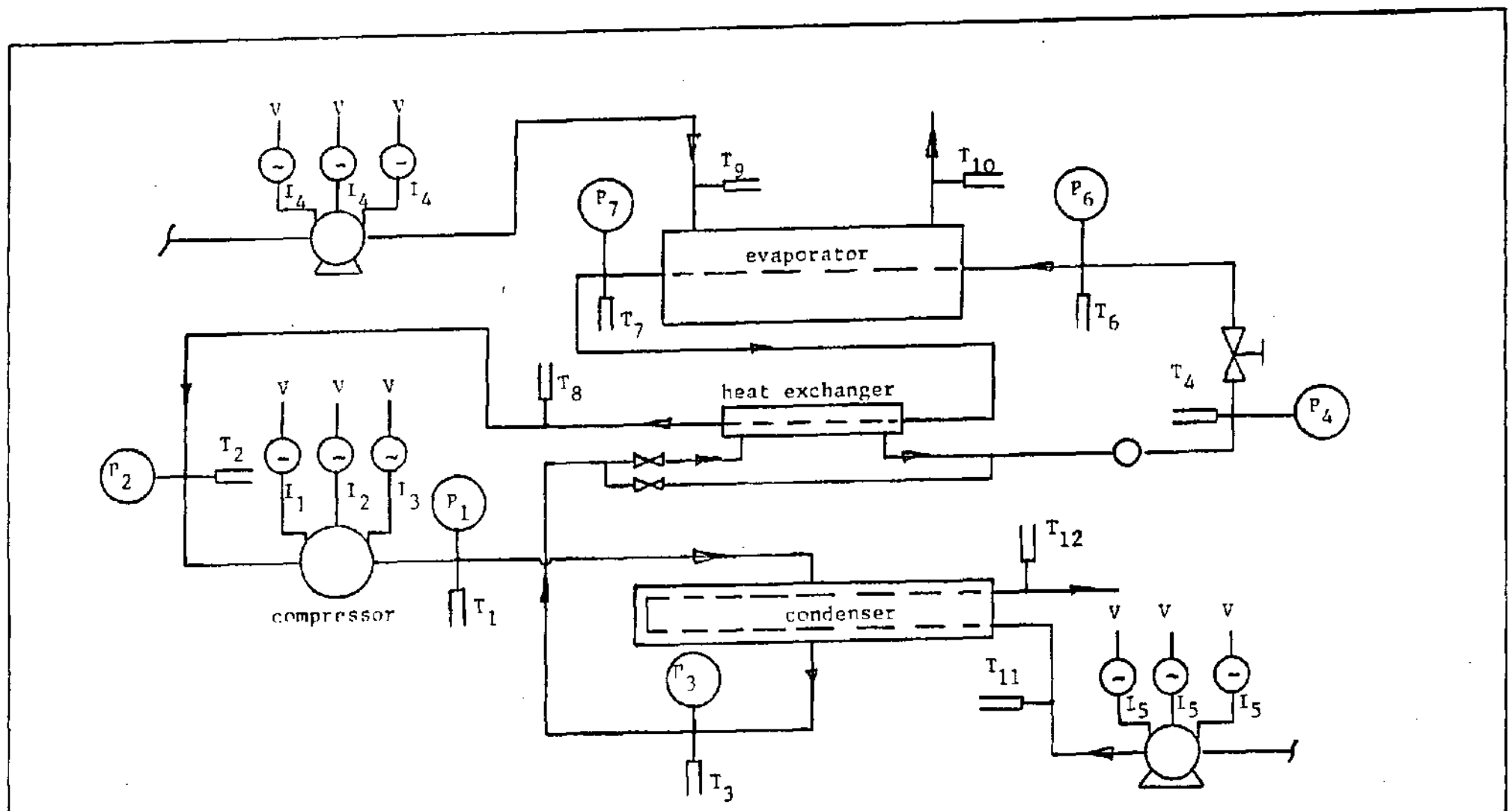


FIGURE (A.II.2) INSTRUMENTATION OF THE EXPERIMENTAL WATER TO WATER HEAT PUMP

APPENDIX III

DESIGN OF THE ABSORBER COLUMN

APPENDIX III

A.III.1 INTRODUCTION

The design decision was made to construct the absorber column, with an external cooling arrangement, using stainless steel. Approximate methods were used for the design using standard equations from text books by:

i) Astarita, G., "Mass transfer with chemical reaction", Elsevier Publishing Company, Amsterdam, (1967).

ii) Backhurst, J.R., Harker, J.H. and Porter, J.E., "Problems in heat and mass transfer", Edward Arnold, London (1974).

Smith, ["Heat pump absorbers", Smith, I.E., School of Mechanical Engineering, Cranfield Institute of Technology, Bedford, U.K., (1981)] has described various types of heat pump absorbers. He gave relations governing the absorption process and the design of the absorbers.

In this work, the assumptions made for designing the absorber column were as follows:

i) The equilibrium concentration at the liquid surface is unaffected by the absorption process.

ii) The stainless steel guaze in the absorber has similar characteristics to Raschig rings.

iii) The pressure drop inside the absorber is 0.0533 bar (40mm Hg) per metre of packing.

iv) The average column inside diameter is 0.05m.

Using water-lithium bromide mixture, the following conditions were assumed:

i) The evaporator heat load Q_{EV} is 1.2kW at an evaporator temperature T_{EV} of 100°C.

ii) Referring to Figure (A.III.1), the lithium bromide concentrations in the solution leaving the generator and in the solution leaving the absorber are X_5 = 55 per cent and X_8 = 50 per cent respectively.

Under these conditions, the temperature in the absorber T_{AB} is 132°C.

A.III.2 MATERIAL AND ENERGY BALANCE

Taking mass balance around the generator

$$M_{10} = M_5 + M_1 \qquad \text{(A.III.1)}$$

and

$$M_{10}\, X_{10} = M_5\, X_5 \qquad \text{(A.III.2)}$$

from which

$$M_{10}/M_1 = \frac{X_5}{X_5 - X_{10}} = \frac{X_5}{X_5 - X_8} \qquad \text{(A.III.3)}$$

since $X_{10} = X_8$

$$M_{10}/M_1 = \frac{55}{55-50} = 11$$

Taking energy balance around the evaporator

$$M_4 = \frac{Q_{EV}}{H_4 - H_3} \qquad \text{(A.III.5)}$$

where H_3 and H_4 are the enthalpies of the saturated liquid and saturated vapour respectively. The values of H_3 and H_4 were obtained from the "Steam Tables" of Keenan, Keyes, Hill and Moore (1978).

$$H_3 = 419.06 \text{ kJ kg}^{-1}$$

$$H_4 = 2676.0 \text{ kJ kg}^{-1}$$

Therefore,

$$M_4 = \frac{4320}{(2676-419.06)} = 1.914 \text{ kg h}^{-1}$$

Since $M_1 = M_4$ (A.III.6)

$$M_{10} = 1.914 \times 11 = 21.054 \text{ kg h}^{-1}$$

and

$$M_5 = 21.054 - 1.914 = 19.14 \text{ kg h}^{-1}$$

It was assumed that the solution in the absorber was recirculated at a reflux rate equal to the mass flow rate of the concentrated solution M_5. Hence, the mass flow rate at stream 7,

$$M_7 = 38.28 \text{ kg h}^{-1}$$

Taking a mass balance around the absorber,

$$M_4 + M_7 = M_8 \quad \text{(A.III.7)}$$

and

$$M_7 X_7 = M_8 X_8 \qquad \text{(A.III.8)}$$

from which

$$X_7 = \frac{(M_4 + M_7) X_8}{M_7} \qquad \text{(A.III.9)}$$

Hence, $X_7 = \frac{(1.914 + 38.28)}{38.28} \times 50 = 52.50$ per cent

The possibility of flooding was checked using Figure (8.5) in "Problems in Heat and Mass Transfer" by Backhurst, Harker and Porter (1974). The figure shows a correlation between the liquid and vapour mass velocities in the absorber column as follows:

$$\frac{M_L}{M_G} \left(\rho_G/\rho_L\right)^{0.5} \quad \text{against} \quad \frac{M_G^2 \, F\psi\mu^{0.2}}{\rho_G \rho_L \, g} \qquad \text{(A.III.10)}$$

where, M_L and M_G are the mass flow rates of the solution going into the absorber and the working fluid vapour respectively in kg s^{-1}. ρ_G and ρ_L are the densities of the working fluid vapour and the absorber solution respectively in kg m^{-3}.

M_G is the flow rate of working fluid vapour per unit cross sectional area, kg s^{-1} m^{-2}

F is the packing factor, dimensionless.

Ψ is the ratio of the density of water to the density of the solution, dimensionless.

μ is the viscosity kg m^{-1} s^{-1}.

g is the acceleration due to gravity, m s^{-2}.

$$M_L = M_7 = \frac{38.28}{3600} \text{ kg } s^1$$

$$M_G = M_4 = \frac{1.914}{3600} \text{ kg } s^1$$

$$M_L/M_G = 20$$

All properties were taken at 132°C.

From the 'Steam Tables' of Keenan, Keyes, Hill and Moore (1978)

$$\rho_G = 0.5977 \text{ kg } m^{-3}$$

From Equation (8.12)

$$\rho_L = 1488 \text{ kg } m^{-3}$$

$$\Psi = \frac{958.13}{1488} = 0.6439$$

By approximation from 'Foote Technical Data' by Boryta,

$$\mu = 6.8 \times 10^{-4} \text{ kg m}^{-1} \text{ s}^{-1}$$

$$M_G = \frac{1.914 \times 4}{3600 \times (0.05)^2} = 0.271 \text{ kg s}^{-1}\text{m}^{-2}$$

The packing factor F was found from "Problems in Heat and Mass Transfer", by Backhurst, Harker and Porter (1974) for a surface area of 150m^2 per m^3 of space volume.

Thus,

$$F = 130$$

Hence,

$$\frac{M_L}{M_G}(\rho_G/\rho_L)^{0.5} = 20\left(\frac{0.5977}{1488}\right)^{0.5} = 0.4008$$

and

$$\frac{M_G^2 F \psi \mu^{0.2}}{\rho_G \rho_L g} = \frac{(0.271)^2 \times 130 \times 0.6439(0.00068)^{0.2}}{0.5977 \times 1488 \times 9.81}$$

$$= 1.64 \times 10^{-4}$$

The above two values fix a point, in Figure (8.5) in "Problems in Heat and Mass Transfer" by Backhurst and Porter, well below the flooding line. Therefore, an

absorber with a diameter of 0.05m could be used.

A.III.3 DETERMINATION OF THE ABSORBER HEIGHT

The absorption coefficient K_L of water vapour into the solution in the absorber was calculated from the relation given by Astarita (1967) as,

$$K_L = 2\sqrt{\frac{D}{\pi t'}} \qquad \text{(A.III.11)}$$

where D is the diffusion coefficient of the gas through the liquid, $m^2\ s^{-1}$,

and t' is the life time of a liquid surface element in seconds; t' was given by Astarita (1967) for a wetted wall column as

$$t' = \frac{2}{3} Z \left[\left[\frac{\pi d}{V_L} \right]^2 \cdot \frac{3\mu}{g\rho} \right]^{\frac{1}{3}} \qquad \text{(A.III.12)}$$

where Z is the height of the absorber column, m
d is the column diameter, m
V_L is the liquid flow rate, $m^3\ s^{-1}$

The value of K_L was determined directly from the absorption rate from the equation presented by Astarita (p.3, 1967)

$$K_L = \frac{M_G}{X_W^* - (X_W)_7} \qquad \text{(A.III.13)}$$

where X^* is the equilibrium concentration of water vapour at the interface, in mole m^{-3},

$(X_W)_7$ is the water in the bulk of the solution, in mole m^{-3}.

$$M_G = \frac{1.914 \times 10^3}{3600 \times 18 \times \quad \times 0.05 \times 2Z}$$

$$= 0.0386/Z \text{ mole } m^{-2}\ s^{-1}$$

$$X_W^* = \frac{0.50 \times 1488 \times 10^3}{18} = 41333 \text{ mole } m^{-3}$$

$$(X_W)_7 = \frac{0.475 \times 1525 \times 10^3}{18} = 40243 \text{ mole } m^{-3}$$

From Equation (A.III.13),

$$K_L = \frac{0.0386}{Z(41333-40243)} = 3.54 \times 10^{-5}/Z \text{ m } s^{-1} \qquad \text{(A.III.14}$$

substituting in (A.III.11)

$$2\sqrt{\frac{D}{\pi t}} = 3.54 \times 10^{-5}/Z \qquad \text{(A.III.14)}$$

A typical value of the diffusion coefficient of gas through liquid is 2×10^{-9} m^2 s^{-1} (Smith, 1981).

Therefore,

$$t' = 2.032Z^2 \qquad \text{(A.III.15)}$$

$$V_L = \frac{38.28}{3600 \times 1525} = 6.9727 \times 10^{-6}\ m^3\ s^{-1}$$

Hence, from Equation (A.III.12),

$$t' = \frac{2}{3}Z\left[\left[\frac{\pi \times 0.05}{6.9727 \times 10^{-6}}\right]^2 \times \frac{3 \times 6.8 \times 10^{-4}}{9.81 \times 1525}\right]^{\frac{1}{3}}$$
$$= 2.737Z$$

From Equation (A.III.15)

$$Z = \frac{2.737}{2.03} = 1.348m$$

The absorber was made from a double pipe heat exchanger, a mixing vessel and a receiver with a total length of 1.5m.

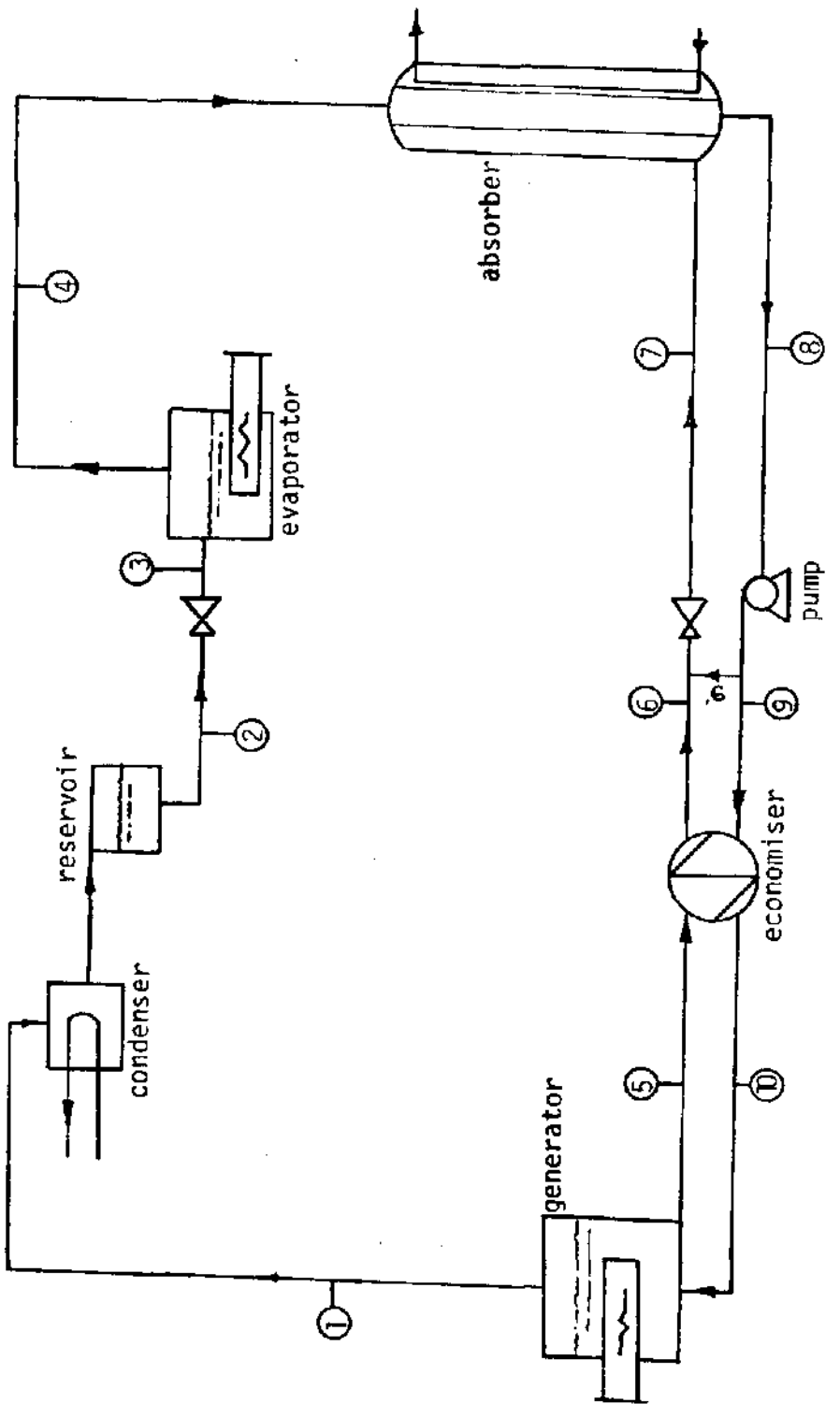


FIGURE (A.III.1) CONVENTIONAL ABSORPTION HEAT PUMP UNIT

APPENDIX IV

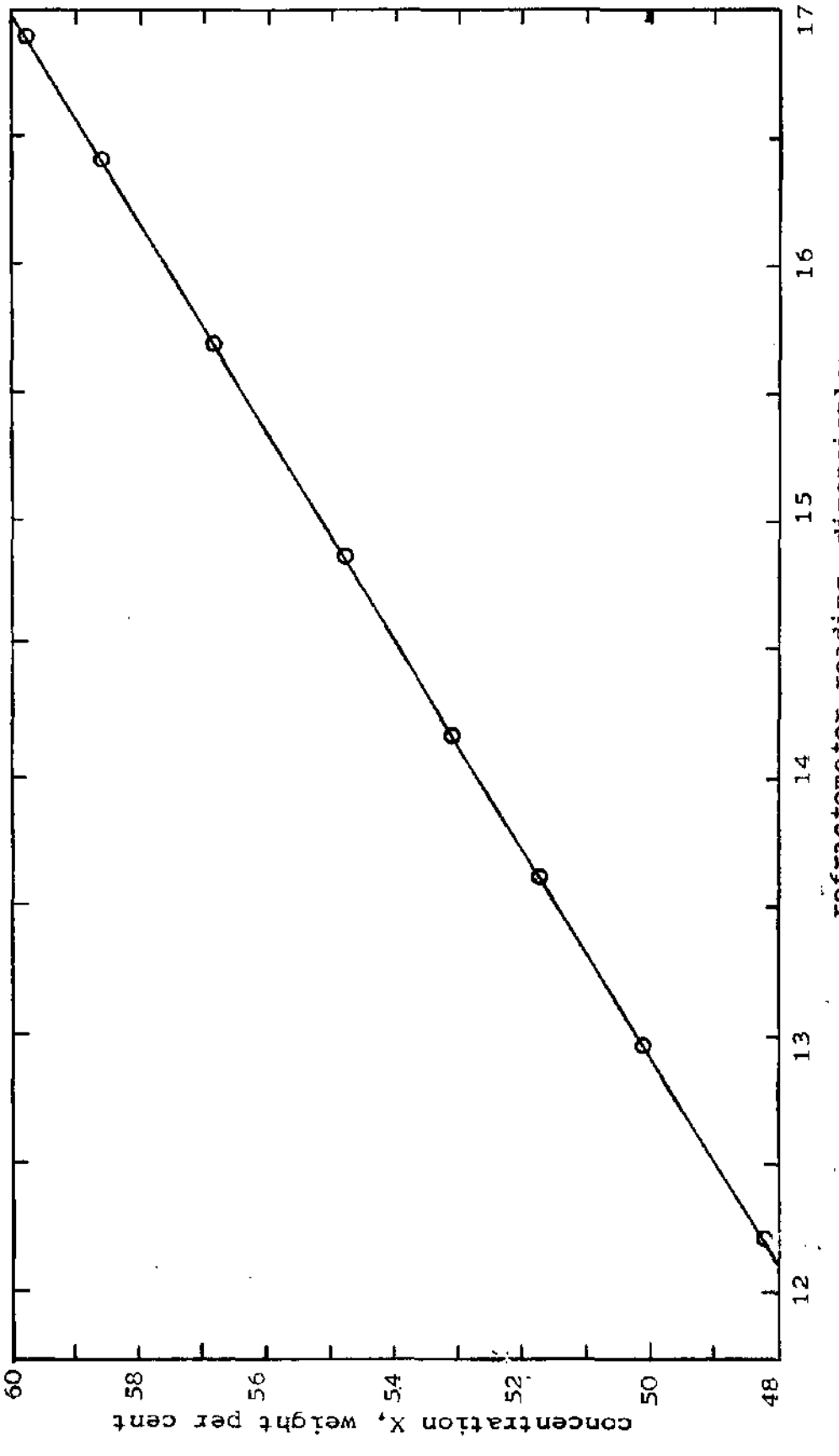
PROPERTIES OF LITHIUM BROMIDE

chemical	composition, per cent	
	typical	guaranteed
LiBr	99.6	99.0 min.
H_2O	0.29	1.0 max.
alkalinity as Li_2CO_3	0.03	0.04 max.
Cl	0.076	0.15 max.
SO_4	0.015	0.02 max.
Ca	0.005	0.01 max.
Mg	0.001	0.001 max.
suspended matter	0.003	0.05 max.

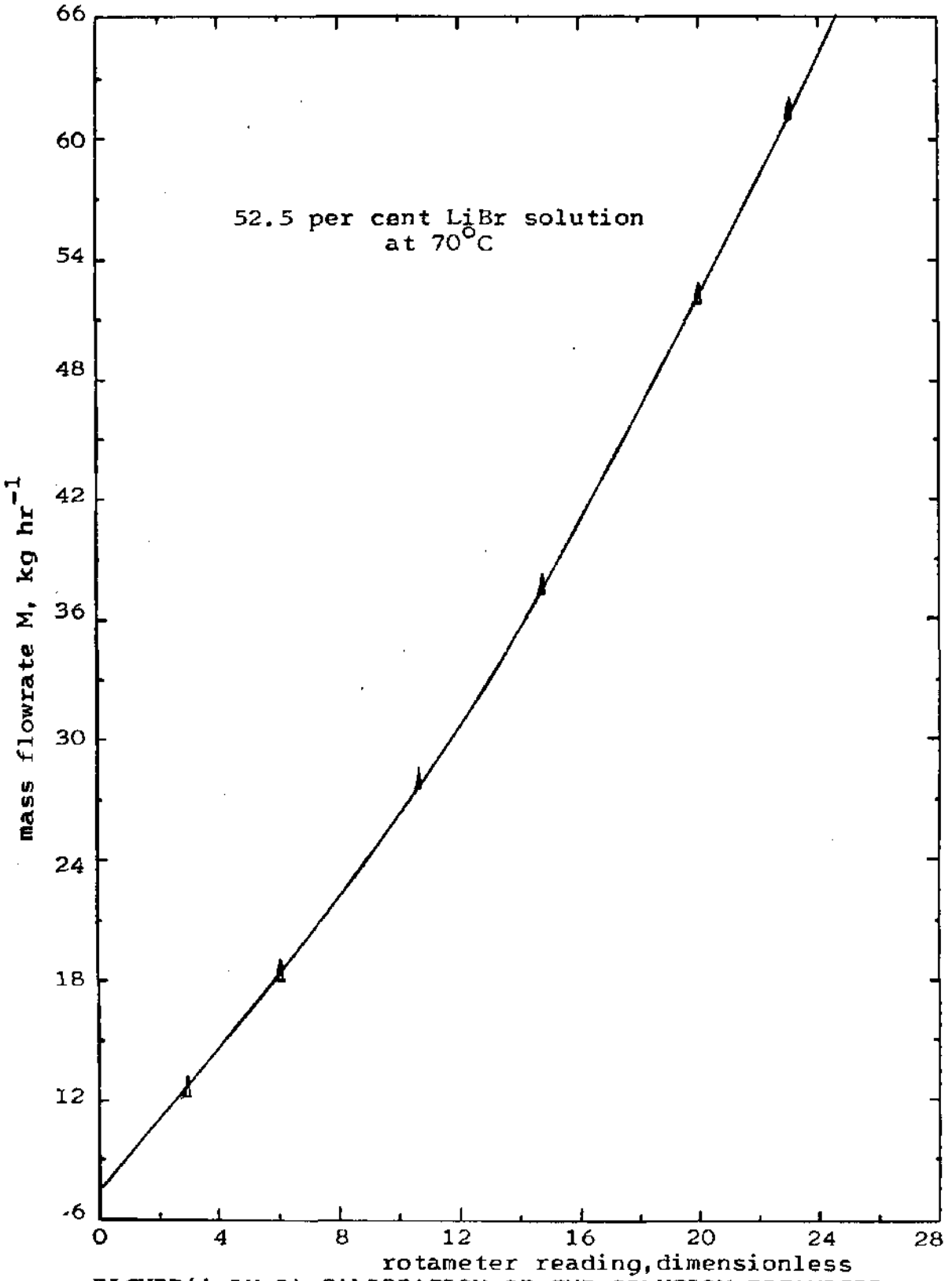
TABLE (A.IV.1) SPECIFICATIONS OF THE ANHYDROUS LITHIUM BROMIDE SUPPLIED BY "FOOTE MINERAL COMPANY, U.K."

hydrate	molecular weight	per cent LiBr by weight	solid phase transition	transition temperature °C
$LiBr.H_2O$	104.86	83.5	$LiBr.H_2O \rightleftharpoons LiBr$	156.0
$LiBr.2H_2O$	122.87	70.7	$LiBr.2H_2O \rightleftharpoons LiBr.H_2O$	42.8
$LiBr.3H_2O$	140.89	61.7	$LiBr.3H_2O \rightleftharpoons LiBr.2H_2O$	2.9
$LiBr.5H_2O$	176.92	49.1	$LiBr.5H_2O \rightleftharpoons LiBr.3H_2O$	-51.2

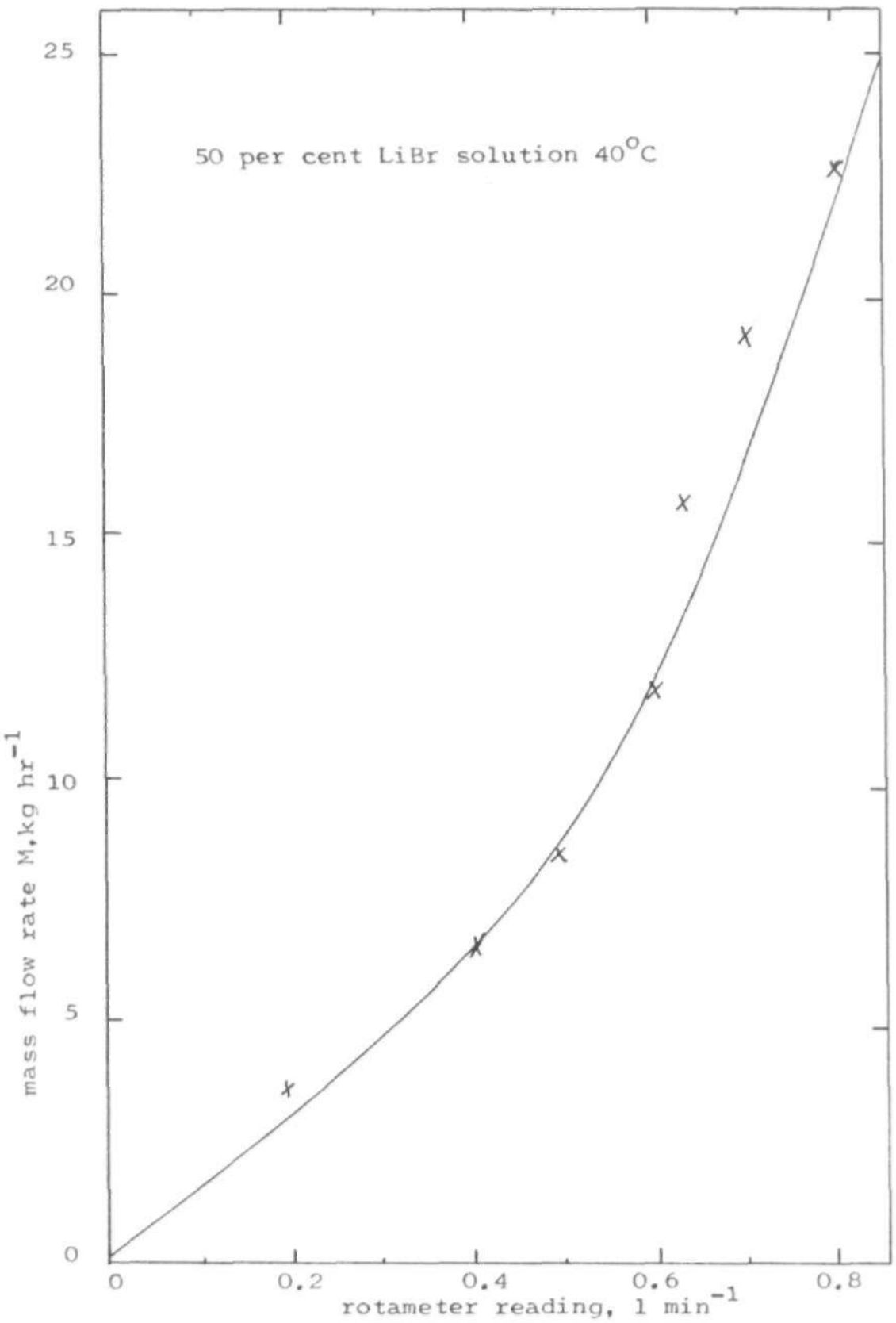
TABLE (A.IV.2) PROPERTIES OF HYDRATED LITHIUM BROMIDE (reproduced from "Technical data", Boryta, D.A.. Bulletin 145, Foote Mineral Company, Exton, U.S.A.)



FIGURE(A.IV.1) CALIBRATION OF LITHIUM BROMIDE SOLUTIONS AT 30°C



FIGURE(A.IV.2) CALIBRATION OF THE SOLUTION ROTAMETER FOR THE METAL EQUIPMENT



FIGURE(A.IV.3) CALIBRATION OF THE SOLUTION ROTAMETER FOR THE GLASS EQUIPMENT

APPENDIX V

THERMAL EFFICIENCY OF HEAT PUMPS

APPENDIX IV

THERMAL EFFICIENCY OF HEAT PUMPS

Referring to Figure (A. V.1), the actual coefficient of performance of a vapour compression pump is defined as

$$(COP)_A = \frac{Q_{CO}}{W} \qquad \text{(A. V.1)}$$

Similarly, the actual coefficient of performance of a conventional absorption heat pump is defined as

$$(COP)_{AHA} = \frac{Q_{CO} + Q_{AB}}{Q_{GE}} \qquad \text{(A. V.2)}$$

However, a more basic measure of the performance of a heat pump is the primary energy ratio (PER).

$$(PER) = \frac{Q_D}{E} \qquad \text{(A. V.3)}$$

where Q_D is the heat energy delivered and E is the primary energy input. For a vapour compression heat pump, using a mechanical compressor, the primary energy ratio can be written as

$$(PER)_A = \eta_{OV}(COP) \qquad \text{(A. V.4)}$$

or

$$(PER)_A = \eta_{OV}\left(\frac{Q_{CO}}{W}\right) \qquad \text{(A. V.5)}$$

where η_{OV} is the over-all efficiency of the compressor in terms of primary energy input.

For an electrically driven compressor with an over-all efficiency of electricity generation from power stations of 25 per cent and a motor efficiency of 80 per cent,

$$(PER)_A = 0.2(COP)_A \qquad \text{(A. V.6)}$$

For a conventional absorption heat pump, the primary energy ratio is

$$(PER)_{AHA} = \eta_{OV}(COP)_A \qquad \text{(A. V.7)}$$

or

$$(PER)_{AHA} = \eta_{OV}\left(\frac{Q_{CO} + Q_{AB}}{Q_{GE}}\right) \qquad \text{(A. V.8)}$$

where η_{OV} is the over-all efficiency of the heat supply system.

For an absorption heat pump system which is heated directly with primary energy,

$$\eta_{OV} \approx 1 \qquad \text{(A. V.9)}$$

Therefore,

$$(PER)_{AHA} = (COP)_{A} \qquad \text{(A. V.10)}$$

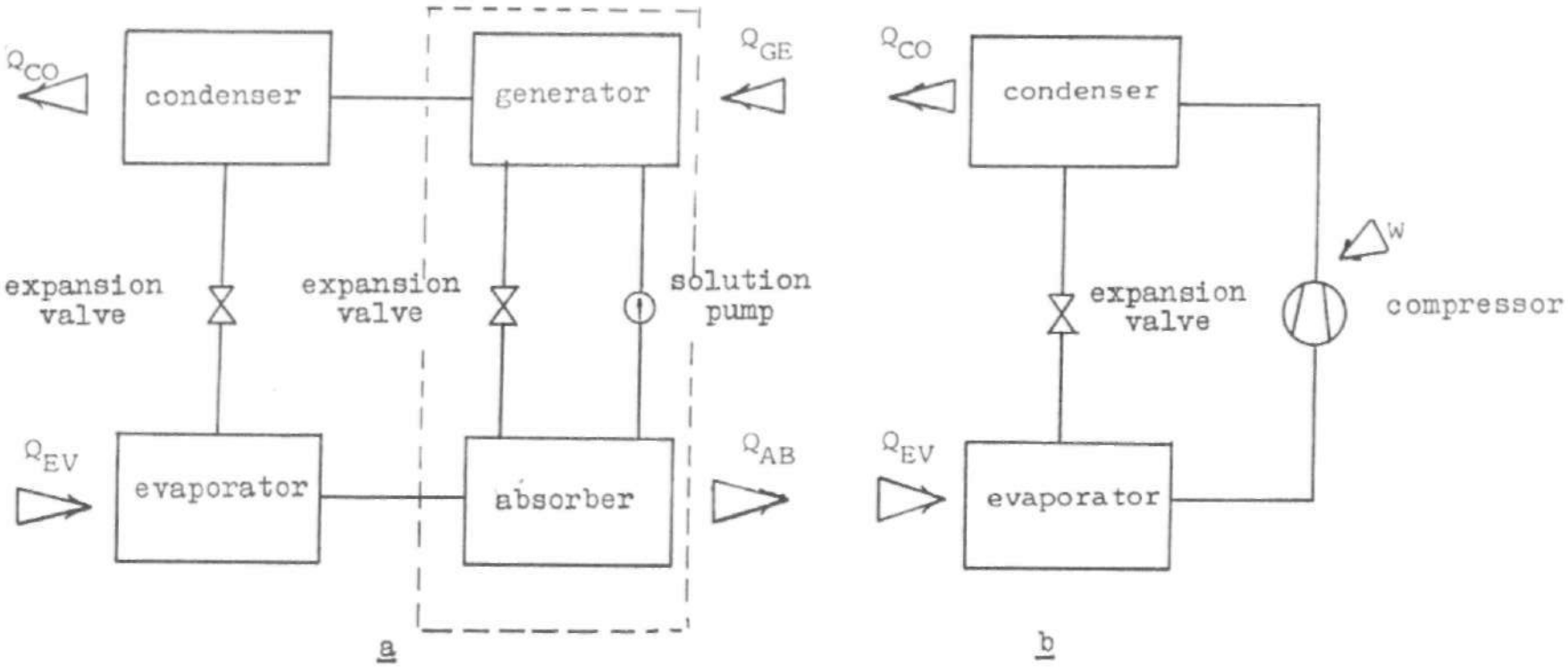


FIGURE (A.V.1) a) SIMPLIFIED ABSORPTION HEAT PUMP

b) SIMPLIFIED VAPOUR COMPRESSION HEAT PUMP